

Behavioural and Physiological Responses of *Myzus persicae* to Ultraviolet Light for the Development of New Pest Control Technologies



A thesis submitted in fulfilment of the
requirements for the degree of

Doctor of Philosophy

by

Joseph Fennell, B.Sc.



Centre for Global Eco-Innovation



I confirm that the contents of this thesis is my own work and has not been submitted for the award of a higher degree elsewhere. Any third-party material has been clearly identified within the text.

Cover Photograph: A mature apterous *Myzus persicae* individual feeding on *Brassica oleracea*.
Photograph by J. Fennell.

Abstract

This project sought to deliver new understanding of the responses of pest insects to light for the purpose of improved agricultural pest control. Through access to experimental polyethylene horticultural films with novel transmission properties, I exploited new opportunities for exploring separate short- and long-wavelength mechanisms for pest suppression. The early experimental work of the project tested the effect of short- and long-wavelength ultraviolet light on the population growth of the generalist aphid, *Myzus persicae*, on cabbage (*Brassica oleracea*) plants. These polytunnel field experiments established new hypotheses for the role of long-wavelength ultraviolet radiation as an environmental cue for damaging short-wavelength ultraviolet radiation. Through a series of methodological developments, I quantified both the dose-response of environmentally-relevant ultraviolet on *M. persicae* mortality, and proposed a colour behavioural model for the feeding behaviour of *M. persicae* under different illumination conditions. Through synthesising these findings into a model of aphid hazard-avoidance, I show that the behaviour of *M. persicae* may be manipulated to increase its exposure to solar short-wavelength radiation, with consequences for population growth rate. As such, this mechanism may be used in protected agricultural practice as part of a wider integrated pest management strategy.

Acknowledgments

I would like to thank the European Regional Development fund and Arid Agritec, who provided the funding for this project as a part of the Centre for Global Eco-Innovation.

There are so many people who have played major and minor parts in the creation of this thesis, it would be impossible to name you all, however I wish to express my particular gratitude to a few groups.

Firstly, to my supervisors: Nigel Paul, Andy Wilby and Jason Moore. Thank you for your continuous support through the many hours of supervisory meetings, the review of countless manuscripts and your patience with the endless string of 'side projects' that I brought to meetings. I've learnt plenty and this is, in no small way, down to you.

I would like to thank all of my friends and colleagues at the Lancaster Environment Centre who, not only gave me essential technical advice, helping hands, administrative support and loaned equipment; but, even more importantly, provided essential moral support, black coffee, cake and office humour.

To all of my friends and family: the old cliché is true, I couldn't have done it without you or the many adventures on which you took me, when I should have been working. In particular I wish to thank my parents for their unrelenting support and encouragement throughout my education.

This thesis is dedicated to my brother, Laurie, who shared my childhood love of all things invertebrate.

Contents

Contents	iv
List of Figures	vii
Acronyms	xiii
1 General Introduction	1
1.1 Project scope	1
1.2 UV-attenuation and insect herbivores	2
1.2.1 Introduction to solar illumination	2
1.2.2 Experimental techniques for studying the effects of spectrally-modifying claddings	4
1.2.3 Effect on immigration	5
1.2.4 Effect on within-crop movement	6
1.2.5 Effect on birth rate	8
1.3 Chromatic vision in insects	9
1.3.1 Introduction to insect visual systems	9
1.3.2 Spectral balance and insect flight	12
1.3.3 Colour as a host cue	14
1.3.4 Moving from monochromatic experiments to a trichromatic model of insect vision	14
1.4 Indirect effects of UV exposure on insects	15
1.4.1 Alkaloids and polyamines	16
1.4.2 Glucosinolates	17
1.4.3 Isoprenoids	18
1.4.4 Phenolics	20
1.5 Summary and project aims	22
2 General Materials and Methods	26
2.1 The experimental system	26
2.1.1 The glasshouse environment	26
2.1.2 Life-cycle and characteristics of <i>Myzus persicae</i>	27
2.1.3 Rearing and use of <i>Myzus persicae</i>	27
2.1.4 Cultivars and growing procedure	28
2.2 Experimental polytunnel field site	28
2.2.1 Design principles	29
2.2.2 Structure design	29
2.2.3 Site layout	30
2.3 Light and insect photobiology experiments	32
2.3.1 Definitions and units	32
2.3.2 Hardware tools for measuring light	32
2.3.3 Software tools for processing spectral data	32
2.3.4 Measuring irradiance	33
2.3.5 Measuring material transmission	33
2.3.6 Biological Spectral Weighting Functions	34
2.3.7 Colourspace derivation and use	35

2.3.8	Third-party solar datasets	36
2.3.9	Film transmission spectra	37
2.3.10	Experimental light sources	37
2.3.11	Standardised canopy transmission spectra	39
3	Population and behavioural effects of ultraviolet radiation on <i>Myzus persicae</i> in field experiments	41
3.1	Introduction	42
3.2	Methods	43
3.2.1	Light environment	43
3.2.2	Plants and insects	43
3.2.3	Aphid PGR experiment	44
3.2.4	Statistical methods	44
3.3	Results	45
3.3.1	Light Environment	45
3.3.2	Effect of light treatment on plant morphology	45
3.3.3	Effect of light treatment on <i>Myzus persicae</i> PGR	46
3.3.4	Effect of light treatment on spatial distribution	48
3.4	Discussion	51
3.4.1	Plant-mediated effects of UV on aphid PGR	51
3.4.2	UV-induced changes in canopy position	52
3.4.3	Novel light environment generates new hypotheses	53
3.5	Conclusions	55
4	Characterising the direct effects of UV radiation on <i>Myzus persicae</i>	56
4.1	Introduction	57
4.2	Methods	58
4.2.1	Plants and insects	58
4.2.2	Light treatments	58
4.2.3	Exposure procedure	59
4.2.4	Population growth procedure	59
4.2.5	Statistical analyses	60
4.2.6	Further population modeling	60
4.3	Results	61
4.3.1	Aphid mortality	62
4.3.2	Identification of appropriate BSWF	62
4.3.3	Sublethal effects	67
4.3.4	Applying the models to real-world scenarios	69
4.4	Discussion	71
4.4.1	Identifying a direct UV mortality effect	73
4.4.2	Sublethal effects of UV radiation	74
4.4.3	Towards better insect photobiology experiments	76
4.4.4	Using mortality data for prediction	78
4.5	Conclusions	78
5	A new method for the rapid quantification of aphid behaviour in different light environments	80
5.1	Introduction	81
5.2	Methods	82
5.2.1	Light environments and measurement	82
5.2.2	Behavioural assay platform configuration	83
5.3	Plants and aphids	83
5.3.1	Software and aphid tracking methods	85
5.3.2	Statistical Analyses	86
5.4	Results	87
5.4.1	Software calibration	87
5.4.2	Illumination	87
5.4.3	Aphid behavioural quantification	87
5.5	Discussion	90

5.5.1	Measuring aphid responses to light environment	90
5.5.2	Changing light in commercial and laboratory growth environments	92
5.6	Conclusions	94
6	Evidence for a novel functional role of the UV photoreceptor in <i>Myzus persicae</i>	95
6.1	Introduction	96
6.2	Methods	97
6.2.1	Plants and aphids	97
6.2.2	Behavioural assay technique	97
6.2.3	Light treatments	98
6.2.4	Statistical analyses	98
6.3	Results	100
6.3.1	Effect of UVA (Experiments 1-3)	100
6.3.2	Effect of UVB (Experiment 4)	102
6.3.3	Defining the aphid colourspace	102
6.3.4	Using the aphid colourspace to predict behavioural responses	103
6.3.5	Experiment 5: Expanding the aphid colourspace model	106
6.3.6	Applying the colourspace model as a predictive tool	108
6.4	Discussion	110
6.4.1	A new model for visually-mediated feeding behaviour	110
6.4.2	UV and green as behavioural cues	112
6.4.3	Green-Blue opponency for host finding	114
6.4.4	Using the colourspace model to predict behaviour	114
6.4.5	Implications for horticulture	115
6.5	Conclusions	115
7	General Discussion	117
7.1	From initial aims to revised hypotheses	117
7.2	Key methodological developments	119
7.2.1	A novel light environment for research	119
7.2.2	Action spectra for understanding mortality and vision	119
7.2.3	No-plant mortality assays in <i>Hemiptera</i>	120
7.2.4	Image analysis tools for behavioural research	121
7.3	A new model of aphid hazard perception	121
7.3.1	Do aphids overestimate the risk of ultraviolet (UV) exposure?	121
7.3.2	Ultraviolet-A (UVA) as a cue for increased plant defence	124
7.3.3	Influencing hazard perception for pest suppression	124
7.4	Conclusions	127
	Bibliography	128

List of Figures

1.1	Summer mean daily CIE dose for 2013. Satellite data (OMUVBd) obtained through the Giovanni interface (NASA, 2016). Geographical region shown is 14°E 34°N to 23°W 60°N. CIE dose is measured in effective $\text{kJ m}^{-2} \text{day}^{-1}$	3
1.2	Diagram of insect visual structures, based on the images presented by Matsumoto et al. (2014). (A) Arthropods perceive light with compound eyes and ocelli (Oc.). (B) These eyes are formed of many tubular light-collecting structures called ommatidia (Om.), each of which has its own cornea (Co.). (C) Each ommatidium collects light using the cornea (Co.), which then passes through the crystalline cone (CC.). Photoreceptor cells (R) surround a central light-transmitting tube, the rhabdom (Rh.). This is formed from interlocking microvilli which contain the chromophores for photoperception. <i>Inset photograph: Sam Droege, used under the Creative Commons 2.0 license</i>	10
1.3	Diversity of spectral perception across insect orders, adapted from Briscoe and Chittka (2001). Individual points show the wavelength of peak electroretinogram sensitivity recorded for an insect photoreceptor (λ_{max}). The boxplots represent the mean, minimum and maximum wavelengths of peak sensitivity for six insect orders. Colour indicates the approximate sensitivity waveband (purple = 300 - 400 nm, blue = 401 - 500 nm, green = 501-560 nm, red = 561 - 700 nm). The grey spectra shows a normalised standard solar spectrum (ASTM G173 Direct). Dashed lines show the upper (400 nm) and lower (315 nm) boundaries of the UVA waveband.	11
1.4	Photoreceptor and behavioural responses of <i>Hemiptera</i> and <i>Thysanoptera</i> to monochromatic light. (A) shows electroretinography (ERG)-derived mean and range photoreceptor peak wavelength sensitivity for <i>Hemiptera</i> (Sp.: <i>A. pisum</i> , <i>M. persicae</i> , <i>N. lugens</i> , <i>T. vaporariorum</i>) and thrips (<i>F. occidentalis</i> , <i>S. dorsalis</i>). (B) shows normalised plots of (1) take-off in thrips (Mazza et al., 2010), (2) attraction of aphids in flight (Hardie, 1989), (3) attraction of whitefly (Coombe, 1982), (4) attraction of thrips (Kishi et al., 2013), and (5) relative increase in probing activity of aphids (Döring et al., 2007). In B.2, line colour represents either summer or autumn dispersal (winged) morphs. Shaded boxes show approximate range of dominant photoreceptor in waveband. The dashed line represents a zero value which differs between experimental setup, but may be broadly interpreted as a null-response. For each subplot of B: (B.1): no take-off, (B.2)-(B.4): no attraction compared to an achromatic source of equivalent intensity, (B.5): equivalent attraction between target and achromatic source of equivalent intensity.	13
1.5	Colourspace diagrams for the behavioural responses identified in Figure 1.4. The three ternary plots have an axis for each class of photoreceptor in the insect eye and the arrows show the effect that movement in each of these axes is hypothesised to have on (A) take-off behaviour in thrips, (B) attractiveness to flying insects, and (C) probing behaviour in <i>Myzus persicae</i>	15
1.6	Simplified phenyl-propanoid pathway	20

1.7	Effects of light on aphids. During dispersal flight, UV light (A) is used to orientate flight. Green light reflected from vegetation (B) attracts dispersing aphids which land on the plant material. Plant chemistry is affected by spectral balance (C) and this can affect birth and death (D). When alates are produced, these use UV as a take-off cue for secondary dispersal (E).	24
2.1	Measured irradiance at plant growing level inside the glasshouse at Lancaster University. Measurement was made in mid-August at approximately solar noon when the sun was un-obscured by clouds. Dashed lines show the lower and upper limit of the UVA waveband (315 nm and 400 nm).	27
2.2	Final structure design. A small, steel-framed polytunnel (A), on temporary supporting plates (B). A timber frame supported a galvanised steel weld mesh growing platform (C), allowing the user to work within the tunnel (D).	30
2.3	Site layout. The top image shows a Google Sketchup simulation of the site to check for possible shading issues. The bottom image shows the site layout as used for the field experiments.	31
2.4	Normalised photoreceptor responses for the three <i>Myzus persicae</i> receptor types	34
2.5	Ternary plot showing the conceptual application of a visual colourspace. The ASTM G173 direct spectrum is defined as the centrepoint and shifts in each of the three axes represent relative changes in the stimulation of each photoreceptor type.	36
2.6	Commercially available polyethylene (PE) film transmission spectra. Measured transmissions as described above for (A) UV-transparent, (B) standard, (C) UV-opaque films and (D-F) three experimental films. The red-shaded region shows the UVB component and the blue-shaded region shows the UVA component of the transmission spectrum. The dashed line shows 100% transmission. The transmission profile for Tex (D) shows transmission values above 100% due to fluorescent emission in this region.	38
2.7	Transmission and reflectance measurements of naturally-occurring aphid feeding environments. Figures A. shows the transmission through a single <i>Brassica oleracea</i> leaf. Figure B. shows the average canopy transmission and Figure C. shows the compost reflectance. Markers in the method diagram show (A) metal halide source lamp, (B) UVA-340 and UVB-313 EL fluorescent tubes, (C) <i>Brassica oleracea</i> seedlings, (D) M3 compost, (E) spectroradiometer cosine-corrected head.	40
3.1	UVA and UVB % transmission for experimental structures. Points show the mean values (n = 3 structures per treatment) and error bars show the measured range.	46
3.2	Aphid plant final population sizes and population growth rates (PGRs). Boxplots show the median, interquartile range and range for each light treatment. Panels show v. Derby Day, experiment 1 (A), v. Derby Day, experiment 2 (B) and v. Volta, experiment 2 (C). Red letters show significantly different treatments (model coefficients in Table 3.3). Mean PGRs are shown for each light treatment by tunnel % UVA transmission (D) and tunnel % UVB transmission (E). Line colours show experiment and cultivar: red = v. Derby Day, experiment 1; blue = v. Derby Day, experiment 2; green = v. Volta, experiment 2.	47
3.3	Proportion of aphids feeding in exposed positions. Boxplots show the median, interquartile range and range for each light treatment. Panels show v. Derby Day, experiment 1 (A), v. Derby Day, experiment 2 (B) and v. Volta, experiment 2 (C). Red letters show significantly different treatments (model coefficients in Table 3.3). All three treatments are shown by tunnel % UVA transmission (D) and tunnel % UVB transmission (E). Line colours show experiment and cultivar: red = v. Derby Day, experiment 1; blue = v. Derby Day, experiment 2; green = v. Volta, experiment 2.	50
3.4	GLMM predicted mean (solid line) and 95% confidence intervals for the proportion of aphids inhabiting exposed parts of the plant at different UVA transmission values. Red dots and markers show the tunnel transmission values of the four films used in the experimental work.	51

3.5	Putative mechanism for direct effect of UV on aphids. Solar UVA and UVB (A) is selectively filtered by spectrally-manipulating films (B). When UVA is transmitted into the tunnel, it is perceived by the aphid (C), causing it to move to sheltered feeding sites within the plant (D). However when UVA is not transmitted, aphids do not move to sheltered feeding sites. When UVB is transmitted but UVA is not, aphids are exposed to UVB (E) which has a direct, negative effect on PGR.	54
4.1	Exposure Procedure. Aphids were placed on moistened filter paper (A) which was taped securely to the base of an aluminium block (B) with a circular hole cut through it. Optical filters (C, specified in Table 4.1) were taped in place with masking tape (D) so that they completely covered the circular hole (shown partially covered for illustration purposes). The metal moulding was placed on a temperature controlled plate (E) in the exposure chamber, beneath the fluorescent tubes (F).	60
4.2	Mortality and model predictions by lamp type and UV irradiance (\log_{10} scale). Individual points show the proportional mortality for each treatment (as described in table 4.1). The lines and confidence bands show the prediction of mortality and 95% confidence intervals as predicted by the GLM $y \sim \ln(\text{dose}) + \text{lamp}$	63
4.3	Lamp and action spectra for identifying appropriate Biological Spectral Weighting Functions (BSWFs) for UV-induced aphid mortality. (A) shows lamp spectra normalised to one with dashed lines showing the approximate waveband centres. (B) shows four candidate action spectra for aphid mortality on a log scale, standardised to one at 309 nm. The red line and coloured dots show the relative effect size (normalised to one at 309 nm) of lamp type on mortality for each of the three lamp types at the approximate waveband centres identified in (A).	64
4.4	Aphid mortality described by different BSWFs. For all plots, individual points show the proportional mortality for each treatment (as described in table 4.1) and the lines and confidence bands show the estimated mortality and 95% confidence intervals respectively. (A-D) show the mortality predictions for CIE (erythemal), ICNIRP (human exposure), Quaite (<i>in vivo</i> DNA) and Setlow (naked DNA). (E-G) show the mortality predictions for unweighted UVB, UVA and UV, respectively. . .	66
4.5	Effect of temperature on final population size for aphids surviving exposure to UV. The plots are paneled by aphid morph: Alatae (winged) or Apterae (wingless). Individual points show the final population size after seven days of a population originating from a single aphid. Individual point colour shows the treatment $\text{Dose}_{\text{Quaite}}$ value. The trendlines and ribbons show the estimated mean and 95% confidence interval from the GLM fitted for each aphid morph.	68
4.6	UV-induced effect on aphid population growth rate under horticultural tunnels in the UK. Point ranges show the predicted mean \pm the 95% confidence intervals (where applicable) for aphids exposed to mean UK summer day doses. (A) shows the predicted single-exposure growth rate, (B) shows the single-exposure mortality rate and (C) shows the continuous exposure growth rate. No meaningful confidence intervals could be computed for (C) and so only the predicted means are shown.	70

- 5.1 Image capture and aphid detection stages. In the fluorescent tube supplementation experiments, open-cell foam islands (A.i) were placed in a water filled 90 mm Petri dish (A.ii) with leaf discs (A.iii) placed on top. Various filtered fluorescent tubes (A.iv) were used to supplement UV with human visible light supplied by a Valoya LED unit (B.i). Images were captured by dSLR cameras (B.ii) mounted directly above the Petri dishes. The two arenas were separated by opaque screens (B.iii). In second set of experiments (LED only), all light was supplied by an LED unit (C.i) and a larger Petri dish was used to allow 12 replicates (C.ii). An example frame is shown pre-analysis as it would be displayed in the GUI (D). (E) Shows the different regions identified by the aphid detection script. Circle (E.i) is the perimeter of the leaf disc and is identified manually by the user. This is expanded by 10% to generate (E.ii). All image data outside this perimeter is excluded from analysis. Non-aphid areas (E.iii) which pass through the colour filter are excluded by size and aspect ratio to correctly identify the centre (X_3, Y_3) of the aphid (E.iv) when $X_1, Y_1 = (0, 0)$ and $X_2, Y_2 = (5.5, 5.5)$. An example frame is shown post-colour filtering (F) to illustrate how colour filtering improves the contrast of the aphid (F.i) against the leaf and background. 84
- 5.2 Aphid tracking raw data. These plots show examples from a control (UVA-) and a UVA+ LED treatment for single aphids. Traces show two individual aphids under either LED Control (left column) or LED UVA+ (right column) lighting. For each aphid, velocity (A and B), whether or not the aphid was detected on the leaf (C and D), whether or not this was interpreted as a probing phase (E and F) and the aphid distance from leaf Disc Centre (G and H) is presented against time (seconds). The dashed lines in (A) and (B) show the movement threshold of 0.014 mm s^{-1} which determined whether or not an aphid was classified as probing during that time period. Aphids with a velocity under 0.014 mm s^{-1} were classified as probing whereas those detected with a higher velocity were classified as not probing. 88
- 5.3 Spectra for the four experimental treatments and an ASTM G173 standard sunlight spectrum (scaled to 0.3 of the modeled irradiances to allow qualitative comparison with the treatment spectra). 89
- 5.4 Raw data and GLM predictions for measures of aphid sensitivity to light. Time proportion in feeding positions (A), Time Proportion in Feeding Position (TPiFP) (B) and average velocity (C) is presented for each aphid under four light treatments: white LED lighting with (FT UVA+) and without (FT Control) fluorescent tube UVA and LED lighting with (LED UVA+) and without (LED Control) LED supplemental UVA. Red point-ranges show quasibinomial GLM-fitted values the predicted standard error in figures A and B. Red point-ranges show the quasi GLM-fitted the predicted standard errors are presented in figure C. 91
- 5.5 Contextual Spectral Diagram. UVA:PAR ratios of experimental, commercial and naturally occurring light sources. FT UVA+, LED UVA+, FT Control and Light-Emitting Diode (LED) Control are the light treatments used in the experimental work reported here (white labels). The yellow labels show the UVA:PAR ratios for four typical plant growth spectra. Metal Halide is a typical metal halide lamp, measured as described previously. Solar is a surface-level modeled spectrum (ASTM G173 global) from the photobiology R package. G2 and NS1 are commercially available LED lamps from Valoya Ltd. (spectral percentages obtained from valoya.com). A measure of relative insect response ($100 - (\text{Time Proportion in feeding position} \times 100)$) is shown on the x-axis for the four experimental treatments. The error bars show the predicted standard errors and the regression line is a linear fit for the four points. 93

6.1	Aphid responses and light treatments for Experiments 1-3 using Philips TL(D)/08 fluorescent tubes. The left-hand column (plots (A), (C) and (E)) show the measured irradiance for each treatments. Grey bars show the total measured unweighted irradiance between 280 nm and 800 nm. The red bars show the unweighted UVA (315 nm - 400 nm) irradiance. The right-hand column shows the proportional aphid response to the light treatments. Each black point represents one measured aphid. For (B) and (D), the red point-range shows the estimated fit and 95% confidence interval from the Generalised Linear Models (GLMs). For (F), the point-range shows the calculated mean and 95% confidence interval for the raw data. The red solid line is the intercept-only model mean and the dashed lines show the 95% confidence intervals.	101
6.2	Aphid behavioural responses and light treatments for Experiment 4 using Q Panel QUV UVB-313 EL fluorescent tubes. (A) shows the measured irradiance for each treatment. Grey bars show the total measured irradiance between 280 nm and 800 nm. The red bars show the total UV (280 nm - 400 nm) irradiance and the blue bars show the total UVB (280-315nm) irradiance. (B) shows the proportional aphid response to the light treatments. Each black point represents one measured aphid. The point-range shows the calculated mean and 95% confidence interval for the raw data. The red solid line is the intercept-only model mean and the dashed lines show the 95% confidence intervals.	103
6.3	<i>Myzus persicae</i> photoreceptor responses (see 2.3.7 for description of plot construction). (A) is an ASTM G173 Direct Solar Spectrum shown unweighted (grey) and convolved with each of the three aphid visual action spectra (purple = UV, Blue = Blue, Green = Green). (B) shows the relative proportion of UV, blue and green experienced by the aphid under each light treatment. The dashed vertical line shows the relative, aphid-weighted UV photoreceptor response of the standard ASTM G173 Direct Solar Spectrum model as a reference. (C) is a ternary plot with three proportional axes, each representing a photoreceptor response. The proportional values were scaled so that the aphid response to ASTM G173 Direct Solar spectrum is the central point in the plot. Arrows show the difference in colourspace between treatments for Experiments 1-4 (Figure 6.1 and 6.2)	104
6.4	Aphid behavioural responses to UV. The proportion of time in a feeding position for all UVA light treatments plotted against (A) aphid-weighted irradiance (E_{UV}^*) and (B) aphid-weighted UV proportion (R_{UV}). Each black point represents a single aphid from a UVA+ or UVA- treatment. The red trendlines show the log-linear GLM predictions and estimated 95% confidence interval for the seven UVA+ and UVA- treatments. Data from the UVB+ experimental treatment are shown independently as small blue points (individual aphids) and a blue point-range representing the mean \pm 95% confidence intervals. The dashed vertical line in (B) shows the proportion aphid-weighted UV for the standard ASTM G173 Direct Solar Spectrum model as a reference.	105
6.5	Aphid colourspace experiment raw data. Plot shows the proportional aphid response to all light treatments (Time Proportion in Feeding Position). Each small point is an individual aphid. Point-ranges show the mean and estimated 95% confidence intervals for each treatment group. The treatments are expressed in categories determined by the unweighted irradiance from each of the three treatment LEDs (not by aphid visual-weighted response). Blue irradiance category is split by faceting, green irradiance category is shown by point shape and colour and UV irradiance category expressed as a percentage of the maximum on the x axis.	106

6.6	Model predictions for effect of irradiance and spectral balance on aphid feeding behaviour. Estimated mean time proportion in feeding position and 95% confidence intervals are shown for the aphid-weighted irradiance model (A). The two line colours represent the extreme experimental aphid-weighted irradiance values ($E_{\text{Green}}^* = 0.6$ to 6.6). These predictions are shown as a response surface (B) where colour represents the predicted TPiFP and aphid-weighted green and UV irradiances are the x and y values respectively. The white points represent the experimental treatments. Estimated TPiFP and 95% confidence intervals are shown for the aphid-weighted proportional model (C). The two line colours represent the extreme experimental aphid-weighted Green-Blue Proportion (GBP). For this experiment, the extreme values were 0.23 and 0.78. The dashed line shows the aphid-weighted UV proportion of the reference sunlight spectrum ($R_{\text{UV}} = 0.046$) These predictions are shown as a response surface (D) where cell colour represents the predicted mean and GBP and aphid-weighted UV proportion are the x and y values respectively. The white points represent the experimental treatments and the green point shows the spectral balance coordinates of the sunlight reference spectrum.	107
6.7	Estimated time proportion in feeding position for aphids under different simulated light environments (A,B) and light treatments in aphid colourspace (C). Estimated means and 95% confidence intervals were generated for (A) the proportional model (Table 6.8) and (B) the irradiance model (Table 6.7) computed previously. Red point-ranges are predictions for exposure to spectral balance experienced in natural habitats. Blue point-ranges show the predictions for spectral balance under six horticultural PE film claddings. The solid vertical line shows the prediction for the solar reference spectrum ASTM G173 direct and the dashed line shows the 95% confidence limits for the ASTM prediction. Light environments are shown on a scaled axis (C) with the ASTM G173 direct spectrum at the centre. Light treatments are described in Table 6.9.	109
6.8	Example image stacks from Experiment 1 for Control (E1 UVA-) and UVA+ (E1 UVA+) treatments. Images have been stacked additively to view the positions of a single aphid at each 30 second time point over the one hour experimental duration.	112
7.1	Integrated mortality and behaviour models for <i>Myzus persicae</i> under different light environments. The mortality hazard is the probability of mortality after a single day dose equivalent (4.3) and the avoidance response is $1 - [\text{Total proportion in feeding position}]$ (6.3). Plots panel: (A) UK summer mean dose ($\text{Dose}_{\text{CIE}} = 1.3 \text{ kJ m}^{-2}$) filtered through the mesh insect cages used in 3.x, (B) UK summer mean dose ($\text{Dose}_{\text{CIE}} = 1.3 \text{ kJ m}^{-2}$), (C) Mediterranean summer mean dose ($\text{Dose}_{\text{CIE}} = 7 \text{ kJ m}^{-2}$). Label position shows the environment coordinates. Translucent boxes show the 95% confidence intervals in both axes. Environment type grouped by colour: green = naturally-experienced environments, blue = commercially-available films, red = experimental UVA-attenuating/UVB-transmitting films. The green line represents the model trajectory through naturally-experienced environments.	122
7.2	Differences in pigmentation between alate and apterous morphs of <i>Myzus persicae</i> . Two morphs are shown (A) apterous (asexual) female (B) alate (asexual) female.	124
7.3	Total insects trapped on sticky traps under different PE film claddings. Data are paneled by insect order and each point represents a trap count. Raw data were collected by C. Wood in 2013 for her M.Sc. project and text interpretation are guided by her final report (C. Wood, <i>personal communication</i>).	126

Acronyms

BSWF Biological Spectral Weighting Function.

CSV Comma-Separated Value.

ERG electroretinography.

GBP Green-Blue Proportion.

GLM Generalised Linear Model.

GLMM Generalised Linear Mixed Effect Model.

GUI Graphical User Interface.

IPM Integrated Pest Management.

LED Light-Emitting Diode.

ND neutral density.

PAR Photosynthetically-Active Radiation.

PE polyethylene.

PGR Population Growth Rate.

ROS Reactive Oxygen Species.

SME Small and Medium sized Enterprise.

SWF Spectral Weighting Function.

TPiFP Time Proportion in Feeding Position.

UV ultraviolet.

UVA ultraviolet-A.

UVB ultraviolet-B.

UVC ultraviolet-C.

VAS Visual Action Spectra.

VOC Volatile Organic Compound.

General Introduction

1.1 Project scope

This project, conceived under the preliminary title ‘Novel Approaches to Sustainable Pest Control Through Light Manipulations’, was funded by the Centre for Global Eco-Innovation as a collaborative partnership between Lancaster University and Arid Agritec, a horticultural consultancy and polyethylene (PE) polytunnel cladding supplier for the protected crop industry. As one of fifty industrially-focused research projects located in north-western England, there were requirements from the funders that the project delivered environmental and economic benefits. The Centre for Global Eco-Innovation defined its objectives as:

1. Increase the innovation performance of the regions Small and Medium sized Enterprises (SMEs).
2. Increase the level of collaboration between SMEs and universities.
3. Capitalise on the use of graduate talent to overcome low levels of absorptive capacity in SMEs.
4. Increase the export performance of the regions SMEs in markets for low carbon and environmental goods and services.
5. To increase the economic performance of the region.
6. To deliver significant savings in greenhouse gas emissions, water, waste and material use.

The scope of the project was therefore defined as ‘*Developing knowledge which could bring environmental and economic benefit through improving pest control in protected cropping environments*’. This would specifically include work on commercially-relevant pest species and would focus on manipulations of light attainable through the filtering of sunlight using current and prototype claddings. As such, this introductory chapter begins with an analysis of the use of wavelength-selective claddings for pest control (section 1.2). Whilst the initial section (1.2) focuses on applied experiments, in subsequent sections, I expand the review to link the findings of these large-scale applied experiments to the fundamental ecological literature describing insect inter-

action with light, both directly (section 1.3) and indirectly through spectrally-induced changes in plant chemistry (section 1.4).

1.2 UV-attenuation and insect herbivores

Spectral manipulation for agricultural pest control includes, but is not limited to: the use of spectral manipulation for trapping invertebrates, the use of reflective ground coverings (mulches) to repel dispersing pests, and the modification of the crop light environment, either through selective attenuation of sunlight, or through the use of artificial lighting (Antignus, 2000). Many spectral bands and methods for modifying the light environment have merits which have been previously discussed (for review see: Johansen et al., 2011; Vänninen et al., 2010), however the role of ultraviolet (UV)-attenuation for inhibiting insect population growth in horticultural systems has been of particular interest to the horticultural community (Antignus, 2000; Diaz and Fereres, 2007). As such, I begin this thesis with a comprehensive review of the use of UV-attenuating filters in horticulture, for the purposes of pest control.

1.2.1 Introduction to solar illumination

The Earth's primary source of illumination is from solar electromagnetic radiation. This is filtered by the various layers of the atmosphere, resulting in a spectral balance which has heavily influenced the evolution of almost all terrestrial organisms (Rozema et al., 1997). The highest irradiance solar electromagnetic radiation is that in the human visible region (380 nm-760 nm) (Nathans, 1999), with the peak between 450 nm and 550 nm. UV light between 290 nm and 400 nm is present at surface level and makes up approximately 8.4% (ASTM G173 standardised spectrum, see General Materials and Methods for details) of the total UV-Human visible (380 nm-760 nm). Although the Sun emits light with wavelengths shorter than 290 nm, they are filtered or reflected by the atmosphere and so do not reach the Earth's surface (Brasseur and Solomon, 2006). Of the UV energy reaching the surface, 98.5% of the UV energy is in the ultraviolet-A (UVA) waveband (315 nm-400 nm), with only 1.5% in the ultraviolet-B (UVB) waveband (280 nm-315 nm).

UV irradiance and spectral balance varies considerably with time of day, season, latitude and atmospheric composition. Seasonality and latitude determine the amount of solar radiation intersecting the outer atmosphere, whilst radiative transfer through the atmosphere is determined by the ozone column thickness and cloud density (Fioletov et al., 2010). For example, within Europe, the mean erythemally-weighted daily summer dose (see Chapter Two for an introduction to spectral weighting functions) varies between $\sim 1 \text{ kJ m}^{-2} \text{ day}^{-1}$ in the far north and $\sim 7 \text{ kJ m}^{-2} \text{ day}^{-1}$ in southern Spain 1.1. Due to the broad geographical distribution of experimental work in spectral manipulation for agriculture (Raviv et al., 2004), there is undoubtedly large variation in the doses of solar UV received by the experimental systems. To further complicate analysis of the existing literature, experimental irradiances and doses are typically not reported, with most studies reporting only the transmission of the claddings used (Table 1.1). As such, quantitative comparison of the effects of UV-attenuation is not an appropriate method for examining this body of literature and so I take a predominantly qualitative approach in synthesising the results of studies of wavelength-selective claddings.

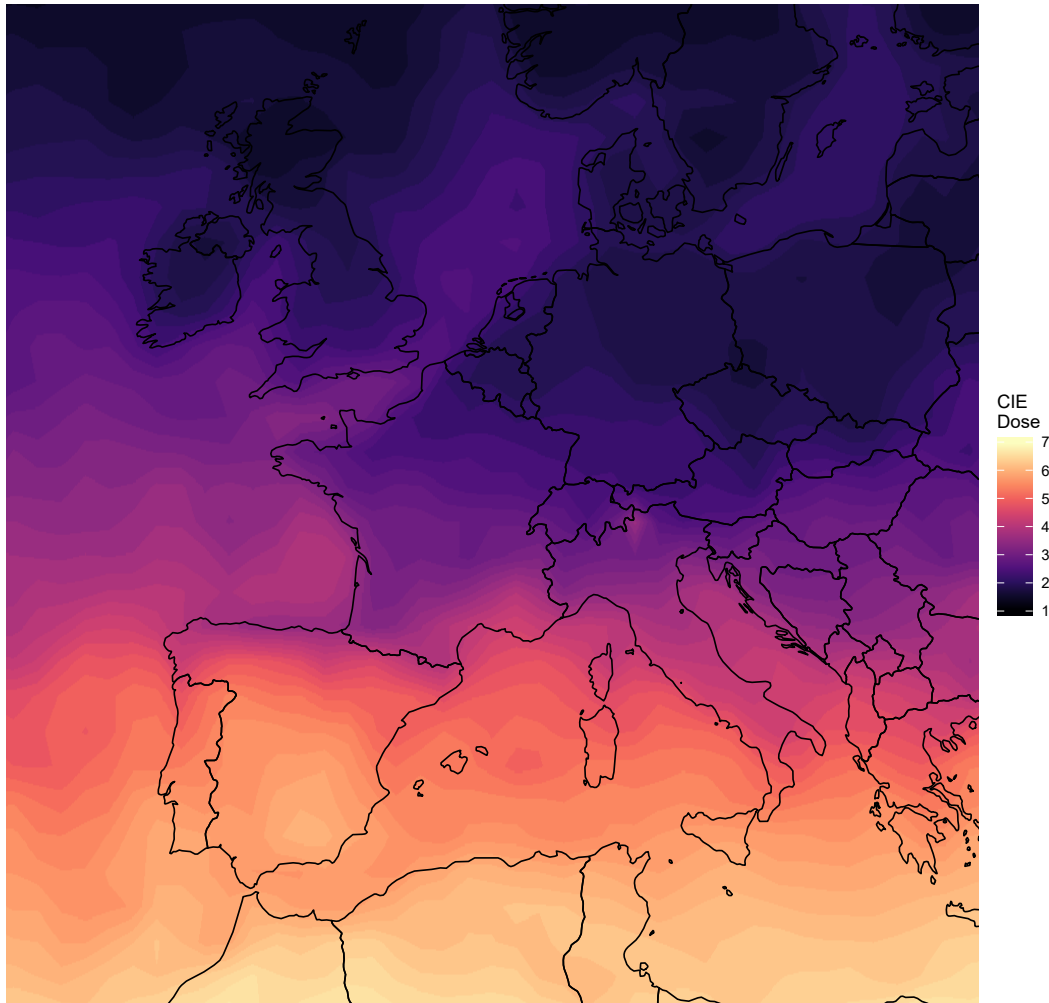


Figure 1.1: Summer mean daily CIE dose for 2013. Satellite data (OMUVBd) obtained through the Giovanni interface (NASA, 2016). Geographical region shown is 14°E 34°N to 23°W 60°N. CIE dose is measured in effective $\text{kJ m}^{-2} \text{day}^{-1}$

Table 1.1: Light Treatments for experiments described in Table 1.2. ¹No Spectral Data available. ²Approximate minimum transmitted wavelength (threshold for UV-blocking cladding). ³% UV transmitted through cladding.

Study	NSD ¹	Type	High UV		Low UV	
			λ_{cut}^2	% UV-trans. ³	λ_{cut}^2	% UV-trans. ³
Antignus et al. (2006)		Film		56%		20%
Antignus et al. (2001)		Film		56%		20%
Burdick et al. (2015)		Film	290 nm		380 nm	
Chyzik et al. (2003)		Film		39%		7%
Costa et al. (1999)	x	Film				
Costa et al. (2002a)		Film	360 nm		380 nm	
Costa et al. (2003)		Film	360 nm		380 nm	
Dader et al. (2014)		Film	360 nm	12%		<1%
Diaz et al. (2006)		Film		15%		2%
Doukas and Payne (2007)		Film	290 nm		385 nm	
Gonzalez et al. (2001)	x	Film				
Kigathi and Poehling (2012)		Film		92%		42%
Kuhlmann and Müller (2009)		Glass	300 nm		400 nm	
Kumar and Poehling (2006)		Film			400 nm	
Legarrea et al. (2010)		Net		70%		40%
Legarrea et al. (2012a)		Net		80%		38%
Legarrea et al. (2012b)		Net		80%		38%
Legarrea et al. (2012c)		Net		80%		38%
Mutwiwa et al. (2005)		Film		78%		10%
Paul et al. (2012)		Film		92%		6%
Sal et al. (2008)		Net		70%		40%

1.2.2 Experimental techniques for studying the effects of spectrally-modifying claddings

Methods for testing the effect of UV-attenuation on pest insects are diverse with many different cladding types, crop species and measurement techniques employed (Raviv et al., 2004). This review was limited to those studies which (i) used some form of optical filtering material to cover the experimental site and (ii) compared two or more materials which had different UV transmission properties. Although the majority of studies were typical field trials, lasting many weeks and investigating immigration, spread, Population Growth Rate (PGR) or trap capture through a crop, studies which tested the short term behavioural responses of insects released under different claddings were also included.

Spectral filters

The majority of studies (75%) used PE films as the spectral filter. 20% of studies used nets of unspecified material whilst one study used glass treated with a metal film coating (Table 1.1). Transmission varied widely between claddings and so it is not possible to classify high and low UV treatments by their spectral characteristics. ‘High UV’ film transmission varied between 12% and 92 % total UV transmission whereas ‘Low UV’ films transmitted below 42% of the UV. Studies using nets varied less in the transmission properties, presumably because all of the relevant studies were conducted by the same research group. These studies used high UV transmission nets (70-80% UV transmission) and low UV transmission (38-40% transmission) (Table 1.1 for references).

Although transmission values give a reference point for comparison, additional information may be gained when the cut wavelength (λ_{cut}) is reported. A commercial UV-transparent cladding is considered to be partially transparent to wavelengths down to 290 nm, therefore exposing the crop to UVA and UVB (see Materials and Methods for commercial UV-transparent transmission profile). Standard commercial claddings typically cut above this in the 360 nm range and a number of studies used these standard claddings as the ‘high UV’ treatment (Table 1.1), comparing them to claddings which blocked wavelengths below 380 nm (e.g. Costa et al. (2002a, 2003)). Others compared UV-transparent films to UV-blocking films (e.g. Doukas and Payne (2007)). The variation in definition of what may be described as ‘high’ and ‘low’ UV clearly makes quantifiable comparison of effect sizes between studies highly difficult. This, combined with the inherent temporal and geographical variation in UV dose likely to have been delivered during the experiments (e.g. Figure 1.1), means that only the direction of the effect can be compared between studies.

Measurement of infestation

All of the studies where crop plants were used, compared insect population sizes using either on-plant assessment (counts, scoring of infestation, etc.) or trapping with coloured traps (yellow sticky traps, blue sticky traps, etc.). For studies where insects were released into tunnel spaces with no plants, trapping with coloured traps was used (Legarra et al., 2012c; Kigathi and Poehling, 2012). *Hemiptera* were typically identified on yellow sticky traps (Costa et al., 2002a; Doukas and Payne, 2007) whereas thrips were more commonly found trapped on blue sticky traps (Diaz et al., 2006; Doukas and Payne, 2007) with the exception of the yellow tea thrip (*Scirtothrips dorsalis*) which was also recovered from yellow sticky traps. This preference may be due to its folivorous nature, as opposed to those thrips which feed predominantly on flowers and therefore may be attracted to various colours.

On-plant assessment typically relied on a discrete-point scale indicating different levels of infestation (e.g. Doukas and Payne, 2007) rather than direct counts. Whilst this may limit the resolution of our understanding of the spatio-temporal dynamics of insect spread through a crop, it provides an adequate measure of infestation for factors of commercial relevance. For example, the incidence of aphid-vectored disease in a crop may not be related to the population size of the resident aphid colony and spread may occur even by short-term feeding of a transient individual (Legarra et al., 2012a).

1.2.3 Effect on immigration

Experiments where the immigration of wild pests into the crop area was monitored, demonstrated that UV-attenuation consistently reduced trap capture across species of *Hemiptera*, *Thysanoptera*, *Diptera* and *Coleoptera* (Table 1.2). Thrips (*Thysanoptera: Thripidae*) and whiteflies (*Hemiptera: Aleyroididae*) are monomorphic and so no differentiation can be made between feeding and dispersing groups, however in aphids (*Hemiptera: Aphididae*), winged (alate) dispersers can be differentiated from sedentary wingless (apterous) morphs. Trap capture was predominantly of winged aphids during their dispersal stage (Doukas and Payne, 2007) and so, trap counts from early stages in the experiments can be considered a proxy for immigration into the crop. Where no effect was seen (Costa et al., 2002a, 2003), it may be explained by the similarity in transmission properties between the high UV and low UV claddings (Table 1.1). The two studies where

no effect on trap capture was seen used filters which cut at 360 nm and 380 nm for high and low UV, respectively. Either the degree of UV attenuation was insufficient to affect the insect population immigration, or it was equally efficient at excluding insects in both treatments.

Smaller-scale studies showed that insects from across the taxa showed reduced preference for entry into structures which transmitted less UV (Costa et al., 1999; Kigathi and Poehling, 2012; Legarrea et al., 2012c; Mutwiwa et al., 2005). Winged morphs of the potato aphid (*Macrosiphum euphorbiae*) (Legarrea et al., 2012c), greenhouse whitefly (*Trialeurodes vaporariorum*) (Mutwiwa et al., 2005), and silverleaf whitefly (*Bemisia tabaci*) (Costa et al., 1999) had a strong preference for chambers clad in UV-transmitting materials compared to those clad in UV-attenuating materials when presented with two chambers in a choice test. Similarly, western flower thrip (*Frankliniella occidentalis*) was nine times more likely to enter a chamber clad in UV transparent materials (Kigathi and Poehling, 2012). In this study, different trapping techniques were compared and no difference was found between trap captures on clear traps and counts on host plants. This indicates that dispersing thrips (i.e. those not already located on a plant) are directly attracted to high UV environments. If the attenuation of UV simply made the host plant visually indistinguishable from the background, thrips would be expected to find high UV and low UV equally attractive in the absence of a plant. As this was not the case, thrips appear to use UV as a direct target towards which they fly.

Feeding thrips were also shown to rapidly respond to attenuation of UVB, showing reduced preference for tunnels with high UVB (Mazza et al., 1999). This suggests that thrip behavioural responses to light may be context dependent: thrips engaged in feeding behaviour may seek reduced UV or increased green environments, whereas those in dispersal phases are attracted to high UV areas. Behavioural responses to UVB are unusual but most insect UV photoreceptors have some sensitivity in the UVB waveband Briscoe and Chittka (2001) and so a UVA+UVB treatment would appear more UV-bright than a UVA-only treatment (as was compared by Mazza et al. (1999)). Thrips in this study were only twice as likely to choose UVB-attenuated treatments over full sun control during feeding (compared to nine times more likely to choose a high UV environment during dispersal, as reported by Kigathi and Poehling (2012)), suggesting that spectral discrimination between UVA and UVB is more difficult than between low and high UV.

1.2.4 Effect on within-crop movement

Once a population of pest insects has entered a crop, the rate at which the population spreads between plants is an important contributory factor in the overall PGR. Methods where insect populations were quantified on plants (as opposed to on traps) suggested that there was a negative effect of UV-attenuation on insect movement within the crop, but that it was less consistent than the effect on immigration (Table 1.2). UV-attenuation was shown to reduce dispersal in western flower thrip (Kigathi and Poehling, 2012), greenhouse whitefly (Mutwiwa et al., 2005) and alate potato aphid (Legarrea et al., 2012c) in short-duration experiments using laboratory-reared insects released in the centre of an arena with traps at different distances from the release point. Under UV-attenuating claddings, more insects were recovered from traps close to the release site compared to under UV-transmitting claddings where aphids were more likely to be recovered further from the release point. As such, it appears that either flight duration is shorter, and so insects land more rapidly under UV-attenuated environments, or less flight occurs and insects disperse by other means (i.e. walking). In longer-duration experiments, artificially-introduced potato aphid were found at lower densities on crop plants and in more spatially-aggregated hotspots

Table 1.2: Effect of UV-attenuation on insect performance. Response variables were: ¹Trap Capture (typically yellow sticky traps for *Hemiptera* and blue sticky traps for *Thysanoptera*), ²Plant Infestation (either number of plants infested or on-plant population size), ³Flight Preference (attractivity or flight activity), ⁴Caged Population Growth (for insects caged to exclude immigration/emigration). Effect of UV-attenuation indicated by green (+) as positive, grey 0 as no effect, and red (-) as negative. Light treatments are described in Table 1.1.

Study	Plant	Insect	Effect of UV-attenuation			
			TC ¹	PI ²	FP ³	CPG ⁴
<i>Hemiptera: Aphididae</i>						
Antignus et al. (2006)	Cucumber	<i>A. gossypii</i>	(-)			
Burdick et al. (2015)	Soybean	<i>A. glycines</i>				0
Chyzik et al. (2003)	Pepper	<i>M. persicae</i>	(-)	(-)		(-)
Costa et al. (2002a)	Solidago	-	(-)	0		
Costa et al. (2002a)	Chrysanthemum	-	(-)	(-)		
Dader et al. (2014)	Pepper	<i>M. persicae</i>				(-)
Diaz et al. (2006)	Lettuce	<i>M. euphorbiae</i>		(-)		
Diaz et al. (2006)	Lettuce	<i>A. lactucae</i>		(-)		
Doukas and Payne (2007)	Cucumber	<i>A. gossypii</i>	(-)	(-)		
Kuhlmann and Müller (2009)	Broccoli	-		(-)		
Kumar and Poehling (2006)	Tomato	<i>A. gossypii</i>	(-)	(-)		
Legarra et al. (2012b)	Lettuce	<i>M. euphorbiae</i>		(-)		
Legarra et al. (2012a)	Lettuce	<i>M. euphorbiae</i>		(-)		
Legarra et al. (2012c)	Lettuce	<i>M. euphorbiae</i>			(-)	
Legarra et al. (2012c)	Turnip	<i>M. persicae</i>			(-)/0	
Paul et al. (2012)	Lettuce	<i>M. persicae</i>				(-)
Sal et al. (2008)	Lettuce	<i>M. euphorbiae</i>		(-)/0		
<i>Hemiptera: Aleyroididae</i>						
Antignus et al. (2006)	Cucumber	<i>B. tabaci</i>	(-)			
Antignus et al. (2001)	Tomato	<i>B. argentifolii</i>	(-)	(-)		
Costa et al. (1999)	-	<i>B. argentifolii</i>			(-)	
Costa et al. (2002a)	Solidago	-	0	0		
Costa et al. (2002a)	Chrysanthemum	-	0	(+)		
Costa et al. (2003)	Lisianthus	<i>T. vaporariorum</i>	0	0		
Dader et al. (2014)	Eggplant	<i>B. tabaci</i>				(+)
Diaz et al. (2006)	Lettuce	<i>T. vaporariorum</i>	(-)	0		
Gonzalez et al. (2001)	Pepper	<i>T. vaporariorum</i>	(-)			
Gonzalez et al. (2001)	Pepper	<i>B. tabaci</i>	(-)			
Kuhlmann and Müller (2009)	Broccoli	-		(-)		
Kumar and Poehling (2006)	Tomato	-	(-)	(-)		
Legarra et al. (2010)	Pepper	<i>B. tabaci</i>	(-)			
Legarra et al. (2012c)	Tomato	<i>B. tabaci</i>			(+)	
Mutwiwa et al. (2005)	-	<i>T. vaporariorum</i>			(-)	
<i>Hemiptera: Cicadellidae</i>						
Diaz et al. (2006)	Lettuce	<i>Empoasca sp.</i>	(+)			
Doukas and Payne (2007)	Cucumber	-	(-)			
<i>Thysanoptera</i>						
Antignus et al. (2006)	Cucumber	<i>F. occidentalis</i>	(-)			
Costa et al. (1999)	-	<i>F. occidentalis</i>			(-)	
Costa et al. (2002a)	Solidago	-	(-)	0		
Costa et al. (2002a)	Chrysanthemum	-	(-)	0		
Costa et al. (2003)	Lisianthus	<i>F. occidentalis</i>	0	0		
Diaz et al. (2006)	Lettuce	<i>F. occidentalis</i>		0		
Doukas and Payne (2007)	Cucumber	<i>T. tabaci</i>	(-)			
Kigathi and Poehling (2012)	-	<i>F. occidentalis</i>			(-)	
Kuhlmann and Müller (2009)	Broccoli	-		0		
Kumar and Poehling (2006)	Tomato	-	(-)	(-)		
Legarra et al. (2010)	Pepper	<i>S. dorsalis</i>	(-)	(-)		
<i>Other Orders</i>						
Costa et al. (2003)	Lisianthus	<i>Diptera: Lyriomiza sp.</i>	(-)			
Doukas and Payne (2007)	Cucumber	<i>Coleoptera</i>	(-)			
Doukas and Payne (2007)	Cucumber	<i>Diptera</i>	(-)			

under UV-attenuating claddings, compared to higher UV controls (Legarrea et al., 2012b,a). This supports the findings of the small-scale experiments, demonstrating that UV-attenuation reduces movement in the crop, and that the likely mechanism is disruption of the insect visual system which controls flight.

Whilst the initial amount of movement within a crop was lower, this may not affect the final population size, as was observed in a number of studies (Legarrea et al., 2012c; Sal et al., 2008). When aphids were forced to disperse, by release onto a non-host substrate, the initial rate of host-location was slower under the UV-attenuated environment, however after 24 hours there was no difference in population size, compared to a high UV control (Legarrea et al., 2012c). This indicates aphids are still be able to disperse, albeit by slower methods (i.e. walking) under low UV environments, possibly using olfactory cues from the plant to locate it, as has been observed in other aphids which use a combination of colour- and volatile-cues to locate their correct host (Han et al., 2012). Similarly, potato aphid was initially found to be less prevalent in a crop, however, by the time the crop reached harvest (eight weeks after initial introduction of insects), the infestation score was equal across all treatments (Sal et al., 2008). It may be that this was due to the use of a discrete scoring system which was artificially capped at a certain population size - significantly larger populations may have been observed if full counts had been made and so differences between treatments may have occurred. However, their findings still showed that 100% of the crop had been infested with aphids and so, given the very low numbers of feeding aphids needed to spread viruses of commercial importance (Legarrea et al., 2012a), it would suggest that UV-attenuation was of limited benefit as an Integrated Pest Management (IPM) tool in this case.

In experiments which used both trapping and plant-scoring, a number of studies demonstrated differences in trap capture but no differences in on-plant counts (Costa et al., 2002a, 2003; Diaz et al., 2006). Despite the disruption to dispersal, whitefly and thrip appear to perform equally well under UV-attenuation, suggesting birth rate might be higher to offset the reduced population spread. The continuous dispersal strategy of whitefly and thrip may allow better compensation for disrupted dispersal. All thrip and whitefly individuals are winged (compared to aphids, which only produce winged morphs under certain conditions) and so are able to disperse by flight. Even though UV-attenuated environments are clearly less attractive to them (see previous section) and have reduced within-crop spread in some examples (Kumar and Poehling, 2006; Legarrea et al., 2010), it may be that under conditions where on-plant birth rate is high (or death rate is low), enough dispersal occurs to infest a crop to the same degree that occurs under non-attenuating claddings. Conversely, during the spring and summer, aphids only produce dispersal morphs under stressful conditions, typically when the population density is very high (An et al., 2012), meaning that short distance dispersal occurs more periodically than in whitefly and thrip. Aphid within-crop dispersal may therefore be more disrupted by UV-attenuation, explaining the consistently reduced populations found on plants grown under UV-attenuation (Table 1.2).

1.2.5 Effect on birth rate

The effect of UV-attenuation on flight behaviour is well-established as a mechanism by which crop pest population size may reduced, however it is also possible that UV-attenuation may affect insect PGR in other ways. In two studies, the green peach aphid (*Myzus persicae*), when caged on individual leaves (excluding immigration and emigration), had slower PGR under UV-attenuated and partially UV-attenuated treatments, compared to a UV-transmitting control (Dader et al.,

2014; Paul et al., 2012). A third study indicated that birth rate of the green peach aphid was negatively affected by UV-attenuation (Chyzik et al., 2003), however their experimental design did not cage the insects and so immigration/emigration cannot be excluded. Dader et al. (2014) suggest that the effect of UVA on PGR may be due to both direct mechanisms - through direct damage of the insect by UVA-exposure - or indirect mechanisms mediated by changes in plant chemistry. In the silverleaf whitefly, growth of the host plants under UV-attenuated environments, prior to insect-infestation, increased PGR (Dader et al., 2014). UV-induced changes in plant chemistry may therefore be an important factor in insect PGR within protected crops, however few experiments have effectively separated the effect on birth/death rate through changes in host quality, from other extrinsic factors in UV-attenuation experiments.

1.3 Chromatic vision in insects

In the previous section, I identified a consistent, reduced preference for UV-attenuated light environments across a number of insect taxa. The most likely explanation is disruption to the insect visual systems involved in controlling dispersal flight, as suggested by a number of UV-attenuation experiments (e.g. Kigathi and Poehling, 2012; Legarrea et al., 2012c). In order to better understand these behaviours, it is important to place them in the context of the fundamental structure and function of the invertebrate visual system. As such, in this section I briefly review insect colour vision and its role in behaviour.

1.3.1 Introduction to insect visual systems

Visual perception may be divided into achromatic and chromatic perception. Achromatic vision (the perception of light and dark, independently of wavelength) is important for behaviours, such as measuring distance during flight (Giurfa and Menzel, 1997) and perceiving stimuli requiring a rapid response (Gao et al., 2008), whilst chromatic vision (the perception of different wavebands) has diverse roles in inter- (Döring et al., 2007; Dyer et al., 2012; Osorio and Vorobyev, 2008) and intra- (Imafuku, 2008) specific communication. Whilst chromatic and achromatic vision are structurally connected, with a large degree of overlap in the perceptive and processing mechanisms (Gao et al., 2008), this section focuses on the roles of chromatic vision. Light is perceived by photoreceptor cells located in the tubular structures of the insect eye called ommatidia (Figure 1.2). Ommatidia are formed of eight photoreceptor cells in most insects (Borst, 2009) and the differential expression of opsin (Matsumoto et al., 2014) and chromophore (Frentiu et al., 2007) genes provides the basic architecture for wavelength-sensitive (chromatic) perception. Chromatic (used interchangeably with 'colour') vision is simply the ability to discriminate between the relative intensities of two or more spectral bands, through the use of photoreceptors with different spectral sensitivity. The majority of insects have at least three, and as many as six distinct photoreceptor types (Briscoe and Chittka, 2001) which may be either broad or narrow-band receptors. Unlike primates, which have photoreceptors with peak wavelengths above 400 nm ($\lambda_{\max} = 420, 530, 560$, Nathans (1999)), most insects have three (trichromatic) sensitivity peaks: in the UV (< 400 nm), blue (400-500 nm) and green (500-570 nm). Additional longer wavelength (> 570 nm) sensitivity has been identified extensively in *Lepidoptera*, with many tetrachromatic species. Some *Hymenoptera* and *Coleoptera* were also identified as tetrachromates with additional long-wavelength sensitivity, however this was unusual (Figure 1.3). Considerable intra- and inter- species variability in photoreceptor peak wavelength exists due

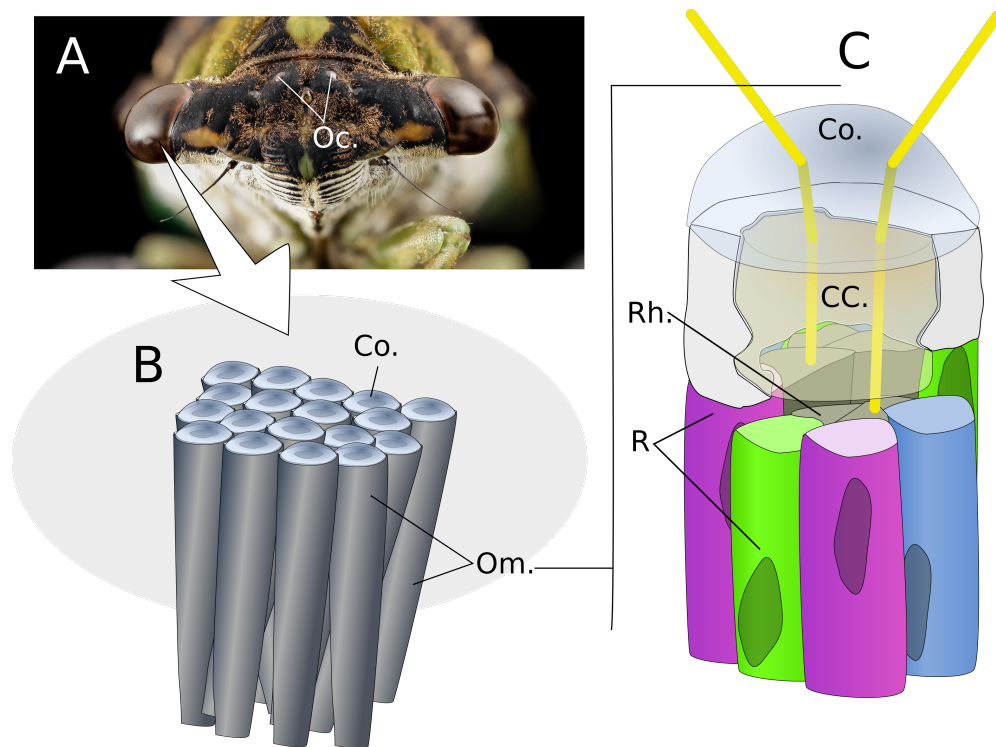


Figure 1.2: Diagram of insect visual structures, based on the images presented by Matsumoto et al. (2014). (A) Arthropods perceive light with compound eyes and ocelli (Oc.). (B) These eyes are formed of many tubular light-collecting structures called ommatidia (Om.), each of which has its own cornea (Co.). (C) Each ommatidium collects light using the cornea (Co.), which then passes through the crystalline cone (CC.). Photoreceptor cells (R) surround a central light-transmitting tube, the rhabdom (Rh.). This is formed from interlocking microvilli which contain the chromophores for photoperception. *Inset photograph: Sam Droege, used under the Creative Commons 2.0 license*

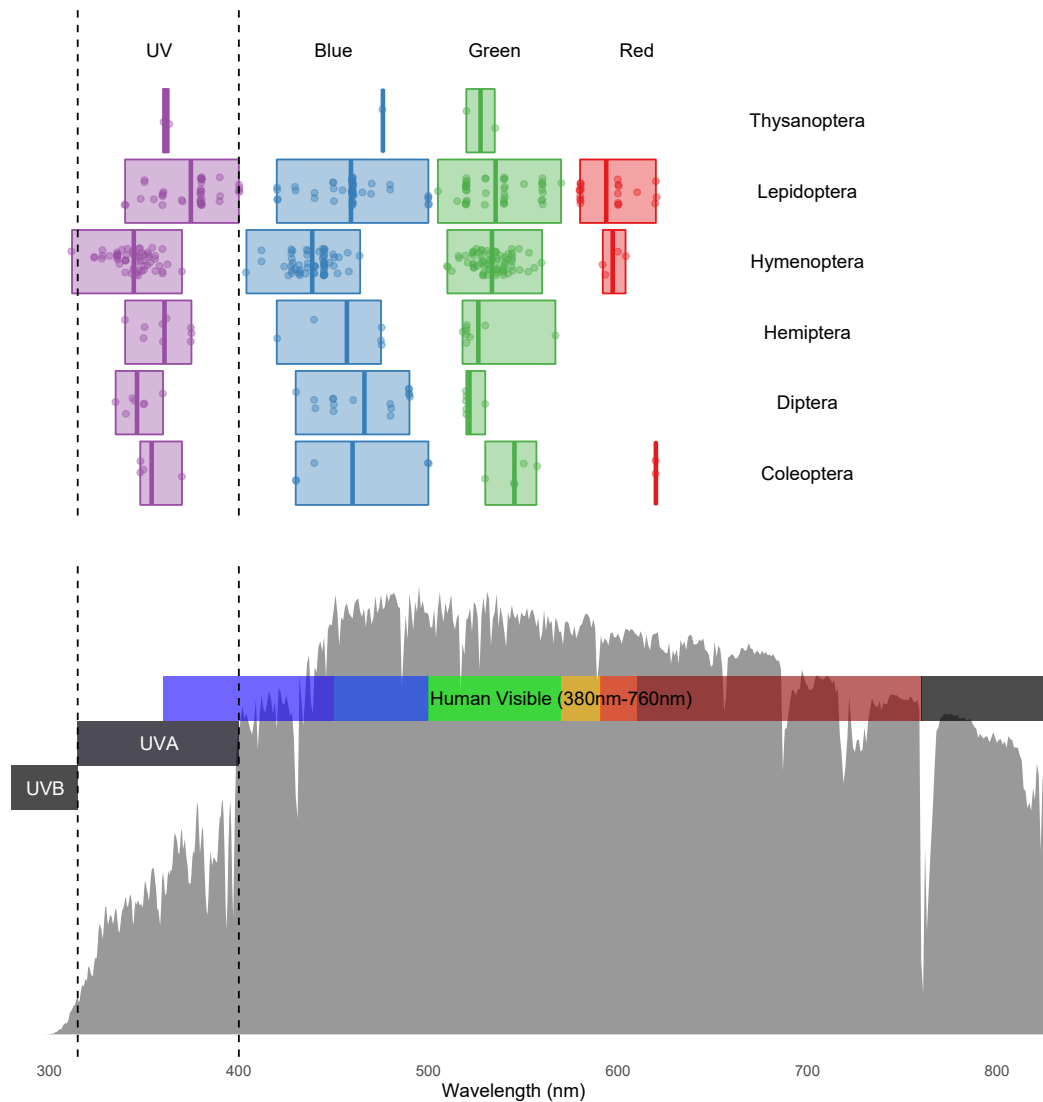


Figure 1.3: Diversity of spectral perception across insect orders, adapted from Briscoe and Chittka (2001). Individual points show the wavelength of peak electrophoretogram sensitivity recorded for an insect photoreceptor (λ_{max}). The boxplots represent the mean, minimum and maximum wavelengths of peak sensitivity for six insect orders. Colour indicates the approximate sensitivity waveband (purple = 300 - 400 nm, blue = 401 - 500 nm, green = 501-560 nm, red = 561 - 700 nm). The grey spectra shows a normalised standard solar spectrum (ASTM G173 Direct). Dashed lines show the upper (400 nm) and lower (315 nm) boundaries of the UVA waveband.

to diversity of genes controlling chromophore, opsin and crystalline cone (filters light before it reaches the photoreceptor, Figure 1.2) production, allowing diverse colour sensitivity to occur across evolutionary gradients (Briscoe and Chittka, 2001).

Photoreceptor sensitivity is strongly linked to the broad requirements of the insect to discriminate between host and non-host. For example, the honey bee (*Apis mellifera*) has a trichromatic colour space (colour space concepts discussed further in this section) which allows for much greater theoretical discrimination between flowers than would occur in the primate colour space (Osorio and Vorobyev, 2008). This is clearly important for identifying the correct host plant, in particular where species-specific mutualisms occur between plant and insect. Additionally, there is evidence that diversity in angiosperm colouration is evolutionarily driven by the fundamental limitations of the visual systems of their most important pollinators, the *Hymenoptera* (Dyer et al., 2012). Similarly, autumn colouration has been argued to have evolved by plants to signal their defensive status to herbivorous insects (Hamilton and Brown, 2001). Thus, the fundamental limits of photoreceptor sensitivity are important constraints for the co-evolution of plant-insect interaction.

1.3.2 Spectral balance and insect flight

Solar radiation may be perceived either directly (i.e. directly sensing the sun) or indirectly, when solar radiation is reflected off a surface. As such, modification of spectral balance can be considered both in terms of a change in colour of the illumination source and a change in the perceived colour of an object. Experiments using monochromatic light have shown UV light to be an important take-off cue to *Caliothrips phaseoli*, which flew towards UV sources when exposed on a non-host substrate (Mazza et al., 2010, data presented in Figure 1.4). Thrips did not respond to any other monochromatic wavelength in this experiment and so it appears that UV radiation acts as a proxy for the sun or open-sky. Similarly, the greenhouse whitefly and the folivorous thrip, *Scirtothrips dorsalis*, were attracted to UV light (Figure 1.4) in preference to blue light. Although the studies showed this to be a weaker response than their response to green light, neither study tested wavelengths below 350 nm, and so it is possible that the peak behavioural sensitivity was lower than 350 nm, as in the case of *C. phaseoli* which had a peak sensitivity at approximately 320 nm (Mazza et al., 2010).

Broadband UV light has also been shown to attract day-flying (Chu et al., 2005; Shimoda and Honda, 2013) and night-flying (Cowan and Gries, 2009; Sambaraju and Phillips, 2008) insects. The reason for this is not known but it may act as a reliable sky cue under many different light conditions, including moonlight (Barta and Horváth, 2004). Perceiving the ratio of green to blue light has been identified as offering the best contrast (and so most reliable discrimination) between ground and sky under cloud cover and through different times of the day (Möller, 2002). Additionally, polarised UV light from the sky offers a reliable indicator of unreflected sunlight and so can be utilised both under the canopy and under heavy cloud cover to permit the insect to orientate itself to the sky (Barta and Horváth, 2004). When UV was attenuated, flight behaviours were inhibited in folivorous insects (Kigathi and Poehling, 2012; Legarra et al., 2012a) however there is some indication that certain nectarivorous *Hymenoptera* are able to adapt to flight in UV-attenuated environments (Dyer, 2004). It is not known to what extent these more complex behaviours occur in other insect orders, however present evidence suggests that aphid, whitefly and thrip do not adjust to UV-attenuation (Table 1.2). As such, it is likely

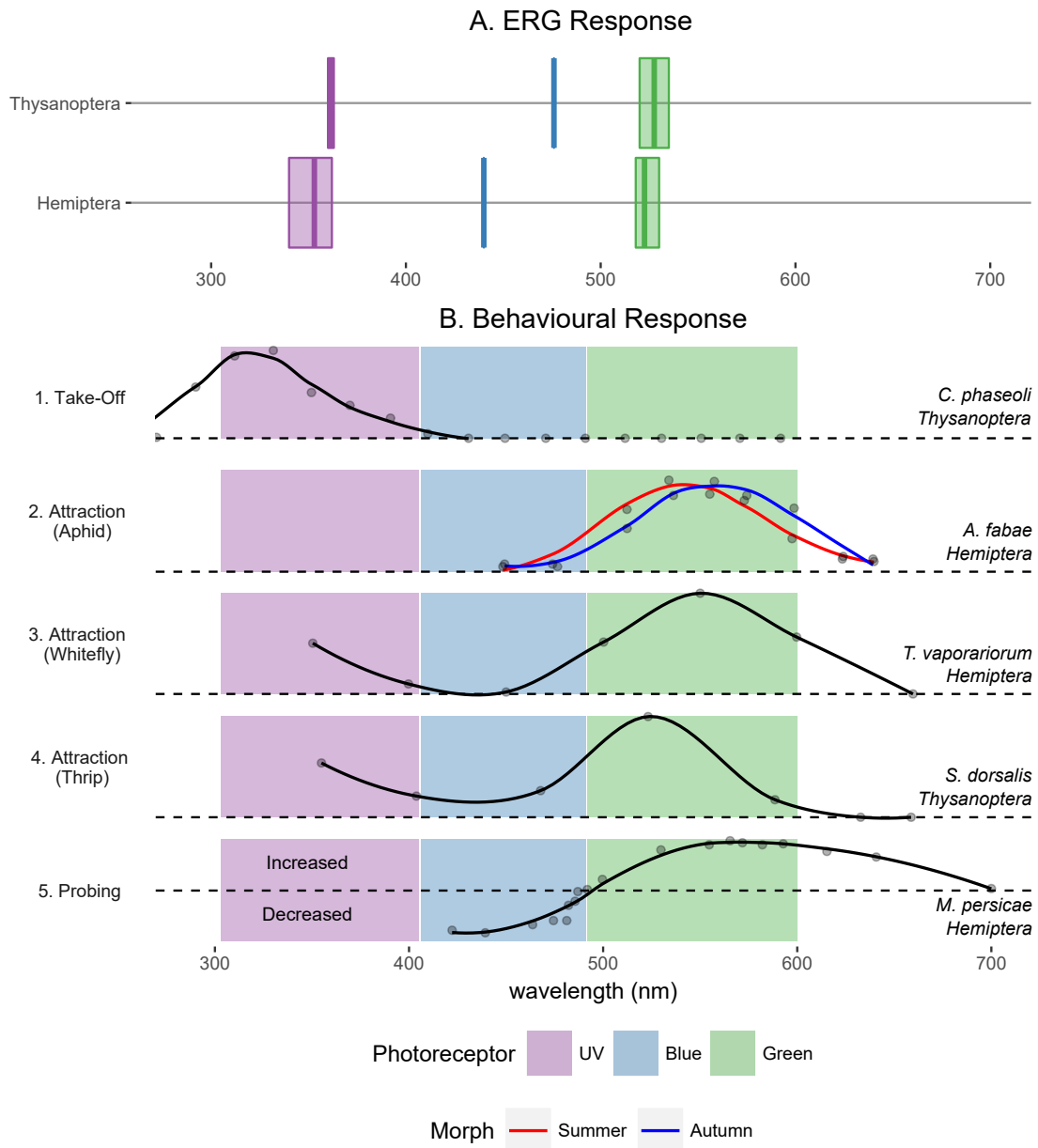


Figure 1.4: Photoreceptor and behavioural responses of *Hemiptera* and *Thysanoptera* to monochromatic light. (A) shows electroretinography (ERG)-derived mean and range photoreceptor peak wavelength sensitivity for *Hemiptera* (Sp.: *A. pisum*, *M. persicae*, *N. lugens*, *T. vaporariorum*) and thrips (*F. occidentalis*, *S. dorsalis*). (B) shows normalised plots of (1) take-off in thrips (Mazza et al., 2010), (2) attraction of aphids in flight (Hardie, 1989), (3) attraction of whitefly (Coombe, 1982), (4) attraction of thrips (Kishi et al., 2013), and (5) relative increase in probing activity of aphids (Döring et al., 2007). In B.2, line colour represents either summer or autumn dispersal (winged) morphs. Shaded boxes show approximate range of dominant photoreceptor in waveband. The dashed line represents a zero value which differs between experimental setup, but may be broadly interpreted as a null-response. For each subplot of B: (B.1): no take-off, (B.2)-(B.4): no attraction compared to an achromatic source of equivalent intensity, (B.5): equivalent attraction between target and achromatic source of equivalent intensity.

that insects are attracted to UV as a direct cue for the sun, and so attenuation of UV removes the stimulus needed to take off in the correct direction and maintain level orientation in flight.

1.3.3 Colour as a host cue

It is well established that pollinators use colour to identify host species (Osorio and Vorobyev, 2008), however less is known about the extent to which foliar-feeding insects use chromatic cues for host identification. Monochromatic green illumination sources and surfaces reflecting narrow-band green light were shown to attract and induce landing (Coombe, 1982) in aphid, whitefly and thrip (Figure 1.4). This was presumably a broad host-seeking behaviour, relying on contrast between green vegetation and non-plant surfaces which typically reflect proportionally more blue or UV (Möller, 2002). Experimentally, *Hemiptera* show strong preference for yellow targets with low UV reflectance (Doring et al., 2004). The study found the strongest positive correlation with attractiveness of coloured traps was with green reflectance and the strongest negative correlation was with UV reflectance, thus suggesting that insects seeking vegetation use the contrast between UV and green to identify hosts. Additionally, this preference may be species- (Doring et al., 2004) and morph- (Hardie, 1989) specific. Döring et al. (2007) propose that different species may use very subtle variation in colour to discriminate visually between host species, however very few aphid photoreceptors have been characterised with ERG techniques and so this hypothesis has not been extensively studied across species. The black bean aphid (*Aphis fabae*) showed slightly different colour preference between summer and autumn migrants exposed to monochromatic light (Hardie, 1989). This was hypothesised to be due to the red-shifted (more yellow, less blue) colouration of the overwintering host.

Monochromatic green illumination promoted aphid feeding behaviour (Figure 1.4), causing aphids to increase probing activity (Döring et al., 2007). In the same study, illumination with blue light had a negative effect on aphid feeding compared to illumination with an achromatic (white) source, and so blue light may be considered a feeding inhibitor. Short wavelength radiation was not tested in this study and so the probing response of aphids to UV is not known, however thrips were shown to respond to high UVB when feeding, moving preferentially to areas of lower UVB (Mazza et al., 1999). Therefore, for folivorous insects, green stimuli are generally associated with hosts, however blue and UV stimuli may also play inhibitory roles in feeding behaviours. It should also be noted that predominantly florivorous species are attracted to other colours, for example the Western Flower Thrip is preferentially attracted to blue sticky traps (Doukas and Payne, 2007) and white or pink inflorescences (McCall et al., 2013).

1.3.4 Moving from monochromatic experiments to a trichromatic model of insect vision

Experiments using monochromatic illumination sources (as shown in Figure 1.4) are useful in identifying peak behavioural sensitivity, however they are not representative of real-world, polychromatic illumination. Figure 1.4.A shows the ERG-derived peak sensitivity of photoreceptors located within thrip and aphid eyes which broadly align with the peak behavioural responses in .B and so behavioural responses may be linked with stimulation of different photoreceptors. Stimulation of the UV photoreceptor is associated with take-off, whereas stimulation of the green photoreceptor is linked to landing, settling and feeding behaviours. A polychromatic visual stimulus, such as sunlight reflected off a leaf, excites all three photoreceptor types. However due

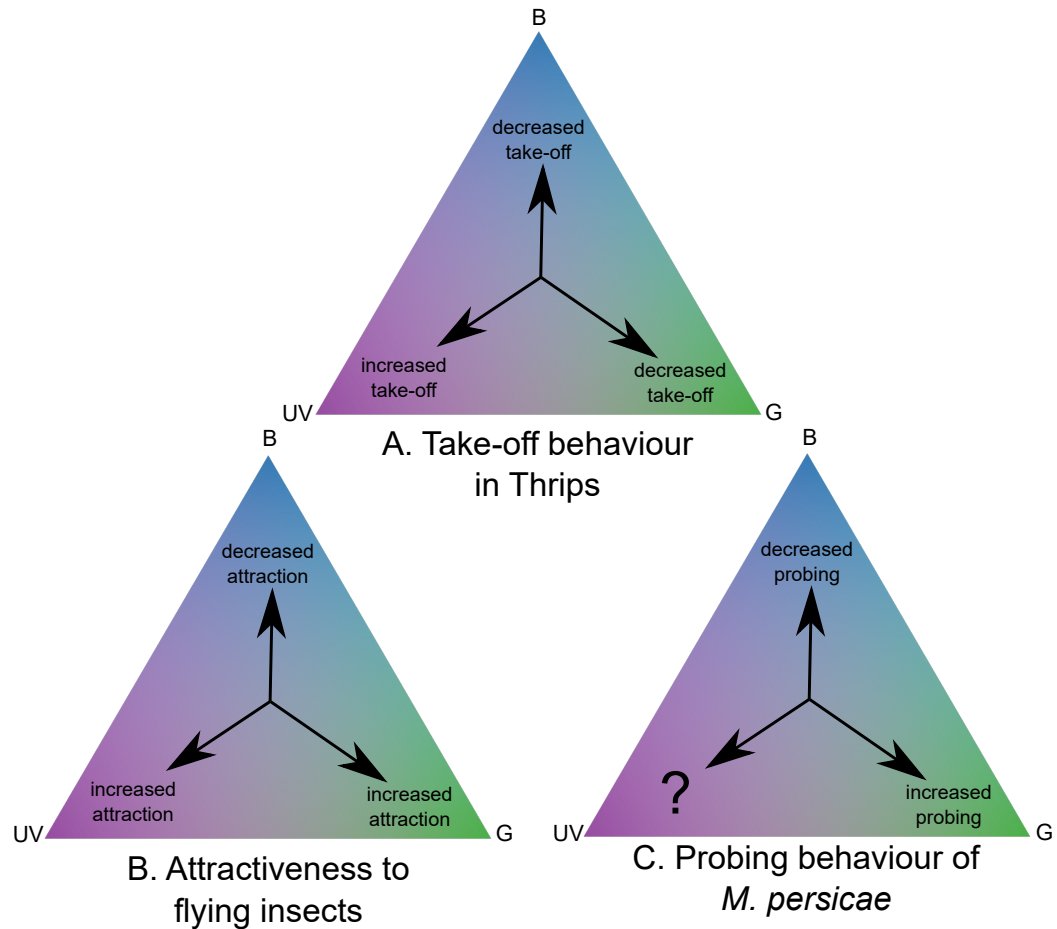


Figure 1.5: Colourspace diagrams for the behavioural responses identified in Figure 1.4. The three ternary plots have an axis for each class of photoreceptor in the insect eye and the arrows show the effect that movement in each of these axes is hypothesised to have on (A) take-off behaviour in thrips, (B) attractiveness to flying insects, and (C) probing behaviour in *Myzus persicae*.

to the different wavelength sensitivities of each, the three colour channels (UV, blue and green) are stimulated to different extents. The perceived colour of a visual stimulus may therefore be thought of as the relative stimulation of each photoreceptor type as a proportion of the total neural response (Döring et al., 2007). This may be represented in 3-dimensional space as in Figure 1.5 where the behavioural responses presented in Figure 1.4 were used to generate broad hypotheses in the colourspace models. For thrips on a non-host substrate, increased stimulation of the UV channel, compared to the blue and green channels is predicted to increase take-off (Figure 1.5.A). Whereas for flying insects, as the UV and green channels receive proportionally more stimulation compared to the blue channel, targets become increasingly attractive (Figure 1.5.B). Finally, as green channel stimulation is increased, proportional to blue channel stimulation, increased probing behaviours are expected (Figure 1.5.C). The behavioural response (whilst feeding) of increased UV channel stimulation in *M. persicae* is not known.

1.4 Indirect effects of UV exposure on insects

In section 1.2, large-scale field studies suggested that UV-induced changes in host plant chemistry may affect the birth and death components of insect PGR (Chyzik et al., 2003; Dader et al.,

2014; Paul et al., 2012). In this section I review the literature concerning UV-induced changes in plant phytochemical composition and identify the effect this may have on herbivores. Some studies linked both UV-induced changes in phytochemical composition with changes in invertebrate performance, however this was not always the case. For some classes of chemical, the effect of UV exposure on production, and the broad effect of the chemical class on invertebrates have been studied separately and so I synthesise these findings where possible.

1.4.1 Alkaloids and polyamines

Alkaloids and polyamines are grouped here as nitrogenous compounds with overlap in their biosynthetic pathways (Ghosh, 2000). Although their structures and syntheses are numerous, their toxicity and inhibition of herbivore feeding make them one of the most important plant anti-herbivore defences (Wink, 1992). There has been relatively little research conducted into the relationship between UV-induced changes in the concentration of different alkaloids and the effect which this may have on the feeding behaviours, mortality or fecundity of insect herbivores (Hectors, 2010), however given the importance of nitrogenous compounds in insect defence, the inter-dependencies of these mechanisms on UV should be considered (Hatcher et al., 1997).

Alkaloids from a number of plant taxa have been shown to play a role in UV photoprotection through their oxygen radical-scavenging properties (Hectors, 2010; Gregianini et al., 2003; Lydon et al., 2009). In *Psychotria brachyceras*, the alkaloid brachycerine increased by an order of magnitude in response to short wavelength UVB and ultraviolet-C (UVC) (Gregianini et al., 2003) and in *Erythroxylum novogranatense*, total truxilline concentration was greater in plants exposed to ambient UV compared to plants grown in the absence of UV (Lydon et al., 2009). Although it is difficult to draw comparison between ambient solar UV treatments (such as that delivered by Lydon et al., 2009) and treatments which include high doses of UVC (Gregianini et al., 2003), production of these antioxidant compounds is clearly linked to plant UV exposure.

Whilst alkaloids produced in response to UV exposure have antioxidant properties, these compounds have not been shown to affect herbivore reproduction or behaviour. A study using another member of the *Psychotria* genus (*Psychotria leiocarpa*) demonstrated that whilst N,-D-glucopyranosyl vincosamide had strong antioxidant activity and was therefore a likely component of the plant UV response, it was not an antifeedant for *Helix aspersa* or *Spodoptera frugiperda* (Matsuura and Fett-Neto, 2013).

Polyamine accumulation has been identified as transient and highly variable but increases are generally associated with the initial stages of UV acclimation (Hectors, 2010). Similarly, feeding of the aphid *Rhopalosiphum padi* stimulated an initial increase in poly- (putrescine and spermine) and mono- (tryptamine) amines in cultivars of a hybrid monocot (*Triticosecale*). After one week of aphid feeding, the overall polyamine content fell before again rising (Sempruch et al., 2012). *In vitro* polyamine supplementation of plant material provided some evidence that they are involved in herbivore regulation, causing reduced survival and growth of an aphid, *Sitobian avenae* (Sempruch et al., 2012) however the methods used were not sufficient to determine whether polyamines acted directly on the herbivores or as elicitors of other plant responses (Hussain et al., 2011). Considering the relatively transient presence of polyamines in response to biotic stressors, it would appear likely that their role is either in their capacity to produce anti-herbivore Reactive Oxygen Species (ROS) during the early stages of infestation or as a signalling component of the wider antiherbivore response (Hussain et al., 2011).

Although plant alkaloid and polyamine profiles are sensitive to both UV and herbivore attack, current evidence does not suggest an important functional overlap between plant responses to these two stressors. There is, therefore, little evidence to suggest that UV-exposed plants will be better defended against herbivore attack due to increases in antioxidant nitrogenous compounds, however future approaches which explore this link further are encouraged.

1.4.2 Glucosinolates

Glucosinolates are sulfur-containing glucosides which play a number of roles in mediating the interactions between cruciferous plants, herbivores and their natural enemies. As precursors to toxic isothiocyanates, they are a key part of the antiherbivore defensive system in crucifers. Additionally, they are used by a number of specialist herbivores as oviposition and phagostimulatory cues, are sequestered as defensive compounds by specialist aphids and act as tritrophic signals for natural enemies (Hopkins et al., 2009).

The effect of UVB on glucosinolate concentration in *Brassicas* is not clearly understood. An experiment using *Brassica oleracea* exposed to ambient UVB showed decreases in total indolyl glucosinolate concentration compared to UVB- controls (Kuhlmann et al., 2010). However a further study showed the opposite, with rapid increases in tissue aliphatic glucosinolates under supplementary UVB (up to one $\text{kJ m}^{-2} \text{day}^{-1}$) whilst slower (< 24 hours) increases were observed in indolyl glucosinolate concentration (Mewis et al., 2012). This study also demonstrated mixed responses in transcription of glucosinolate-related genes with up- and down-regulation occurring after UV exposure. Whilst these studies broadly describe total aliphatic and total indolyl concentration, it is likely that up- and down- regulation may occur simultaneously *within* these broad groups and that these responses are cultivar- and developmental stage- specific.

Other authors have shown increases in glucosinolate production with increased UVB exposure, but these have often used very high UVB doses ($> 46 \text{ kJ m}^{-2} \text{day}^{-1}$), or short wavelength UVC which is not present in sunlight and the findings should therefore be treated with caution (Schreiner et al., 2012).

Whilst the relationship between glucosinolate composition and the plant's interaction with higher trophic levels has been identified as highly complex (Kos et al., 2011), indolyl glucosinolates have been specifically linked to herbivore success in at least one study (Kim et al., 2008a). Generalist herbivores were negatively affected by high indolyl glucosinolate cultivars. However previous studies which showed UVB-induced reductions in indolyl glucosinolates also showed reduced aphid populations (Kuhlmann et al., 2010) compared to controls with higher indolyl glucosinolate concentrations. Therefore, whilst these compounds are undoubtedly important in plant defence, no simple relationship has been convincingly demonstrated between plant UVB exposure, increase in glucosinolate expression and subsequent decrease in herbivore population.

Changes in glucosinolate concentration may also play a role in the relationship between herbivore and natural enemy. The PGR of a specialist aphid *Brevicoryne brassicae* was shown to be positively affected by indolyl glucosinolate concentration in the plants. Higher concentrations of these compounds sequestered in the aphid was negatively correlated with predator success, although not with parasitoid success (Kos et al., 2012). As before, more work is needed to establish how this mechanism may interact with other competing effects of UV manipulation.

1.4.3 Isoprenoids

Carotenoids

Carotenoids are medium-sized isoprenoids (carotenes) and their oxygenated derivatives (xanthophylls) typically associated with plant colouration and high light protection. Whilst carotenes do absorb long wavelength UV and blue light, it appears that their major role in plants is protection of the photosystems via electron quenching of the chlorophyll molecules during high light stress (Solovchenko and Merzlyak, 2008). Xanthophylls are formed as part of cyclic processes which dissipate thermal energy and therefore also contribute to protection against high light. Carotenoid synthesis has been linked to exposure to UVA and blue light in *Brassica oleracea* (Bohne and Linden, 2002) whilst total carotenes in *Fagus sylvatica* (Laposi et al., 2009) and lycopene in the fruit of *Solanum lycopersicon* (Becatti et al., 2009) increased when plants were exposed to ambient UVB, demonstrating sensitivity to both UVA and UVB.

Plant-derived xanthophylls such as lutein may be used by herbivorous insects as UV photoprotectants. In at least one species of *Lepidoptera* (*Depressaria pastinacella*), larval UV-avoidance behaviour was negatively affected by the concentration of dietary xanthophylls. Insects which were fed higher doses of lutein chose increased exposure to UV (Carroll et al., 1997) and the sequestered concentration of lutein in wild individuals was positively correlated with the typical UV irradiances at the latitudes where they were recovered (Carroll and Berenbaum, 2006). Plant derived carotenes were also shown to be precursors to insect pigments, both in cryptic and aposematic colouration, and in the chromophores used in the visual systems of all animals (Heath et al., 2012).

Carotenoids may also be relevant in antiherbivore defence. Plants have been shown to convert carotenes into volatiles, known as apocarotenes; important natural enemy attractors in tritrophic signalling (Heath et al., 2012). However, as most of the work in this area has demonstrated a positive effect of dietary carotenoids (Carroll et al., 1997; Carroll and Berenbaum, 2006), it is likely that any increases in carotenoid production elicited by UVB exposure has little effect on tritrophic interactions.

Saponins and other Triterpene derivatives

The triterpene squalene is the precursor to saponins and phytosterols. Both positive and negative changes in triterpene concentration has been linked to UV exposure and there is some disagreement in the literature as to whether they are produced as part of the long-term UVB acclimation response (Gil et al., 2012) or as short-term mediators of oxidative stress associated with UVC and environmentally-unrepresentative UVB doses (de Costa et al., 2013). In *Vitis vinifera*, increases in leaf sitosterol, stigmasterol and lupeol were observed under field-representative doses of UVB (4.75 kJ m⁻² over 16 hours) (Gil et al., 2012). Similar doses applied to the tropical plant *Quillaja brasiliensis* showed no significant change in triterpene concentration however an effect was seen when a 'high stress' UVC treatment was applied (de Costa et al., 2013).

Saponins have a well documented negative effect on the mortality of herbivorous insects and their production is known to be sensitive to insect feeding. The saponins hederogenin cellobioside and oleanolic acid from the crucifer *Barbarea vulgaris* were identified as the strongest influences on mortality of *Phyllotreta nemorum* (Kuzina et al., 2009). Further work on *B. vulgaris*

identified the saponin biosynthetic pathway and candidate transcription factors which were also activated by feeding of *Plutella xylostella* (Wei et al., 2013). In *Medicago sativa*, saponin concentration was higher in plants which had been subjected to feeding by *Spodoptera littoralis* larvae (Agrell et al., 2003). In the same study, a 14% reduction in larval mass was observed in insects fed on previously challenged plants compared to feeding on undamaged plants.

Considering the important role saponins have in the protection against herbivores, UV-controlled changes in composition or concentration are likely to be important predictors of herbivore success, however more work is needed to establish the magnitude and direction of the response across species.

Volatile Terpenes

The volatile terpenes form a large proportion of the functional group termed Volatile Organic Compounds (VOCs). These are small polymers with lipophilic properties which allow them to move readily across cell membranes and into the air surrounding the plant. This allows them to act as chemical messages to other organisms ('kairomones') whether that is pollinators, herbivores or natural enemies of herbivores (Dudareva et al., 2013). Additionally, every major insect Order uses plant volatiles or their precursors for inter- or intra-specific signalling. These are obtained during feeding and may be modified or sequestered intact before release as alarm, aggregation or sex pheromones (Müller et al., 2011).

Short-term UVB exposure of plants after growth in a UVB-deficient environment was generally linked to increased volatile terpene production. Exposure in growth chambers showed increases in volatile terpene production in *Mentha piperita* (Dolzhenko et al., 2010) and *Vitis vinifera* (Gil et al., 2012), however both of these experimental approaches relied on the use of plants which had not been grown in the presence of UVB. Although the doses were field-relevant, the plants were exposed to relatively high UVB irradiances with no acclimation. The responses may therefore be somewhat different to the responses which might be expected had the plant been grown under UVB from germination, as in typical UVB removal field experiments.

Where field exclusion methods were used, the pattern of VOC emission was less pronounced where some species showed either small increases (longifolene in *Daphne gnidium* (Llusia et al., 2012)), no change (overall volatile terpene content of *Mentha piperita* (Dolzhenko et al., 2010)) or even a decrease (α - and β - pinene in *Pistacia lentiscus* (Llusia et al., 2012)). The differences in response to field compared to growth chamber was reflected in different gene expression patterns: whereas high irradiance, short-term exposure of unacclimated plants may have elicited an antioxidant stress response—it has been suggested that volatile terpenes are involved in ROS scavenging and thylakoid stabilisation (Gil et al., 2012)—chronic UV exposure likely lead to prioritisation of production of more typical UV-induced photoprotectants at the expense of volatile terpene synthesis.

The role of plant volatiles, especially small terpenes, in insect-insect and insect-plant communication has been reviewed extensively by Müller et al. (2011) but the potential influence of UVB on this system has been little-studied. VOC emission from *Picea abies* was not affected by UVB exposure, however when the plant was exposed to the herbivorous beetle, *Hylobius abietus*, VOC emission increased (Blande et al., 2009). As with the carotenoids, there is no consistent relationship between environmental UVB exposure and change in emission. It is likely that any volatile used as a tritrophic feeding cue (i.e. an attractant to predators and parasitoids) would need to

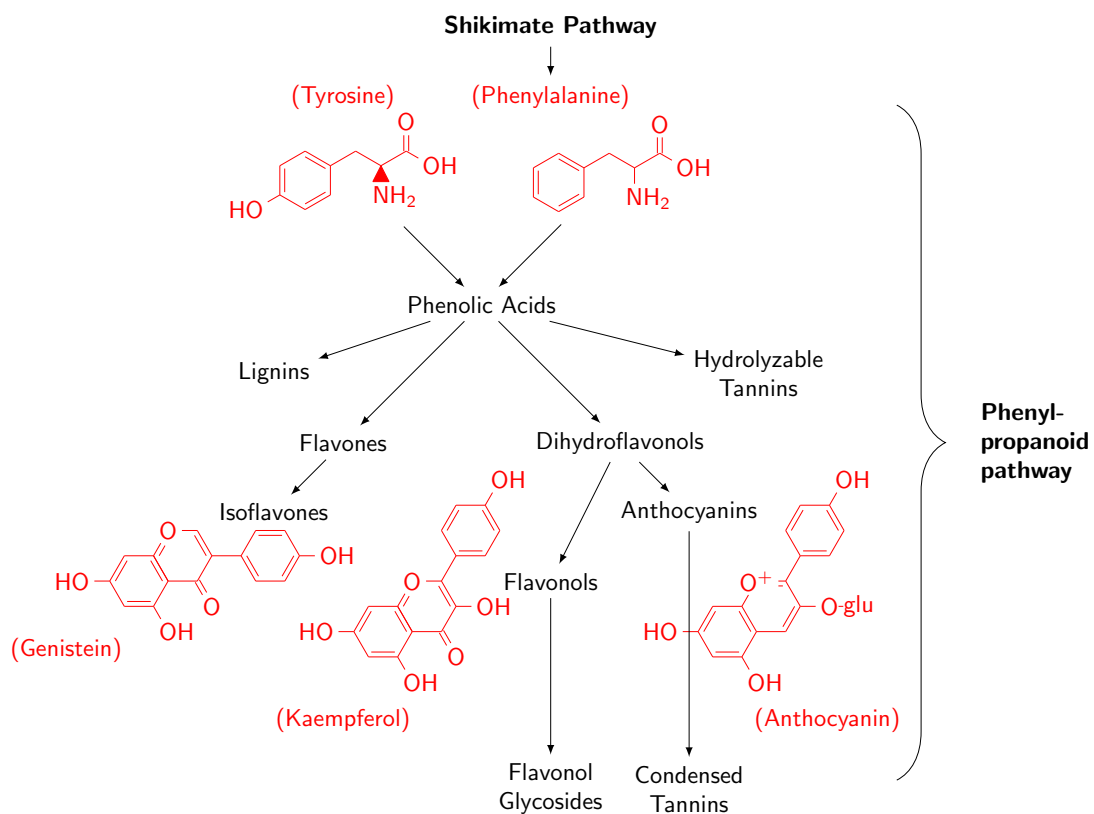


Figure 1.6: Simplified phenyl-propanoid pathway

be insensitive to UV exposure in order to prevent ‘false alarm’ messages being released during periods of high UVB exposure, but no herbivory. Therefore mechanisms such as that described by Blande et al. (2009), where there is little or no overlap in the UV- and herbivore- initiated VOC synthesis mechanisms, are expected to be the most common.

1.4.4 Phenolics

Plant phenolics are a large and varied class of plant secondary metabolite, characterised by the presence of one or more phenol group. All are derived from the amino acid phenylalanine which is synthesised via the Shikimate pathway from C₃ and C₄ carbohydrate derivatives. Synthesis then occurs via the phenylpropanoid pathway (figure 1.6) where the phenolic acid, p-coumarate, is converted into lignin precursors (Hydroxycinnamic acids such as caffeic, ferulic and sinapic acid), flavonoid precursors (Chalcones) or isoflavonoid precursors (Meijkamp et al., 1999). Whilst there are many molecular species in the phenolic pathway, the terminal products predominantly exist as glycosides (such as the flavonol glycosides and anthocyanins). Perhaps the most well known group are the flavonoids; compounds based on a 3-ring phenolic (C₆C₃C₆) framework in either monomer or polymer form (Sisa et al., 2010). This large group includes the anthocyanidins, flavonols, flavones and their respective glycosides.

Anthocyanins

Anthocyanins are glycosides (most commonly glucosides) of anthocyanidins and are responsible for much of the dark blue through to red pigmentation in flowers, leaves and stems (Close

et al., 2003). Whilst it is accepted that UV induces the biosynthesis of anthocyanins, large accumulations in palisade and spongy mesophyll cells - compared to the epidermal cells where the majority of UV light is absorbed - has led to speculation that they are not used for UV absorption in mature leaf tissue (Close et al., 2003). However, studies have shown that anthocyanins in young leaves have strongly UV-absorbing properties and their distribution in expanding leaf tissue offers protection against UV-induced photoinhibition (Domingues et al., 2012; Fondom et al., 2009; Woodall and Stewart, 1998).

The roles of anthocyanins in antiherbivore defence are difficult to identify as genes identified in the biosynthetic pathways of anthocyanins typically have a high degree of pleiotropy with other flavonoids (Schaefer and Rolshausen, 2006). *Nicotiana tabacum*, expressing an *Arabidopsis thaliana* transcription factor (AtMYB75/PAP1) known to be responsible for anthocyanin production, was fed to lepidopteran tobacco pests in choice and no-choice assays (Malone et al., 2009). Larval growth rate (*Helicoverpa armigera*, *Spodoptera litura*) and larval survival (*H. armigera*) were lower for individuals fed on plant material from the anthocyanin-expressing mutant. Although this might suggest an inhibitory effect of the anthocyanin, there were also increases in leaf tissue concentration of caffeic acid and its derivatives, known to have a suppressive effect on survival in dietary supplementation experiments, making the results hard to interpret.

Anthocyanins are likely to be most important in host-herbivore signalling. In a feeding assay, feeding rate and larval growth rate were low on a solid purple leafed phenotype, compared to both the purple-veined phenotype (which had higher anthocyanin concentrations than the wild type) and the wild-type green phenotype (Johnson and Dowd, 2004). There was no difference in survival between larvae reared on the purple-veined and green phenotypes, indicating a likely antifeedant effect rather than a response to the toxicity of anthocyanins. *Lepidoptera* that typically feed on green foliage have also been shown to identify and selectively feed on green leaf tissue (low in anthocyanin) over anthocyanin-pigmented leaf tissue, even though larval survival was little affected by feeding on anthocyanic leaf tissue compared to green tissue of the same plant (Markwick et al., 2013). Therefore it is likely, as proposed by Close et al. (2003) and termed the Defence Indication hypothesis by Schaefer and Rolshausen (2006), that a major role of anthocyanins in herbivore defence is in the visual cues which they provide to herbivores, indicating the likely phenolic status of the plant. Anthocyanin expression is typically — although not universally (Hughes et al., 2010) — associated with high concentrations of other phenolics which have a negative impact on survival. Anthocyanins are thought of as ‘red’ pigments in human colour perception, however many insects lack photoreceptor sensitivity to red light and so are unable to discriminate long wavelength colour. However anthocyanin-rich tissue also reflects proportionally less green light than tissue with low concentrations of anthocyanin, whilst the reflectivity of blue light remains unchanged (Gitelson et al., 2009). As such, insects with green- and blue-sensitive photoreceptors may perceive this relative decrease in the green:blue ratio and respond by showing reduced feeding effort or attraction (Döring et al., 2007). Therefore, as the mechanism of repulsion is likely a visual one, exposure of anthocyanin-expressing crop species and cultivars to UV will be important for maximum induction of signal colouration which acts as a pre-contact repellent of pest insects.

Flavonols, Isoflavonols and their Glycosides

Flavonols and isoflavonols, known widely for their antioxidant activity (Pollastri and Tattini, 2011) have been shown to deter feeding and inhibit fecundity in a number of aphid species. Lat-

tanzio et al. (2000) identified that cultivars of *Vigna unguiculata* high in flavonols and isoflavonols (quercetin, kaempferol and isorhamnetin) were often designated as resistant cultivars. When phenolic content was manipulated *in vitro* by introducing methoxylated phenolics into excised leaf material, a range of phenolics were shown to have an inhibitory effect on larval deposition of *Aphis fabae*. This was verified *in vivo* where larval deposition was lower in chemotypes high in the flavonols quercetin and isorhamnetin. Exposure to near-ambient UVB has been shown to increase total leaf flavonols and their corresponding flavonol glycosides in a number of species (Josuttis et al., 2010; Kuhlmann et al., 2010; Ryan et al., 2001). Kuhlmann et al. (2010) showed that exposure to near-ambient UVB increased the concentration of quercetin and kaempferol in phloem compared to UVA-only exposure. Whilst plant UVB-exposure had a negative effect on birth rate in the specialist aphid *Brevicoryne brassicae*, the generalist aphid *Myzus persicae* was unaffected by UV exposure, probably because other *Brassica* defensive mechanisms (e.g. glucosinolates, see above.) had a strong negative effect on birth rate.

Not all interactions between plant-produced flavonols and herbivores had negative implications for the herbivore. In at least two species of *Lepidoptera* (*Bombyx mori* and *Polyommatus icarus*) larvae sequestered derivatives of kaempferols and quercetins, either directly or through conversion into other flavonol glycosides (Simmonds, 2003). These relationships were often highly specialised with different derivatives of the same flavonol acting very differently (Simmonds, 2003). Therefore, UVB-induced changes in the relative concentration of different flavonols may particularly affect specialists and, potentially, their ability to defend against predation.

Flavones, Isoflavones and their Glycosides

Closely-related to the flavonols, some flavones and isoflavones have been shown to have similar antifeedant properties. In an artificial media experiment, elevated concentrations of the flavone, luteolin, and the isoflavone, genistein, reduced the duration of salivation and ingestion behaviours in *Acyrtosiphon pisum*, indicating that these compounds are detected by, and likely harmful to, this species (Golawska et al., 2012a). However, the exact behavioural response is dependent on both the pest species and the identity of the compound: some flavones, such as 4-Hydroxywogonin had no effect on feeding behaviour whilst others, such as acacetin, seemingly affected certain species but not others (Castillo et al., 2013). Whilst total flavonoids increased with UVB exposure (Harborne and Williams, 2000), flavones have more complex expression patterns. In one study, the overall flavone glycoside concentration did not change with UVB exposure, however the luteolin:apigenin glycoside concentration significantly increased (Markham et al., 1998). Thus, the effects of UVB on herbivores, mediated via the flavone biosynthetic pathway, is hard to predict and likely to vary widely between different plant species and their various generalist and specialist herbivores.

1.5 Summary and project aims

Experiments using spectrally-modifying claddings have consistently identified a negative trend in the overall (incorporating direct and indirect effects) PGR of aphid, whitefly and thrip in tunnels clad with UV-attenuating claddings (section 1.2). The effect on extrinsic factors (immigration and emigration) appear to be the dominant mechanisms, with experimental evidence for (i) reduced movement into low UV environments (section 1.2.2) and (ii) reduced preference for low

UV environments in dispersing insects (section 1.2.3). There is also some evidence that disruption to insect vision, caused by UV-attenuation, results in spatial aggregation within tunnels (section 1.2.4). This was due to the use of UV perception in flight as a direct cue for the sun (section 1.3.2). When UV was removed, insects did not take-off, even when exposed to wavelengths associated with host plants. I therefore conclude that UV is a critical component in the long distance dispersal behaviours of aphid, whitefly and thrip.

Most of the work in this area focused on *Hemiptera* and *Thysanoptera* and so little is known about the effect of UV-attenuation on other orders, however there is some indication that UV-attenuation also inhibits the spread of *Diptera* and *Coleoptera* (Table 1.2). The effect of UV-attenuation on *Lepidoptera* is largely unknown, however most species have more advanced visual processing requirements than *Hemiptera* and *Thysanoptera* (e.g. locating nectar sources, correctly identifying mates, etc.) and so their vision may be less susceptible to UV-attenuation. Additionally, many commercially-relevant pest species are predominantly night flying (section 1.3.2) and so may be less reliant on visual cues for flight. As such, applications for the use of spectrally-modifying claddings are most appropriate as an IPM tool for control of aphid, whitefly and thrip and it is in these species where future investigative work should concentrate.

Whilst control of immigration and spread within a crop had a strong effect on limiting PGR, there was some evidence of a second mechanism by which UV-attenuation affected insect PGR. In a number of cases, immigration was shown to be reduced by UV-attenuation, however overall thrip and whitefly PGR within the tunnels was unaffected (Table 1.2). UV-attenuation also appeared to have a variable effect on birth/death rate when extrinsic factors were controlled for (section 1.2.5). These findings suggest that there is a secondary mechanism controlling overall PGR in tunnels which is linked to UV exposure, but is not due to insect behaviour. As UV (especially UVB) is known to affect many plant processes which interact with herbivore defence (section 1.4, since reviewed by Ballaré (2014)), it is to be expected that spectral modification in the UV will affect the plant phytochemical composition and that this will affect feeding herbivores. Across a wide range of plant taxa, there were many species-specific responses to UV-exposure and extensive evidence of UV-induced changes in the concentration of these compounds which have roles in both photoprotection and herbivore defence (section 1.4). Particularly important chemical classes for UV-induced herbivore defence are the isoprenoids (including carotenoids, section 1.4.3) and phenolics (section 1.4.4), and so any plant-herbivore interactions which are strongly influenced by these chemical classes are likely to be affected by UV exposure.

I identified two major areas in which spectral modification is likely to have an effect on insect PGR: (i) the direct effect on the insect, through manipulating dispersal and host-finding behaviours, and (ii) the indirect effect on the insect, through the interaction between UV-exposure and herbivore defence. The applied research community has established a strong basis for the use of UV-attenuation to control dispersal behaviours, however little is known about the indirect effects (plant-mediated) of UV-attenuation on the birth or death rate of insects under UV-attenuated light environments. Whilst some small-scale laboratory studies had been conducted by the fundamental research community, predominantly testing the effects of UV-supplementation of plant material on *Lepidoptera*, very little was known about the effects of UV-attenuation on phloem-feeding insects.

Given the established scope of the project (section 1.1) and the findings of this introductory chapter, the initial aims of the project were:

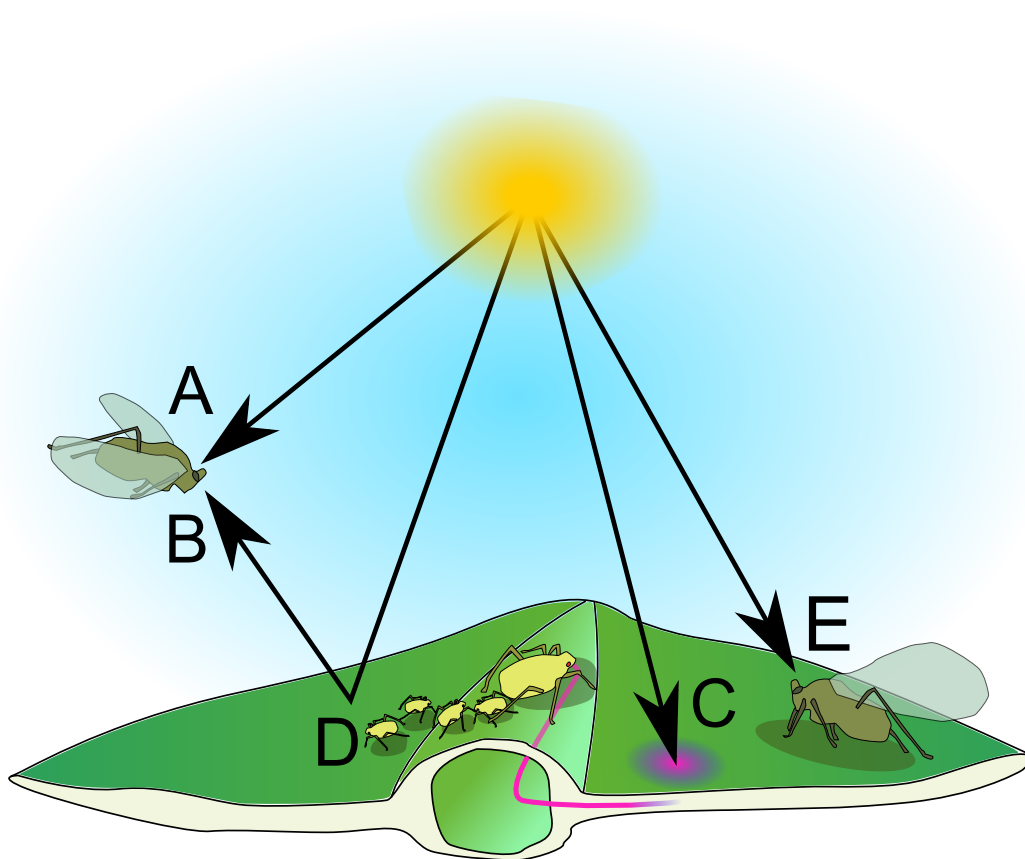


Figure 1.7: Effects of light on aphids. During dispersal flight, UV light (A) is used to orientate flight. Green light reflected from vegetation (B) attracts dispersing aphids which land on the plant material. Plant chemistry is affected by spectral balance (C) and this can affect birth and death (D). When alates are produced, these use UV as a take-off cue for secondary dispersal (E).

1. To establish a model system using a phloem-feeding pest (Order:*Hemiptera*) for experimental work testing the effects of UV-attenuation on birth and death rate.
2. To assess the relative importance of UV in mediating plant defence against phloem-feeding pests (indirect), compared to other mechanisms (indirect) by which UV may affect their population growth.
3. To utilise methods applicable to protected cropping practice (i.e. attenuation of solar UV rather than UV supplementation).
4. To synthesise the findings of experimental work in the context of both the fundamental and applied literature, in order to produce new hypotheses for the methods by which selective UV-attenuation may act in a suppressive capacity against phloem-feeding pests.

General Materials and Methods

2.1 The experimental system

In the general introduction, I identified a need to develop a robust system for testing the effects of ultraviolet (UV)-attenuation on a model phloem-feeding herbivore. *Myzus persicae* has been identified as a commercially-important pest in protected cropping (Legarra et al., 2010), used extensively as a model in UV-manipulation experiments of *Hemiptera* (Kuhlmann et al., 2009, 2010; Mewis et al., 2012; Paul et al., 2012), and identified as a polyphagous aphid capable of feeding on more than 400 plant species (Zhang et al., 2016). In comparison to other aphids, the visual sensitivity and visual ecology is somewhat better understood: the photoreceptors have been characterised using electroretinography (ERG) (Kirchner et al., 2005) and probing activity, in response to colour, measured (Döring et al., 2007). As such, *M. persicae* was an obvious choice as an aphid model for investigating the effects of UV on aphid population growth. *Brassica oleracea* had been previously used for the study of UV on the interaction of *M. persicae* with its host (Mewis et al., 2012; Kuhlmann et al., 2010) and so was chosen as the host plant for use in initial experiments.

2.1.1 The glasshouse environment

Glasshouses were located at the Lancaster Environment Centre (54.04°N, 2.80°W). Each glasshouse had a floor area of approximately 4 m × 4 m. Temperature was partially controlled by temperature-controlled passive ventilation, thermal blinds and heating. Over the course of the glasshouse practical work undertaken between February 2014 and January 2016, the mean (\pm one standard deviation) temperature was $22.4 \pm 5.0^\circ\text{C}$ and relative humidity was $43.5 \pm 13.4\%$. Supplementary lighting was supplied by eight sodium lamps until January 2015 and then by eight Senmatic FL300 Sunlight Light-Emitting Diode (LED) units to maintain a daytime total irradiance of at least 115 W m^{-2} . Measured maximum Photosynthetically-Active Radiation (PAR), ultraviolet-A (UVA), and ultraviolet-B (UVB) irradiances were 225.7 W m^{-2} , 14.9 W m^{-2} , $< 0.01 \text{ W m}^{-2}$ respectively (Figure 2.1). For experimental work and maintaining insect stocks, a day:night photoperiod of 16:8 hours was used.

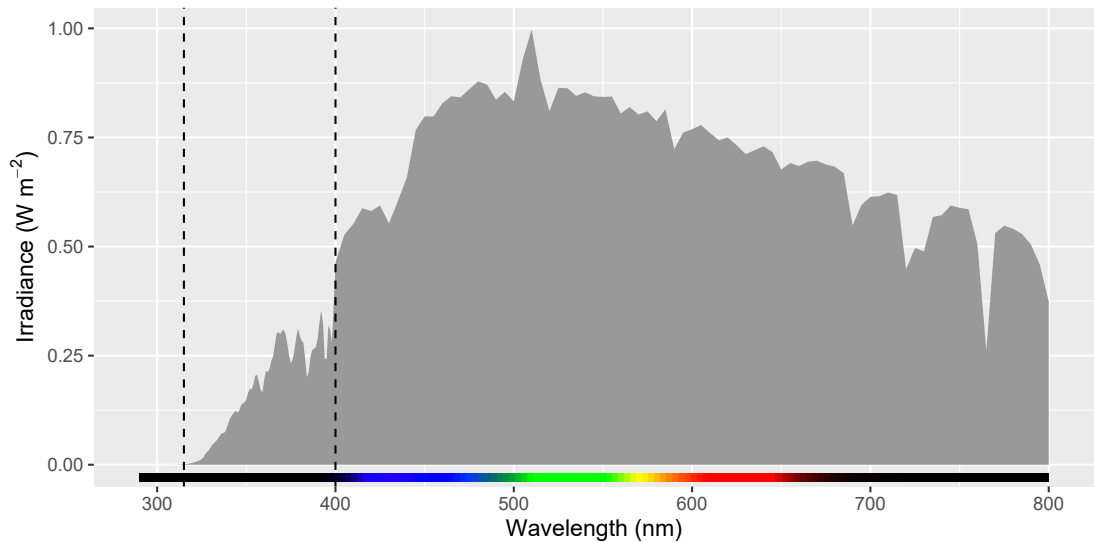


Figure 2.1: Measured irradiance at plant growing level inside the glasshouse at Lancaster University. Measurement was made in mid-August at approximately solar noon when the sun was un-obscured by clouds. Dashed lines show the lower and upper limit of the UVA waveband (315 nm and 400 nm).

2.1.2 Life-cycle and characteristics of *Myzus persicae*

Myzus persicae, like many heteroecious aphid species, has a complex life cycle (Irwin et al., 2007). In early spring asexual winged females hatch from overwintering ova and move from the winter hosts (*Prunus spp.*) to a diverse range of summer host plants. These asexual winged females give birth to asexual wingless females and subsequently, rapid population growth occurs. As the colony increases in size and the relative aphid density increases, production of asexual winged ‘dispersal morphs’ occurs (Irwin et al., 2007). In *M. persicae*, this is triggered by a reduction in phloem quality and, to a lesser extent, spatial crowding (Müller et al., 2001). These dispersal aphids make short flights, or may even walk, to new host plants in close proximity where they produce more asexual wingless females (Irwin et al., 2007). This is distinct from the autumn migration, where production of winged males and winged sexual females occurs, allowing the population to move back to the primary hosts (*Prunus spp.*) and undertake sexual reproduction. This process is triggered by reduced day length (Searle and Mittler, 1982), moderated by a generational “interval timer” (Margaritopoulos et al., 2002).

During the asexual component of the life cycle of *M. persicae*, individual fecundity and longevity may be heavily influenced by a number of biotic and abiotic factors, however for a colony reared at a typical glass house temperature of 25°C on chinese cabbage (*Brassica rapa*), the intrinsic rate of increase (population growth rate) was between 0.23 and 0.36 aphids/aphid/day (Davis et al., 2006). In the same study, the mean generation time was between 9 and 14 days.

2.1.3 Rearing and use of *Myzus persicae*

Myzus persicae (Sulzer) was used throughout the experimental work from a colony held at Lancaster University and originally collected locally. Aphids were reared on the *B. oleracea* cultivar currently being used for the experimental work (Derby Day, Volta or Zen, as described above). Stock plants were reared as described above but were potted into larger pots at four weeks to lengthen the duration on which the culture could be kept on them. Aphids were kept in mesh

tent cages (0.5 m × 0.5 m × 0.5 m) on three to five stock plants per cage. Cages were located on benches within the experimental glasshouses and were therefore under the same climatic conditions as the experimental plants for each experiment (see above for details). New stock plants were added and old or damaged plants were removed every two weeks. The 16:8 hour day:night regime ensured the aphid culture remained in its summer state with asexual female apterous aphids produced continuously and asexual female alate aphids produced when the colony was placed under mild stress by reducing the interval between plant replacement.

Apterous (wingless) aphids of a similar size and pigmentation were selected for experimental work. Whilst this guaranteed that all aphids were asexual females (males are relatively easy to differentiate), separation of immature asexual winged females from wingless females was difficult because immature winged females also lack wings and so are easy to mistake for wingless females. Later instars are more easily differentiated by visual patterning on the back (lighter colouration around the perimeter of the abdomen in winged immatures) and so were more easily avoided. Therefore, to control for this during experimental work, later instar aphids were used and, in order to reduce the proportion of alates in the stock culture, host plants were replaced regularly (maintaining lower population density reduced alate production (Müller et al., 2001)).

2.1.4 Cultivars and growing procedure

A number of cultivars of *Brassica oleracea* were used throughout the experimental work. The cabbage cultivar ‘Derby Day’ (supplied by Nickys Nursery Ltd. Fairfield Road, Broadstairs, Kent. CT10 2JU) was used in the initial field experiments. A calabrese, ‘Volta’ (supplied by Nickys Nursery Ltd. Fairfield Road, Broadstairs, Kent. CT10 2JU) was selected for polytunnel field experiments and mortality assays due to a more open leaf structure during early growth stages (no head formation). This cultivar was chosen because of its wide range of sowing dates (and so presumed tolerance to a wide range of temperatures), moderate *Botrytis* tolerance and green foliar material. Due to supply problems, experimental work was moved to a second cultivar of calabrese, ‘Zen’ (supplied by Tozer Seeds Ltd. Pyports, Downside Bridge Road, Cobham, Surrey, KT11 3EH), for the behavioural experiments. This cultivar had similar sowing requirements and appearance to ‘Volta’.

Seeds were sown at 0.5 cm depth in Levington’s M3 high nutrient compost (supplied by LBS Worldwide Ltd, Standroyd Mill, Cottontree, Colne, Lancashire BB8 7BW) and allowed to germinate under perspex propagator hoods in the glasshouse. Depending on experiment, polystyrene module trays (field experiments, behavioural experiments) or transparent polypropylene cups (mortality experiments) were used to contain individual plants. Three seeds per container were sown and all but one seedling were removed a few days after germination. Containers were grouped in plastic trays which allowed proper drainage. Plants were well watered with tap water and no fertilisation was applied due to the high nutrient content of the substrate and short duration of the experiment.

2.2 Experimental polytunnel field site

Whilst latter stages of this project used small, typical, plant science laboratory facilities and growing environments to dissect the mechanisms of aphid responses to UV, the initial work was

concerned with identification of broad aphid population responses to both current commercial and prototype light environments in small scale field experiments. These experiments necessitated the design and construction of a suitable field site to test horticultural films, allowing sufficient replication for experimental power in addition to simple management and usability. The following section describes the design and layout of the site.

2.2.1 Design principles

1. **The field site allows sufficient replication of up to four prototype plastics.** Previous studies on the effects of UV-attenuation on insect populations often had limited true replication, with a number of studies using only one (Legarrea et al., 2012b,a) or two (Doukas and Payne, 2007) simultaneous structure replicates per treatment. Although these previous studies have used replication within the light treatments (i.e. within tunnels), a preferable approach is to have replicate tunnel structures organised in a randomised block design, as used by Antignus et al. (2006). This approach controls for any spatially-determined covariance of the site, such as temperature, humidity or shading. During the planning phase of this research project, four horticultural polyethylene (PE) film claddings of interest were identified, based on their spectral properties. Therefore, with four treatments and a minimum replication of three per treatment, the minimum number of structures needed was 12.
2. **The structures should be structurally sound and adequately support the film claddings.** Lancaster is subject to occasional strong winds and so any external structures should be suitably anchored with ground anchors and strong enough to resist moderately high winds. Additionally, the films should be supported far enough from the experimental plants and cages such that if they are changed midway through an experiment, this will not affect the experimental plants.
3. **The structures allow some ventilation to prevent excessive temperatures and maintain lower relative humidity.** High humidity is favourable to the propagation of some fungal pathogens. Additionally, very high air temperatures are also considered unfavourable for plant development.
4. **The user should be able to work within the tunnel structure.** Many experiments require *in situ* measurements to be made (such as aphid counts, chlorophyll fluorimetry etc.). Removal of the plants from the experimental light environment may stimulate physiological changes and so should be minimised where possible. Similarly, movement of plants with resident insect populations may cause their dislodgement and subsequently affect their survival or Population Growth Rate (PGR).
5. **The site was irrigated by drip irrigation to maintain plants in a well-watered state.** Maintaining adequate soil moisture content throughout the growing period is essential as droughting or over-watering would introduce a second stress which may interact with the herbivore population growth.

2.2.2 Structure design

Based on the design principles described previously, a tunnel structure was designed from standard and bespoke parts (fabrication and supply: NP Structures Ltd. Mill Green, Waterside Road,

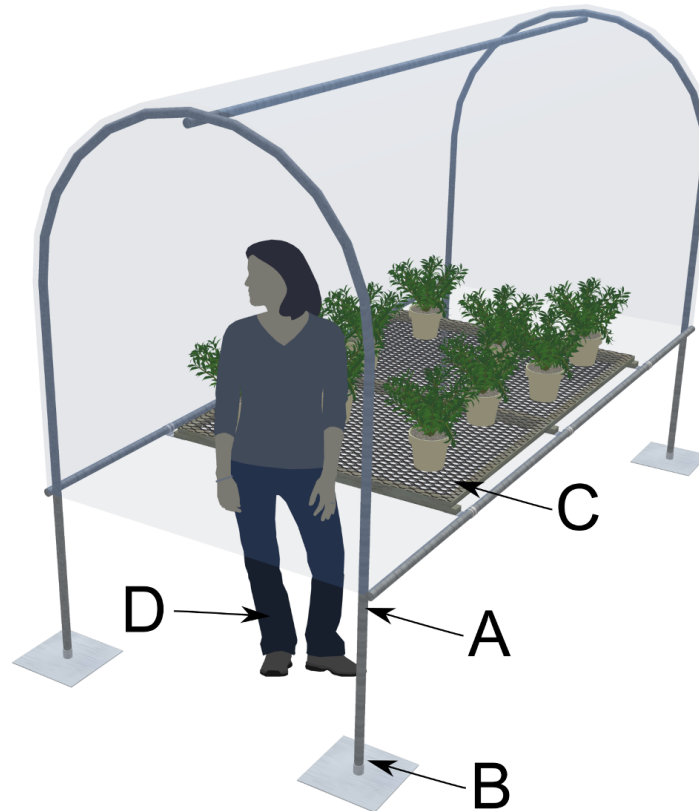


Figure 2.2: Final structure design. A small, steel-framed polytunnel (A), on temporary supporting plates (B). A timber frame supported a galvanised steel weld mesh growing platform (C), allowing the user to work within the tunnel (D).

Colne, Lancs, BB8 0TA) (Figure 2.2) which gave a 1.9 m × 1.2 m growing area constructed of weld-mesh on a timber frame. The timber frame was assembled and coated with a green timber treatment. This growing bench was housed within a tunnel of height 2.2 m, width 1.3 m and length 3.1 m, providing adequate space at both ends for a user to make measurements. The growing area was suspended from the two side support beams on brackets designed to hold a door unit. The tunnel was anchored using cargo tape and a screw-in ground anchor. Horticultural film claddings (details below) were used to clad all sides of the tunnel structure to the level of the bench. Below the bench was left unclad to allow ventilation below the growing space.

A Galcon DC irrigation timer and manifold connected to the mains water supply was used to irrigate the tunnels on a single circuit. Each tunnel had a terminal with 12 dripper nozzles. Irrigation was programmed twice a day for various durations, depending on the size of the plants.

2.2.3 Site layout

The tunnels were oriented so that the ends were un-obscured by other tunnels or structures, and were facing approximately south to provide maximum exposure to solar radiation (Figure 2.3). At the western end of the compound, there was a partially opaque fence and so the first tunnels were positioned three metres east of this. To the north of the site was a glasshouse array and the main laboratory building. Tunnels were positioned a minimum of three metres from the

buildings. In order to estimate the best positioning of tunnels on the available site, a shadow model was constructed in Google SketchUp (now Trimble SketchUp) which allowed the approximate position of shadows to be estimated at different points through the growing season (Figure 2.3). I concluded that tunnels were best spaced 1 m apart to reduce the shading effect from neighbouring tunnels, however as the tunnels were oriented south, the shading effect from other tunnels was minimal. The area beneath the tunnel was covered with a light-coloured landscaping ballast over a weedproof membrane and was regularly controlled for weeds with glyphosphate herbicide.

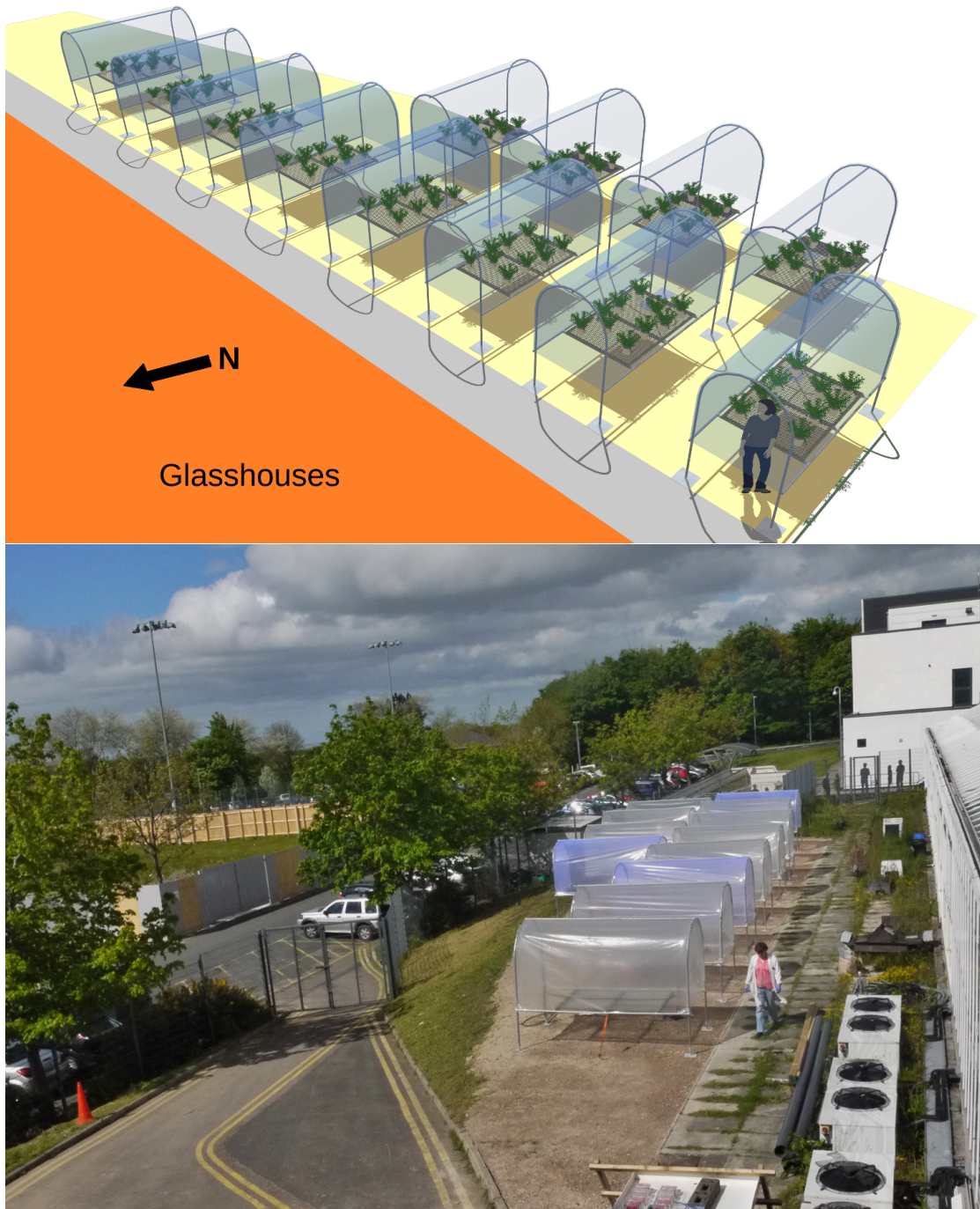


Figure 2.3: Site layout. The top image shows a Google Sketchup simulation of the site to check for possible shading issues. The bottom image shows the site layout as used for the field experiments.

2.3 Light and insect photobiology experiments

As the interaction of organisms and light is the central theme of this thesis, the fundamental principles, measurement and expression of light treatment is of great importance.

2.3.1 Definitions and units

As light is of central importance to this thesis, I briefly define the terminology and concepts of light and its units. Light may be thought of as both a wave and a particle and, as such, may be measured either as an energy or a quantity. Dose is defined as the energy (J) or quantum (μmols) intersecting a 2-dimensional plane and the units are either energy per unit area (J m^{-2}) or quantum per unit area ($\mu\text{mols m}^{-2}$). Irradiance is the energy transferred per second with units of W m^{-2} or mW cm^{-2} . The analogous unit for quantum is photon fluence which is the quantity of photons transferred per second with units of $\mu\text{mols m}^{-2} \text{s}^{-1}$. UV light is the band of electromagnetic radiation with wavelengths between 100 nm and 400 nm. This region is further divided into Ultraviolet C (100 nm-280 nm), Ultraviolet B (280 nm-315 nm), and Ultraviolet A (315-400 nm). Human visible light is defined as the waveband between 400 nm and 900 nm (although it is acknowledged that humans are capable of perceiving light beyond this range).

2.3.2 Hardware tools for measuring light

A Macam SR9910 double monochromator spectroradiometer (Macam Ltd. No longer trading) was used for spectral measurements. This was regularly calibrated against deuterium and QTH reference sources. For measurement of irradiance, a cosine corrected head on a 1.5 m shielded quartz fibre was used. Irradiances were recorded at a minimum resolution of 1 nm between 250 nm and 400 nm, and 5 nm between 400 nm and 800 nm.

For transmission measurements of a material, a 20 cm diameter Macam integrating sphere was used for light collection, allowing the total (diffuse and direct) transmission to be measured. A 1 m quartz fibre connected the top collection port to the spectroradiometer. A 6283NS mercury-xenon arc lamp (supplied by Newport Spectra-Physics Ltd. Unit 7, Library Ave, Harwell Oxford, Didcot OX11 0SG) housed in an Oriel lamp housing was used for illumination of the sample.

2.3.3 Software tools for processing spectral data

As much of the statistical analysis for the experimental work in this thesis was conducted using the R statistical programming environment, this was also used to perform calculations on the recorded spectra. Within this, the 'photobiology' package (Aphalo et al., 2012) was used as the primary processing tool for the spectroradiometer raw data. Raw data from the spectroradiometer, stored as line-separated value text files with a .dti or .dta file extension, was read directly into R and further calculations applied from that point. The package makes use of the object-oriented environment in R to import spectra or groups of spectra as objects and apply user-specified transformations. This may include simple multiplication to convolve a spectra with a spectral weighting function, or a division to calculate a transmission. The 'raster' package was used to import and process GeoTIFF irradiance maps. Plots were generated with either the 'ggspectra' or parent package 'ggplot2'.

2.3.4 Measuring irradiance

All irradiance measurements were made in accordance with standard photometric procedures (Labsphere, 2015). For a typical irradiance measurement, the cosine head was orientated vertically so the sensor surface was parallel with the sky. Measurements were taken with an integration time of 100 ms for solar and 200 ms for non-solar sources. Solar measurements were conducted within one hour of solar noon (13.00 BST) and under cloudless conditions. Shorter integration times were used under sunlight to reduce the overall measurement time and therefore reduce the likelihood of a change in atmospheric conditions which would give inaccurate measurement.

Analyses for insect experiments relied on the use of weighted or unweighted integrated irradiances as predictors in the statistical models. Unweighted irradiance integrals (such as total UVA, UVB, PAR, etc.) were calculated as

$$E = \sum_{\lambda_{\min}}^{\lambda_{\max}} E(\lambda) \cdot \Delta(\lambda) \quad (2.1)$$

where E is the total integrated irradiance between λ_{\min} and λ_{\max} , $E(\lambda)$ is the irradiance over a given waveband, and $\Delta(\lambda)$ is the width of the waveband.

In some circumstances, it is desirable to calculate effective irradiance, where an unweighted irradiance (e.g. an illumination source) is convoluted with a Spectral Weighting Function (SWF) (e.g. the wavelength sensitivity function of a photoreceptor). The integral of an effective irradiance spectrum is a dimensionless value, E^* , which can be thought of as the effective response of a system to a given spectrum. SWFs are referred to as Biological Spectral Weighting Functions (BSWFs) when the target system is biological (e.g. photoreceptors, other chromophores, etc.) Effective irradiances were calculated as:

$$E^* = \sum_{\lambda_{\min}}^{\lambda_{\max}} E_{\text{eff}}(\lambda) \cdot E(\lambda) \cdot \Delta(\lambda) \quad (2.2)$$

where E^* is the total effective integrated irradiance between λ_{\min} and λ_{\max} and $E_{\text{eff}}(\lambda)$ is the weighting for a given waveband.

2.3.5 Measuring material transmission

Transmission measurements of material samples were made using an integrating sphere illuminated as described above. The lamp beam was focused through a quartz lens into the front port of the integrating sphere. The rear port was obscured with a calibrated polytetrafluoroethylene (PTFE) reflectance reference disc and the top collection port connected to the spectroradiometer with a 1m quartz fibre. After allowing a 30 minute warm-up period for the lamp, a 100% reference scan was made with the entry port of the integrating sphere un-obscured. The entry port was then covered with a single layer of the measured material and a second scan recorded. Transmission calculations were made in the 'photobiology' R package. For each wavelength, the transmission was calculated as

$$t(\lambda) = \frac{E(\lambda)_{\text{filtered}}}{E(\lambda)_{\text{reference}}} \quad (2.3)$$

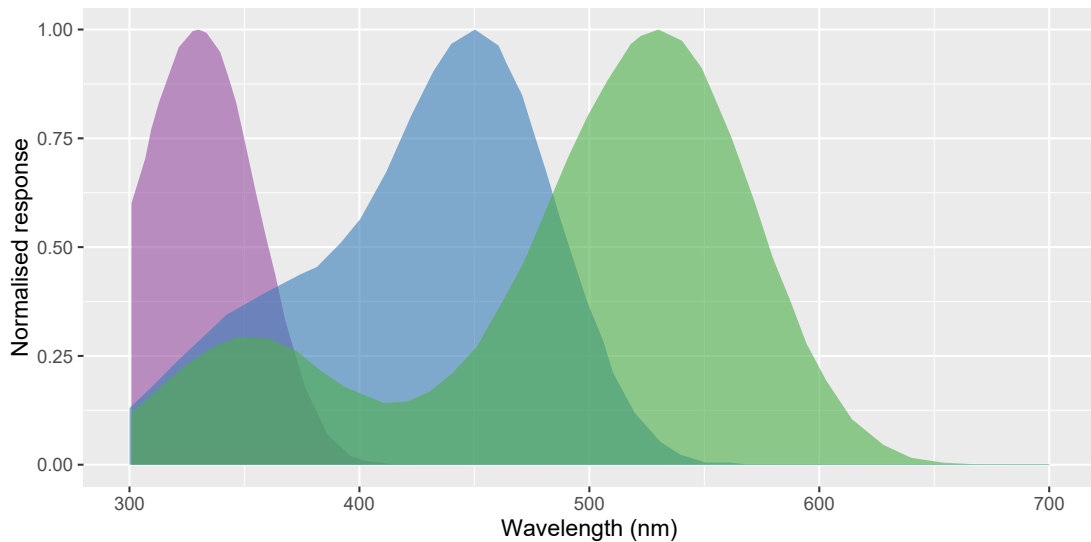


Figure 2.4: Normalised photoreceptor responses for the three *Myzus persicae* receptor types

where $E(\lambda)_{\text{filtered}}$ is the irradiance of the filtered light source at a given wavelength and $E(\lambda)_{\text{reference}}$ is the irradiance of the same light source unfiltered.

It was often useful to estimate the effective irradiance transmission of the material under an environmentally representative illumination source, for example the % transmission of erythemally-weighted solar UV into a polytunnel, clad with a PE film of known transmission. The transmission spectrum was first convolved with a standard surface-level solar reference spectrum (in this case ASTM G173 direct, see section 2.3.8 for description) to obtain the transmission spectrum. The transmission spectrum and the reference spectrum were each convolved with the desired spectral weighting function (see above) and the final effective transmission for a known filter under a known spectra was calculated as

$$T = \frac{E_{\text{filtered}}^*}{E_{\text{reference}}^*} \quad (2.4)$$

Some caution must be applied when using this, as the percentage transmission estimate is only applicable for similar illumination spectra. If, for example, a solar spectrum has been used to estimate the erythemally-weighted transmission of a material, that transmission percentage only applies to transmission of a similar solar spectrum through the material.

2.3.6 Biological Spectral Weighting Functions

A number of BSWFs were used throughout the thesis. The visual action spectrum for *Myzus persicae* (Figure 2.4) was extracted from Döring et al. (2007) and was used to calculate the effective stimulation of the trichromatic aphid visual system (see next section for description of colourspaces). Other BSWFs were used in Chapter Four to approximate alignment with known action spectra of UV-induced damage. BSWFs used were:

1. The erythemally-weighted CIE action spectrum, Commission Internationale d'Eclairage (1999)
2. Combined spectra for human health risk factors, International Commission on Non-Ionising Radiation (2004)

3. Naked DNA action spectrum, Setlow (1974)
4. *In vivo* DNA damage in *Alfafa sp.*, Musil (1995)

All were used directly within the 'photobiology' package in R (Aphalo et al., 2012).

2.3.7 Colourspace derivation and use

Insect visual perception of light is determined by the sensitivity of the insect eye to different wavelengths. When normalised, these Visual Action Spectras (VASs) can be used as BSWFs to measure the effective stimulation of a photoreceptor by a given illumination source. The use of these insect VAS as BSWFs provides a convenient way of describing the effective irradiance perceived by the insect and so the VAS for short- ('UV'), medium- ('Blue') and long-wavelength ('Green') photoreceptors for *M. persicae* were used to generate a *M. persicae* 3-dimensional colourspace. Modifying an approach used by Osorio and Vorobyev (2008), this was calculated as follows:

The illumination spectrum was first convolved with each of the three photoreceptor VAS such that

$$E_{\text{photoreceptor}}^* = \sum E_{\text{eff}}(\lambda) \cdot E(\lambda) \cdot \Delta(\lambda) \quad (2.5)$$

where E_{eff} was the normalised photoreceptor response spectrum for a given photoreceptor type. The effective response for each photoreceptor was then converted to a proportion of the total photoreceptor stimulation (the sum of all three photoreceptor types):

$$R_{\text{UV}} = \frac{E_{\text{UV}}^*}{E_{\text{UV}}^* + E_{\text{Blue}}^* + E_{\text{Green}}^*} \quad (2.6)$$

$$R_{\text{Blue}} = \frac{E_{\text{Blue}}^*}{E_{\text{UV}}^* + E_{\text{Blue}}^* + E_{\text{Green}}^*} \quad (2.7)$$

$$R_{\text{Green}} = \frac{E_{\text{Green}}^*}{E_{\text{UV}}^* + E_{\text{Blue}}^* + E_{\text{Green}}^*} \quad (2.8)$$

This generated a set of three colour coordinates for each illumination source, such that

$$aR_{\text{UV}} + bR_{\text{Blue}} + cR_{\text{Green}} = 1 \quad (2.9)$$

where a,b and c are weighting values determined by the signal processing neural network. Neuronal weightings for the different photoreceptor types are context dependent and will change as the insect-eye is colour-adapted to the light environment (Chittka et al., 1992), therefore the absolute position within the unweighted colourspace (where $a = b = c = 1$) is arbitrary. Instead, it is the relative position of one illumination source to another that is of interest, and so, for graphical representation, the colourspace may be scaled about a convenient reference spectrum. For the work undertaken in this thesis, the centrepoint was defined as the aphid response to a standard solar spectra (similar to chromaticity diagram principles developed by Vorobyev and Brandt (1997)). The ASTM G173 direct spectrum was used and all measured values were scaled such that the ASTM spectrum was at the centre of the ternary diagram (Figure 2.5). This allowed interpretation of spectra as increased or decreased photoreceptor responses, relative to sunlight.

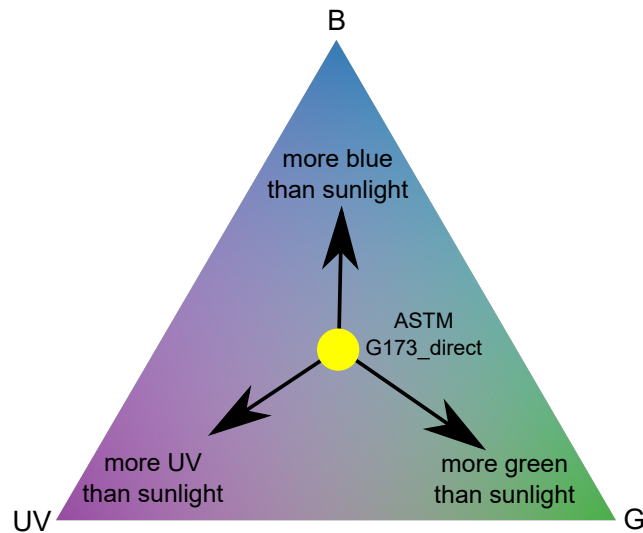


Figure 2.5: Ternary plot showing the conceptual application of a visual colourspace. The ASTM G173 direct spectrum is defined as the centrepoint and shifts in each of the three axes represent relative changes in the stimulation of each photoreceptor type.

2.3.8 Third-party solar datasets

Certain data modeling and interpolation required the use of standardised modeled and measured spectra from external sources. Here, a description of those datasets and their source is provided:

ASTM G173 Direct

This is a representative solar reference spectrum. The spectrum was designed to be a representative mean for all regions of the U.S.A, over all seasons (ASTM International, 2012). As environmental irradiance and dose vary widely in time and space, this was considered a typical clear sky spectrum and was predominantly used for spectral balance calculations, rather than for irradiance or dose calculations. The spectrum was obtained from the 'photobiologySun' R package.

DEFRA measured dataset

Erythemally-weighted solar irradiance averages recorded at 30 minute intervals for a site at Reading, UK (51.44°N, 0.94°W). The dataset retrieved from the DEFRA radiation data repository (DEFRA, 2016). A subset of the data from 20th June 2013 to 31st of August 2013 (to coincide with the field experiment) was used to calculate daily dose integrals for erythemally-weighted solar radiation as a spectral dataset broadly representative of British summertime.

SoDa modeled dataset

Mean hourly erythemal dose for a given location, retrieved from the SoDa website (SoDa, 2016) (actual data service supplied by Meteotest, Fabrikstrasse 14 3012 Bern, Switzerland). Values were calculated using a modified version of the radiation transfer model described by (Rigollier et al., 2000). The parameter values entered into the interface on the website are presented in

Table 2.1: Input parameter values for the SoDa radiation transfer model interface.

Parameter	Value
Latitude and Longitude	Reading: 51.44°N, 0.94°W Lancaster: 54.04°N, 2.80°W
Spectral part of UV	Erythemal all sky
Radiation unit	Irradiance
Select time unit	hourly
type of ground	grass
chain method	Erythemal all sky

Table 2.1. The model returned hourly mean irradiance values. These were used to calculate daily dose integrals for erythemally-weighted solar radiation (comparable with the above measured dataset).

Aura-OMI Daily Gridded Surface UV

Satellite surface daily erythemally-weighted UV doses in a $1^\circ \times 1^\circ$ grid obtained through the Giovanni interface (NASA, 2016). A time-averaged dataset for the period 21st of June 2013 to 31st of August 2013 (to temporally align with the DEFRA dataset described above) was obtained, providing mean daily surface erythemally-weighted UV dose at a $1^\circ \times 1^\circ$ resolution. A subset area over western Europe and north Africa was selected for use. Using the Giovanni tool, a single-colour colourscale was selected with 65 separate colour levels, smoothing was applied and the dose range scaled between 1 kJ m^{-2} and 7 kJ m^{-2} . This map was then exported from the web interface in the GeoTIFF format. The GeoTIFF image was processed in R using the 'raster' package. After importing the GeoTIFF as a raster brick, colour channel values, longitude and latitude were transformed into a data frame. The colour values, from each of the three colour channels, for each pixel were summed and the result scaled between one and seven to produce a geo-referenced map of erythemal daily dose.

2.3.9 Film transmission spectra

The industrial element to this research project allowed access to commercial PE film claddings with various transmission profiles. Whilst there was a commercial research component to their use in field experiments, the optical properties and stability of these films meant that they were highly suitable as UV-manipulating filters for laboratory work. Four different films were used for experimental work at Lancaster: a commercial UV-transparent film (Lumisol, Figure 2.6.A), a commercial 'standard' film (Lumitherm, Figure 2.6.B), a commercial UV-opaque film (Lumivar, Figure 2.6.C) and an experimental film (referred to as 'Tex', Figure 2.6.D). All were supplied by BPI-Visqueen, Lundholm Road, Ardeer, Stevenston, KA20 3NQ. Additionally, spectra for two experimental films not used in the experimental work are presented here, predominantly for modeling purposes (referred to as 'C1' and 'C6', Figure 2.6.E and 2.6.F).

2.3.10 Experimental light sources

A number of illumination sources were used for laboratory experiments. For UVB supplementation, UVB-313 EL fluorescent tubes were used (supplied by Q-LAB EUROPE, LTD., Express Trad-

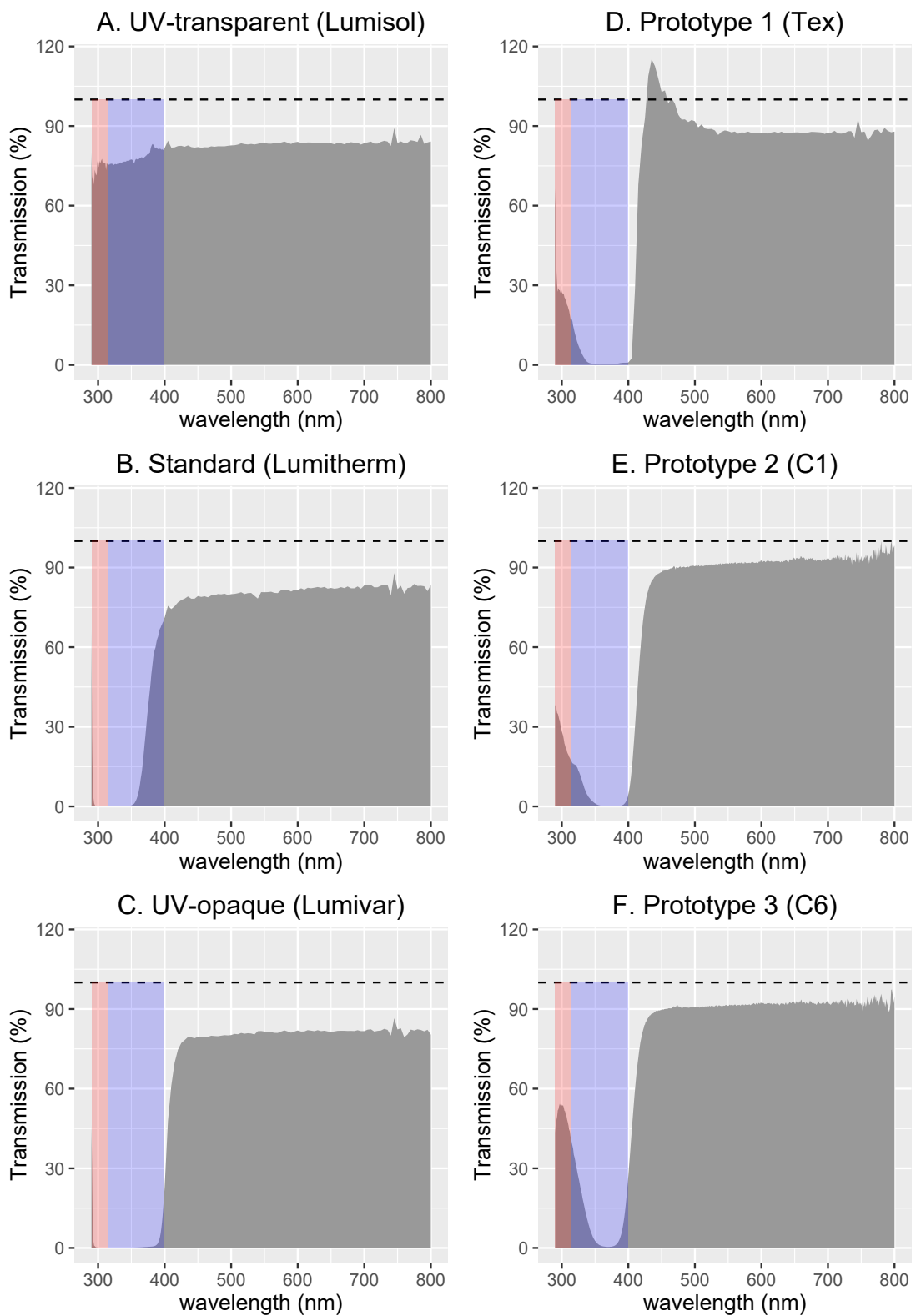


Figure 2.6: Commercially available PE film transmission spectra. Measured transmissions as described above for (A) UV-transparent, (B) standard, (C) UV-opaque films and (D-F) three experimental films. The red-shaded region shows the UVB component and the blue-shaded region shows the UVA component of the transmission spectrum. The dashed line shows 100% transmission. The transmission profile for Tex (D) shows transmission values above 100% due to fluorescent emission in this region.

ing Estate, Stone Hill Road, Farnworth, Bolton, BL4 9TP). For short wavelength UVA, UVA-340 fluorescent tubes were used (supplied by Q-LAB, address as above). Long wavelength UVA supplementation was provided by Philips TL 6 W BLB fluorescent tubes (supplied by Philips-Lighting UK). Where necessary for experimental work, Valoya NS-1 LED units (supplied by Valoya Ltd., Melkonkatu 26, 00210 Helsinki, Finland) were used for non-UV, broadband supplementation. LED units were used for work carried out in Chapters five and six. Four colours were used: Deep Blue (455 nm peak, i-LED part number: ILH-ON04-DEBL-SC211-WIR200), True Green (528 nm peak, i-LED part number: ILH-ON04-TRGR-SC211-WIR200), Hyper Red (656 nm peak, i-LED part number: ILH-ON04-HYRE-SC211-WIR200) and UV (365 nm peak, i-LED part number: ILH-XS01-S365-SC211-WIR200.). These were supplied by RS Components (Green Lane Industrial Estate, Kennedy Way, Stockport SK4 2JT). These were controlled with a raspberry Pi via a 5V motor controller board (also supplied by RS Components, see above).

2.3.11 Standardised canopy transmission spectra

As discussed in 1.3, insect vision is highly sensitive to spectral balance, and so quantifying the light environment typically experienced by the aphid was a significant development in understanding the mechanisms by which it influences behaviour. In order to produce a simple model of the effect of the canopy on solar radiation, the transmission of light through the canopy was measured in a controlled illumination environment. Calabrese (v. Zen) was grown (as described in section 2.1) in 5 cm × 5 cm × 5 cm module units, grown as a single 3×4 cell module tray. Plants were grown for four weeks (approximately five true leaves present) to produce a seedling canopy environment, representative of the experimental work conducted elsewhere in this study. The measurement arena was established within a CE room, using UVA-340 (UVA), UVB-313 (UVB) and Valoya NS-1 LED units (400-700nm) for illumination.

For the single leaf transmission measurement, the sensor was clamped in position and a representative leaf (either second or third leaf) was positioned directly over the sensor head so that it was touching the probe (Figure 2.7.A). The plant was then removed and a 100% reference scan was made. This was repeated three times and the averaged values used to calculate the through-leaf transmission.

For canopy transmission measurements, the cosine head was clamped in position, pointing up, towards the lamp sources which were positioned directly above the measurement arena. Five measurements were made with the head under the canopy and five were made at different positions around the arena, once the tray of plants had been removed. Under-canopy and control spectra were averaged and the average transmission calculated (Figure 2.7.B).

A direct measurement of the compost reflectance was made by orientating the cosine head downwards, measuring the spectra and then orientating the head towards the lamps and adjusting the height so that the measurement was made in the same vertical plane (Figure 2.7.C).

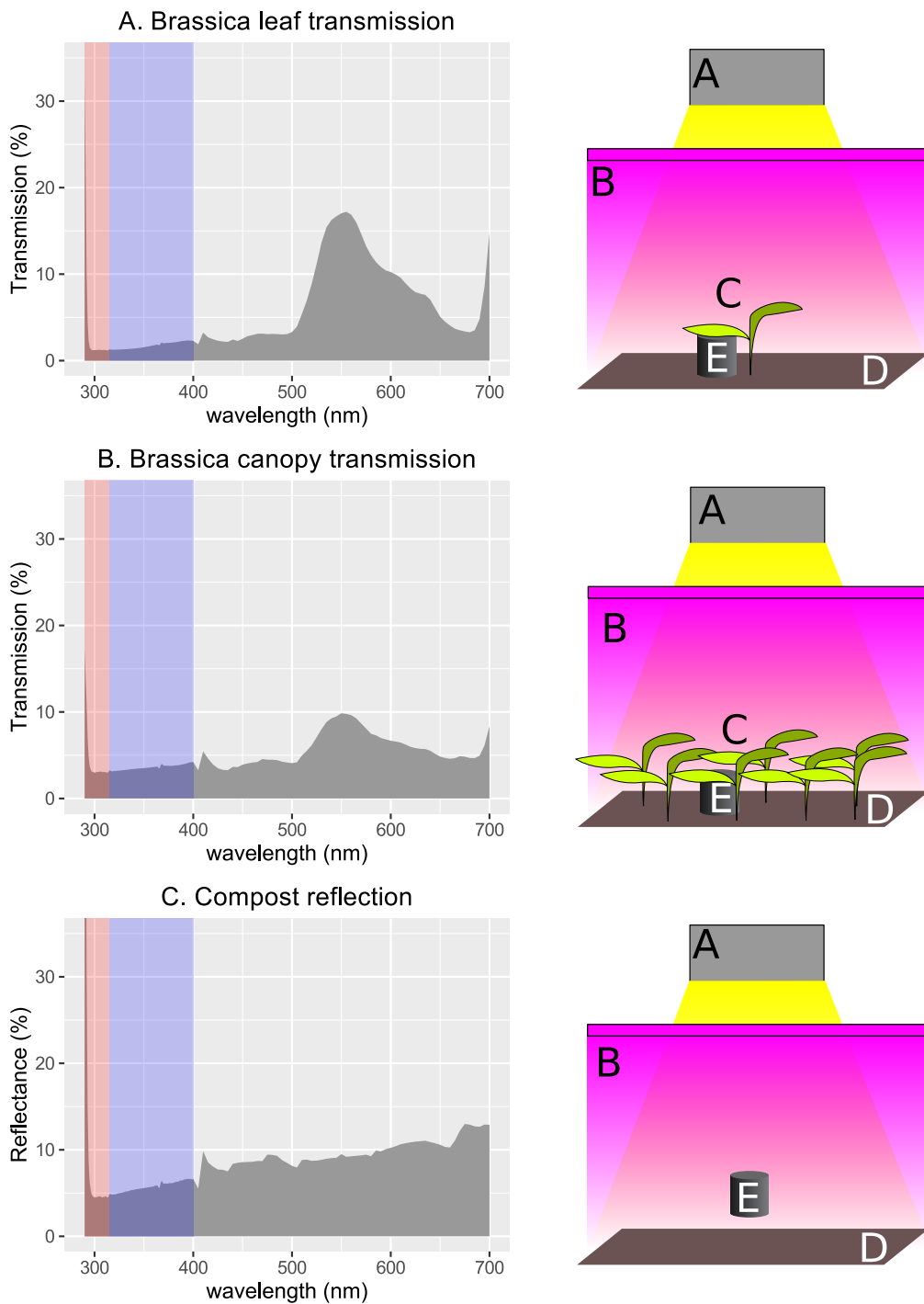


Figure 2.7: Transmission and reflectance measurements of naturally-occurring aphid feeding environments. Figure A. shows the transmission through a single *Brassica oleracea* leaf. Figure B. shows the average canopy transmission and Figure C. shows the compost reflectance. Markers in the method diagram show (A) metal halide source lamp, (B) UVA-340 and UVB-313 EL fluorescent tubes, (C) *Brassica oleracea* seedlings, (D) M3 compost, (E) spectroradiometer cosine-corrected head.

Population and behavioural effects of ultraviolet radiation on *Myzus persicae* in field experiments

Abstract

Background: Ultraviolet-B (UVB) radiation has previously been shown to influence pest success by inducing plant responses which alter antiherbivore defence. This mechanism is of interest in protected cropping, where crops are covered with films or nets, as spectral balance may be manipulated through changes in the optical transmission properties of the cladding. Very little is known about the plant-mediated effects of UVB on aphids and so the initial experiments of the project were designed to test the responses of the aphid, *Myzus persicae*, to ultraviolet-A (UVA) and UVB. This work was conducted in 2013 in small scale polytunnels, utilising polyethylene (PE) films with different transmission properties to provide a gradient of UVA and UVB transmissions.

Results: UVB was not found to significantly determine birth or death rate of *M. persicae*, however there were treatment differences. The lowest aphid Population Growth Rates (PGRs) on two cultivars of *Brassica oleracea* were seen when UVA was attenuated but some UVB was transmitted into the growing environment. For both cultivars studied, canopy distribution differences were observed between treatments. Under UVA-attenuated light environment, approximately twice as many aphids were recovered from exposed feeding sites (upper leaf surfaces of the upper canopy), compared to high UVA treatments.

Conclusion: UVB-induced changes in plant defensive chemistry were not thought to explain aphid PGR in this study, however, possible behavioural changes exposed the aphids to higher levels of damaging UVB radiation in some treatments. This was hypothesised to explain the PGR differences between treatments and identified new targets for research in subsequent chapters of this thesis.

3.1 Introduction

From the early 1980s, there has been interest in the use of horticultural polytunnel claddings that modify the solar spectrum for pest control (Antignus, 2000). Study of insect flight behaviour has determined, both mechanistically (Kirchner et al., 2005) and experimentally (Raviv et al., 2004), that UVA (315 nm–400 nm) is both detected and utilised for flight orientation (Pfeiffer and Homberg, 2007). Exclusion of ultraviolet (UV) radiation through the use of UV-attenuating nets had an inhibitory effect on pest PGR: aphids and whiteflies (Order: *Hemiptera*) were more likely to land when they entered a UV-attenuated environment (Legarrea et al., 2012c) and, if presented with a choice, were less likely to enter areas with lower UV irradiances (Costa et al., 1999) resulting in fewer infected plants and smaller pest populations in the crop as a whole. Similarly, under UV-attenuating films, thrips (Order: *Thysanoptera*) remained closer to their point of release and showed reduced preference for UV-attenuated environments (Kigathi and Poehling, 2012). As such, these claddings offer a powerful tool for the control of arthropod pests in horticulture.

Whilst it has been shown that removal of UV may reduce the spread of pest insects via a visual mechanism, other studies have shown that exposure of plants to short wavelength UV—UVB—had an inhibitory effect on *Lepidoptera* (Caputo et al., 2006; Hatcher and Paul, 1994), *Coleoptera* (Ballare et al., 1996) and *Hemiptera* (Paul et al., 2012; Mewis et al., 2012). For *Lepidoptera*, larval weight, feeding preference and oviposition were reduced on plants grown under solar UVB (Caputo et al., 2006) and reduced PGR in the generalist aphid, *Myzus persicae*, was attributed to increases in brassica glucosinolates (Mewis et al., 2012). UVB-induced increases in flavonoid concentration have been shown to negatively affect aphid birth rate (Paul et al., 2012), likely due to the strong antifeedant effect of flavonoid and flavonoid derivatives (Golawska et al., 2012b; Lattanzio et al., 2000). However, it has been previously noted that UVB-induced changes in plant chemistry do not always correspond with better defended plants (e.g. Izaguirre et al., 2007, for a review of UVB-induced antiherbivore defence, see 1.4) and as such the UVB-induced plant response may have no effect (Kuhlmann et al., 2010), or even a positive effect (Dader et al., 2014) on herbivores.

It is therefore of interest to establish the relative importance of insect-mediated (visual response, flight behaviour, movement within crop, etc.) and plant-mediated (UVB-induced increases in defence) mechanisms that may affect pest insects within a crop. Accordingly, the aims of the experimental work presented in this chapter were to first quantify the effect of UVA and UVB on insect PGR through putative changes in plant defensive chemistry as well as identify any obvious morphological responses in the plants (such as reduced leaf area, as has been observed in previous studies (Paul et al., 2005)). As such, the experimental method excluded migratory and dispersal behaviours by inoculating caged plants with small populations of wingless aphids and measuring the PGR. Using three commercial and one prototype film with different UV-attenuating properties, a novel factorial experimental design was employed where the effect of UVA and UVB could be tested in both combination and isolation (Table 3.1). In accordance with a previous study (Mewis et al., 2012), The primary hypothesis was that PGR would be high under UV-opaque (Lumivar) and commercial standard (Lumitherm) films due to the absence of UVB and low and medium, respectively, under UV-transparent and prototype (Tex) films, due to the respective high and moderate UVB transmission.

Film	Waveband		
	UVA	UVB	PGR
Lumivar	-	-	High
Lumitherm	+	-	High
Lumisol	+	+	Low
Tex	-	+	Medium

Table 3.1: Predicted effect of cladding type on Population Growth Rate (PGR) of aphids inhabiting polytunnels. This is expressed in terms of their UVA and UVB transmission (+) or attenuation (-).

3.2 Methods

3.2.1 Light environment

The experiment was located on a south-facing site at Lancaster University. Twelve purpose-built polytunnel structures (3 m×1.3 m×2 m) were spaced 1.5 m apart (see 2.3 for further details). Each tunnel was clad in one of four film claddings: Lumitherm (a Standard film with no specific UV-manipulating properties), Lumisol (a UV-transparent film), Lumivar (a UV-blocking film) and Tex (a prototype film which attenuated UVA and transmitted some UVB). All films were produced and supplied by BPI Visqueen Ltd. Lundholm Road, Ardeer, Stevenston KA20 3NQ. Full spectrum irradiance measurements were taken in each tunnel on 9th July 2013 using a Macam spectroradiometer (model SR9910, Macam Photometrics Ltd.) and a five metre quartz fibre optic with a cosine corrected head. Measurements were made within one hour of midday when no clouds were present. 100% reference measurements were made outside the tunnels, before and after tunnel measurements. The mean spectrum was used to calculate the tunnel transmission for each tunnel.

3.2.2 Plants and insects

For the first experiment, *Brassica oleracea* (cabbage, c.v. Derby Day supplied by Nickys Nursery, Kent, UK) was sown in Levington's M3 compost (supplied by LBS Horticulture Ltd., Standroyd Mill, BB8 7BW) in 134 mL modules in a partially temperature controlled glasshouse. 72 plants (six per tunnel) were moved to the tunnels on 10th of June (five days after sowing) and watered in trays by flood irrigation.

In the second experiment, two cultivars were compared: Derby Day (as above) and a calabrese (c.v. Volta, supplied by Marshalls Seed Ltd., Cambridgeshire, UK). Seeds were sown in trays of M3 compost in a partially temperature controlled glasshouse and left to germinate uncovered. After six days, 36 plants of each cultivar (72 total) were transplanted individually into 500 mL pots and moved into mesh cages inside the experimental structures (11th August).

Stocks of *Myzus persicae* were kept on Derby Day or Volta as described previously (2.1) before transfer to plants of the same experimental cultivar.

3.2.3 Aphid PGR experiment

In the first experiment, plants were transferred into individual standard mesh insect tent cages (approximate volume = 35L) suspended from the tunnel structure at 29 days post-germination. Ten apterous (wingless) *M. persicae* were transferred to a leaf fragment in a Petri dish and placed at the base of the plant, allowing aphids to colonise the plants. Plants were harvested two weeks after inoculation with aphids (43 days post-germination) which approximates a single generation of *Myzus persicae* (see 2.1.2 for description of life cycle).

In the second experiment, the plants were grown in the mesh cages from six days post-germination. At 23 days post-germination, five apterous (wingless) *M. persicae* were transferred to a leaf fragment in a Petri dish and placed at the base of the plant, allowing aphids to colonise the plants. Plants were harvested two weeks after inoculation with aphids (37 days post-germination).

For both experiments, *in situ* measurements of leaf temperature were made with an infrared thermometer on three separate days during the experiments. For the final harvest, plants were dissected and the number of aphids on upper and lower surfaces of each leaf was recorded. Leaf area was measured with a LICOR LI-3000C portable leaf area meter (LI-COR Environmental - UK Ltd, St.John's Innovation Centre, Cowley Road, Cambridge, CB4 0WS). Above-ground plant fresh mass was also measured.

3.2.4 Statistical methods

All statistical analyses were conducted using the R Statistical Computing Environment (R Core Team, 2013). The effect of light treatment on plant leaf area and leaf temperature was tested with a one-way ANOVA.

To compensate for the nested experimental design (replication within tunnels), Generalised Linear Mixed Effect Models (GLMMs) were used to test the effect of light treatment on the final population size for each experiment, whilst accounting for the nested experimental design of cages within tunnels. The 'MCMCglmm' package was used to implement the Markov Chain Monte Carlo technique to provide more reliable parameter and 95% confidence interval estimates than can be achieved using the 'lme4' package (for introduction to this method see Baguley, 2012). For final population size, a Poisson family was specified as the count data followed an approximate Poisson distribution.

PGR for estimated mean final population sizes was calculated with Equation 3.1 (after Renshaw (1993)) where N_0 is the start population and N_t is the population after time period t (days).

$$\text{PGR} = \frac{\text{Ln}\left(\frac{N_t}{N_0}\right)}{t} \quad (3.1)$$

To test the effect of light treatment on aphid position, the 'MCMCglmm' package was used with a 'multinomial2' family, to predict the proportion of aphids in an exposed position. Proportion of aphids in an exposed position (proportion exposed) was defined as the number of aphids on the upper surface of the first and second true leaves divided by the total plant population. All MCMCglmm models used the default weak priors and models were checked by testing for chain autocorrelation as specified by Hadfield (2010). Chain length was set to 100,000 and the default burn-in (3000) and thinning interval (10) was used for all models, unless otherwise specified.

3.3 Results

3.3.1 Light Environment

On the day of measurement (9th July, 2013). Photosynthetically-Active Radiation (PAR) was recorded between 1835 mol m⁻² s⁻¹ to 2142 mol m⁻² s⁻¹ within one hour of noon. The transmission spectra for all structures were measured on this day and were broadly in keeping with the expected transmission profiles (see 2.4.9 for transmission spectra measured on an integrating sphere). Percentage transmission for total UV, UVA and UVB were calculated for each treatment (Table 3.2, Figure 3.1). The Lumisol (UVA+|UVB+) film had uniform transmission of 69% across the UV waveband. Both Lumivar (UVA-|UVB-) and Tex (UVA-|UVB+) blocked UVA, allowing transmission in this waveband of less than 3%. Tex and Lumisol both transmitted in the UVB with Tex transmitting 19% and Lumisol transmitting 69% UVB. Lumitherm (UVA+|UVB-) allowed some transmission in the UVA (18%) but not in the UVB (< 0.1%). PAR transmission varied across treatments, between 67% (Lumitherm) and 82% (Tex).

These transmission profiles allowed a semi-factorial experimental design where the effect of UVB in isolation (Tex), UVA in isolation (Lumitherm), and UVA and UVB in combination (Lumisol) could be compared to a UV-attenuated control (Figure 3.1). As such, the light treatments are referred to by their UVA and UVB transmission (e.g. Lumisol: UVA+|UVB+, etc.), rather than by the film brand names.

Table 3.2: % Transmission of sunlight through four horticultural films measured *in situ* at the field site (n = 12). Mean values are shown for three tunnels ± 1 standard error of the mean.

Film	Total UV	UVA	UVB	PAR	Light Treatment
Lumivar	0.7 \pm 0.1	0.8 \pm 0.1	0.0	68.5 \pm 3.7	UVA- UVB-
Lumitherm	15.2 \pm 0.5	17.9 \pm 0.5	0.1 \pm 0.1	67.4 \pm 3.7	UVA+ UVB-
Tex	4.7 \pm 0.1	2.2 \pm 0.1	19.2 \pm 0.8	82.0 \pm 2.2	UVA- UVB+
Lumisol	69.1 \pm 2.1	69.1 \pm 1.8	69.1 \pm 3.5	76.3 \pm 2.0	UVA+ UVB+

3.3.2 Effect of light treatment on plant morphology

Total leaf area of cabbage (v. Derby Day) was not significantly affected by light treatment in experiment 1 ($F_{3,68} = 1.058$, $p = 0.373$). The mean leaf area was 241 \pm 13 cm². In the second repeat of this experiment, leaf area of Derby Day was larger than in the first experiment, but was not significantly affected by light treatment ($F_{3,31} = 0.483$, $p = 0.697$) with a mean leaf area of 513 \pm 10 cm² across all treatments. Calabrese (v. 'Volta') total leaf area was also not significantly affected by light treatment ($F_{3,30} = 1.853$, $p = 0.159$) with a mean leaf area of 382 \pm 8 cm².

An infrared thermometer was used to measure the radiative temperature of plants grown during experiment 1. The upper leaves of the plant were measured three times and the mean recorded as the temperature. The mean leaf temperature was 29.6 \pm 0.2°C. There was no significant effect of light treatment on leaf temperature ($F_{3,68} = 2.146$, $p = 0.102$).

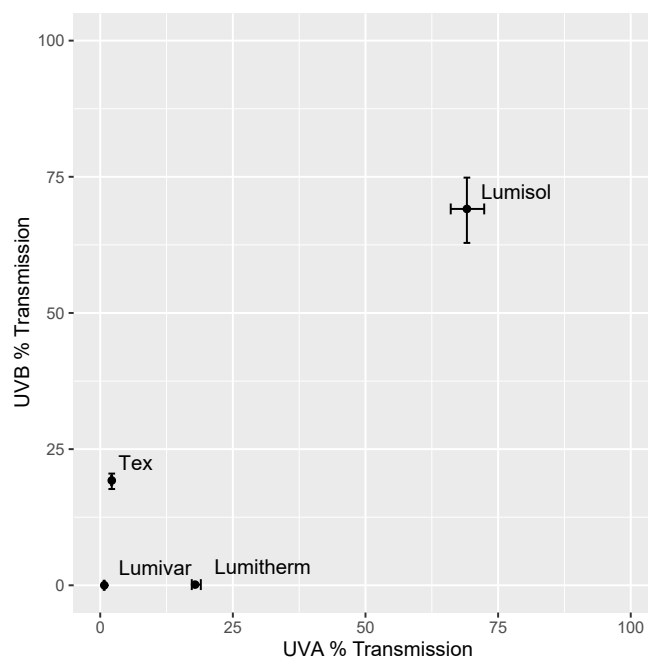


Figure 3.1: UVA and UVB % transmission for experimental structures. Points show the mean values ($n = 3$ structures per treatment) and error bars show the measured range.

3.3.3 Effect of light treatment on *Myzus persicae* PGR

In both experiments, light treatment had a significant effect on the final population size of *M. persicae* (Table 3.3, Figure 3.2). In the first experiment, *M. persicae* final population size was significantly lower ($p = 0.012$, Table 3.3, Figure 3.2.A) on Derby Day grown under UVA-|UVB+ (57 aphids plant⁻¹) than on Derby Day grown under UVA+|UVB+ (209 aphids plant⁻¹). Final population sizes under UVA+|UVB- (161 aphids plant⁻¹) and UVA-|UVB- (124 aphids plant⁻¹) were not significantly different to final population sizes under UVA+|UVB+ (Table 3.3, Figure 3.2.A).

Table 3.3: GLMM model coefficients for two separate models (cv. ‘Derby Day’ and cv. ‘Volta’) for aphid final population size. Parameters presented are: ¹ Posterior Mean. ² Lower 95% Confidence Interval. ³ Upper 95% Confidence Interval. Significance codes: * = $p < 0.05$, ** = $p < 0.01$, *** = $p < 0.001$

Experiment	Predictor	β^1	LCI ²	UCI ³	p-MCMC
Experiment 1 v. Derby Day	Intercept	5.15	4.41	5.92	< 0.001***
	UVA- UVB+	-1.41	-2.52	-0.39	0.012*
	UVA+ UVB-	-0.50	-1.54	0.59	0.338
	UVA- UVB-	-0.61	-1.75	0.40	0.241
Experiment 2 v. Volta	(Intercept)	5.11	4.64	5.60	< 0.001***
	UVA- UVB+	-0.93	-1.65	-0.27	0.011*
	UVA+ UVB-	-0.27	-0.98	0.47	0.447
	UVA- UVB-	-0.02	-0.72	0.65	0.946

In the second experiment, there was no significant effect of light treatment on final population size in Derby Day ($\beta < 0.2$, $p > 0.5$ for all treatments, Figure 3.2.B). The mean population size across all treatments was relatively high (193 aphids plant⁻¹) compared to aphids on the same cultivar in the first experiment.

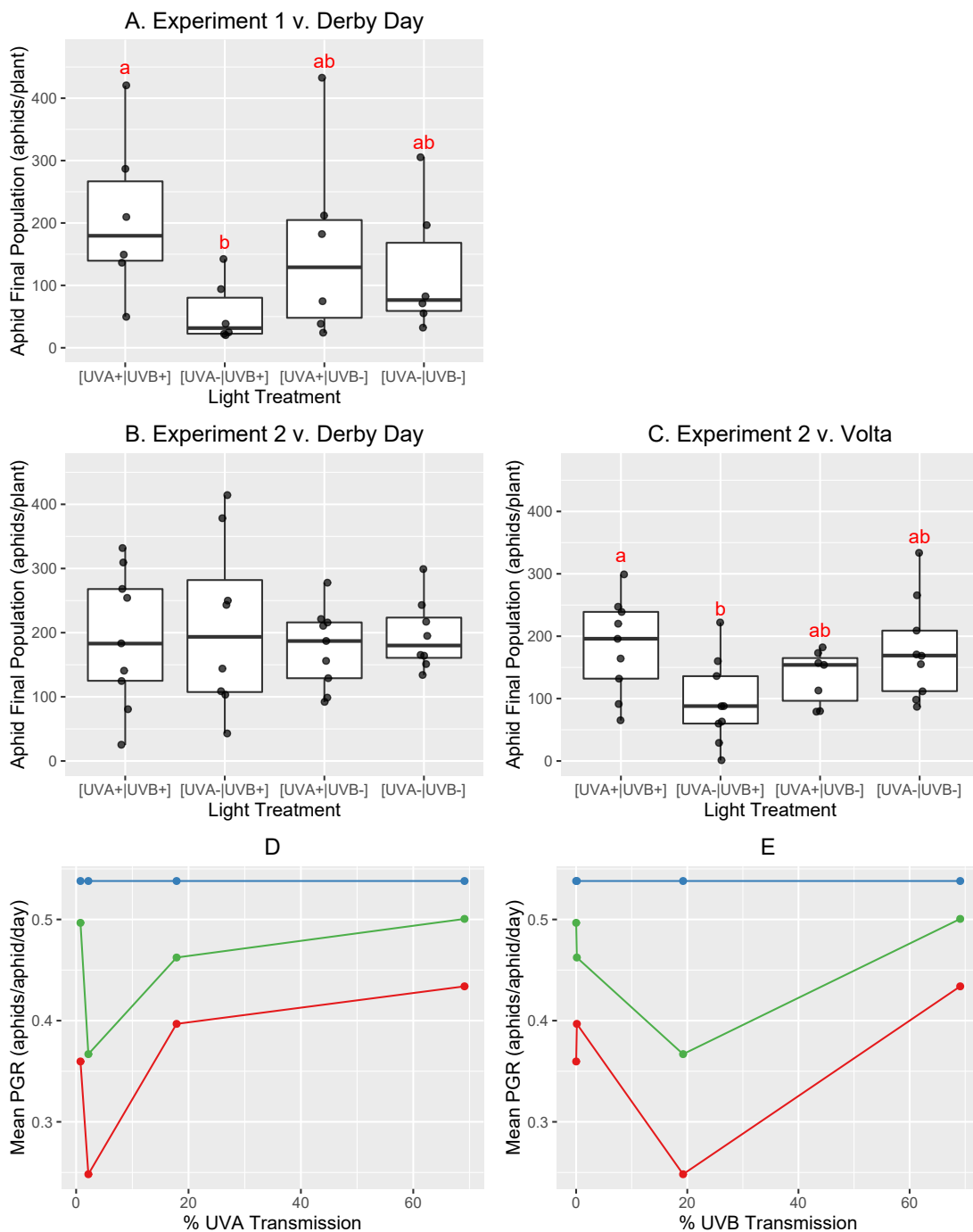


Figure 3.2: Aphid plant final population sizes and population growth rates (PGRs). Boxplots show the median, interquartile range and range for each light treatment. Panels show v. Derby Day, experiment 1 (A), v. Derby Day, experiment 2 (B) and v. Volta, experiment 2 (C). Red letters show significantly different treatments (model coefficients in Table 3.3). Mean PGRs are shown for each light treatment by tunnel % UVA transmission (D) and tunnel % UVB transmission (E). Line colours show experiment and cultivar: red = v. Derby Day, experiment 1; blue = v. Derby Day, experiment 2; green = v. Volta, experiment 2.

Aphid final population size was significantly lower ($p = 0.011$, Table 3.3, Figure 3.2.C) for aphids on Volta under UVA-|UVB+ (65 aphids plant⁻¹) compared to aphids on Volta under UVA+|UVB+ (166 aphids plant⁻¹). Final population sizes under UVA+|UVB- (127 aphids plant⁻¹) and UVA-|UVB- (162 aphids plant⁻¹) were not significantly different to final population sizes under UVA+|UVB+ (Table 3.3, Figure 3.2.C).

In order to adjust for the different size starting populations ($n=10$ in experiment 1, $n=5$ in experiment 2) in the two experiments, the PGR was calculated from the model coefficients for each light treatment and cultivar in both experiments (Table 3.4). PGR was similar between *M. persicae* on Derby Day in the first experiment and on Volta in the second experiment. The PGR for *M. persicae* on Derby Day in the second experiment was not affected by light treatment and was higher than the PGRs for Volta and Derby Day in experiment One (PGR = 0.52 aphids aphid⁻¹ day⁻¹).

In order to explain the differences between PGRs in terms of the UVA and UVB transmission of the tunnels, in the two experiments where an effect of light treatment was seen (Experiment 1, Derby Day and experiment 2, Volta), PGRs were calculated and the two datasets analysed together. The GLMM was specified as $y \sim \text{UVA} \times \text{UVB} + (1|\text{Tunnel}) + (1|\text{Experiment})$ ('Tunnel' and 'Experiment' fitted as individual random effects) where UVA and UVB were the % tunnel transmissions for the respective wavebands. The minimum adequate model was found to include the interaction term (UVA×UVB), which was highly significant ($p = 0.001$, Table 3.5). This showed that attenuation of UVA had a negative effect on aphid PGR, but only when UVB was not attenuated. As such, there was no linear relationship between PGR and UVA (Figure 3.2.D) or UVB (Figure 3.2.E) transmission of the tunnels.

Table 3.4: Mean Population Growth Rates (PGRs) for *M. persicae* on two cultivars of *B. oleracea* under four different light treatments. GLMM predicted means were used for the Derby Day, experiment 1, and Volta, experiment 2. Group mean was used for Derby Day, experiment 2 as there was no significant effect of light treatment.

	LT	Film	Cultivar	PGR
Experiment 1	UVA+ UVB+	Lumisol	Derby Day	0.43
	UVA- UVB+	Tex	Derby Day	0.25
	UVA+ UVB-	Lumitherm	Derby Day	0.40
	UVA- UVB-	Lumivar	Derby Day	0.36
Experiment 2	UVA+ UVB+	Lumisol	Derby Day	0.54
	UVA- UVB+	Tex	Derby Day	0.54
	UVA+ UVB-	Lumitherm	Derby Day	0.54
	UVA- UVB-	Lumivar	Derby Day	0.54
	UVA+ UVB+	Lumisol	Volta	0.50
	UVA- UVB+	Tex	Volta	0.37
	UVA+ UVB-	Lumitherm	Volta	0.46
	UVA- UVB-	Lumivar	Volta	0.50

3.3.4 Effect of light treatment on spatial distribution

Aphids in both experiments and on both cultivars were significantly differently distributed in the plant under different light treatments (Figure 3.3). Under UVA+|UVB+, 0.6% to 2.3% of aphids were found in exposed positions. Under light treatments with low UVA transmission (UVA-|UVB+, UVA-|UVB-), significantly more aphids (Table 3.6) were located in exposed feeding positions (2.2% to 5.9%). The UVA+|UVB- and UVA-|UVB+ treatments were not significantly

Table 3.5: GLMM model coefficients for the model $PGR \sim UVA * UVB$. Parameters presented are: ¹ Posterior Mean. ² Lower 95% Confidence Interval. ³ Upper 95% Confidence Interval. Significance codes: * = $p < 0.05$, ** = $p < 0.01$, *** = $p < 0.001$

Predictor	β^1	LCI ²	UCI ³	p-MCMC
(Intercept)	4.7×10^{-1}	-7.4×10^{-1}	1.54×10^0	0.1361
UVA %	-9.0×10^{-3}	-1.4×10^{-2}	-4.2×10^{-3}	< 0.001***
UVB %	-3.7×10^{-3}	-8.2×10^{-3}	6.8×10^{-4}	0.105
UVA x UVB	1.7×10^{-4}	7.2×10^{-5}	2.8×10^{-4}	0.001**

different to the UVA+|UVB+ control, apart from in experiment 2, v. Derby Day where significantly more aphids were found in exposed feeding positions under UVA-|UVB+ compared to the UVA+|UVB+ treatment ($p = 0.012$, Table 3.6, Figure 3.3.B). 3.9% of the total population were found in exposed positions under the UVA-|UVB+ treatment compared to only 0.6% of the total population under UVA+|UVB+.

Table 3.6: GLMM model coefficients for three separate models for proportion of aphids found in exposed positions. Parameters presented are: ¹ Posterior Mean. ² Lower 95% Confidence Interval. ³ Upper 95% Confidence Interval. Significance codes: * = $p < 0.05$, ** = $p < 0.01$, *** = $p < 0.001$

Experiment	Predictor	β^1	LCI ²	UCI ³	p-MCMC
Experiment 1 v. Derby Day	(Intercept)	-4.48	-5.54	-3.48	< 0.001***
	UVA- UVB+	1.28	-0.04	2.83	0.074
	UVA+ UVB-	0.68	-0.70	2.12	0.316
	UVA- UVB-	1.39	0.06	2.77	0.041*
Experiment 2 v. Derby Day	(Intercept)	-5.14	-6.29	-4.15	< 0.001***
	UVA- UVB+	1.93	0.47	3.31	0.012*
	UVA+ UVB-	1.15	-0.29	2.57	0.104
	UVA- UVB-	1.54	0.10	2.91	0.033*
Experiment 2 v. Volta	(Intercept)	-3.73	-4.25	-3.19	< 0.001***
	UVA- UVB+	0.60	-0.19	1.41	0.136
	UVA+ UVB-	0.33	-0.48	1.10	0.400
	UVA- UVB-	0.88	0.19	1.62	0.022*

When proportion exposed was plotted against UVA transmission, there was a negative trend (Figure 3.3.D). There did not appear to be a relationship between proportion exposed and UVB transmission (Figure 3.3.E). The relationship between UVA and UVB transmission and proportion of aphids found in exposed positions was formally tested by fitting a second GLMMs using data from the two experiments (all cultivars). Model simplification of the full model rejected the interaction (UVA \times UVB) and main effect of UVB to give the minimum adequate model: $y \sim UVA + (1|Tunnel) + (1|Experiment)$. This was fitted and checked as described previously (Materials and Methods)

Tunnel UVA transmission had a significant negative effect ($p < 0.001$, $\beta = -0.017$) on the proportion of aphids inhabiting exposed parts of the plants (Figure 3.4). The two UVA- treatments (tunnels clad in Lumivar and Tex) were predicted to have the highest proportion of aphids feeding in exposed positions (3.9% and 3.8%, respectively). The UVA+|UVB- treatment (tunnels clad in Lumitherm) was predicted to have fewer aphids inhabiting an exposed feeding position (3.0%) UVA+|UVB+ treatment was predicted to have the lowest proportion (1.3%).

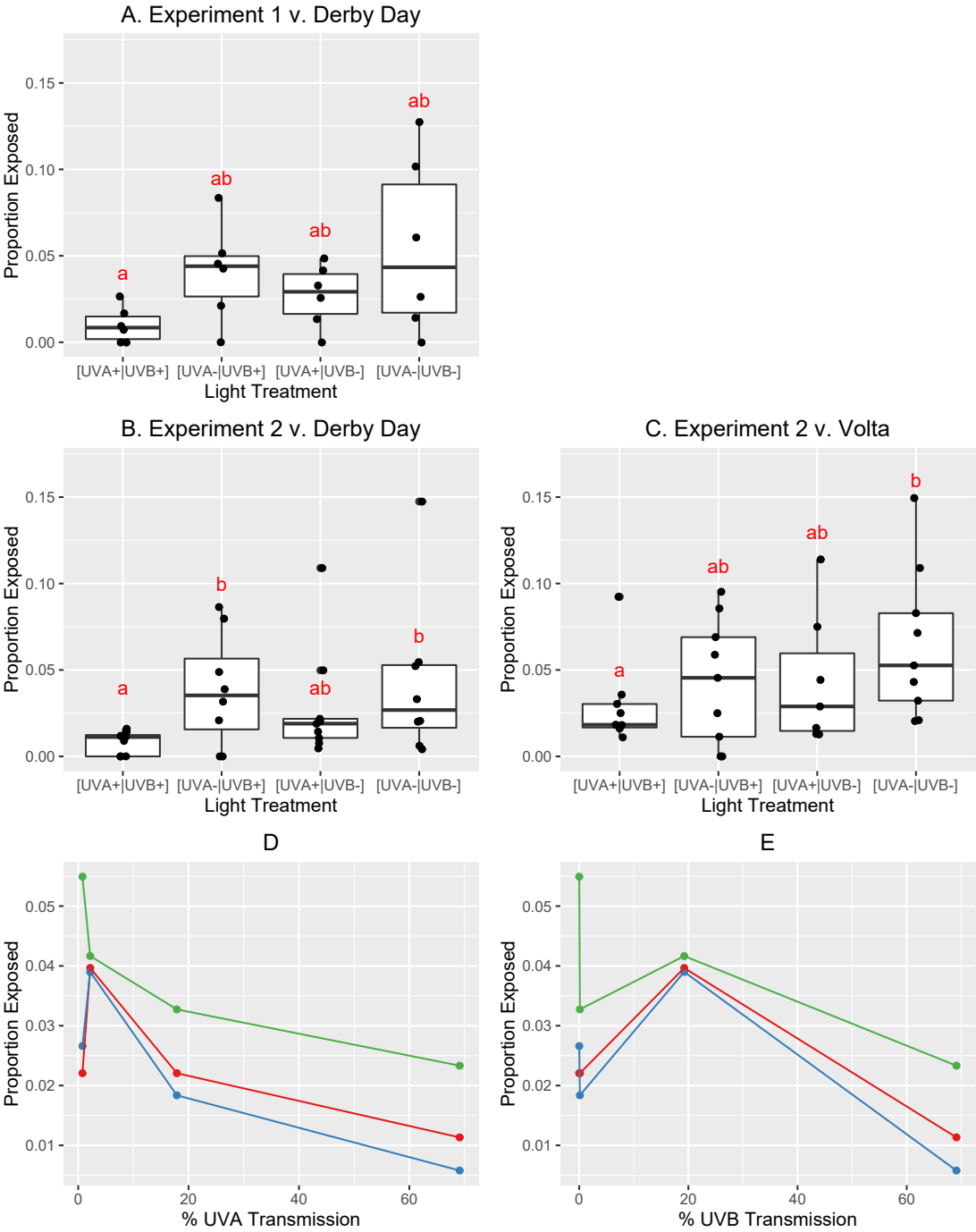


Figure 3.3: Proportion of aphids feeding in exposed positions. Boxplots show the median, interquartile range and range for each light treatment. Panels show v. Derby Day, experiment 1 (A), v. Derby Day, experiment 2 (B) and v. Volta, experiment 2 (C). Red letters show significantly different treatments (model coefficients in Table 3.3). All three treatments are shown by tunnel % UVA transmission (D) and tunnel % UVB transmission (E). Line colours show experiment and cultivar: red = v. Derby Day, experiment 1; blue = v. Derby Day, experiment 2; green = v. Volta, experiment 2.

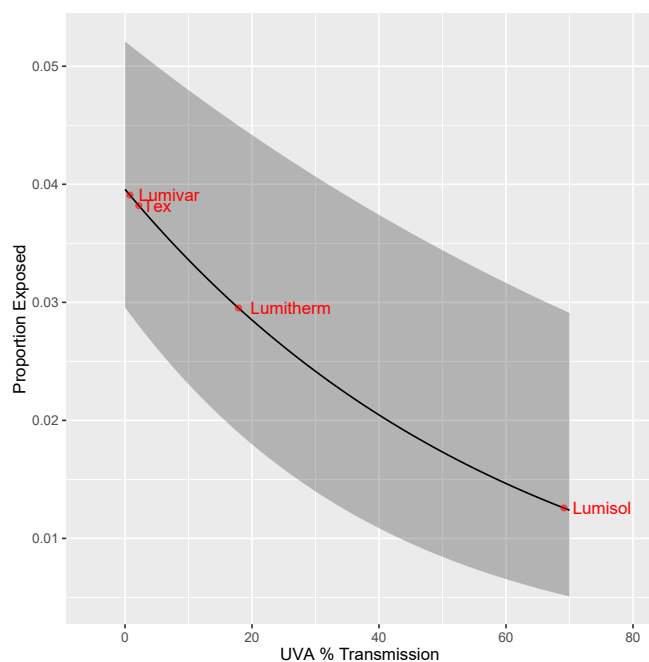


Figure 3.4: GLMM predicted mean (solid line) and 95% confidence intervals for the proportion of aphids inhabiting exposed parts of the plant at different UVA transmission values. Red dots and markers show the tunnel transmission values of the four films used in the experimental work.

3.4 Discussion

3.4.1 Plant-mediated effects of UV on aphid PGR

This study did not identify a direct relationship between UVA or UVB exposure and changes in aphid PGR. Both high (UVA+|UVB+) and low (UVA-|UVB-) had similar PGR and so, in this study, UVB-induced changes in plant chemistry are not likely to explain the differences in population size between treatments. UVB-induced changes in plant chemistry have been shown to affect the interaction between plant and insect, particularly in systems where phenolics are an integral part of the antiherbivore defence. UVB irradiation of barley (*Triticum aestivum*) caused increased probing activity and reduced feeding duration in the grain aphid (*Sitobian avenae*) (Zu-Qing et al., 2013). This was likely to have been due to increases in phloem or epidermal flavonoids, which have been shown to decrease salivation and reduce probing behaviours of aphids (Golawska et al., 2012a). UVB-induced increases in flavonoids have also been linked to decreased feeding in *Lepidoptera* (Grant-Petersson and Renwick, 1996; Hatcher and Paul, 1994; Izaguirre et al., 2007; Markham et al., 1998) as well as reduced oviposition and pupal growth (Caputo et al., 2006). Therefore, where antiherbivore defence is linked to plant phenolics, increased UVB often reduces insect fitness, however, where protection from herbivores is reliant on other phytochemicals, UVB exposure may not affect, or even inhibit defence. Some studies have shown that exposure to solar UVB does not reduce aphid PGR (Dader et al., 2014; Paul et al., 2012; Croft, 2006) compared to those grown under UV-attenuated light environments. The reasons for this are not well understood but may be attributed to reduced antiherbivore defence due to allocation of resource to photoprotection, or through UVB-induced increases in the production of compounds beneficial to herbivores (Simmonds, 2003; Carroll and Berenbaum, 2006).

Previous work with *M. persicae* on brassicas has shown varied responses to UV exposure. Excluding the UVA-|UVB+ treatment, my findings are consistent with a study which showed that *M. persicae* PGR was not significantly affected by attenuation of solar UVB (Kuhlmann et al., 2010). Whilst phloem flavonoid concentration increased with UVB exposure, total glucosinolate concentration remained broadly unchanged. As it is the glucosinolate profile, particularly the concentration of indolyl glucosinolates, which has been shown to act in defence of *M. persicae* (Kim et al., 2008b), if there is no change in glucosinolate composition or concentration (as in Kuhlmann et al. (2010)), a change in aphid PGR would not be expected. The same study did demonstrate a negative effect on the specialist aphid *Brevicoryne brassicae*, suggesting that this species may be more susceptible to UV-induced changes in flavonoids. A further study showed that UVB irradiation of brassicas pre-conditioned them against *M. persicae* attack, causing a negative PGR in aphids feeding on UVB-exposed seedlings (Mewis et al., 2012). The study demonstrated that, as well as broad increases in aliphatic glucosinolates (not as important for anti-aphid defence), UVB exposure caused small increases in indolyl glucosinolate concentration which could explain the decrease in aphid performance. I suggest that the effect of UVB-exposure of *Brassica sp.* on phloem-feeding insects may be highly dependent on the specific traits of the insect, as well as being subject to inter- and intra- specific variation amongst plants.

3.4.2 UV-induced changes in canopy position

In this study, increased occupation of the adaxial (upper) leaf surface was seen when UVA transmission into the tunnels was low or absent. Since this work was conducted in 2012, a further study has shown the same effect, in a different system (Soybean and *Aphis glycines*) where aphids were more likely to be located in exposed positions under solar UV-attenuated light treatments compared to full sunlight (Burdick et al., 2015). This suggests that there is a behavioural component in feeding site selection that is sensitive to UVA radiation. Although studies have speculated on the role of UV in feeding site selection (Luft et al., 2001; Naranjo, 2007; Paulsen et al., 2013), the majority of previous work studying aphid behavioural responses to spectral balance has focused on winged aphids during dispersal or migratory flight (see General Introduction for discussion). *M. persicae* has trichromatic vision (Kirchner et al., 2005), perceiving light in the UV (~ 300 – 400nm), blue (~ 400 – 500nm) and green (~ 500 – 550nm) spectral regions. Work on aphid vision has broadly focused on two main areas: the effect of target colour on attractiveness (Döring et al., 2007), and flight behaviours under UV-attenuated environments (Raviv et al., 2004). Alate (winged) aphids were attracted to yellow- or green-reflecting targets and repulsed by blue- or UV- reflecting targets when in dispersal flight, presumably in vegetation-seeking behaviour (Döring et al., 2007). It is also well-evidenced that flight behaviour of *Hemiptera* is disrupted by the use of UV-attenuating claddings (Doukas and Payne, 2007; Fereres and Moreno, 2009; Legarrea et al., 2012c), probably because UV light identifies the sky, allowing the aphid to maintain orientation during flight (Barta and Horváth, 2004). Very little is known about the role of UV illumination in apterous (wingless) aphid behaviour. It has been previously thought that aphids use plant-tactile cues to locate feeding sites (Simmons, 1999), however my data, like that of Burdick et al. (2015), suggest that aphids both detect UVA, and determine their feeding site in response to it.

Whilst many phloem-feeders predominantly inhabit the lower (abaxial) leaf surface (Naranjo, 2007), there are circumstances where inhabiting the upper leaf surface is advantageous, such as when the lower leaf surface has a high population density (Luft et al., 2001), when predation is

higher on lower leaf surfaces (Paulsen et al., 2013) or when plant structural defences are more obstructive on the lower leaf surfaces (Simmons, 1999). Population density has been shown to be a key factor in the prevalence of upper surface inhabitation in *Hemiptera* (Luft et al., 2001). Nymphs of the plant bug *Trioza eugeniae* were more abundant on the upper surfaces of shaded leaves when population density was high. Individual mortality was higher on unshaded, exposed leaves, suggesting that exposure to solar radiation is damaging to insects which typically inhabit sheltered parts of the plant (Luft et al., 2001). This trade-off with the hazards of the upper leaf surface (radiation, predation from the air, dislodgement, etc.) has been shown to occur when predation risk from terrestrial predators increases (Paulsen et al., 2013). The black pecan aphid, *Melanocallis caryaefoliae*, was shown to routinely inhabit the upper leaf surfaces of its host in order to avoid coccinellid predators (Paulsen et al., 2013). The authors note that there were few abundant aerial parasitoids in the bioregion where the experiment was conducted and that their presence may affect the success of this unusual strategy. Other studies have suggested that different rates of movement from the lower to the upper leaf surface may be influenced by the host leaf structure rather than by photo- or geotropisms (Simmons, 1999). Overall, it is likely that a combination of these factors play a part: when there are pressures from intraspecific competition, predation or plant defensive structures such as trichomes, movement to the upper surface may mitigate exposure to the hazards of the upper leaf surface.

3.4.3 Novel light environment generates new hypotheses

In two of the three experiments, populations of aphids grown under the novel UVA-|UVB+ light environment, had lower PGRs than aphids reared both under high UV-transmittance films (UVA+|UVB+) and UV-attenuating films (UVA-|UVB-), which had similar PGRs. As such, the low PGRs observed in the UVA-|UVB+ treatment is not likely to be explained by UVB-induced changes in plant defensive chemistry, and so an alternative hypothesis, explaining the negative effect of UVB, which occurred only when UVA was attenuated, is proposed (see Figure 3.5 for diagram):

1. Aphids were more likely to inhabit exposed feeding sites under light environments with attenuated UVA (UVA-|UVB-, UVA-|UVB+) compared to light environments which did not (UVA+|UVB-, UVA+|UVB+) and so it is likely that *M. persicae* both perceives UVA light and avoids it.
2. Under the novel light environment (UVA-|UVB+), more aphids inhabited exposed feeding sites than under UVA+|UVB+ light environments and so a greater proportion of the population were directly exposed to UV than would be expected under unfiltered sunlight.
3. This increased exposure to UVB had a direct negative effect on individuals in exposed feeding sites, causing a reduction in total plant PGR through mechanisms, as yet, unknown.

It is not known why PGR was affected by light treatment in the first experiment and not in the second experiment on the same cultivar (Derby Day), however plants in the second experiment had approximately twice the leaf area and so there may be a spatial component to this mechanism. We also found variation in the PAR transmissions of the different films. Although PAR was not linearly related to total UV, UVA or UVB transmission, an effect of PAR on aphid PGR cannot be discounted at this stage. This variation in PAR transmission, as well as the inherent variability in environmental conditions (e.g. total irradiance, temperature, humidity etc.) meant that a different approach was needed to isolate the mechanism proposed above. In Chapters 4-6,

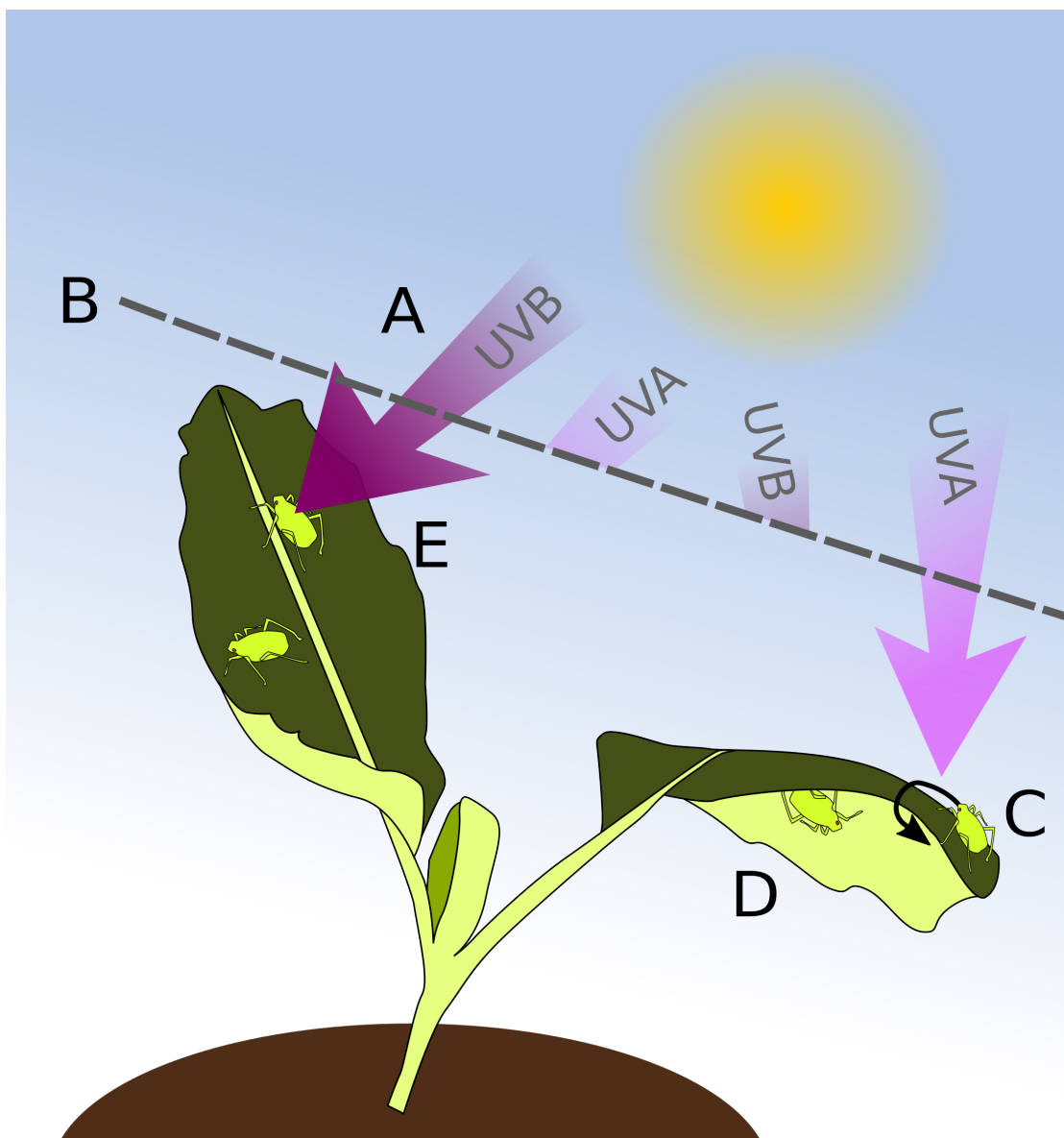


Figure 3.5: Putative mechanism for direct effect of UV on aphids. Solar UVA and UVB (A) is selectively filtered by spectrally-manipulating films (B). When UVA is transmitted into the tunnel, it is perceived by the aphid (C), causing it to move to sheltered feeding sites within the plant (D). However when UVA is not transmitted, aphids do not move to sheltered feeding sites. When UVB is transmitted but UVA is not, aphids are exposed to UVB (E) which has a direct, negative effect on PGR.

I move from field-scale approaches such as this, to refined campaigns of controlled laboratory work in order to test the fundamental hypotheses generated from the work presented here.

3.5 Conclusions

In summary, the results presented here show two important findings: Firstly, that the relationship between UV exposure and the population growth of phloem-feeding insects is not consistent in all varieties of *B. oleracea* and in all *M. persicae* strains. I did not find a relationship between UVB exposure and aphid population size and suggest that plant-mediated UVB responses are unlikely to be an important constraint on aphid population size in the study system. However, this work illustrates how the relationship between UVB exposure and herbivores cannot be easily generalised.

Secondly, through the use of a novel film, for the first time, the effect of UVB in the absence of UVA could be tested, yielding surprising results. This allowed us to identify two new hypotheses that (i) wingless *M. persicae* perceive UVA and use it to position themselves in parts of the plant which are less exposed to solar radiation and (ii) that this is because exposure to solar UVB has a deleterious effect on the aphid population, either through increasing mortality or reducing fecundity. These hypotheses are tested in Chapters Four (Effect of solar UV on *M. persicae* mortality) and Six (Evidence for a novel functional role of the UV photoreceptor in *M. persicae*) of this thesis.

Characterising the direct effects of UV radiation on *Myzus persicae*

Abstract

Background: In the previous chapter, data from a field experiment showed that populations of aphids which, through changes in their behaviour, are directly exposed to solar ultraviolet (UV) may experience lower Population Growth Rate (PGR). Other studies have shown a negative effect on PGR when aphids and plants have been exposed to high UV, however, these studies have failed to isolate the direct effect on the aphid from previously identified plant-mediated effects of UVB.

Results: A dose response was characterised in *Myzus persicae* using different wavebands and doses to irradiate aphids independently of the host plant. Mortality was negatively related to CIE (erythema)-weighted dose ($p < 0.0001$). UK summer mean daily equivalent doses predicted mortality of 41-43%, indicating that aphid populations exposed to full sunlight would have negative PGR.

Conclusions: Ambient UV is highly damaging to *M. persicae* and so this species must have adaptations to mitigate this. Photoprotective physiological responses may form a component of this, however adaptation is also likely to be behavioural whereby *M. persicae* responds to UV and avoids exposure.

4.1 Introduction

The results of field experiments which tested the effect of UV manipulation on the growth of *Myzus persicae* on *Brassica oleracea* led to a hypothesis that aphids had increased exposure to UV under certain light conditions, and that this increased exposure had a negative impact on PGR (3.3.3). Previous studies have demonstrated a plant-mediated effect of UV, where plant photoprotective responses to UV reduced the PGR of aphids, even though the aphids had not been exposed to UV (Mewis et al., 2012). Indirect effects of plant ultraviolet-B (UVB) exposure have been well documented in *Lepidoptera* with insects showing reduced feeding preference and larval weight (Caputo et al., 2006; Grant-Petersson and Renwick, 1996; Hatcher and Paul, 1994), reduced larval survival (Zavala et al., 2001) and reduced preference for UVB-exposed material as oviposition sites (Foggo et al., 2007). This response has been broadly attributed to overlap in UV photoprotective responses of plants with antiherbivore defence (Ballaré, 2014). However, this response may be host-specific (Dader et al., 2014) and depends on the extent to which these two plant mechanisms overlap (Caputo et al., 2006).

Whilst there is evidence that UV exposure may reduce insect PGR through induced changes in plant defence, it may not be the only mechanism by which UV affects insect populations. In Chapter Three, aphids were found to be more numerous in exposed leaf positions under treatments with attenuated UVA. Aphid populations were smallest under treatments that attenuated ultraviolet-A (UVA), but did not attenuate UVB. This was not attributed to plant response to UV because treatments that had higher UVB doses had larger aphid populations and so it was hypothesised that aphids were more likely to expose themselves to UVB under UVA-attenuated treatments, which had a direct effect on their survival or fecundity (3.4.3). Direct effects of UV on survival of *Hemiptera* have not previously been conducted in isolation of the plant, however, there are some experiments that show a negative effect on overall PGR at high UV irradiances, which may be via a direct effect on the aphid (Burdick et al., 2015; Dader et al., 2014; Tariq et al., 2015). In other invertebrates, UVA and UVB exposure has been directly linked to increased egg (Fukaya et al., 2013) and adult (Zhang et al., 2011a) mortality.

UV exposure may also affect insect physiology such that PGR is affected independently of mortality. UV irradiation at moderate doses has been linked with increases in reproductive effort (Dader et al., 2014; Fukaya et al., 2013; Hu et al., 2013; Tariq et al., 2015), possibly as mitigation for increased egg or larval mortality (Murata and Osakabe, 2013). Reproductive effort may also decline as a result of UV stress due to the physiological costs of compensating for UV-induced damage (Meng et al., 2009). These sublethal mechanisms may be as important in predicting UV-induced changes in PGR as mortality effects, although they are, as yet, little understood.

This chapter sought to establish the response of *M. persicae* to UV radiation, independently of potential plant-mediated mechanisms. Both mortality and post-exposure PGR were quantified in order to determine the presence of any dose-dependent lethal or sublethal effects. These findings were then placed into an environmentally relevant context through the use of Biological Spectral Weighting Functions (BSWFs) as an improved method for describing and using radiation dose information.

4.2 Methods

4.2.1 Plants and insects

Brassica oleracea (v. 'Volta') was used as the host for the aphid stock culture and experimental work. Plants were grown in 500 mL drinking cups with 100 mL of compost in the bottom as described previously (2.1.4). The bottom of each cup was pierced and the cup placed on moistened fibre matting in a large seed tray. Seeds were sown directly into the cups three weeks prior to aphid irradiation. After one week of growth under propagator hoods, the hoods were removed and any surplus seedlings removed, leaving one plant per cup. Experimental repeats 1-6 were conducted in a fully temperature controlled glasshouse which was maintained at $15\pm 1^\circ\text{C}$. experimental repeats 7-9 were conducted in a partially temperature controlled glasshouse where the mean temperature for each experiment was between 20°C and 22°C .

Aphid stocks were reared in the same glasshouses as the plants (2.1.3) in large tent cages prior to UV exposure. As discussed in 2.1.3, *Myzus persicae* reproduces asexually and has a generation time of approximately 2 weeks under the glasshouse conditions used for the experimental work (2.1.2). Prior to irradiation of aphids, exposure to short wavelength UVB was expected to be negligible (maximum measured erythema irradiance $\sim 0.006\text{ W m}^{-2}$) as the glasshouse glass does not transmit light in these ranges, however the glasshouse did transmit some longer-wavelength UV ($> 320\text{nm}$).

4.2.2 Light treatments

UV dose and spectral quality was manipulated using various combinations of optical filters and lamps (Table 4.1). Three fluorescent tube lamps were used to deliver UV doses in different parts of the UV spectrum: UVB313 which delivers predominantly UVB and some short wavelength UVA; UVA340 which produces mainly short wavelength UVA; and UVA360 which produces long wavelength UVA. UVA340 tubes were filtered with Mylar ($\lambda_{\text{min}} \approx 340\text{nm}$) to attenuate UVB and ultraviolet-C (UVC). UVB313 and UVA360 tubes were filtered with cellulose acetate ($\lambda_{\text{min}} \approx 290\text{nm}$) low-cut filters to attenuate short wavelength UVB or UVC not experienced under solar illumination (details in Table 4.1). Additional polyethylene (PE) films and steel gauze neutral density (ND) filters were used to further alter spectral quality and intensity (Table 4.1). Further details of lamps and filters are presented in 2.4. These filters and lamp combinations were selected to provide a range of different qualitative and quantitative treatments across the environmentally-relevant UV spectrum (wavelengths $>290\text{nm}$). Using different qualitative treatments (as opposed to varying only irradiance) allowed the use of techniques for assessing different BSWFs as models of aphid response to UV (see 4.3.2).

Light treatments were given in a purpose built fluorescent tube housing with a temperature controlled surface positioned directly below the fluorescent tubes. The irradiation surface was removable such that a cosine corrected head could be located with the light collection surface at the same level as the irradiation surface, below the lamps. Spectroradiometer measurements were made (2.4.4) with the cosine head covered with the filters described in Table 4.1.

Table 4.1: Light Treatments for the experimental work presented in 4.3. Description and transmission of the filters is presented in 2.4

Treatment	Lamp	Position	Low-Cut Filter	Film	ND Filter
1	UVB313	8	Cellulose Acetate	Lumivar	None
2	UVB313	12	Cellulose Acetate	Tex	1x ND
3	UVB313	10	Cellulose Acetate	Tex	None
4	UVB313	14	Cellulose Acetate	Lumivar	None
5	UVB313	8	Cellulose Acetate	2x Tex	None
6	UVB313	12	Cellulose Acetate	3x Tex	None
7	UVB313	8	Cellulose Acetate	Lumisol	1x ND
8	UVA360	8	Cellulose Acetate	Lumisol	None
9	UVA360	10	Cellulose Acetate	Lumisol	1x ND
10	UVA360	12	Cellulose Acetate	Lumisol	2x ND
11	UVA340	10	Mylar	None	1x ND
12	UVA340	8	Mylar	None	None
13	UVA340	12	Mylar	None	2x ND
14	UVA340	14	Mylar	None	None
15	UVA360	14	Mylar	None	None

4.2.3 Exposure procedure

An aluminium block with a 60 mm diameter hole cut through it was used to contain each treatment cohort of aphids (Figure 4.1). On the underside of the block, a square of filter paper was taped into place, forming the base of the containment chamber. This was moistened with DI water and aphids were transferred individually onto the paper, using a fine paint brush. After transferring all aphids to the filter paper, the chamber was sealed by taping the low cut filter (Mylar or cellulose acetate) over the upper surface with masking tape. The other optical filters were similarly taped in place, forming a window through which the aphids could be irradiated. After allowing a 30 minute lamp warm-up period, the sealed containment chambers were placed on the temperature controlled plate in the exposure chamber (Figure 4.1). As the aphids were irradiated independently of plant material, it was expected that this would be somewhat stressful as they would be expected to spend the irradiation period seeking a host plant. In order to reduce the effect of this, a refrigeration unit was used to cool the temperature controlled plate to 10°C in order to slow movement and so reduce energy expenditure from attempting to seek out a host. Aphids were exposed for between one and six hours, depending on treatment. As a component of this chapter involved the identification of appropriate BSWFs for aphid mortality, doses for each treatment are presented and discussed in the results and discussion sections.

4.2.4 Population growth procedure

Once irradiation was complete, the optical filters were carefully removed from the aluminium block to retrieve the aphids. Aphids were tested for instantaneous mortality by gently probing with a fine paintbrush. Each aphid was then placed on a separate 3-week old *Brassica oleracea* (c.v. "Volta") seedling, grown in a 500 mL drinking cup. To secure the aphids within the cups, a domed 'smoothie' cap with a piece of fine muslin grown glued over the drinking hole, was placed on top of each cup. The cups were returned to the glasshouse and the aphid population allowed to grow for a week. At the end of the seven day period, the number of aphids in each cup was recorded as well as whether or not the original aphid was apterous (wingless) or alate (winged)

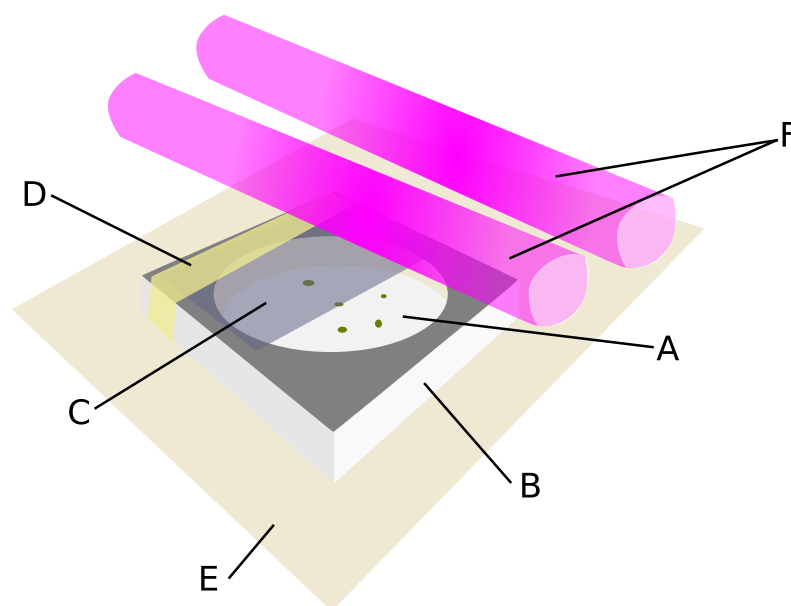


Figure 4.1: Exposure Procedure. Aphids were placed on moistened filter paper (A) which was taped securely to the base of an aluminium block (B) with a circular hole cut through it. Optical filters (C, specified in Table 4.1) were taped in place with masking tape (D) so that they completely covered the circular hole (shown partially covered for illustration purposes). The metal moulding was placed on a temperature controlled plate (E) in the exposure chamber, beneath the fluorescent tubes (F).

at the point of harvest. As the generation time for *Myzus persicae* is approximately 9-13 days under glasshouse conditions (2.1.2), any additional aphids recovered were assumed to be the offspring of the original single individual placed in the cage, and so it was possible to estimate the population growth of a single cohort.

4.2.5 Statistical analyses

The R-statistical package was used for all analyses and plots as described previously (2.4.3). For mortality analysis, binomial Generalised Linear Models (GLMs) were fit to the data, using the quasibinomial family to compensate for overdispersion where applicable. For final population counts, Poisson GLMs were used to estimate the effect of UV, aphid morph and the temperature covariance of the glasshouse, on final population size. Model simplification was conducted using the 'drop1' function in the 'stats' package. In order to establish which BSWF best described aphid mortality in response to UV, a number of similar models were compared. The residual deviances were used as a proxy measure of model fit and so a reduction in residual deviance was considered an improvement in model fit, as described in (Crawley, 2007). Handling of spectral data and subsequent convolutions and calculations were made using the 'photobiology' package.

4.2.6 Further population modeling

In order to establish the effect of repeated exposure (i.e. a daily dose of UV every day throughout the growing period), two separate components must be incorporated into a single, continuous-time model: the mortality effect (a discrete-time model) and the PGR of survivors (a continuous time model). So that this model was more useful in modeling applications, the CIE (erythemal)

dose was used as the dose parameter because CIE dose and irradiance information are more widely available than full spectrum data.

After an aphid has been irradiated, it may either die before reproduction ('died') or survive to reproduce and produce offspring ('survive'). The probability that an individual aphid is killed by a single dose (P_m) can be related to UV dose (d) by using inverse logistic transformation of the GLM such that:

$$P_m = \frac{e^{\beta_0 + \beta_1 \ln(d)}}{1 + e^{\beta_0 + \beta_1 \ln(d)}} \quad (4.1)$$

In this equation, β_0 is the GLM intercept coefficient and β_1 is the coefficient for $\ln(d)$ (Crawley, 2007).

For the second component of the combined population model, the standard PGR model is used to estimate the survivor PGR. Population growth may be calculated using the standard population model (Renshaw, 1993):

$$N_t = N_0 e^{rt} \quad (4.2)$$

rearranged with respect to r :

$$r = \frac{\ln\left(\frac{N_t}{N_0}\right)}{t} \quad (4.3)$$

where N_t is the population size after a given time, N_0 is the starting population, r is the continuous PGR and t is the population growth period.

The effect of UV on survivor fecundity may be quantified by testing for changes in final population size from populations originating from a single survivor. Where there is an effect of UV exposure on fecundity, the GLM equation may be incorporated into the above equation to calculate the effect of UV dose on r . Alternatively, where there is no effect of UV on the subsequent PGR of a population from a single survivor, a constant PGR may be used for r .

Once the continuous-time model for r has been established, this must be combined with the mortality probability of UV exposure to calculate the overall PGR (R) for a repeated exposure scenario:

$$R = \ln((1 - P_m)e^r) \quad (4.4)$$

4.3 Results

Aphids were exposed to a single dose of UV on filter paper. After UV-exposure, aphids were transferred to individually-caged calabrese plants for seven days (one aphid per plant). All aphids survived initial exposure and transfer to host plant and, after seven days growth on the host plant, the final population was counted. If no aphids were present on a plant, the individual was recorded as having died from exposure ('died'). If one or more aphid remained on the plant after seven days, the aphid was recorded as having survived exposure ('survived'). One dataset (out of 9) was excluded due to high mortality in the control treatment, attributed to disease infection.

An analysis of mortality was first examined by spectral treatment (lamp type) and unweighted UV irradiance. Appropriate action spectra were then compared to establish which BSWFs best described the mortality probability of an aphid exposed to a single dose of UV. Aphids that survived exposure and transfer were used to estimate PGR after UV-exposure. These two models (separately describing mortality and PGR) were combined to produce a continuous time model of

aphid PGR under repeated daily UV exposure to standardised UK summer illumination. Finally, this model was used to generate predictions for different films under UK summer conditions.

4.3.1 Aphid mortality

The three lamp types (UVB313, UVA340 and UVA360) provided the core spectral classes for this study with total UV dose the continuous variable. Mortality ('survived' or 'died') for each aphid was fitted in a binomial GLM with unweighted UV dose and lamp type as predictors in the model. Model simplification showed the interaction term to be non-significant and so the additive model $y \sim \ln(\text{dose}) + [\text{lamp type}]$ was determined to be the minimum adequate model. Model fit was improved through use of a quasipoisson family to compensate for overdispersion, and by natural log-transforming UV dose.

Mortality increased with unweighted UV dose and the magnitude of this effect was determined by the spectral balance (lamp type) (Table 4.2, Figure 4.2). For treatments of the same unweighted irradiance, radiation from the UVB313 source was more than an order of magnitude more lethal ($LD_{50} = 30.8 \text{ kJ m}^{-2}$) than the radiation from a UVA340 source ($LD_{50} = 1365 \text{ kJ m}^{-2}$). All aphids survived under UVA360 lamps therefore an LD_{50} could not be estimated and the relative effect size of UVA360 UV irradiation was therefore set to 0.

Table 4.2: Coefficients for the quasibinomial GLM model $y \sim \ln(\text{dose}) + \text{lamp}$ used to test the effect of unweighted UV from three different illumination sources on the mortality of *M. persicae*. Significance codes: * = $p < 0.05$, ** = $p < 0.01$, *** = $p < 0.001$.

	Estimate	Std. Error	t value	Pr(> t)
(Intercept)	-3.8445	0.6408	-5.9998	<0.001 ***
Ln(UV dose)	0.5325	0.0955	5.5745	<0.001 ***
Lamp: UVA360	-17.1860	949.3743	-0.0181	0.9856
Lamp: UVB	2.0199	0.4919	4.1065	<0.001 ***

4.3.2 Identification of appropriate BSWF

The use of two, spectrally-distinct UVA-sources (UVA360 and UVA340) and a UVB source, each clad with different combinations of spectrally-modifying filters (see Table 4.1) gave a broad range of spectral qualities and irradiances. In order to account for the different biological effectiveness of photons of different wavelengths (and therefore different energies), the identification of BSWFs which best describe the relationship between *M. persicae*, irradiance and spectral balance was an essential part of this study. Two separate approaches were used to identify BSWFs that best predict aphid mortality following a single UV exposure. In the first, normalised model effect sizes for the three lamp types were compared to candidate BSWFs, to estimate which best approximated the response seen in the data presented here. In the second approach, for each BSWF or waveband of interest, a GLM was fitted, comparing dose to mortality. Measures of model fit were used to rank the models by how well they fitted the data and so identify the BSWFs that best predicted mortality.

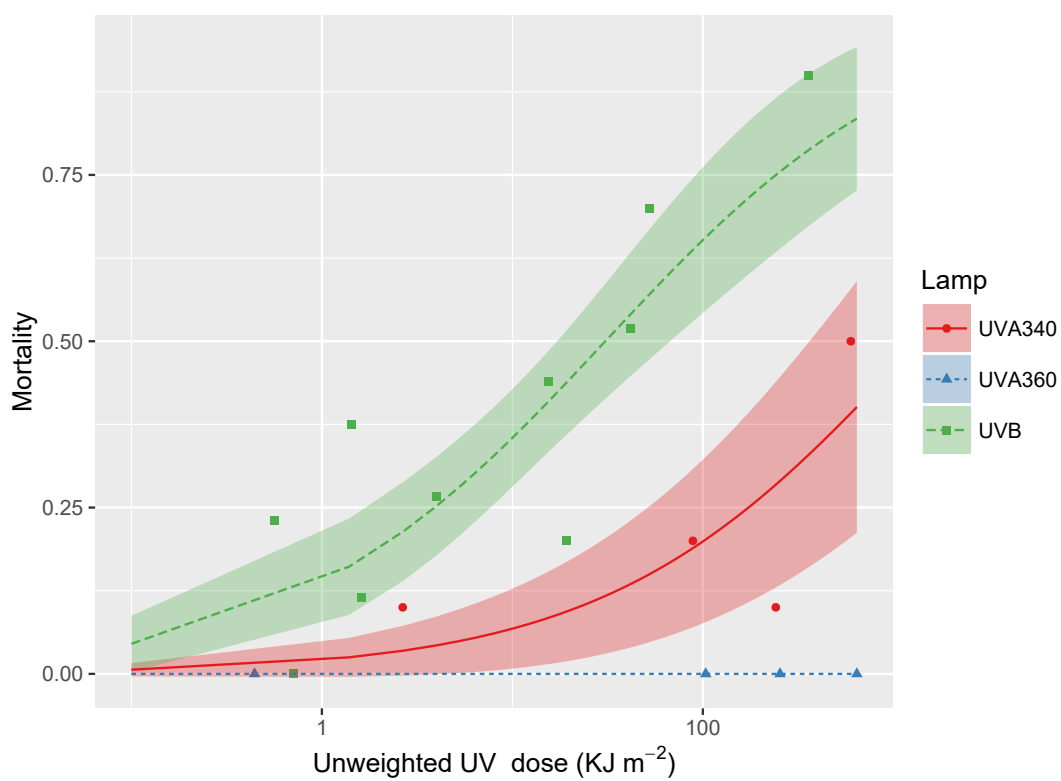


Figure 4.2: Mortality and model predictions by lamp type and UV irradiance (\log_{10} scale). Individual points show the proportional mortality for each treatment (as described in table 4.1). The lines and confidence bands show the prediction of mortality and 95% confidence intervals as predicted by the GLM $y \sim \ln(\text{dose}) + \text{lamp}$.

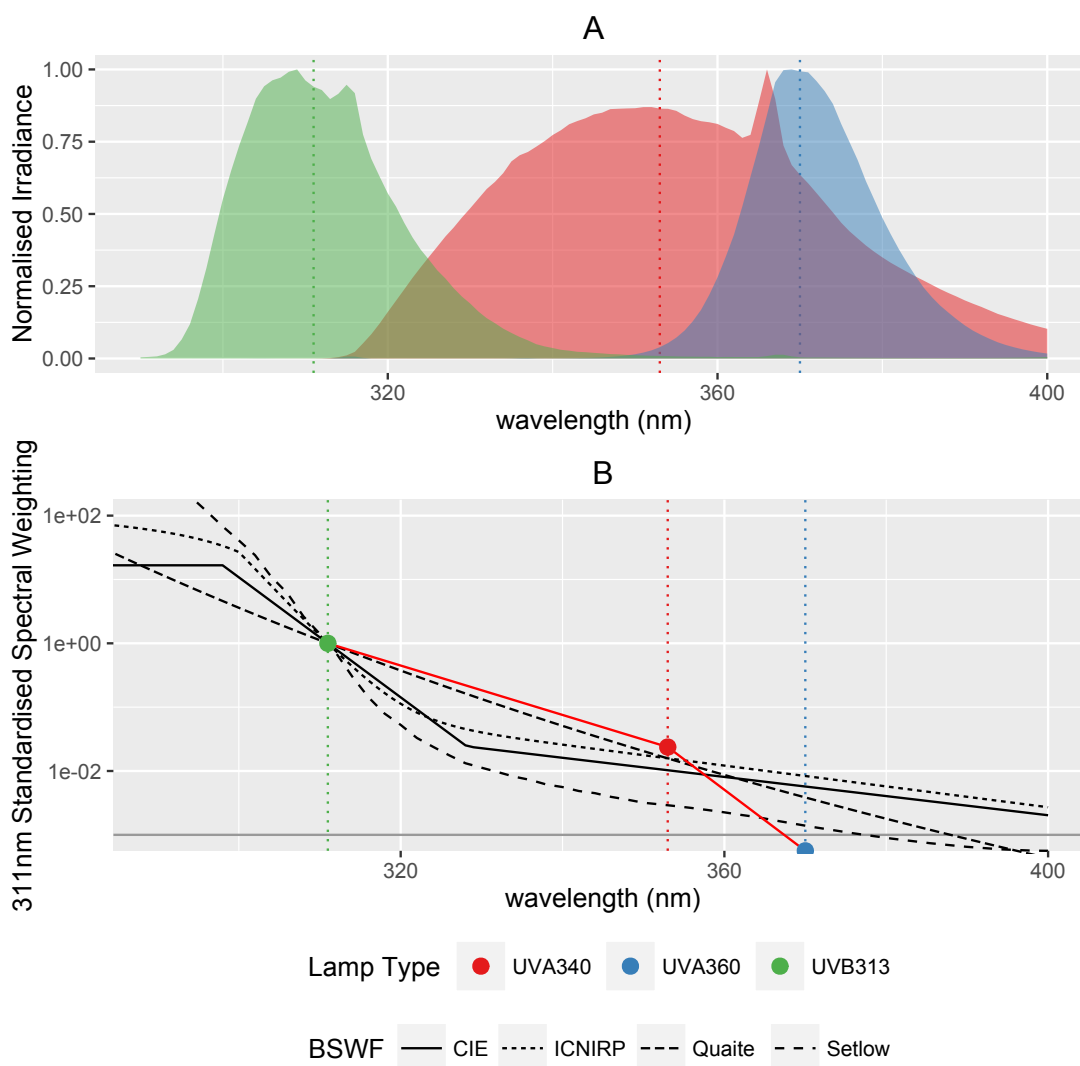


Figure 4.3: Lamp and action spectra for identifying appropriate BSWFs for UV-induced aphid mortality. (A) shows lamp spectra normalised to one with dashed lines showing the approximate waveband centres. (B) shows four candidate action spectra for aphid mortality on a log scale, standardised to one at 309 nm. The red line and coloured dots show the relative effect size (normalised to one at 309 nm) of lamp type on mortality for each of the three lamp types at the approximate waveband centres identified in (A).

Approach One:

Normalised spectra for the three lamp types were used to estimate the peak centre of each (Figure 4.3.A). This was done by finding the central point by integrated irradiance between 290 nm and 400 nm (i.e. the wavelength that divides the spectrum into two equal halves by energy). For UVB313 tubes this was 311 nm, for UVA340 tubes this was 353 nm, and for UVA360 tubes this was 370 nm. The relative effect sizes of each lamp on mortality, estimated by the GLM (Table 4.2), were scaled to one at 309 nm and compared to human health ('CIE' (Commission Internationale d'Éclairage, 1999) and 'ICNIRP' (International Commission on Non-Ionising Radiation, 2004)), naked DNA ('Setlow' (Setlow, 1974)) and *in vivo* plant DNA ('Quaité' (Quaité et al., 1992)) BSWFs (Figure 4.3.B).

Aphids irradiated with the UVA340 source had higher expected mortality than is predicted by any of the human health or DNA BSWFs, suggesting that the BSWF best predicting the effect of UV

Table 4.3: Residual deviances and main effect p -values for seven candidate models predicting aphid mortality. The models are ordered by residual deviance with the lowest deviance (and therefore the best fitting model) first. Significance codes: * = $p < 0.05$, ** = $p < 0.01$, *** = $p < 0.001$.

Model	Residual Deviance	Pr(> t)
died \sim ln(Dose _{Quaite})	263.03	< 0.001***
died \sim ln(Dose _{ICNIRP})	264.32	< 0.001***
died \sim ln(Dose _{CIE})	264.48	< 0.001***
died \sim ln(Dose _{Setlow})	267.32	< 0.001***
died \sim ln(Dose _{UVB})	268.84	< 0.001***
died \sim ln(Dose _{UV})	309.86	0.001**
died \sim ln(Dose _{UVA})	316.03	0.031*

on mortality in this part of the spectrum, had a high relative weighting at 353 nm. Additionally, aphids irradiated with a UVA360 source had 100% survival, suggesting that the relative effect of UV at 370 nm was zero. With the exception of the Setlow BSWF (which predicts an effective weighting of zero), the three other BSWFs predict that there will be a relatively small effect of light with a wavelength of 370 nm. Therefore the best fitting BSWF should balance high effectiveness of radiation at 353nm and very low effectiveness at 370 nm. Setlow predicts zero effectiveness at 370 nm but underestimates irradiation at 353 nm (Figure 4.3). Quaite appears to offer the best fit, slightly underestimating effectiveness at 353 nm and over-estimating at 370 nm.

Approach Two:

For all treatments, the four BSWF-weighted (Quaite, ICNIRP, CIE and Setlow) and unweighted waveband (UV, UVA UVB) doses were calculated and used to fit seven models (model fits and raw data presented in Figure 4.4). Natural log transformation of dose always yielded lower deviances and better fitting models compared to untransformed equivalent models. The models were ranked by residual deviance (Table 4.3). The Quaite *in vivo* DNA model was the best fitting and unweighted UVA the worst. However, the four BSWFs-weighted models (Figures 4.4.A-D) and the UVB model (Figure 4.4.E) all had similar residual deviances and therefore described the data similarly. Unweighted UV and UVA were very poorly-fitting models (Figures 4.4.F-G) with much larger deviances than the other models (Table 4.3). Therefore any of the four BSWFs or unweighted UVB irradiance models can be recommended for use predicting *M. persicae* mortality but should be prioritised in the order presented in (Table 4.3).

Model parameters are presented for the Dose_{Quaite} (Table 4.4) and for the Dose_{CIE} model (Table 4.5). The Quaite model was the best fitting model, with the lowest residual deviance (263.03). The CIE model was the best fitting model (deviance of 264.48) for which there is widespread spatial and temporal data available (DEFRA, 2016; NASA, 2016; SoDa, 2016).

Table 4.4: Quasibinomial GLM model parameters for the model $y \sim \ln(\text{Dose}_{\text{Quaite}})$ predicting the mortality of aphids exposed to different doses of Quaite-weighted radiation. Significance codes: * = $p < 0.05$, ** = $p < 0.01$, *** = $p < 0.001$.

	Estimate	Std. Error	t value	Pr(> t)
(Intercept)	-1.4218	0.2248	-6.3252	< 0.001***
ln(Dose _{Quaite})	0.5733	0.1023	5.6020	< 0.001***

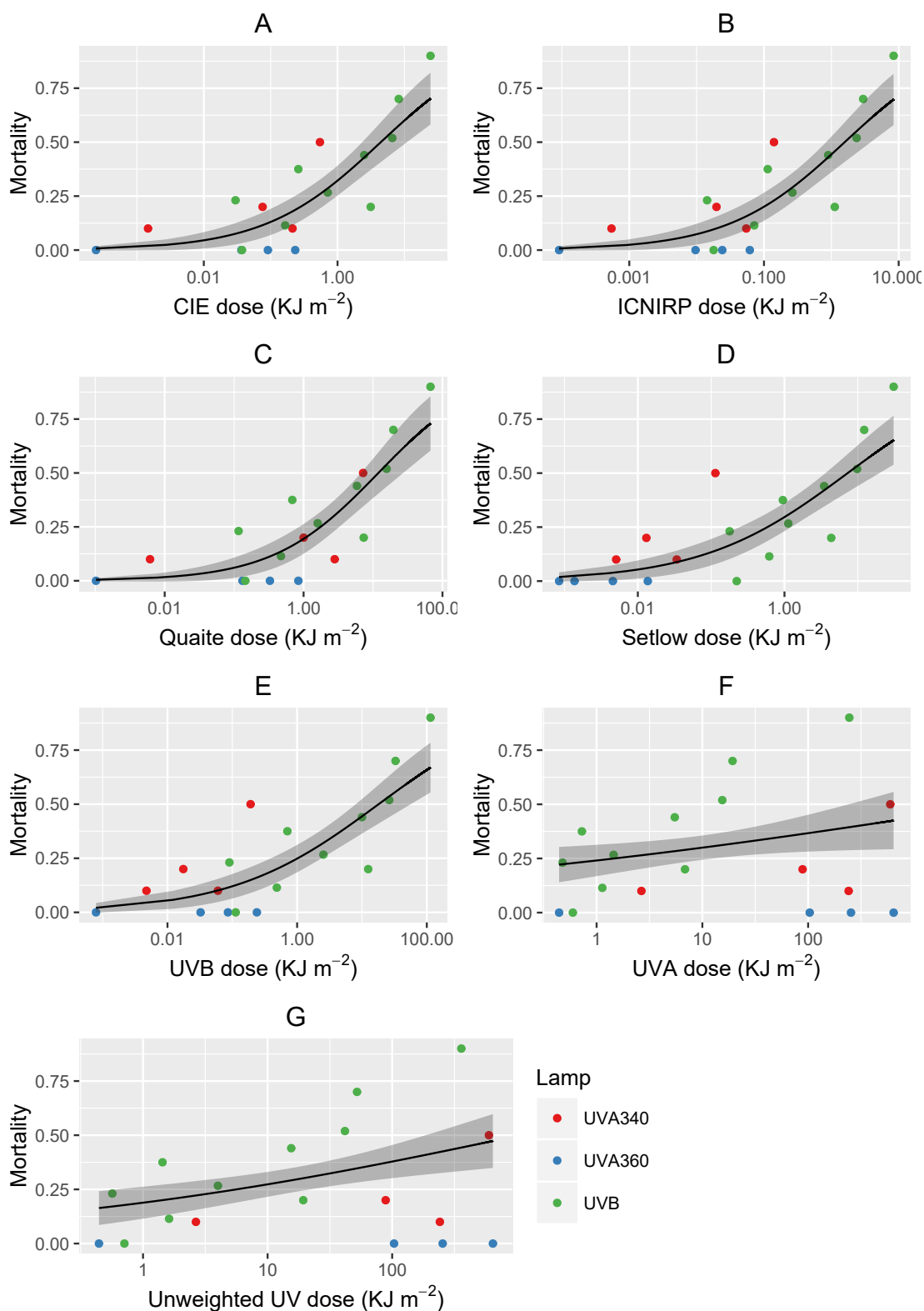


Figure 4.4: Aphid mortality described by different BSWFs. For all plots, individual points show the proportional mortality for each treatment (as described in table 4.1) and the lines and confidence bands show the estimated mortality and 95% confidence intervals respectively. (A-D) show the mortality predictions for CIE (erythemal), ICNIRP (human exposure), Quaité (*in vivo* DNA) and Setlow (naked DNA). (E-G) show the mortality predictions for unweighted UVB, UVA and UV, respectively.

Table 4.5: Quasibinomial GLM model parameters for the model $y \sim \ln(\text{Dose}_{\text{CIE}})$ predicting the mortality of aphids exposed to different doses of CIE-weighted radiation. Significance codes: * = $p < 0.05$, ** = $p < 0.01$, *** = $p < 0.001$.

	Estimate	Std. Error	t value	Pr(> t)
(Intercept)	-0.7458	0.1620	-4.6048	< 0.001***
$\ln(\text{Dose}_{\text{CIE}})$	0.5001	0.0846	5.9111	< 0.001***

Table 4.6: Quasipoisson GLM model parameters for the model $y \sim \text{morph} \times \text{temperature}$ predicting aphid population growth rate of survivors of UV irradiation. Significance codes: * = $p < 0.05$, ** = $p < 0.01$, *** = $p < 0.001$.

	Estimate	Std. Error	t value	Pr(> t)
(Intercept)	0.2376	0.2808	0.8462	0.399
Morph: Alatae	2.4131	0.7684	3.1405	0.002**
Temperature	0.1431	0.0147	9.7383	< 0.001***
Morph: Alatae x Temperature	-0.2019	0.0419	-4.8231	< 0.001***

4.3.3 Sublethal effects

In order to establish the effect of dose on aphid PGR, all aphids irradiated were caged individually and the population counted after seven days in the glasshouse. Experiments 1 to 6 were conducted in a fully temperature-controlled glasshouse ($15 \pm 1^\circ\text{C}$) and experiments 7 to 9 were carried out in a glasshouse with partial temperature regulation. As *M. persicae* development and reproductive rate is largely dependent on temperature (Davis et al., 2006), mean glasshouse temperature over the experimental period was used as a covariate in the statistical model. Additionally, if a winged (alate) aphid was found during the final count, this was assumed to be the original aphid irradiated (as the developmental period for a winged aphid from birth to maturity is greater than one week) and so morph (winged or wingless) was used as a predictor in the model. For aphids exposed to the highest treatment ($\text{Dose}_{\text{Quaite}} = 67 \text{ kJ m}^{-2}$), there was a single surviving aphid and so this was removed from the growth rate analysis.

The full model was specified as $y \sim \ln(\text{Dose}_{\text{Quaite}}) \times \text{morph} \times \text{temperature}$, using the quasipoisson family to compensate for overdispersion. After model simplification, an interaction between morph and temperature remained highly significant, however the effect of Quaite-weighted dose on final population size was non-significant and so it was removed from the model to produce a final model $y \sim \text{morph} \times \text{temperature}$ (Table 4.6). In the combined model, the direction and magnitude of the main effect was different for the different morphs, so for simpler interpretation of the interaction, the data were partitioned by morph and separate models run with temperature as the sole effect (Table 4.7). Temperature had a significant positive effect on the final population size of a population originating from a wingless aphid ($\beta = 0.1431$, $p < 0.001$, Figure 4.5). There was a slight negative effect of temperature on PGR originating from a winged aphid ($\beta = -0.0587$, $p = 0.012$, Figure 4.5).

For further calculations requiring a measure of *M. persicae* survivor PGR, a value predicted by the wingless aphid model at a set temperature of 20°C was used. When converted to PGR this was estimated, by the model presented in Table 4.7, to be $0.4429 \text{ aphids aphid}^{-1} \text{ day}^{-1}$.

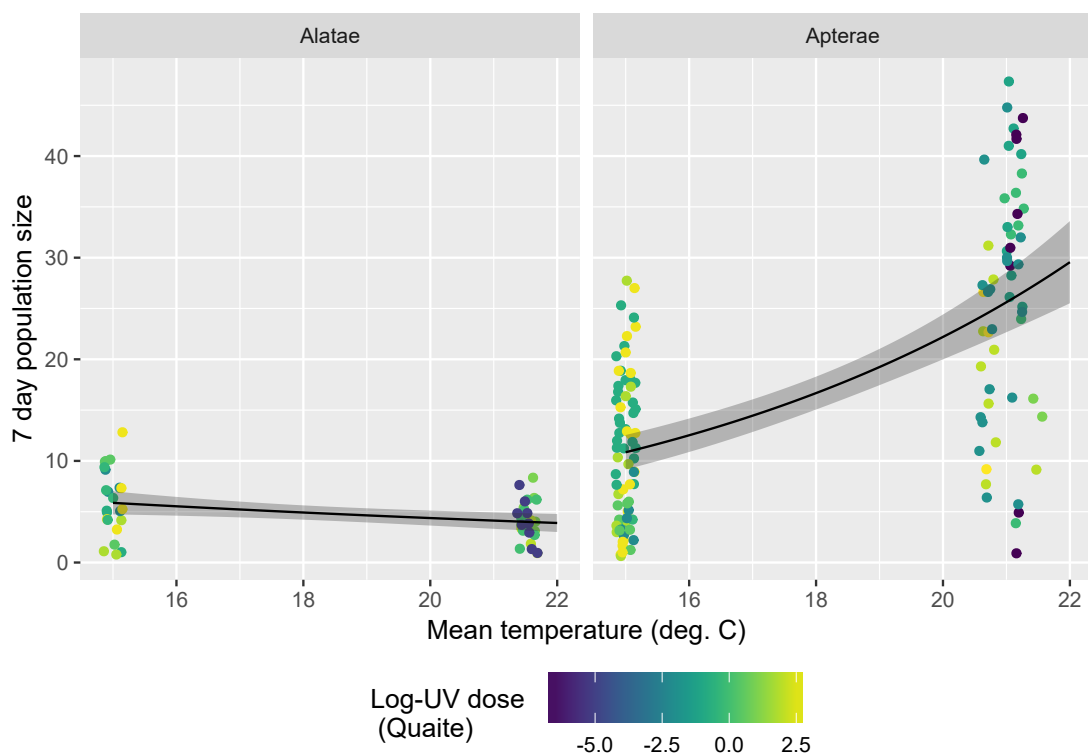


Figure 4.5: Effect of temperature on final population size for aphids surviving exposure to UV. The plots are paneled by aphid morph: Alatae (winged) or Apterale (wingless). Individual points show the final population size after seven days of a population originating from a single aphid. Individual point colour shows the treatment $Dose_{Quaite}$ value. The trendlines and ribbons show the estimated mean and 95% confidence interval from the GLM fitted for each aphid morph.

Table 4.7: Quasipoisson GLM model parameters for two separate models $y \sim$ temperature predicting aphid population growth rate of survivors of UV irradiation for Wingless (*Apterae*) and Winged (*Alatae*) aphids separately. Significance codes: * = $p < 0.05$, ** = $p < 0.01$, *** = $p < 0.001$.

	Estimate	Std. Error	t value	Pr(> t)
Wingless (<i>Apterae</i>)				
(Intercept)	0.2376	0.3148	0.7547	0.452
Temperature	0.1431	0.0165	8.6854	< 0.001***
Winged (<i>Alatae</i>)				
(Intercept)	2.6507	0.4098	6.4683	< 0.001***
Temperature	-0.0587	0.0225	-2.6157	0.012*

Table 4.8: Predicted effects of exposure to UK summer UV. Three solar CIE (erythemal) datasets were used to calculate a mean daily CIE dose ($Dose_{CIE}$) which was then used to calculate daily mortality of *M. persicae*, based on the response of the model $y \sim \ln(Dose_{CIE})$ (Table 4.5). From this, the estimated PGR, based on repeated daily exposure to $Dose_{CIE}$ (the mean value for each dataset), was calculated.

Dataset	Latitude	Longitude	$Dose_{CIE} \pm SE$	Daily Mortality	PGR <i>aphids</i> <i>aphid</i> ⁻¹ <i>day</i> ⁻¹
<i>City, Country, Type</i>	<i>deg.</i>	<i>deg.</i>	<i>kJ m⁻² day⁻¹</i>	<i>%</i>	
Reading, UK, Measured	51.44°N	0.94°W	2.12 ± 0.11	41% ± 4%	-0.08
Reading, UK, Modeled	51.44°N	0.94°W	2.65 ± 0.12	44% ± 4%	-0.13
Lancaster, UK, Modeled	54.04°N	2.80°W	2.59 ± 0.13	43% ± 4%	-0.12

4.3.4 Applying the models to real-world scenarios

Typical UK summertime

Using three third-party datasets, measured and modeled CIE-weighted day doses were averaged for date values between 21st of June, 2013 and 31st of August 2013 (Table 4.8). These values were used to estimate the daily mortality, as predicted by the model (Table 4.5). As no effect of UV on fecundity of survivors was demonstrated in the experimental work presented in this chapter, dose-dependent mortality was combined with a standardised survivor PGR of 0.4429 to estimate the overall PGR. The modeled dataset estimated higher CIE-weighted daily doses than the measured dataset at the Reading site and therefore predicted higher mortality (Table 4.8). Daily mortality for all three datasets varied between 41% and 43% and therefore, the overall PGR was estimated as always negative, varying between -0.08 and -0.13 *aphids aphid*⁻¹ *day*⁻¹. The Reading measured dataset for 2013 predicted an overall PGR approximately 36% higher than the typical-year modeled dataset for the same location. The Lancaster modeled dataset estimated a PGR approximately 4% higher than the Reading measured dataset.

Horticultural growing environments in the UK

To estimate the effect of UV light reaching a crop when filtered through horticultural films, the mean CIE-weighted daily dose values for each solar spectral dataset (Reading Measured, Reading Modeled, Lancaster Modeled) were convolved with the CIE-weighted transmittance of three commercial (Lumisol, Lumivar and Lumitherm) and three experimental (C1, C6 and Tex) films to provide typical daily CIE doses under each film. Estimated under-plastic CIE-weighted

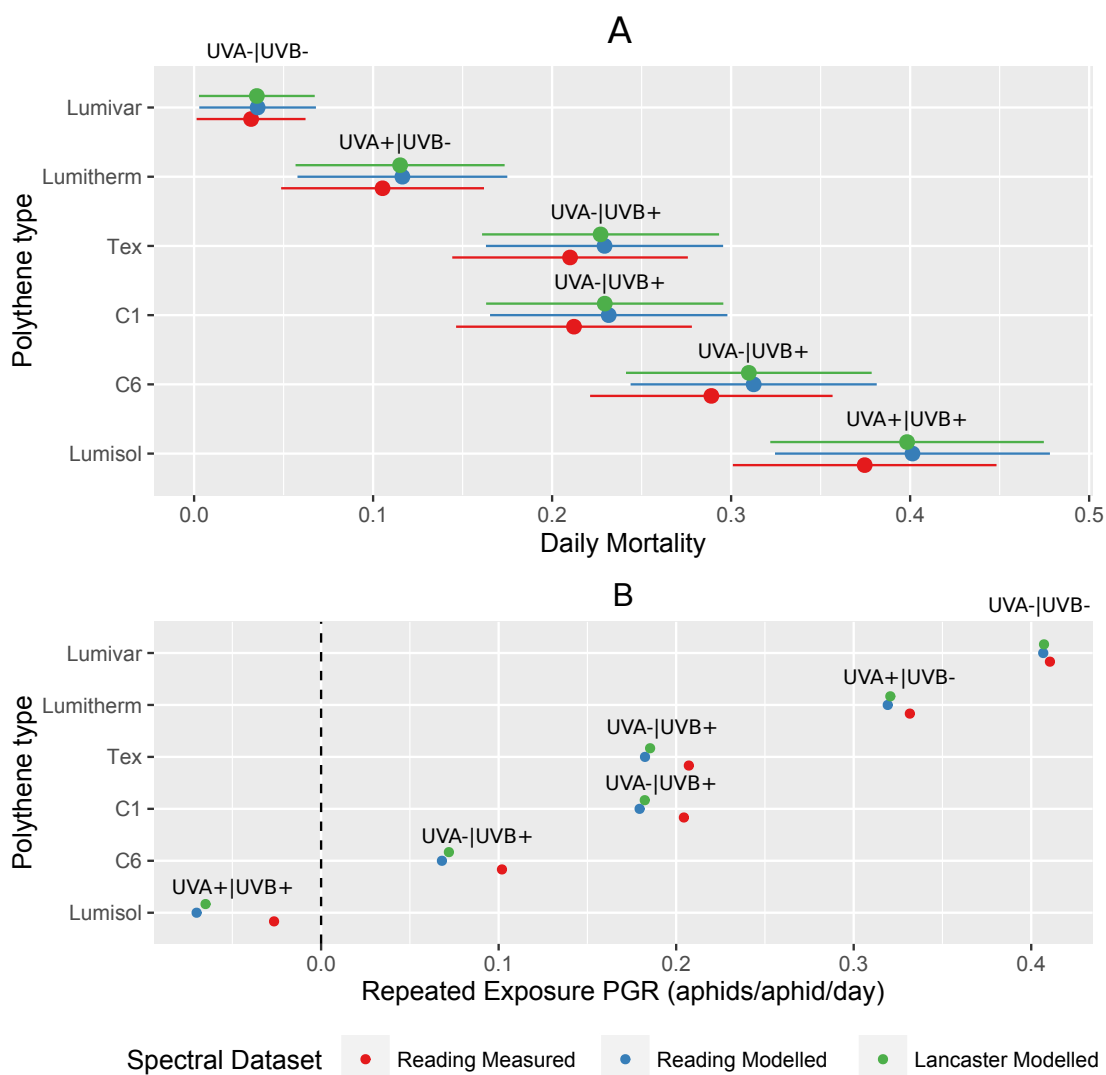


Figure 4.6: UV-induced effect on aphid population growth rate under horticultural tunnels in the UK. Point ranges show the predicted mean \pm the 95% confidence intervals (where applicable) for aphids exposed to mean UK summer day doses. (A) shows the predicted single-exposure growth rate, (B) shows the single-exposure mortality rate and (C) shows the continuous exposure growth rate. No meaningful confidence intervals could be computed for (C) and so only the predicted means are shown.

day doses were then used to compute single exposure mortality (Figure 4.6.A) and repeated exposure PGR (Figure 4.6.B) for aphid populations which are exposed to the full daily dose each day throughout the population growth period.

For the Reading measured dataset, estimated repeated exposure PGR under the UV-transparent (Lumisol) film was only slightly higher than under full sunlight (-0.07 aphids $\text{aphid}^{-1} \text{day}^{-1}$ compared to -0.08 aphids $\text{aphid}^{-1} \text{day}^{-1}$ under full sunlight). For the same spectral dataset, the UV-opaque film (Lumivar), had an estimated PGR of 0.41 aphids $\text{aphid}^{-1} \text{day}^{-1}$. Populations under the ‘standard’ film were predicted to have a PGR of 0.33 aphids $\text{aphid}^{-1} \text{day}^{-1}$. The three experimental films had predicted PGRs between the ‘standard’ film and the UV-transparent film with predicted PGRs of 0.21 , 0.20 and 0.10 for ‘Tex’, ‘C1’ and ‘C6’ respectively. As would be expected, the two modeled datasets showed the films ranked in the same order but, due to their higher predicted daily doses, they predicted higher mortality and therefore lower PGRs under CIE-transmitting films (Figure 4.6).

Table 4.9: Lamp details for Table 4.10. Peak wavelength is the peak below 400 nm * A smaller secondary peak was located at 312 nm

Code	Lamp	Peak Wavelength
s	Solar (non-supplemented)	400 nm
1	Q Panel EL340	344 nm
2	Philips TL40	313 nm
3	Osram Vitalux	364 nm (312 nm)*
4	Panasonic UV	311 nm
5	Honle UVA Hand 100	
6	unknown UVA fluorescent	360 nm

4.4 Discussion

This study sought to isolate the direct effects of radiation on the aphid *M. persicae*, from any effect of UV irradiation of its host plant which may subsequently affect the aphid survival or fecundity. A negative dose response for *M. persicae* survival and exposure to UV radiation was identified and the magnitude of this effect was determined by the radiation source spectrum (Figure 4.2). Longer wavelength UV (UVA) was found to be less lethal to aphids than shorter wavelength UV (UVB). The mortality data were integrated into a CIE-weighted dose response for prediction of aphid mortality under any illumination environment where the CIE-weighted dose is known.

Of the aphids which survived irradiation, no sublethal effect on PGR was observed. As far as the author is aware, this approach — where aphids were irradiated on a non-plant medium and then transferred to non-UV exposed plants — has not been previously used for *Hemiptera* and so this is the first study to conclusively isolate the direct effect of UV radiation on aphids from indirect effects mediated through the host plant.

Previous work has been conducted with a number of invertebrate orders: namely *Hemiptera*, *Lepidoptera* and the spider mites (Order: *Trombidiforma*) (Table 4.10). UV irradiance, dose and supplementation technique vary widely between studies and often the light treatment information provided in the papers is inadequate for drawing comparison between studies (see subsection 4.4.3 for a more in-depth discussion of this problem). In this section, I first review the findings in the context of other studies of insect responses to UV irradiation before considering some of the challenges of designing experiments to test the effect of UV on insects in a way that is both comparable to other work and also allows prediction to be made in real-world contexts.

Table 4.10: Effects of UV on invertebrates. ¹ Pest species name. ² UV illumination source type (see table 4.9 for further details). ³ Exposure type (I - insect only, B - plant and insect) ⁴ Any measure of total UV, UVA, UVB irradiance presented in the paper (unit: $W\ m^{-2}$). Where lamp spectra were available, the CIE (erythral) irradiance was estimated. ⁵ Any measure of total UV, UVA, UVB dose (unit: $kJ\ m^{-2}$, where only a single treatment occurs), or daily dose (unit: $kJ\ m^{-2}\ day^{-1}$, where repeated exposure occurred). Where lamp spectra were available, the CIE (erythral) dose was estimated. ⁶ The life stage used for the study. ⁷ Mortality (+) indicates increased mortality or reduced longevity. ⁸ Reproductive effort ((+) indicates more offspring or more eggs produced). ⁹ Population Growth Rate. * These irradiance and dose values are likely to be incorrectly reported as the light source used is predominantly a UVA-emitting source, yet the study reported very high UVB irradiances.

Study	Sp. ¹	Order	Plant	IS ²	ET ³	Irradiance ⁴			Daily Dose ⁵			LS ⁶	Mort. ⁷	Fec. ⁸	PGR ⁹
						UV	UVA	UVB	CIE	UV	UVA				
Burdick, 2015	<i>A.glycines</i>	Hem.	Soybean	1	B	8.55	8.16	0.40	0.06	92.35	88.09	4.27	0.71		(-)
Burdick, 2015	<i>A.glycines</i>	Hem.	Soybean	2	B	9.05	4.93	4.12	1.40	97.70	53.22	44.47	18.08		(-)
Burdick, 2016	<i>A.glycines</i>	Hem.	Soybean	s	B	11.80	11.63	0.18	0.02	-	-	-	-		0
Dader, 2014	<i>M.persicae</i>	Hem.	Pepper	3	B	1.43	1.42	0.01	0.06	72.22	71.69	0.55	2.80		(+)
Dader, 2014	<i>B.tabaci</i>	Hem.	Aubergine	3	B	1.43	1.42	0.01	0.06	72.22	71.69	0.55	2.80		(+)
Fukaya, 2013	<i>P.citri</i>	Trom.	Citrus	4	I	1.00	0.42	0.58	0.24	3.60	1.51	2.09	0.86		(-)
Fukaya, 2013	<i>P.citri</i>	Trom.	Citrus	s	B	-	-	-	-	-	-	-	-		(-)
Hu, 2013	<i>S.avenae</i>	Hem.	Barley	5	B	-	-	120.00*	-	-	-	864.00*	-		(-)
Hu, 2013	<i>S.avenae</i>	Hem.	Barley	5	B	-	-	120.00*	-	-	-	216.00*	-		(+)
Kuhlmann, 2010	<i>M.persicae</i>	Hem.	Cabbage	s	B	-	-	-	-	-	-	-	-		(-)
Kuhlmann, 2010	<i>B.brassicacae</i>	Hem.	Cabbage	s	B	-	-	-	-	-	-	-	-		(-)
Meng, 2009	<i>H.armigera</i>	Lep.	Citrus	6	I	3.00	-	-	-	16.20	-	-	-	0	(-)
Murata, 2013	<i>T.urticae</i>	Trom.	Citrus	4	B	0.45	0.14	0.31	0.77	3.24	1.01	2.23	5.54		(+)
Paul, 2012	<i>M.persicae</i>	Hem.	Lettuce	s	B	-	-	-	-	-	-	-	-		(+)
Tariq, 2015	<i>D.citri</i>	Hem.	Citrus	6	B	3.20	-	-	-	46.08	-	-	-		(+)
Tariq, 2015	<i>D.citri</i>	Hem.	Citrus	6	B	3.20	-	-	-	80.64	-	-	-		(-)
Zhang, 2011	<i>H.armigera</i>	Lep.	Citrus	6	I	3.00	-	-	-	54.00	-	-	-		(+)
Zhang, 2011	<i>H.armigera</i>	Lep.	Citrus	6	I	3.00	-	-	-	75.60	-	-	-		(-)

4.4.1 Identifying a direct UV mortality effect

Effect on *Hemiptera*

Our work indicated a strong mortality effect of UV exposure at environmentally relevant doses — the model predicted that a typical summer’s day in Lancaster, UK would be expected to kill 43% of aphids directly exposed — and whilst other work broadly supports this (Table 4.10), no work has previously studied the effect on *Hemiptera*, independently of the plant. Previous studies of hemipteran responses to UV have almost exclusively started with the hypothesis that plant changes, in response to UV, will affect insect survival and fecundity. Experimental designs where aphids and plants were simultaneously exposed to the treatment light environments have been used (Hu et al., 2013; Kuhlmann et al., 2010; Rechner and Poehling, 2014; Tariq et al., 2015), making separation of direct- and indirect- effects difficult. However, in one of these studies, a high irradiance, short time period exposure, where an aphid was confined to the upper surface of a leaf, demonstrated a strong mortality effect (Hu et al., 2013).

In whole-plant experiments, where the plants and aphids were exposed to daily doses of UV, the grain aphid (*Sitobian avenae*) showed reduced longevity under higher doses of solar and artificial UVB (Hu et al., 2013). The PGRs of *Myzus persicae* and the specialist cabbage aphid *Brevicoryne brassicae* were shown to be negatively affected by exposure to solar UVB (Kuhlmann et al., 2010). This was attributed to increases in plant flavonoids (quercetins and kaempferols) associated with both UV-exposure and antiherbivore defence, however the aphids were also potentially exposed to UV radiation and so a direct effect cannot be excluded.

Exposure to both solar and artificial UVA had a negative effect on *B. brassicae* PGR (Rechner and Poehling, 2014), whilst the citrus whitefly (*Dialeurodes citri*) had significantly higher egg mortality when caged under a UVA source on citrus leaves (Tariq et al., 2015). Therefore, exposure of the plant-aphid system to short wavelength radiation had a negative effect on survival or PGR. However whilst these experiments identify both UVA and UVB as important factors in the PGR of *Hemiptera*, they do not allow us to partition direct effects on the insect from effects that may be mediated through the plant.

More recently, studies have identified plant-mediated effects of UV on aphids through pre-exposure of plants to UV, prior to aphid inoculation. Plants irradiated with UVB prior to *B. brassicae* inoculation had significantly fewer aphids after a period of three days compared to aphid populations on control plants (Mewis et al., 2012), supporting the claims made by Kuhlmann et al. (2009) and Rechner and Poehling (2014) that UV triggers up-regulation of plant defence and that these changes in plant defence negatively affect aphid performance.

UV exposure was not always shown to negatively affect aphid PGR. A study using *M. persicae* reared on *Capsicum annuum* (pepper) pre-exposed to UVA demonstrated that aphid PGR was 10% higher in populations feeding on UVA-exposed plants compared to aphids feeding on plants which had not been exposed to UVA (Dader et al., 2014). In the same study, *M. persicae* on UVA pre-exposed plants did not have significantly different PGRs when grown under high UVA, compared to low UVA, suggesting that there was no direct effect of UVA on the insects in this study. Similarly, *M. persicae* on lettuce (*Lactuca sativa*) had higher PGRs when exposed to solar UV, compared to populations where solar UV was excluded (Paul et al., 2012), indicating a lethal effect of UV exposure to be unlikely. The plant-mediated negative effect on insect survival, seen in brassicas (Mewis et al., 2012), does not appear to occur in pepper or lettuce, potentially due

to a lesser degree of overlap between plant herbivory and plant UV defence responses (Izaguirre et al., 2007).

UV lethality in other invertebrates

In *Lepidoptera*, various responses to UV exposure have been seen. In *Ephestia kuehniella* (Güven et al., 2015) and *Helicoverpa armigera* (Zhang et al., 2011b), larvae irradiated with artificial UVA-emitting lamps, independently of their food source were shown to have increased mortality. McCloud and Berenbaum (1999) separated plant-mediated- from direct- effect, demonstrating that Cabbage Looper (*Trichoplusia ni*) only suffered increased mortality when reared on plants under supplemental UVB, and not when fed UVB-supplemented plant material in the absence of UVB, demonstrating the presence of a direct (but no plant-mediated) effect of UVB. However, in experiments using exposure to ambient solar radiation, a mortality effect of combined UVA and UVB has not been seen. *Anticarsia gemmatalis* showed no decrease in survival following exposure to ambient UV (Zavala et al., 2001), nor did *Thaumetopoea pinivora* (Battisti et al., 2013), where individuals exposed to direct sunlight actually had higher mass, compared to individuals shaded. The authors attributed this increase to the higher temperatures experienced in full sunlight, rather than a UV effect.

Longer wavelength light has also been associated with increased mortality. Continuous exposure to monochromatic violet light (peak wavelength of 417 nm) has been shown to induce greater larval mortality in two species of *Diptera* (*Drosophila melanogaster* and *Culex pipiens*) than UVA or wavelengths longer than 417 nm (Hori et al., 2014). Little is known about the mechanisms which may drive this response, however it is possible that the mortality effect here is due to the absence of other wavelengths, rather than the presence of the specified wavebands. Longer wavelengths than 500 nm are only implicated in mortality when used at highly artificial intensities, such as that delivered as pulsed laser light, which was also shown to induce mortality in *Diptera* (Keller et al., 2016). Mortality occurred via a direct thermal effect on the insect, however this is clearly not relevant to general understanding of insect photoecology.

Two species of spider mite showed varying degrees of susceptibility to UV exposure, depending on species and life stage. Egg mortality increased with both UVA and UVB exposure in *Panonychus citri* (Fukaya et al., 2013) and the two-spotted spider mite, *Tetranychus urticae*, (Murata and Osakabe, 2014) when eggs laid in UV-absent environments were irradiated with a UVB-emitting lamp. Egg mortality of *P. citri* was also found to be higher for eggs laid in direct sunlight, compared to those laid in shaded parts of the plant. Plant mediated effects are unlikely to affect egg survival (most plant-mediated effects rely on ingestion of plant material) and so this was identified as a direct effect of UV. Similarly, there was a dose dependent effect of UVB radiation on *T. urticae* nymphs (Fukaya et al., 2013; Murata and Osakabe, 2014) and adults (Murata and Osakabe, 2013) with adults showing higher resistance to UV than nymphs or eggs.

4.4.2 Sublethal effects of UV radiation

We found no evidence that the fecundity of aphids exposed to a single UV dose was affected by UV dose, however, multiple non-lethal effects of exposure to short wavelength light have been observed in invertebrates. These include changes in morphology and physiology, changes in fecundity and reproductive effort, and changes in behaviour. As discussed above, it is often difficult to identify a direct response to UV, rather than a response mediated through the plant and so

some caution must be used when interpreting studies which did not isolate the invertebrate from the host.

In the same way that plants produce photoprotectants in response to UV and high light (Ballaré, 2014), increases in invertebrate-derived photoprotectants occurs in individuals (Alkhedir et al., 2010) and populations (Herbert and Emery, 1990). The grain aphid (*S. avenae*) has been shown to increase production of carotenoids and other photoprotective compounds, in response to increased non-UV light intensity (Alkhedir et al., 2010). Whilst this change occurred in individuals over a number of days, light-induced increases in melanin pigmentation occurred only at the population level in *Daphnia pulex* moved from a low light environment to a high light environment (Herbert and Emery, 1990). As well as UV-absorbing compounds, insects also have higher antioxidant capacity under higher UV (Meng et al., 2009), however, it is not clear if this increase occurs entirely through increased insect synthesis, or through increased dietary intake of antioxidants when feeding on plants grown under high UV conditions (Carroll and Berenbaum, 2006).

Reproductive effort has been shown to increase with low UV doses, but decrease under high UV doses (Tariq et al., 2015; Zhang et al., 2011a; Dader et al., 2014). Under low UVA daily doses the citrus whitefly, *D. citri*, had higher egg mortality than in the UV-absent control, but fecundity was higher (Tariq et al., 2015), suggesting a possible compensation mechanism for the offspring lost to increased egg mortality. Similarly, *M. persicae* fecundity increased when exposed to UVA (Dader et al., 2014), however the same light treatment caused a reduction in the number of *Bemisia tabaci* eggs per female, demonstrating that the threshold between compensation and damage is likely to be species-specific. In addition to a change in the number of offspring produced, there is also some evidence that the viability of offspring is reduced after exposure of the adult. The grain aphid, *S. avenae* produced higher numbers of deformed offspring (Zhang et al., 2016) after exposure to moderate UVA doses. The study also demonstrated that this effect is partially mitigated by feeding on a host species which supplies a higher concentration of antioxidants.

In the *Lepidoptera* *H. armigera*, post-exposure oviposition rate increased at low UVA doses but decreased at high doses (Zhang et al., 2011a). It appears that *H. armigera* can effectively respond to UVA irradiation at low doses by increasing its antioxidant capacity, but at higher doses, the antioxidant system becomes overwhelmed (Meng et al., 2009). Therefore, the temporary increases in fecundity may occur as a compensation strategy, whilst the insect still has the capacity to mitigate oxidative stress. However at higher doses, the insect can no longer compensate and reproductive effort decreases along with a general decline in other physiological functioning.

Finally, invertebrates have been shown to respond behaviourally to high solar UV (Gencer et al., 2006; Murata and Osakabe, 2014; Paulsen et al., 2013). The two-spotted spider mite (*T. urticae*) avoided exposed areas, which would be advantageous feeding sites, during periods of high solar UV irradiation (Murata and Osakabe, 2014). Earlier larval stages of the psyllid *Homotoma ficus* avoided areas subject to high light exposure, perhaps due to increased UV-susceptibility (Gencer et al., 2006), and the pigmented aphid *Melanocallis caryaefoliae* was more commonly found in exposed feeding sites than less pigmented aphids. As well as responding directly to the light environment, both *Hemiptera* (Zu-Qing et al., 2013) and *Lepidoptera* (Caputo et al., 2006) have been shown to show feeding preference for plant material grown without UVB. These behavioural responses to UV, whether responding directly to the light or to the change in food quality, clearly have implications for survival and fecundity, through both the benefits of avoiding exposure to

harmful doses of UV, and through the costs of feeding at less nutritious sites within the plant. Insect behavioural responses to light are discussed further in Chapter 6.

4.4.3 Towards better insect photobiology experiments

The results presented in this chapter demonstrate a significant mortality effect of wavelengths in both the UVA and UVB wavebands in isolation of the host (Figure 4.2), however it is difficult to draw comparison directly with other studies as information about UV dose and spectral quality is often not available. In this section I briefly review the major pitfalls of UV photobiology experiments and present recommendations for improvement. The main areas of focus are the use of biological spectral weighting functions, experiments using UVC sources and the confounding effects of photoreactivation.

From wavebands to spectral weighting functions

In this study, short wavelength radiation was shown to be significantly more lethal than radiation with longer wavelengths. As such, doses expressed in the somewhat arbitrary unweighted UV, UVA or UVB wavebands did not explain the mortality response of *M. persicae* as well as doses expressed with BSWFs (Figure 4.4), which shows that light in all parts of the spectrum has an effect on organisms, however different wavelengths will be more effective than others in the induction of a response. In this case, that response was aphid mortality and, as there is no *M. persicae* mortality action spectrum, commonly-used action spectra were ranked according to their degree of explanation of the experimental data.

We identified a number of BSWFs which apply a larger effective weighting to shorter wavelengths than longer wavelengths and, as such, better describe *M. persicae* mortality than any of the unweighted measures of dose (Figure 4.4). Although an action spectrum describing the damage of DNA in alfalfa (Quaite et al., 1992) was found to best fit the data, CIE-weighted dose is perhaps the most useful effective BSWF as CIE daily dose data are widely available, either directly from satellite data (NASA, 2016), or as UV-index values obtained through meteorological services. Unfortunately, the use of BSWFs to describe light treatments in insects mortality experiments has not been adopted, with most studies reporting the source type and the measured UVA, UVB or total UV irradiance. Where the experimental work used sunlight, it is appropriate to use unweighted irradiance to compare the experimental treatments to other field conditions because the spectrum shape (i.e. the ratio of one wavelength to another) will not vary hugely. However, if the experimental work relied on supplementation using fluorescent tubes or other short-wavelength emitting source, it is very likely that the effective UV dose will be much higher than the field unweighted equivalent due to a bias towards short wavelength UVB and even UVC emitted by these lamps.

As an illustration of the magnitude of error which may be introduced, in a hypothetical scenario where a UVB dose of 1 kJ m^{-2} is desired, a typical lamp choice might be a Q Panel EL-UVB313. Unfiltered, this would provide a CIE-weighted dose 82% higher than the same unweighted UVB dose delivered from sunlight (Table 4.11). Adding a cellulose acetate filter, which removes short-wavelength UVB and completely excludes UVC radiation, would improve this, but would still result in an overestimation of 55% in effective dose terms. Failure to take this into account may explain observed higher insect mortality in lamp experiments, compared to field experiments (Fukaya et al., 2013; Burdick et al., 2015, data presented in Table 4.10) and smaller effect sizes

of experiments using solar UVB compared to experiments using UV lamps (Rechner and Poehling, 2014).

Table 4.11: Under-estimation of effectiveness of solar simulators. The unweighted UVA and CIE (erythemal) doses for five different radiation sources, standardised to a UVB dose of 1 kJ m^{-2} . The radiation sources are the modeled ASTM G173 direct solar model (solar), a Philips TL 6 W BLB (UVA360), a Q Panel EL-UVA340, an unfiltered Q Panel EL-UVB313, and a Q Panel EL-UVB313 filtered with a single layer of cellulose acetate. The final column shows the percentage estimation in erythemal effective dose of each artificial source.

	Radiation Source	UVB kJ m^{-2}	UVA kJ m^{-2}	CIE kJ m^{-2}	% change from solar CIE
1	solar	1	66.57	0.13	
2	Philips TL 6 W BLB (UVA-350 nm)	1	2689.09	0.97	+625%
3	Q Panel EL-UVA340	1	20.65	0.14	+6%
4	Q Panel EL-UVB313	1	1.46	0.24	+82%
5	Q Panel EL-UVB313+CA	1	1.64	0.21	+55%

Use of artificial UVC

Certain studies have used UVC sterilisation sources for studies on insect response to oxidative stress (Gunn, 1998; Güven et al., 2015; Ghanem and Shamma, 2007). Doses of high-energy UVC had a large effect on the survival of *Lepidoptera* (Gunn, 1998; Güven et al., 2015) and *Coleoptera* eggs (Ghanem and Shamma, 2007), however this is relevant only in the context of the use of artificial UVC sterilisation sources for pest control purposes, as UVC radiation is not present under ambient solar conditions. As UVC has not been encountered as a selective pressure by organisms in their recent evolutionary history, adaptations for UVC protection have not evolved. Typical organism-produced photoprotectants may have some coincidental protective properties against UV, however, there is evidence that melanin does not provide protection against UVC (Gunn, 1998) and that it is largely transparent to UVC when *in vivo* (Kollias, 1995). Therefore, UVC experiments cannot be considered suitable proxies for invertebrate responses to solar UV. In the experimental work presented here, a low-cut filter such as cellulose acetate was used to prevent exposure to these wavelengths and it is recommended that, unless the work seeks specifically to evaluate the effectiveness of UVC, that all insect work use an equivalent low cut filter.

Photoreactivation as a confounding factor

Photoreactivation is the process of activation of photosensitive photolyase enzymes with long wavelength UVA and human-visible light, in order to repair cyclobutane pyrimidine dimers formed by exposure to shorter wavelength UV radiation (Britt, 1996). This mechanism can dramatically reduce the effective lethality of short-wavelength radiation and has been studied extensively in plants (Sakai et al., 2011a) and bacteria (Bohrerova et al., 2007). In *T. urticae* mortality was much higher when nymphs and eggs were irradiated with only UVB compared to those irradiated with UVB then exposed to UVA or short-wavelength visible light (Murata and Osakabe, 2014). Photolyase activation and subsequent DNA repair by long wavelength light has also been demonstrated in the common pill woodlouse (*Armadillidium vulgare*) (Sato et al., 2010), demonstrating that photoreactivation is a highly important mitigation of short wavelength radiation damage.

Our study did not specifically control for possible photoreactivation effects during the UV exposure procedure (a period of 1-6 hours), however aphids were moved to a UVB-absent glasshouse (with supplementation in the Photosynthetically-Active Radiation (PAR) region), post-exposure, where photoreactivation was expected to have occurred. Future experiments may consider using an additional solar source (with all UV light removed by filtration) at an appropriate intensity, in order to properly quantify the photoreactivation effect.

4.4.4 Using mortality data for prediction

Predicted effect of UV on aphids under UK summer conditions

The model generated from the mortality data were used to produce population models for different illumination scenarios, using widely-available CIE data (Table 4.8). In full sunlight on an average UK summer day, the model predicts that an aphid population will have a negative PGR, meaning that the population will be in decline. Clearly this is not the case as *M. persicae* is a ubiquitous global species, both in natural and agricultural environments, and so this demonstrates that aphids must have behavioural or physiological responses to mitigate the effect of UV. This raises important questions as to the mechanisms that determine aphid exposure to harmful UV radiation, however, these are considered extensively elsewhere in this thesis (Chapter 6) and will not be discussed here. The predicted effect of UV may therefore be considered a mortality maximum value (for mortality induced by direct exposure to UV), however the true mortality of *M. persicae* in field experiments is predicted to be lower.

Predicted effect under horticultural films

The model also allowed the evaluation of six horticultural films in terms of the likely mortality effects of an aphid population in direct sunlight (Figure 4.6). Although the absolute mortality rate may not be accurate, they do allow the films to be ranked in order of their lethality to unprotected insects. UV-transparent plastics yield near-ambient UV conditions and, therefore, have very high expected mortality rates for unprotected aphids. Similarly, prototype films which allow some UVB transmission also increase the risk of mortality for those aphids which expose themselves to direct solar radiation, filtered through these plastics.

4.5 Conclusions

1. In conclusion, this chapter quantified the dose-mortality response of *M. persicae* in response to UV radiation in isolation of any plant-mediated effect. This finding is the first instance of a mortality effect of UV to be identified in *Hemiptera*, independently of plant-mediated UV effects.
2. UV is clearly an important abiotic stress for *M. persicae* and so I predict that it has evolved a mechanism(s) which mitigates the effect of UV as an inhibitory factor in its survival and subsequent PGR.
3. After evaluating the literature in this area, it is recommended that future work studying the effects of UV on insect survival or physiology consider the following when designing experiments:

- (a) Where artificial sources are used as a proxy for solar UV, use sources which, as closely as possible, mimic the spectral balance of sunlight.
- (b) Do not use UVC as a proxy for solar UV and use an appropriate low cut filter to exclude wavelengths with a shorter wavelength than are present in sunlight.
- (c) Consider using a broadband illumination source to avoid inhibition of photoreactivation mechanisms in the target organism. Illumination between 370 nm and 600 nm is typically required.
- (d) Use doses weighted with an appropriate Biological Spectral Weighting Function for the system in question. A CIE (erythemal) action spectrum broadly approximated the mortality response of *M. persicae* to broadband UV sources and could be appropriate for insect mortality studies, however more work is needed to establish the confidence with which this BSWF can be used.
- (e) Report all UV dose and irradiance information, ideally with full-spectrum irradiance data where lamps have been used as solar simulators. Reporting of cumulative or daily CIE dose information for solar experiments may also provide a data reference which could aid in the future collation of studies.

A new method for the rapid quantification of aphid behaviour in different light environments

Abstract

Background: As the plant science research community and the horticultural industry progress towards more energy efficient crop illumination through designer spectra, made possible by recent advances in affordable Light-Emitting Diode (LED) lighting units, we should consider not only how plants will respond, but how pests and pathogens might be affected by these unusual light environments.

Results: I present an affordable approach for testing the short term effects of light environment on an aphid pest species, *Myzus persicae*, using off-the-shelf camera equipment and Open Source software for image analysis. To demonstrate the capability of the system, aphid behaviour was measured for one hour under high, field-like Ultraviolet-A (UVA) environments and low ultraviolet-A (UVA) environments similar to LED-illuminated growth chambers. I showed that a simple metric could be calculated to demonstrate that aphids spent 35-48% more time in a stationary feeding position under the low UVA light environments compared to aphids under high UVA treatments. I suggest that this is indicative of a UVA avoidance mechanism for avoiding damage from solar ultraviolet radiation.

Conclusion: This method extends previous techniques for automated measuring of insect behaviour to be robust under different light environments. I used Open Source programming environments and off-the-shelf camera equipment to make this a highly customisable, cost-effective technique for measuring insect responses to their light environment.

5.1 Introduction

Fast-throughput behavioural assay techniques for pest insects are emerging as a rapid way of screening for resistant crop phenotypes (Kloth et al., 2015; Thoen et al., 2016), but there is potential to extend this technique to measure insect responses to other factors that may affect their impact on a crop. New lighting technologies such as high-efficiency LEDs are increasingly employed in plant growth facilities in both research facilities and in commercial production. The light environment produced by LEDs is different from that produced by previous technologies such as fluorescent, metal halide or high pressure sodium lamps. One consistent difference is that unlike glasshouses and most traditional growth room lighting systems, LED-based plant lighting systems produce little or no ultraviolet (UV). Different lighting environments have the potential to affect not only the plants but also their interaction with invertebrate pests and microbial pathogens (Paul et al., 2012). Methods to assess the effects of light environment on plant-pest interactions remain relatively limited. Simple clip-cage experiments and feeding assays are useful for establishing plant-mediated mechanisms affecting plant-pest interaction, such as light-mediated resistance (see below). However, approaches that assess the direct effects of the lighting on the insect are also required if we are to understand fully how the light environment affects plant-pest interactions. That need applies, not only in experiments designed to investigate this aspect of plant biology, but more generally wherever there is a risk of plants being challenged by pests.

The expectation that different light environments will affect plant resistance to pest attack is based on understanding of the role of light in regulating plant defence against pest and pathogen (Ballaré, 2014). Changes in the spectral balance have been linked extensively to changes in plant defensive chemistry with implications for herbivorous invertebrates (Roberts and Paul, 2006). For example, exposure to UV radiation, especially ultraviolet-B (UVB) radiation (280 nm-315 nm), has been shown to cause increases in UV-absorbing flavonoids (Dolzhenko et al., 2010; Markham et al., 1998; Ryan et al., 2001), most likely produced to protect the plant from photoinhibition and photooxidative stress caused by UV high irradiances (Agati et al., 2012). A secondary effect of flavonoid production is enhanced resistance of the plant to invertebrate pests. Many flavonol glycosides which are broadly known to increase with UV exposure, such as quercetin, kaempferol and their derivatives, are known to play a role in pest resistance (Golawska et al., 2012a; Zu-Qing et al., 2013; Lattanzio et al., 2000). Other classes of phytochemical, such as glucosinolates (Hopkins et al., 2009), polyamines (Sempruch et al., 2010) and alkaloids (Wink, 1992) have also been shown to inhibit feeding, reduce survival and limit Population Growth Rate (PGR) in insects, however, their interaction with UV is not well understood (Schreiner et al., 2012). Other studies using both phloem feeding (Kuhlmann et al., 2010) and chewing (Izaguirre et al., 2007) insects have explicitly demonstrated the relationship between UVB exposure, subsequent change in phenolic profile, and decreases in insect PGR or reproductive success.

Whilst there is undoubtedly a strong case that UVB-induced changes in plant chemistry can affect resistance, the effect of UV on the invertebrates themselves may result in them incurring significant fitness costs. Reduced survival associated with exposure to UV has been demonstrated in spider mites (Ohtsuka and Osakabe, 2009; Sakai et al., 2012) and also in various aphid species (Dong et al., 2014; YiMin et al., 2014). Additionally, there is strong mechanistic evidence that many invertebrates, including pests such as aphids, have the photoreceptors and neural process-

ing capability to perceive UV light, particularly the long wavelength UVA radiation (315 nm-400 nm) (Döring et al., 2007). The UV environment can have major effects on insect behaviour, such as in Red-Spotted Spider mite (Ohtsuka and Osakabe, 2009) and in Soybean Aphid (Burdick et al., 2015) which show preference for low UV environments.

In order to understand the effect of different light environments on aphid behaviour, it was necessary to establish a fast-throughput method which allowed the quantification of aphid behaviour under various light environments. Recent advances in photogrammetric techniques have accelerated the speed at which insect behavioural responses may be quantified (Kloth et al., 2015; Noldus et al., 2002) and through extending this robust technique to cope with unusual light conditions, I sought to develop this as an approach for screening insect responses to light. The aims of this research were to:

1. Establish a cost-effective method of recording and measuring the behaviour of wingless aphids under different lighting environments.
2. Use this system to quantify wingless aphid responses to UV-supplementation of white light (LED or fluorescent tube), using both UV-LEDs and UVA-emitting fluorescent tubes.

Wherever possible, I made use of open source software tools and coding environments, both to minimise cost and increase the accessibility of this method.

5.2 Methods

5.2.1 Light environments and measurement

Two separate sets of experiments were conducted with the behavioural assay platform. These experiments were conducted with simultaneous UVA+ and UVA- treatment groups (four UVA+ and four UVA- aphids per experimental run). The first (Fluorescent Tube Supplementation, see Figure 5.1.A and B) used a Valoya B-series NS1 white LED lamp, supplying Photosynthetically-Active Radiation (PAR) (400-700 nm) and two Philips TL(D)/08 fluorescent tubes for UVA supplementation (peak 360 nm). UV-blocking polyethylene (PE) film (Lumival, supplied by BPI Visqueen Ltd. Lundholm Road, Ardeer, Stevenston KA20 3NQ) was used to filter-out UV from the UVA- (control) treatment and a UV-transparent PE film (Lumisol, supplied as above) was used in the UVA+ treatment.

For the second set of experiments (LED only), all light in the chamber was provided by high power red (720 nm), green (530 nm), blue (450 nm) and UV (375 nm) LEDs which were independently dimmed by high frequency (KHz) pulse-width modulation to deliver a high UVA+ and a UVA- (control) treatment. Experimental runs were conducted individually, alternating between a UVA+ treatment and a UVA- (control) treatment. As aphids possess three photoreceptors, this allowed the spectrum in the experimental chamber to be easily manipulated to represent any aphid colour.

Spectra were measured using a Macam 9910 series spectroradiometer (Macam Photometrics Ltd.) and a cosine corrected head positioned at leaf disc height with the sensor surface parallel to the arena surface. Spectra were processed in R using the 'photobiology' (<http://www.r4photobiology.info/>) package to calculate spectral band irradiances and all plots were generated using the 'ggplot2' package.

5.2.2 Behavioural assay platform configuration

For the fluorescent tube supplementation experiments, foam (5 mm open-cell polyurethane) was cut to 25 mm × 25 mm pieces and attached to the interior of a 90 mm Petri dish (Figure 5.1.A and B) to provide four replicate platforms per treatment. 11 mm diameter (95.1 mm²) leaf discs were punched from a single leaf from a Calabrese plant aged between four and six weeks. These were placed in the centre of the foam squares with the adaxial leaf surface orientated upwards. Tap water was added to the Petri dishes, flooding the areas between the foam squares and preventing the aphids from moving between replicate leaf discs. The water also served to prevent desiccation of the leaf discs. The Petri dishes were then placed on a raised platform (approx. 40 mm high) directly beneath the camera lens and fully exposed to the experimental light sources.

Two areas of the cabinet housing the experiment were isolated by an opaque screen (Figure 5.1.B, marked .iii) with a camera mounted in each, allowing simultaneous operation of a control and an experimental treatment. With a Petri dish containing four replicates in each half of the chamber, eight aphids and two treatments were measured simultaneously.

In the LED-only experiments, two layers of filter paper were placed between the leaf disc and the foam squares. Additionally, the Petri dish was replaced with a 96-well assay plate lid to provide space for 12 replicates instead of four (Figure 5.1.C). A single LED lighting unit was used and to avoid any temporal bias, replicate runs of the experiment were alternated between treatments.

Two Canon 1200D cameras fitted with Canon EF 50 mm f/2.5 Compact Macro lenses were controlled by a PC using the Astro Photography Tool (<http://www.ideiki.com/>) software package, which allowed full control of the cameras and time-lapse functionality. Images were captured at f/13 with a shutter speed of between 1/10 and 1/15 seconds (depending on treatment). Camera white balance and exposure program was set to Manual to ensure consistent image processing. Cameras captured JPEG images at 30 second intervals for one hour.

5.3 Plants and aphids

Calabrese (*Brassica oleracea*, v. 'Volta' supplied by Nickys Nursery Ltd., Broadstairs, Kent, UK) was used for fluorescent-tube supplementation experiments. Plants were grown in a glasshouse at Lancaster University (54.0470°N, 2.8010°W) with supplementary illumination from 4x 600 W Senmatic FL300 Sunlight LED units. Humidity was recorded at an average relative humidity of 47%. Glasshouse air temperature was recorded at an average of 20.2C. Plants were grown in Levington's M3 compost (supplied by LBS Horticulture Ltd., Standroyd Mill, BB8 7BW) and were well watered throughout the experiment. Experiments were conducted with plants 4-6 weeks after germination. Due to variation in solar radiation intensity and temperature in the glasshouse, there was some variation in size of similarly-aged plants and this was standardised by choosing similarly-sized leaves for the experimental work (those with an approximate leaf area of 25 cm²). Plants were isolated from exposure to aphids or other invertebrates by growing within a mesh cage after germination. In the LED-only experiments, calabrese (*B. oleracea*, v.'Zen' supplied by Tozer Seeds Ltd., Cobham, Surrey, UK) was used as a variety with reported similar characteristics to 'Volta'. Growth conditions were as above.

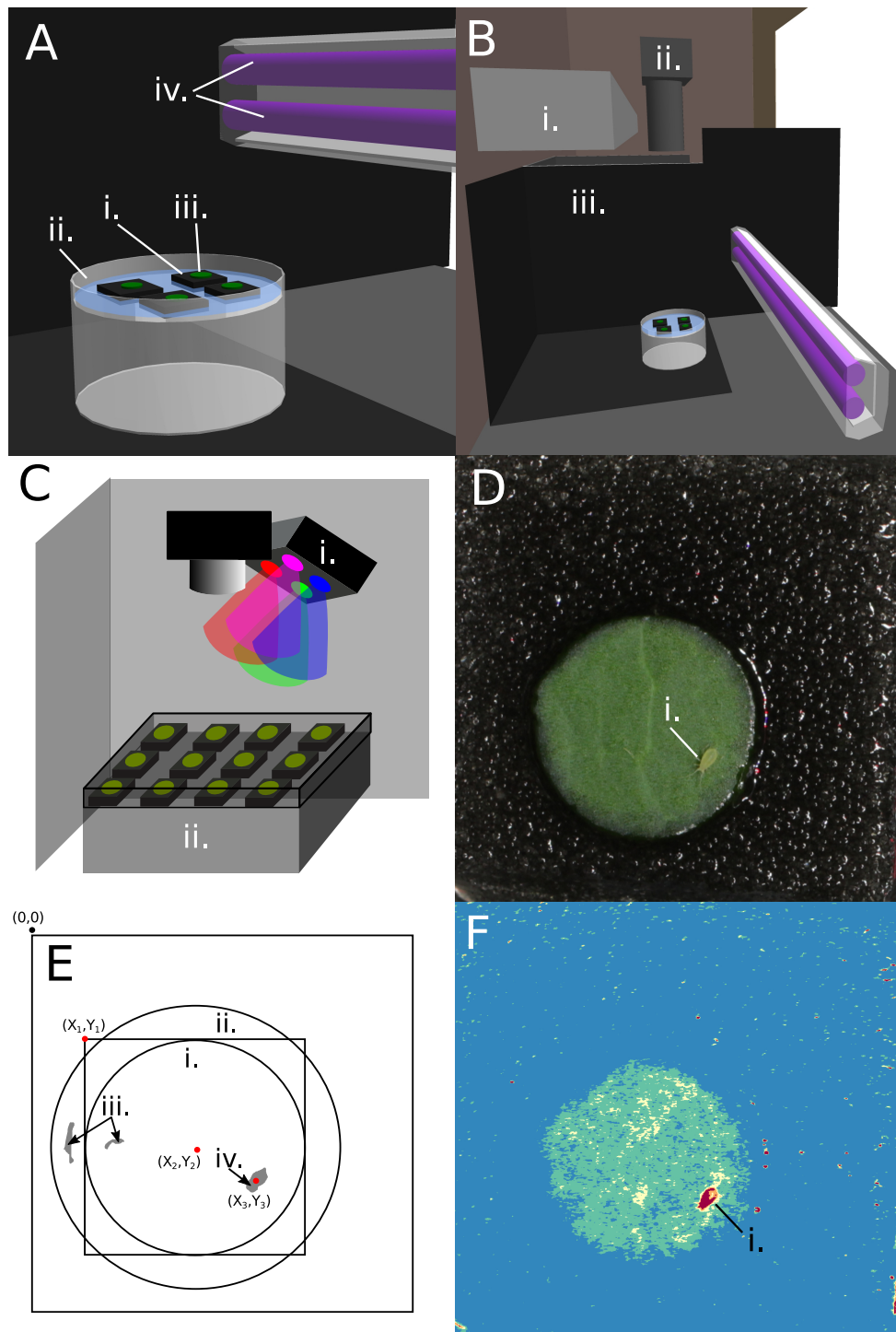


Figure 5.1: Image capture and aphid detection stages. In the fluorescent tube supplementation experiments, open-cell foam islands (A.i) were placed in a water filled 90 mm Petri dish (A.ii) with leaf discs (A.iii) placed on top. Various filtered fluorescent tubes (A.iv) were used to supplement UV with human visible light supplied by a Valoya LED unit (B.i). Images were captured by DSLR cameras (B.ii) mounted directly above the Petri dishes. The two arenas were separated by opaque screens (B.iii). In second set of experiments (LED only), all light was supplied by an LED unit (C.i) and a larger Petri dish was used to allow 12 replicates (C.ii). An example frame is shown pre-analysis as it would be displayed in the GUI (D). (E) Shows the different regions identified by the aphid detection script. Circle (E.i) is the perimeter of the leaf disc and is identified manually by the user. This is expanded by 10% to generate (E.ii). All image data outside this perimeter is excluded from analysis. Non-aphid areas (E.iii) which pass through the colour filter are excluded by size and aspect ratio to correctly identify the centre (X_3, Y_3) of the aphid (E.iv) when $X_1, Y_1 = (0, 0)$ and $X_2, Y_2 = (5.5, 5.5)$. An example frame is shown post-colour filtering (F) to illustrate how colour filtering improves the contrast of the aphid (F.i) against the leaf and background.

Myzus persicae was reared on the same variety as was used in the assays and was grown as above in separate mesh cages, but in the same glasshouse and conditions. New plants were introduced weekly and plants showing visible symptoms of stress removed.

Aphids were transferred from glasshouse to laboratory on a leaf from the culture. Mature wingless aphids of approximately similar size and colouration were selected for the experiment. One aphid per leaf disc was transferred by paintbrush directly from the culture plant. This was carried out under laboratory fluorescent lighting. The Petri dish or tray was then transferred to the platform underneath the camera and the image capture process started.

5.3.1 Software and aphid tracking methods

The OpenCV 3.0 C++ library was used with Python 2.7 bindings to produce general tools for cropping areas of interest, locating the aphid and outputting a calibrated Comma-Separated Value (CSV) file with information relating to aphid position and direction. Python scripts were developed to implement the C++ library and to organise the resulting files. Any required Graphical User Interface (GUI), to allow user-adjustment of detection parameters, were generated using OpenCV. Four key processing steps were identified: image subsetting, spatial calibration, aphid location, and data processing. The software processing steps are described as follows:

Image subsetting

The original image sequences, containing multiple aphid repeats in each, are cropped to produce new image sub-sequences with a single aphid in each (example in Figure 5.1.D). This is achieved using a simple interface that allows users to manually identify single aphid areas within the image sequence. All of the files within the original image sequence are then exported as a new subsequence of individual images.

Spatial calibration

Spatial calibration and identification of the boundary of the leaf disc is achieved by generating a GUI displaying an image (Figure 5.1.D) from the data folder with a user-defined circle overlaid. The user adjusts the position and diameter of the circle to mark the boundary of the 11 mm leaf disc within a single frame of the image subsequence. The user then views the circle overlaid over the other frames in the subsequence to verify that the boundary is a good fit throughout the image subsequence. Once the diameter and centre coordinates have been confirmed, this information is exported as a JPEG file which is used as a mask image in the Aphid Location processing stage

Aphid location

Each image in an image subsequence is masked using the mask file generated in the previous step. This excludes all areas of the image (excluded area is the area outside the largest circle in Figure 5.1.E) from analysis, apart from the leaf disc (Figure 5.1.E.iii) and a border zone (Figure 5.1.E.ii) to allow detection of aphids on or close to the leaf disc. This masked image is separated into red, green and blue colour channels. To improve aphid contrast with the background, the blue colour channel was subtracted from the red colour channel to produce a single-channel

image (figure 5.1.F shows false-colour representation of the single channel image). This is passed through a binary threshold filter with a user-adjustable threshold value to produce a binary (black and white) image.

The binary image is searched for contours (the perimeters of solid white areas in the image) using the OpenCV `findContours` function. These contours are filtered by minimum size, maximum size and aspect ratio to exclude non-aphid areas (Figure 5.1.E.iv) and identify the aphid (Figure 5.1.E.v). This is graphically represented with a detection ellipse drawn around the aphid in the GUI. The filter parameters may be adjusted by the user until the aphid is tracked reliably throughout the subsequence.

The centre point of the detection ellipse in each frame is referred to as the aphid's position. During the processing, if no appropriate contour is located or if the position is not within the leaf disc perimeter, the position information is recorded as absent. The pixel positional information is then converted to X and Y values (in mm) relative to the top left-hand corner of the square box bounding the leaf disc circle (point X_1, Y_1 in figure 5.1.f) and the displacement between current and previous frame is calculated. For two consecutive frames in the subsequence, positional information for both must be present to record a displacement value. If either lack positional information (i.e. the aphid is recorded as off the leaf), displacement is recorded as NA in the output file. For each image subsequence, a CSV file is generated containing positional and displacement information for each time interval.

Data processing

Each image subsequence produces a single CSV file in a subfolder. Image subsequences may be (manually) grouped by treatment and sequence during image import. A python script which retrieves all of the individual CSV files and collates them into a single data file and a single summary file was written to facilitate rapid import into R for statistical analysis.

5.3.2 Statistical Analyses

Analyses were run in the R statistical programming environment. Data from the two experiments (Fluorescent Tube Supplementation and LED-Only) were analysed together. Three candidate indices of aphid behaviour were tested: (i) proportion of time on leaf, (ii) proportion of time stationary on leaf and (iii) average velocity. The two proportional indices were not expected to be normally distributed and so were tested with Generalised Linear Model (GLM) with a quasi-binomial error structure to account for the overdispersion in the data as described by Crawley (2007). Average velocity data also exhibited a non-normal distribution with some evidence of over-dispersion and was therefore tested using a GLM with an unspecified quasi error structure (Crawley, 2007).

Table 5.1: Irradiances and UVA percentages for experimental treatments. Spectra measured at 1nm intervals using a Macam sr.9910 spectroradiometer. Spectra for a Valoya LED unit and a fluorescent UVA source, filtered with UV-transparent (FT UVA+) and UV-opaque (FT Control) PE films are presented. Spectra for UVA+ (LED UVA+) and UVA- (LED Control) LED-only irradiation are also presented.

	Irradiance (W m^{-2})			
	Total	PAR	UVA	UVA %
FT UVA+	14.25	12.35	1.70	12
FT Control	13.95	13.59	0.15	1
LED Control	17.32	17.12	0.00	0
LED UVA+	19.52	17.24	2.08	11

5.4 Results

5.4.1 Software calibration

In order to differentiate normal aphid movement that occurs during feeding (i.e. the wiggle of a feeding aphid) from locomotion, a threshold of 0.014 mm s^{-1} was set as a movement threshold to identify time periods when movement was occurring (Figure 5.2.A and B). When the aphid was located on the leaf (Figure 5.2.C and D) and the velocity was recorded as less than the movement threshold (Figure 5.2.A and B), aphids were recorded as in a probing status (Figure 5.2.E and F). The aphid tracking system also allows analysis of the positional information of the aphid over the test period, such as the distance from the leaf disc centre (Figure 5.2.G and H). For the two aphid examples presented, the control (UVA-) aphid showed relatively little movement and maintained a position near the leaf disc centre whereas the UVA+ aphid moved at higher velocities and moved off the leaf disc for part of the measurement period.

5.4.2 Illumination

Irradiance was measured for the four light treatments at 1 nm intervals between 300 nm and 750 nm (Figure 5.3). Integrated irradiances were calculated for the four treatments for UVA, PAR and total irradiance (Table 5.1). The fluorescent tube experiments were set up to yield similar irradiances between the UVA+ and UVA- treatments (approximately 14 W m^{-2}) with UVA 10% of the combined UV-visible spectral irradiance under the high UV treatment. The overall irradiance under the LED-only array was higher (17 W m^{-2} and 20 W m^{-2} for the UVA- and UVA+ treatments, respectively). In the LED UVA+ treatment, UVA was 11% of the total UV-visible irradiance. Solar UVA is approximately 6% of the UV-visible spectral band.

5.4.3 Aphid behavioural quantification

Three different metrics of aphid behaviour were examined: (i) Time Proportion in Feeding Position (TPiFP) (Figure 5.4.A), (ii) the proportion of time spent on the leaf (Figure 5.4.B), and (iii) the mean velocity of the aphid measured on the leaf disc (Figure 5.4.C).

Aphids under low UVA environments remained settled in the probing position for 86-87% of the time, but under high UVA environments spent significantly less time (D.f. = 79, $p < 0.0001$) in a feeding position (57%-58%). The interaction between lamp type (LED or Fluorescent tube)

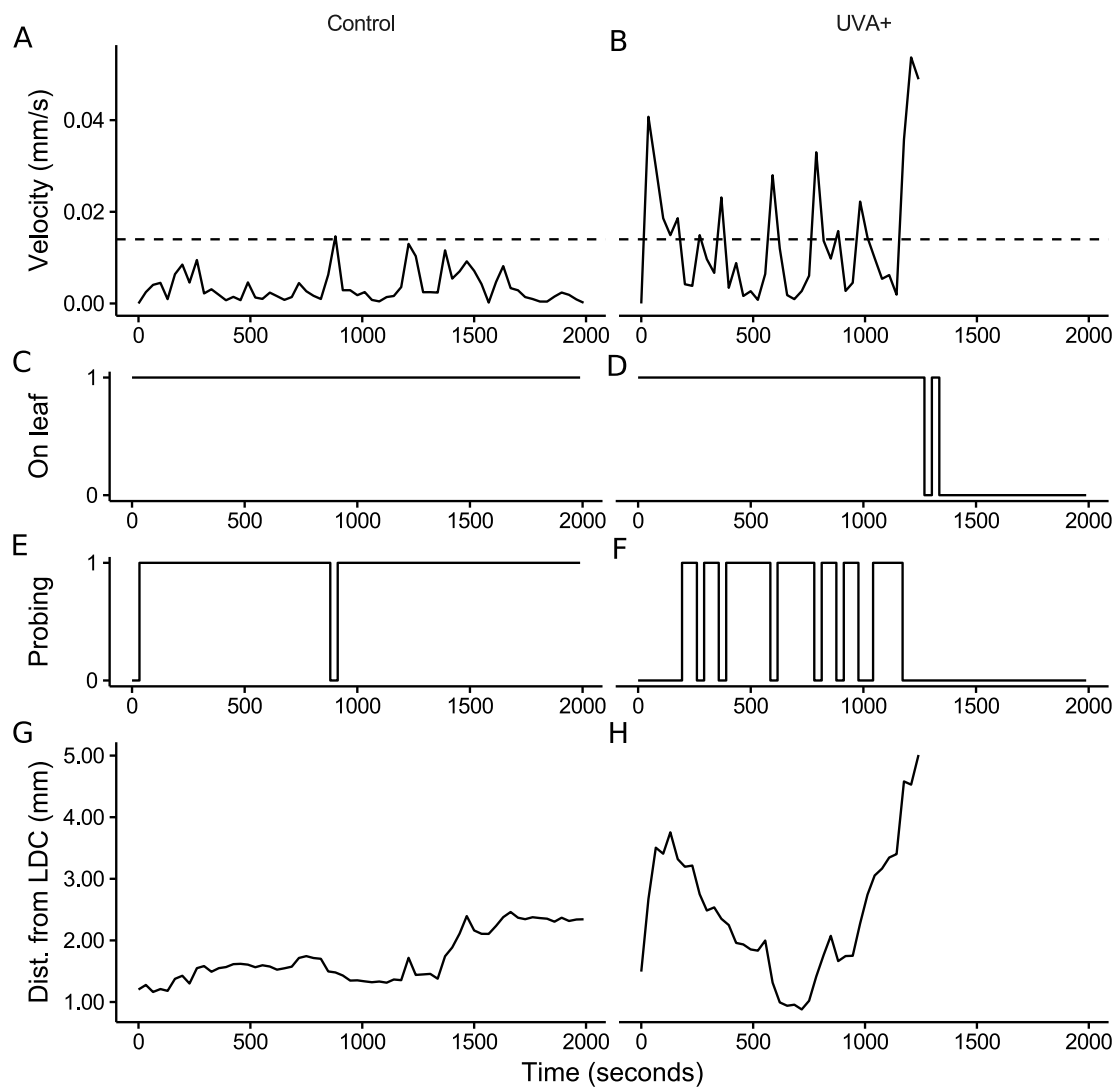


Figure 5.2: Aphid tracking raw data. These plots show examples from a control (UVA-) and a UVA+ LED treatment for single aphids. Traces show two individual aphids under either LED Control (left column) or LED UVA+ (right column) lighting. For each aphid, velocity (A and B), whether or not the aphid was detected on the leaf (C and D), whether or not this was interpreted as a probing phase (E and F) and the aphid distance from leaf Disc Centre (G and H) is presented against time (seconds). The dashed lines in (A) and (B) show the movement threshold of 0.014 mm s^{-1} which determined whether or not an aphid was classified as probing during that time period. Aphids with a velocity under 0.014 mm s^{-1} were classified as probing whereas those detected with a higher velocity were classified as not probing.

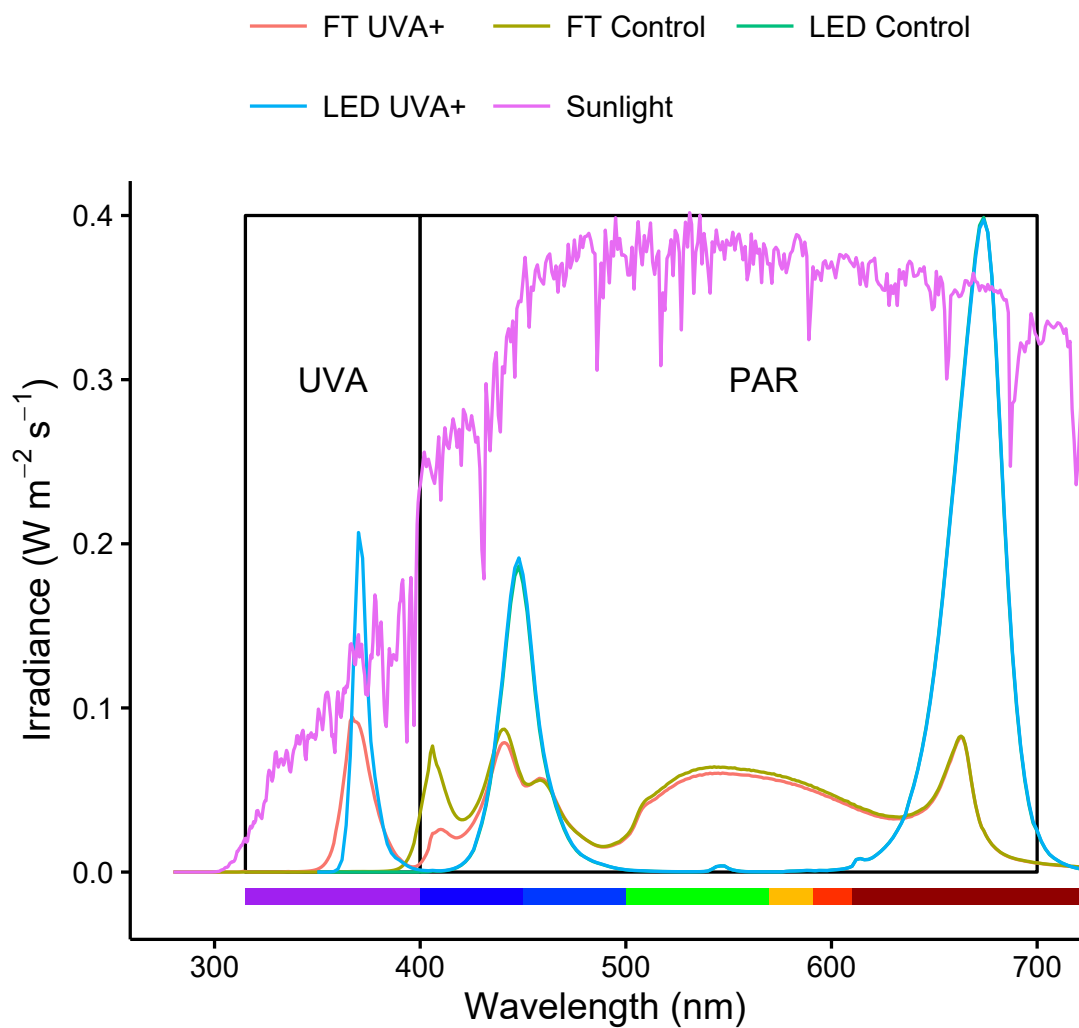


Figure 5.3: Spectra for the four experimental treatments and an ASTM G173 standard sunlight spectrum (scaled to 0.3 of the modeled irradiances to allow qualitative comparison with the treatment spectra).

Table 5.2: Model coefficients for three separate models describing aphid behavioural responses to light stimuli. Response variables were model 1: Time Proportion in Feeding Position, model 2: Time Proportion on Leaf, model 3: Mean Velocity. Two light treatments were compared: UVA- (n = 38), UVA+ (n = 42). Significance codes: * = $p < 0.05$, ** = $p < 0.01$, *** = $p < 0.001$.

Response Variable	Predictor	β	SE	t-value	p
Time Proportion in Feeding Position	(Intercept)	1.6070	0.3326	4.831	<0.001***
	UVA	-1.5524	0.4523	-3.432	0.001***
Time Proportion on Leaf	(Intercept)	1.8624	0.3781	4.926	<0.001***
	UVA	-1.7253	0.4082	-4.227	<0.001***
Mean Velocity	(Intercept)	0.0065	0.0021	3.047	0.0032***
	UVA	0.0067	0.0029	2.3000	0.0241*

and UVA treatment (UVA+ or UVA-) was non-significant ($p = 0.58$) in predicting the TPiFP. The main effect of lamp type was also non significant in the additive model ($p = 0.7231$), therefore aphid TPiFP was predicted only by the UVA treatment (Figure 5.4.A).

Aphids under UVA+ lighting spent 31-35% less time (D.f. = 79, $p = 0.001$) on the leaf discs than under the control. Both the lamp type interaction with UVA treatment ($p = 0.90$) and the main effect of lamp type ($p = 0.94$) were non significant and so aphid duration of time on leaf disc was predicted only by UVA treatment (Figure 5.4.B and Table 5.2).

Aphids under high UVA+ lighting moved 51% faster (D.f. = 79, $p = 0.02$) under UVA+ treatments compared with those under UVA- treatments. The interaction between lamp type and UVA treatment ($p = 0.68$) and the main effect of lamp type ($p = 0.30$) were non significant, therefore the final model included the UVA treatment term only (Figure 5.4.C and Table 5.2).

5.5 Discussion

5.5.1 Measuring aphid responses to light environment

Using the raw data from the image tracking scripts (in this case, aphid position and time), three secondary measures of aphid movement behaviour in response to light environment were compared: proportion of time in a feeding position, proportion of time on the leaf disc, and average velocity. As proportion of time in a feeding position is an aggregate of velocity and time on the leaf disc, this metric is the most convenient metric of aphid response, sensitive to changes in velocity and whether or not the aphid moved to an area of non-leaf (where velocity information was not measured). Proportion of time spent on the leaf disc and aphid average velocity may be applicable to test specific hypotheses but may not be as sensitive measured of behaviour as the TPiFP. Other research has used similar aggregate metrics, derived from identifying periods of aphid inactivity and calibrating these against other techniques that explicitly identify feeding activity (Kloth et al., 2015). As they sought to identify aphid preference for different host phenotypes, their method was necessarily more complex, allowing differentiation of short and long probes in order to distinguish between the exploratory pathway phase and ingestive phloem phase (Pettersson et al., 2007). Here, I sought to quantify the response of aphids to the light environment, and these were amenable to simpler measures of behaviour: aphids attempting to feed compared with aphids moving away from feeding sites in response to the light environment.

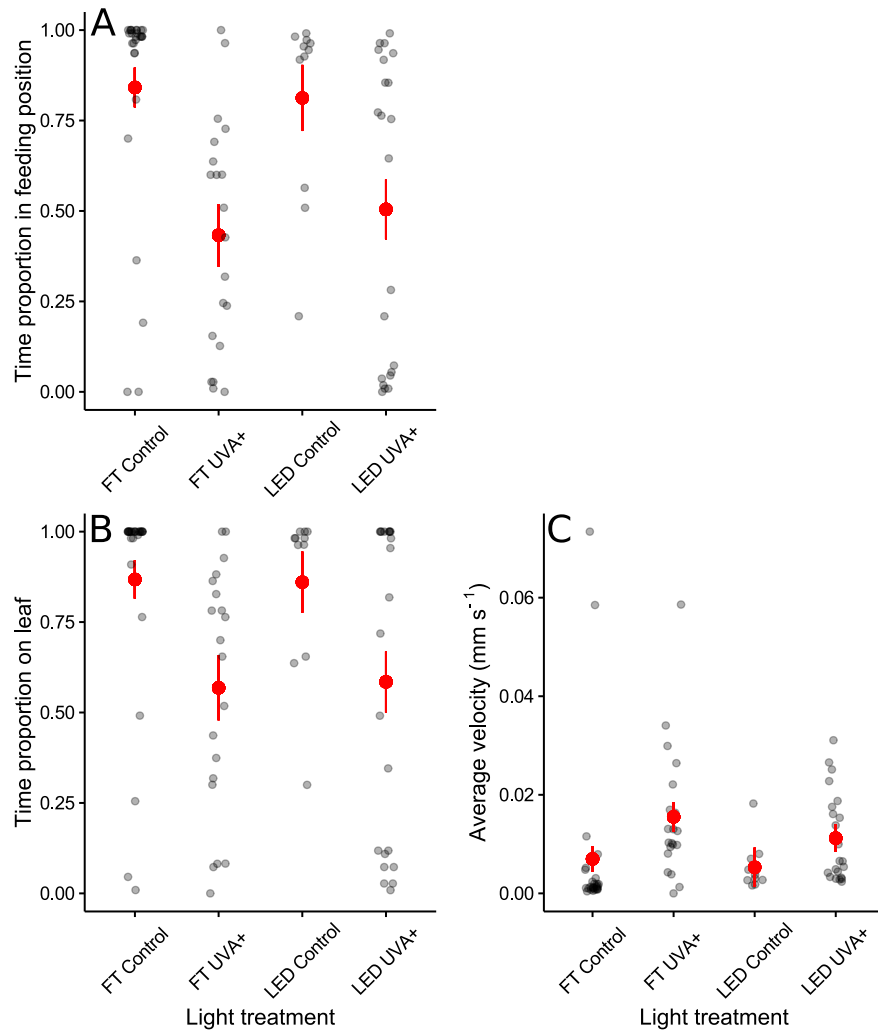


Figure 5.4: Raw data and GLM predictions for measures of aphid sensitivity to light. Time proportion in feeding positions (A), TPiFP (B) and average velocity (C) is presented for each aphid under four light treatments: white LED lighting with (FT UVA+) and without (FT Control) fluorescent tube UVA and LED lighting with (LED UVA+) and without (LED Control) LED supplemental UVA. Red point-ranges show quasibinomial GLM-fitted values the predicted standard error in figures A and B. Red point-ranges show the quasi GLM-fitted the predicted standard errors are presented in figure C.

This simpler method, which takes into account both short and long probes as attempted feeding, appears to be suitable as a simple, rapid screen for the effects of light environment on aphids.

A threshold velocity of 0.014 mm s^{-1} was used in the experimental setup which is somewhat lower than previously used (0.020 mm s^{-1} was used by Kloth et al. (2015)), therefore making this system more conservative in identifying a feeding event. However as the effect size for the TPiFP metric was largely determined by the presence or absence of the aphid on the leaf disc, rather than the the low velocity whilst on the leaf disc, it is unlikely that varying this threshold would significantly alter the conclusions. Previous studies tested the efficacy of camera tracking systems against manual observation of feeding behaviour, demonstrating a strong correlation between user-verified probing events and periods where the aphid was stationary on the leaf disc (Kloth et al., 2015; Noldus et al., 2002).

Our work successfully established a method for short term (< 1 hour) quantification of behavioural responses to light. The technique presented here is a quick, cost-effective approach for measuring insect behavioural parameters under various light conditions. The system was robust under various types of lamp and spectral balance (Figure 5.3) and, as all source code was written using Open Source programming environments (OpenCV, Python and R), the code can be modified for different insect species and testing layouts.

All of the steps are described in the Materials and Methods section (5.2) and so an informed user may construct similar scripts for their own tracking requirements. Code is provided to illustrate approaches which may be taken when designing scripts, however this is not provided as an off-the-shelf software package.

5.5.2 Changing light in commercial and laboratory growth environments

Field sunlight, glasshouses and controlled environment rooms lit with conventional lighting systems (fluorescent tubes or metal halide lamps) all contain UVA radiation (Aphalo et al., 2012). The rapid expansion of commercially available LED systems for plant lighting means that for the first time light environments without UV radiation are becoming commonplace in both research and commercial crop production. Our results demonstrate that aphids spend more time moving in light environments where UV is present compared with those without UV, most likely to find a feeding site with lower UV irradiances, so reducing exposure to shorter wavelength UV (UVB), which is known to have a significant deleterious effect on many invertebrates (Ohtsuka and Osakabe, 2009; Sakai et al., 2012; Dong et al., 2014; YiMin et al., 2014, Chapter Four). We would expect these changes in invertebrate behaviour on the plant (Figure 5.4) to influence pest distribution through the host plant (Burdick et al., 2015), with consequences for both the visibility of pest attacks and accessibility to pest control measures. These response are in addition to the well know effects on UV on the flight behaviour of many insect pests (Diaz et al., 2006) and light-mediated changes in host resistance (Roberts and Paul, 2006).

From the perspective of plant biology light environment is generally characterised in terms of the irradiance or quantum flux of PAR (400-700 nm) and/or specific ratios such red: far red. In considering the effects of light environment on insects, such as aphids, it is useful to consider ratios between different wavebands rather than irradiances since insects use a relatively complex colour opponency mechanism involving green, blue and UV (Döring et al., 2007) for perception of colour (Briscoe and Chittka, 2001). Therefore, it is the relative ratios of one spectral band to another that influences behaviour rather than the overall irradiance. In Figure 5.5 I describe

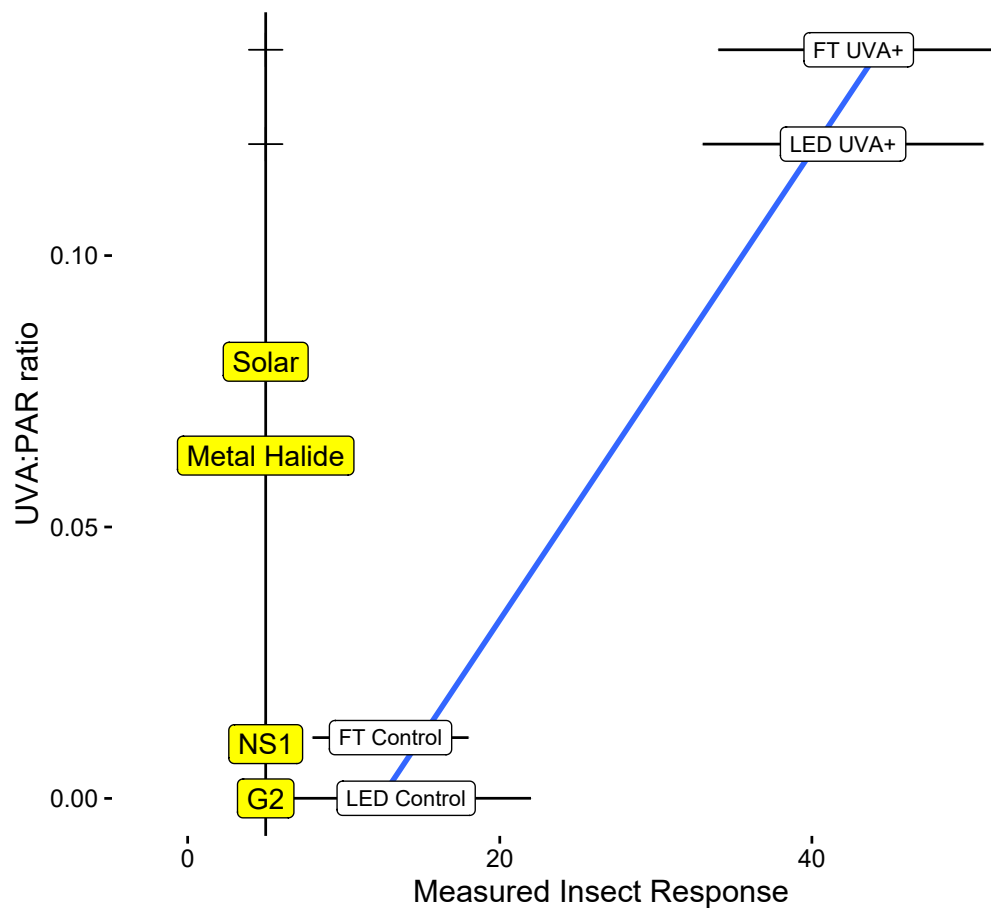


Figure 5.5: Contextual Spectral Diagram. UVA:PAR ratios of experimental, commercial and naturally occurring light sources. FT UVA+, LED UVA+, FT Control and LED Control are the light treatments used in the experimental work reported here (white labels). The yellow labels show the UVA:PAR ratios for four typical plant growth spectra. Metal Halide is a typical metal halide lamp, measured as described previously. Solar is a surface-level modeled spectrum (ASTM G173 global) from the photobiology R package. G2 and NS1 are commercially available LED lamps from Valoya Ltd. (spectral percentages obtained from valoya.com). A measure of relative insect response ($100 \cdot (\text{Time Proportion in feeding position} \times 100)$) is shown on the x-axis for the four experimental treatments. The error bars show the predicted standard errors and the regression line is a linear fit for the four points.

a range of growing environments in terms of the simple ratio between UVA and PAR. Our data demonstrated here that aphids respond predictably to the UV:PAR ratio, spending significantly less time in a feeding position (i.e. they are more disturbed) when UV:PAR is higher (Figure 5.5). Typical metal halide growth rooms are more similar to typical sunlight than to LED units (Figure 5.5) in terms of the UVA:PAR ratio. We would predict that insects seeking to avoid UVA (examples in Ohtsuka and Osakabe (2009) and Burdick et al. (2015)) would respond similarly to sunlight under metal halide (more disturbed, less attempted feeding), whereas under the low UVA:PAR (Figure 5.5) ratios found under most growth lamps, these avoidance responses would be absent. However, whilst broad predictions may be made about insect responses to new lighting through the UVA:PAR ratio (as in Figure 5.5), techniques such as this for rapidly screening insect behavioural responses to lighting environments are important for exploring the effects of the wide range of light environments now provided by different LED lighting systems.

5.6 Conclusions

We present a simple system, utilising open source software resources and inexpensive camera equipment, for the assessment of insect behavioural responses to light. Our system worked robustly under four different light environments and provided a convenient metric to indicate the amount of time aphids spent in a feeding position on the leaf disc. This technique may form part of the early prototyping or development stages in designing new light environments, offering a rapid system for testing an insect species for behavioural avoidance responses to new lighting.

Evidence for a novel functional role of the UV photoreceptor in *Myzus persicae*

Abstract

Background: The results of experimental work in Chapter Three and from the wider literature suggested that perception of ultraviolet light may determine the distribution of invertebrate herbivores within the canopy structure of the host plant. Through a campaign of experimental work using image analysis software to determine settling activity under different illumination, I develop a colourspace behavioural model for apterous morphs of the aphid, *M. persicae*.

Results: Using variable intensity narrow-band Light-Emitting Diodes (LEDs), I demonstrated that increasing the ultraviolet (UV) and blue proportion of the illumination spectrum had an inhibitory effect on the settling behaviour of apterous morphs, whilst increasing the green proportion of the illumination spectrum had a stimulatory effect on settling. Combining these data with previously-derived electroretinography data, a colourspace model for the behaviour of *M. persicae* was produced.

Conclusions: The findings of this chapter demonstrate the use of two colour-opponent visual processing systems in apterous *M. persicae* which initiate behavioural responses. This allows both positioning within the canopy which minimises exposure to harmful solar radiation, and correct identification of green foliar material for feeding.

6.1 Introduction

Understanding insect vision is of fundamental importance in understanding the interaction with its environment. With examples from across the Class, visual mechanisms have been shown to have a central role in navigation (Egelhaaf and Kern, 2002), host plant selection (Döring et al., 2007), predation and parasitism (Langley et al., 2006) and mate selection (Osorio and Vorobyev, 2008). Broadly, we may consider visual mechanisms to fall under two major categories: achromatic and chromatic. Achromatic vision is primarily associated with locomotion or response to moving objects, such as predators (Giurfa and Menzel, 1997). Insects in flight detect vertically orientated textures moving through the visual spatial domain, in order to maintain a straight heading as well as to measure the distance traveled (Egelhaaf and Kern, 2002). The use of achromatic vision in these circumstances allows very fast neuronal processing to occur (Borst, 2009), which is highly advantageous for time-critical functions, for example the takeoff behaviour of a fly in order to evade a predator. Achromatic vision has also been shown to allow discrimination of shapes (Pérez et al., 2011), however this may be unreliable as a method of target identification in structurally complex habitats and for tasks that require associative learning (Benelli and Canale, 2012).

Chromatic vision is the ability to discriminate between different wavelength light and therefore requires that the insect has sensitivity to at least two different wavebands. Wavelength specificity may be achieved either through filtering the light that passes down the insect ommatidia, with wavelength-specific distal cells before it reaches the photoreceptor, or, through altering the sensitivity of the chromophore pigment in the photoreceptor cells (Briscoe and Chittka, 2001). These two adaptive mechanisms allow a very wide range of spectral sensitivities to occur across insect taxa. Whilst many *Lepidoptera* are tetrachromates (four photoreceptor sensitivities), the majority of *Hemiptera*, *Diptera* and *Hymenoptera*, like vertebrates, have trichromatic vision (three photoreceptor sensitivities). The peak sensitivities of the three bands vary somewhat (1.3.1), however, most have a peak in the ultraviolet-A (UVA) ($\lambda_{\max} \sim 350\text{nm}$), blue ($\lambda_{\max} \sim 440\text{nm}$) and green ($\lambda_{\max} \sim 530\text{nm}$) (Briscoe and Chittka, 2001).

Simply having the architecture for perception at different wavelengths does not guarantee that an organism can perceive colour. In order to truly perceive colour, it must process the signals from its photoreceptors in a way that accounts for the overall intensity of the stimulus. *Hymenoptera* have been shown to show preference for monochromatic targets over achromatic (white) targets which had a higher intensity at the same wavelength as the monochromatic target (Chittka et al., 1992). Similarly, aphids showed preference for green and yellow targets even though white targets reflected higher irradiances in the green-yellow wavebands (Doring and Kirchner, 2007, see 1.3.2 for discussion). This spectral preference can occur because insects typically use an opponent coding strategy: the stimuli from each class of photoreceptor are processed such that stimulation of one class of photoreceptor inhibits that of another (Chittka et al., 1992). This robustly allows the identification of target and illumination colour across the vast range of light intensities that occur in different parts of its habitat, as well as at different times of day.

In herbivorous insects, chromatic vision is used extensively for host finding (Doring et al., 2004; Doring and Kirchner, 2007) and in flight behaviour (Barta and Horváth, 2004; Antignus, 2000). Aphids have been shown to be strongly attracted to yellow and green targets, but to be repelled by materials with high UV and blue reflectivity (Doring et al., 2004). This preference for yellow and green is likely a mechanism for detecting vegetation and supports the hypothesis that aphids

use a colour opponent strategy for host selection that is positively stimulated by green light and negatively stimulated by blue and UV light. There is some small variation in aphid green peak wavelength sensitivity between species (Doring and Kirchner, 2007), and it has been suggested that this confers a species-specific ability to detect the subtle variation between host and non-host vegetation (Prokopy and Owens, 1983). During flight, insects probably use UVA to identify the sky (Barta and Horváth, 2004) due to the high degree of contrast that occurs between land and a wide variety of sky conditions (Möller, 2002). Consequently, many studies have examined the impact of UV-attenuation on the spread of flying insects, due to the potential for agricultural pest control. When UV was attenuated, fewer aphids were found in polytunnel crops (Antignus, 2000; Legarrea et al., 2012c) and the population spread more slowly (Legarrea et al., 2012a), as might be expected if dispersal flight behaviour was disrupted.

In Chapter Three, an increased proportion of wingless *M. persicae* was found on the upper leaf surfaces when UVA was attenuated. This was also seen in a previous study (Burdick et al., 2015) in a different system. It has been previously argued that wingless aphids do not choose their feeding sites in response to light stimuli (Simmons, 1999), however, it is evident that there is a mechanism or mechanisms, of response to UVA, which affects aphid choice of feeding site. As such, the aims of this chapter were to (i) establish whether *M. persicae* responds behaviourally to illumination colour, (ii) establish the likely visual processing method with which it translates light perception into behavioural response and (iii) discuss the implications of this in the context of protected cropping technology.

6.2 Methods

6.2.1 Plants and aphids

Aphids were reared as described previously (2.1.1) on calabrese (*Brassica oleracea*) of the same variety as was used for the experimental work. For Experiments 1 to 4, calabrese (c.v. 'Volta', supplied by Nickys Nursery Ltd., Broadstairs, Kent, UK) was grown in a partially-temperature controlled glasshouse with automatic ventilation, heating and supplementary lighting from 4x 600 W Senmatic FL300 Sunlight LED units. Seeds were sown in M3 compost and grown as described previously (2.1.2). At four weeks, the third or fourth leaf was removed from the plant and an 11 mm leaf disc borer was used to remove up to 12 leaf discs from a single leaf, avoiding large veins. These were immediately placed on the moistened foam squares as described below. The same procedure was carried out for Experiment 5, however, the calabrese variety for aphid stock and experimental plants was changed to 'Zen' (supplied by Tozer Seeds Ltd., Cobham, Surrey, UK).

6.2.2 Behavioural assay technique

Full details of the behavioural assay chamber set-up, image capture and image processing technique are described in Chapter Five. Briefly, for Experiments 1-4, two Petri dishes were used, each with four foam squares. The Petri dishes were flooded with deionized water so that only the tops of the foam squares were above the surface. An 11 mm diameter leaf disc was placed on each island upper-surface facing upwards and a single aphid placed on this with a paintbrush.

One Petri dish was placed on each side of the behavioural assay chamber, allowing a side-by-side experimental design for two light treatments simultaneously.

For Experiment 5, 12 foam squares were fixed into a 200 mm x 100 mm perspex tray, which was then flooded with DI water. Each foam square had a double-thickness square of filter paper applied to the top surface and an 11 mm leaf disc placed on top (upper surface facing upwards). An aphid was placed in the centre of the leaf disc and the tray moved into the behavioural assay chamber. In all experiments, each assay was run for one hour with a photograph captured every 30 seconds.

The image sequence data were processed as described in Chapter Five, and the metric Time Proportion in Feeding Position (TPiFP) was used as the primary response variable. This was calculated for each aphid as

$$\text{TPiFP} = \frac{D_{\text{Feeding}} - D_{\text{Moving}} - D_{\text{Off Leaf}}}{D_{\text{Feeding}} + D_{\text{Moving}} + D_{\text{Off Leaf}}} \quad (6.1)$$

where D_{Feeding} is the duration of time an aphid spends on the leaf disc below the threshold velocity of 0.014 mm s^{-1} , D_{Moving} is the duration spent on the leaf disc above that threshold, $D_{\text{Off Leaf}}$ is the duration spent unmonitored off the leaf disc.

6.2.3 Light treatments

Light treatments in experiments 1-4 were designed to test for specific avoidance responses to UVA and UVB by using a high UV irradiance compared to a low UV irradiance control. In experiment 5, the light treatments were chosen to test a broad range of illumination scenarios which covered the range of illumination colours experienced by an aphid in typical canopy environments, as well as allowing the testing of unusual light environments, such as those experienced under polythenes. In experiments 1-4, illumination was provided by a combination of LED and fluorescent tubes, filtered with various polyethylene (PE) claddings and neutral density filters (see Table 6.1). This permitted For experiment 5, a four-LED source was used with variable intensity irradiation peaks at 375 nm, 451 nm, 521 nm and 660 nm (Table 6.2, see 2.3.10 for details of light sources). Full spectrum irradiance was measured for each light treatment with a cosine corrected head (see 2.4.4 for further details) at the leaf disc level for each light treatment.

6.2.4 Statistical analyses

All statistical analyses were conducted in R. The index Total Proportion of Time in Feeding Position was used and so GLMs with a binomial or quasibinomial error structure were used to test the response to aphid visual parameters. Aphid colourspace calculations were made as described previously (2.4.7). Spectral data processing and irradiance calculations were made using the 'photobiology' package and all plots were made with 'ggplot2' or the 'ggspectra' photobiology package.

Table 6.1: Details of light treatments for experiments 1-4. The ‘Treatment’ label refers to the labels used in subsequent plots. Source types were: Valoya NS1 - Valoya NS1 LED array, UVA360 - Philips TL 6W BLB fluorescent tube, UVB313 - QPanel EL313 UVB fluorescent tube. The neutral density (ND) filter used was a medium course aluminium filter. PE films used were: Lumivar - BPI Visqueen Lumivar UV-Opaque, Lumisol - UV-Transparent.

Treatment	Visible Source	Visible Source ND Filter	UV Source	UV Source Film Filter	UV Source ND Filter
E1 UVA-	Valoya NS1	N	UVA360	Lumivar	N
E1 UVA+	Valoya NS1	Y	UVA360	Lumisol	N
E2 UVA-	Valoya NS1	N	UVA360	Lumivar	Y
E2 UVA+	Valoya NS1	Y	UVA360	Lumisol	Y
E3 Hi HVis	Valoya NS1	Y	UVA360	Lumisol	Y
E3 Lo HVis	Valoya NS1	Y (x2)	UVA360	Lumisol	Y
E4 UVB-	Valoya NS1	N	UVB313	Lumivar	N
E4 UVB+	Valoya NS1	N	UVB313	Lumisol	N

Table 6.2: Details of light treatments for Experiment 5. The settings used for a variable control four-LED array as percentages of the maximum available brightness for each LED type. The peak wavelength for each LED type is also displayed.

Treatment	LED Power (% Max.)			
	Red (660 nm)	Green (521 nm)	Blue (451 nm)	UV (375 nm)
1	94	0	47	0
2	94	0	47	50
3	94	0	47	100
4	47	0	24	0
5	47	0	24	50
6	47	0	24	100
7	94	50	47	0
8	94	50	47	50
9	94	50	47	100
10	47	50	24	0
11	47	50	24	50
12	47	50	24	100
13	94	100	47	0
14	94	100	47	50
15	94	100	47	100
16	47	100	24	0
17	47	100	24	50
18	47	100	24	100
19	24	100	12	50
20	24	100	12	100
21	16	100	8	16

6.3 Results

Using the assay technique described previously, aphid behavioural responses to various light environments were tested in a series of one hour experiments. Initial experimental runs (Experiments 1-4) tested for the presence of behavioural responses to UVA (Experiments 1-3) and ultraviolet-B (UVB) (Experiment 4) using UVA360 and EL-UVB313 fluorescent tubes respectively. A second campaign of experiments was then used to explore the effect of modifying the intensity of green, blue and UV light in order to better understand and, ultimately predict the effect of irradiance and spectral balance on aphid behaviour. Both irradiance and spectral balance (proportional) models were fitted to the data and used to generate predictions of aphid behavioural responses to commercially-relevant light environments.

6.3.1 Effect of UVA (Experiments 1-3)

‘Side-by-side’ experiments (UVA- control and UVA+ measured simultaneously, see [methods chapter] for more details) were used to establish the effect of UVA on aphid feeding behaviour (Figure 6.1).

Experiment 1: high UVA irradiance

In Experiment 1, a low UVA, high human visible (E1 UVA-) treatment and a high UVA, reduced human visible (E1 UVA+) treatment was used to test for the presence of a behavioural response (Figure 6.1.A). Aphids under the UVA+ treatment spent significantly less time in a feeding position compared to those under the UVA- treatment (87% and 31% respectively. Table 6.3 and Figure 6.1.B).

Experiment 2: constant total irradiance

In Experiment 2, total unweighted irradiance was standardised across the two experimental treatments to control for the effect of unweighted irradiance. UVA irradiance was adjusted to produce an aphid-weighted UV proportion equivalent to that found in sunlight ($R_{UV} = 0.05$) under the UVA+ (E2 UVA+) treatment and a low UV proportion ($R_{UV} < 0.002$) under the UVA- (E2 UVA-) treatment (Figure 6.1.C). Aphids under the UVA+ treatment spent significantly less time in a feeding position compared to those under the UVA- treatment (53% and 90% respectively. Table 6.3, Figure 6.1.D).

Experiment 3: constant UVA irradiance

In Experiment 3, UVA irradiance was kept constant and human visible irradiance varied to alter the UV ratio without altering the UV irradiance (E_{UV}^*). A high UVA, low human visible treatment (E3 Lo HVis) and a high UVA, high human visible treatment (E3 Hi HVis) were compared (Figure 6.1.E). Aphids under high Photosynthetically-Active Radiation (PAR) and under low PAR did not spend significantly different amounts of time in a feeding position, therefore an intercept-only model was fitted which estimated the time in a feeding position as $37\% \pm 5\%$ for the two treatments (Table 6.3, Figure 6.1.F).

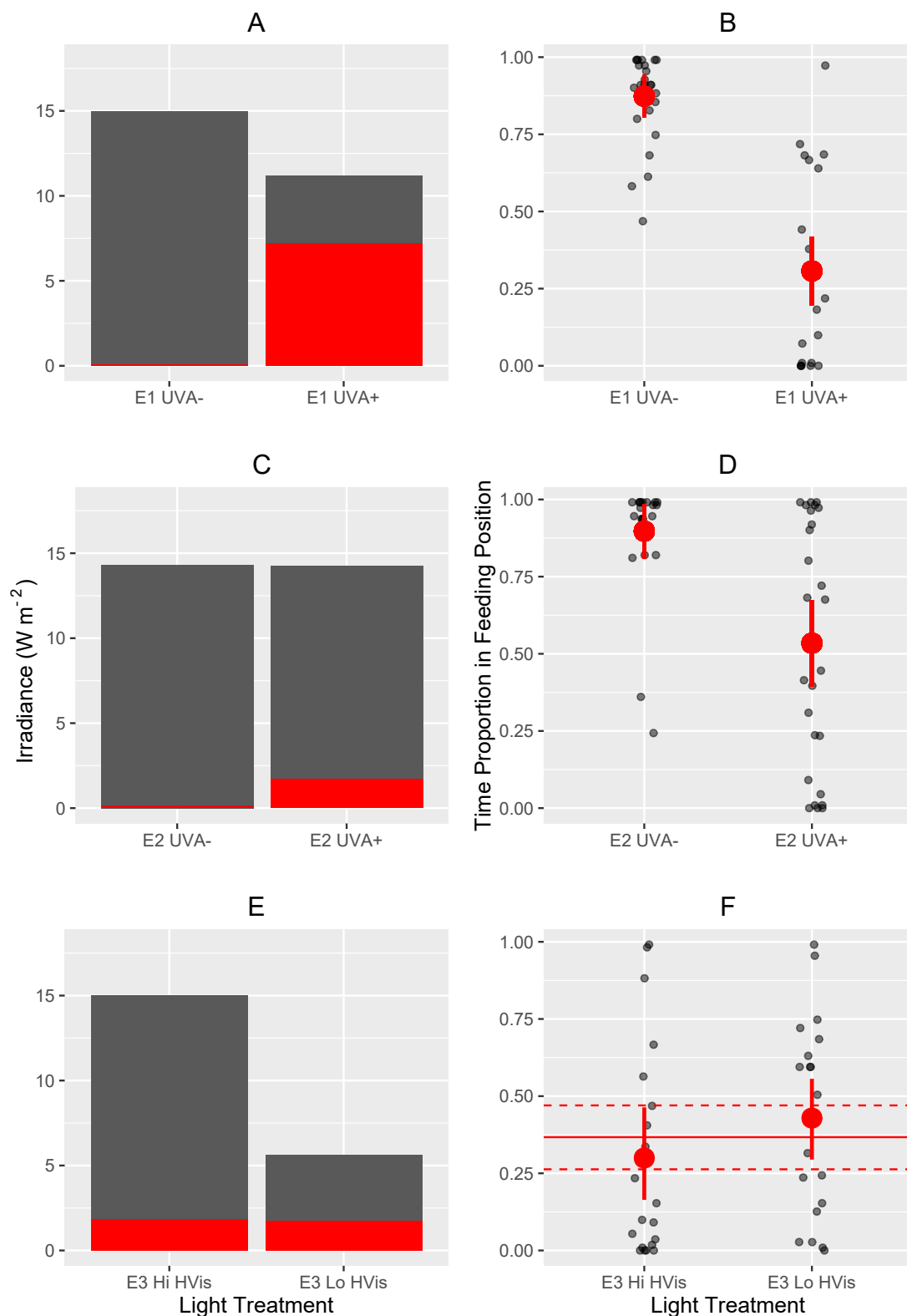


Figure 6.1: Aphid responses and light treatments for Experiments 1-3 using Philips TL(D)/08 fluorescent tubes. The left-hand column (plots (A), (C) and (E)) show the measured irradiance for each treatments. Grey bars show the total measured unweighted irradiance between 280 nm and 800 nm. The red bars show the unweighted UVA (315 nm - 400 nm) irradiance. The right-hand column shows the proportional aphid response to the light treatments. Each black point represents one measured aphid. For (B) and (D), the red point-range shows the estimated fit and 95% confidence interval from the Generalised Linear Models (GLMs). For (F), the point-range shows the calculated mean and 95% confidence interval for the raw data. The red solid line is the intercept-only model mean and the dashed lines show the 95% confidence intervals.

Table 6.3: GLM model parameters for Experiments 1-3. Quasibinomial GLM model parameters for the proportion of aphids in a feeding position for UVA tube experiments. Each experiment was fit with a separate GLM. Experiment 1 compared a UVA+ (UVA = 7.21 Wm^{-2}) to a UVA- (UVA = 0.07 Wm^{-2}) light environment (n = 46). Experiment 2 compared a high UVA (UVA 1.70 Wm^{-2}) to a low UVA (UVA = 0.13 Wm^{-2}) light environment with constant total un-weighted irradiance (n=49). Experiment 3 compared a constant UVA irradiance (UVA = $1.74\text{-}1.84 \text{ Wm}^{-2}$) with a high PAR (PAR = 12.99 Wm^{-2}) and a low PAR (PAR = 3.82 Wm^{-2}) light treatment (n = 39). For Experiment 3, the intercept-only model is shown as light treatment was non-significant. Significance codes: * = $p < 0.05$, ** = $p < 0.01$, *** = $p < 0.001$.

Experiment 1: High UVA irradiance				
	Estimate	Std. Error	t value	Pr(> t)
(Intercept)	1.9307	0.3203	6.0278	< 0.0001 ***
E1 UVA+	-2.7448	0.4178	-6.5693	< 0.0001 ***
Experiment 2: Constant Total Irradiance				
	Estimate	Std. Error	t value	Pr(> t)
(Intercept)	2.1676	0.4889	4.4333	0.0001 ***
E2 UVA+	-2.0298	0.5664	-3.5836	0.0008 ***
Experiment 3: Constant UVA Irradiance				
	Estimate	Std. Error	t value	Pr(> t)
(Intercept)	-0.5437	0.2298	-2.3660	0.0230 *

6.3.2 Effect of UVB (Experiment 4)

In Experiment 4, UVB and UVA irradiance was higher under the UVB+ treatment (E4 UVB+) compared to the control (E4 UV-). PAR irradiance was kept constant for both experimental treatments (Figure 6.2.A). Aphids under high UVB did not spend significantly different amounts of time in a feeding position compared to aphids under a low UVB and low UVA control therefore an intercept-only model was fitted, which estimated the time in a feeding position as $81\% \pm 5\%$ for the two treatments (Table 6.4, Figure 6.2.B).

Table 6.4: GLM model parameters for Experiment 4. Quasibinomial GLM model parameters for the proportion of aphids in a feeding position. Experiment 4 compared a UVB+ (UVA = 1.66 Wm^{-2} , UVB = 1.10 Wm^{-2}) to a UVB- control (n = 49). The intercept-only model is shown as light treatment was non-significant. Significance codes: * = $p < 0.05$, ** = $p < 0.01$, *** = $p < 0.001$.

Experiment 4: High UVB irradiance				
	Estimate	Std. Error	t value	Pr(> t)
(Intercept)	1.4750	0.2949	5.0016	< 0.0001 ***

6.3.3 Defining the aphid colourspace

In order to determine the quantitative relationship between UV and aphid behaviour, light treatment spectral measurements were converted to *M. persicae* photoreceptor-weighted irradiance values. A reference spectrum (ASTM G173 Direct solar spectrum) was chosen as the centre-point for the aphid colourspace and was convolved with the three aphid photoreceptors to produce aphid-weighted irradiances (figure 6.3.A). The convolved spectra had high weighted irradiances in aphid-blue ($E_{\text{Blue}}^* = 110 \text{ Wm}^{-2}$) and aphid-green ($E_{\text{Green}}^* = 156 \text{ Wm}^{-2}$) compared to a relatively low weighted irradiance in aphid-UV ($E_{\text{UV}}^* = 13 \text{ Wm}^{-2}$), due to the low proportion of

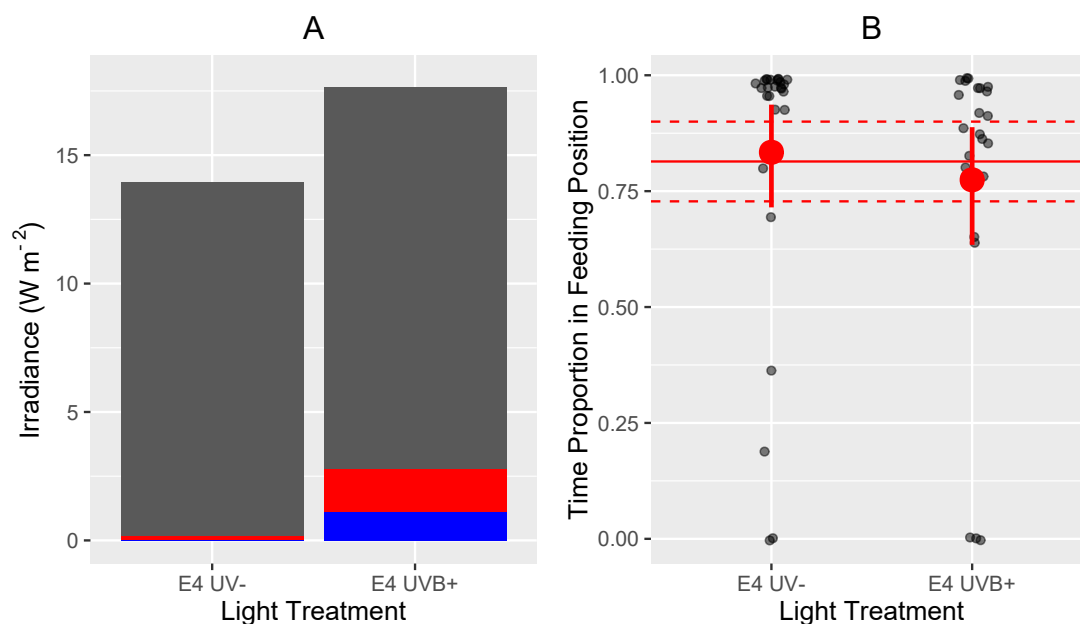


Figure 6.2: Aphid behavioural responses and light treatments for Experiment 4 using Q Panel QUV UVB-313 EL fluorescent tubes. (A) shows the measured irradiance for each treatment. Grey bars show the total measured irradiance between 280 nm and 800 nm. The red bars show the total UV (280 nm - 400 nm) irradiance and the blue bars show the total UVB (280-315nm) irradiance. (B) shows the proportional aphid response to the light treatments. Each black point represents one measured aphid. The point-range shows the calculated mean and 95% confidence interval for the raw data. The red solid line is the intercept-only model mean and the dashed lines show the 95% confidence intervals.

UVA in sunlight (Figure 6.3A). As proportional coordinates: $R_{\text{Green}} = 0.559$, $R_{\text{Blue}} = 0.394$ and $R_{\text{UV}} = 0.047$.

Weighted irradiances and irradiance-independent proportional values for each light treatment used in Experiments 1-4 were calculated in the same way. R_{UV} values for each photoreceptor under the different light treatments varied between 0.001 and 0.221 (Figure 6.3.B) representing a range from well below the sunlight reference ($R_{\text{UV}} = 0.047$) to much higher. These values were then scaled to calculate their position in a *M. persicae* colourspace, centered around the standard ASTM G173 direct solar spectrum model (Figure 6.3.C). The control treatments for Experiments 1, 2 and 4 (E1 UVA-, E2 UVA-, E4 UVA-) were all much less UV-rich, but had a similar Green:Blue ratio to standard field sunlight. E2 UVA+ and E3 Hi PAR were similar to sunlight in all three colour axes. E1 UVA+, E3 Lo PAR and E4 UVB+ were very UV-rich in comparison to sunlight, however, their Green:Blue ratios also remained similar to sunlight. Overall, on the scaled axis in figure 6.3.C UV:[Green+Blue] proportion varied by 0.72 compared to only 0.13 in the scaled Green:Blue proportions.

6.3.4 Using the aphid colourspace to predict behavioural responses

Two models were specified for the time proportion data for Experiments 1-3: a model using aphid-UV weighted irradiance (E_{UV}^*) and a second model using aphid-UV weighted proportion (R_{UV}). For the irradiance model, natural log transformation of E_{UV}^* reduced the residual deviance and was judged a better model fit. The final model identified a highly significant negative log-linear relationship between the UV irradiance and the proportion of time spent in a feeding position, estimating 50% in a feeding position when $E_{\text{UV}}^* = 0.36 \text{ Wm}^{-2}$ (Table 6.5, Figure 6.4.A).

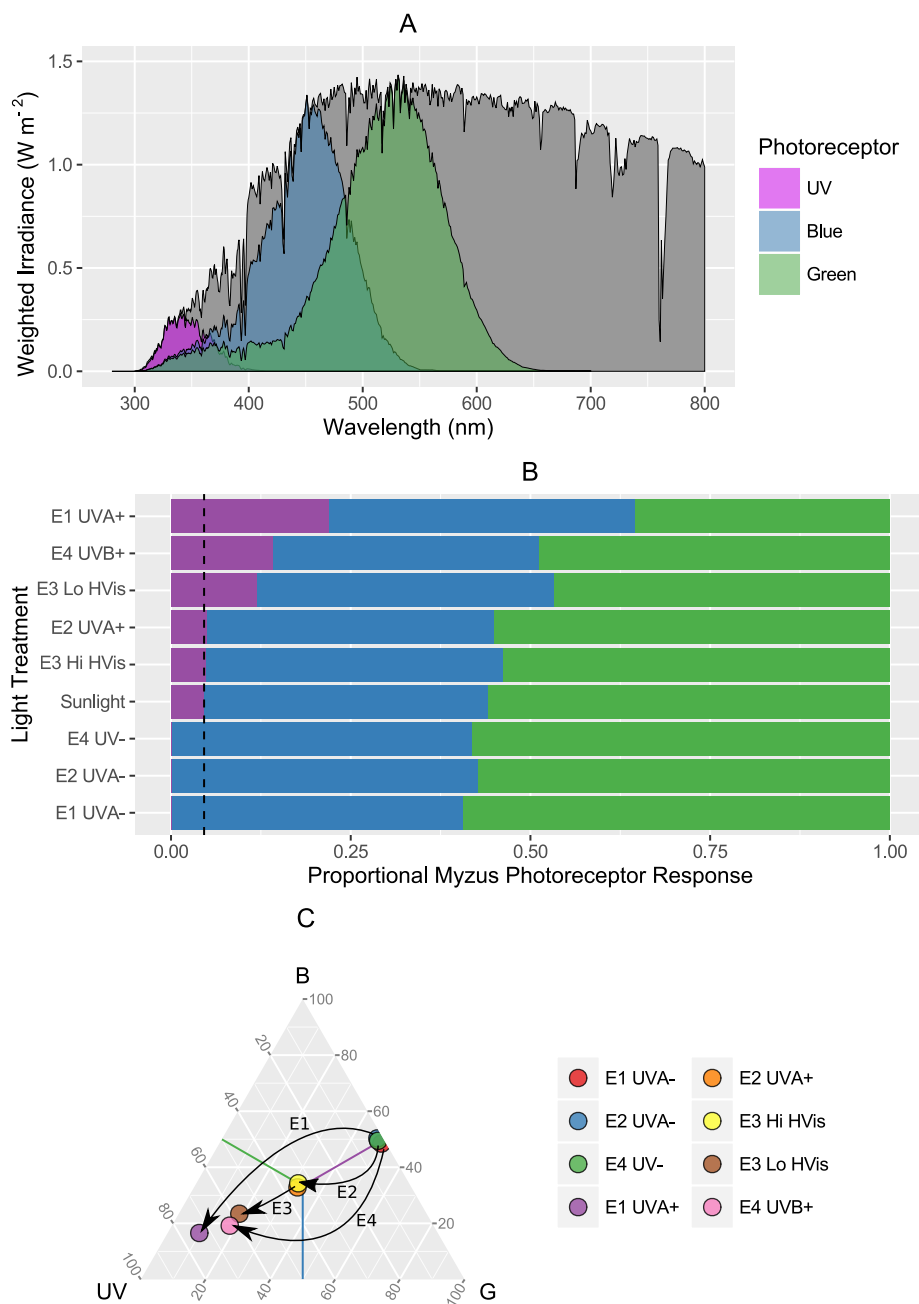


Figure 6.3: *Myzus persicae* photoreceptor responses (see 2.3.7 for description of plot construction). (A) is an ASTM G173 Direct Solar Spectrum shown unweighted (grey) and convolved with each of the three aphid visual action spectra (purple = UV, Blue = Blue, Green = Green). (B) shows the relative proportion of UV, blue and green experienced by the aphid under each light treatment. The dashed vertical line shows the relative, aphid-weighted UV photoreceptor response of the standard ASTM G173 Direct Solar Spectrum model as a reference. (C) is a ternary plot with three proportional axes, each representing a photoreceptor response. The proportional values were scaled so that the aphid response to ASTM G173 Direct Solar spectrum is the central point in the plot. Arrows show the difference in colourspace between treatments for Experiments 1-4 (Figure 6.1 and 6.2)

Table 6.5: Quasibinomial GLM parameters for the proportion of aphids in a feeding position for all UVA tube experiments (Experiments 1-3) with log aphid-weighted irradiance (E_{UV}^*) as a single factor in the model. $n = 163$. Significance codes: * = $p < 0.05$, ** = $p < 0.01$, *** = $p < 0.001$.

	Estimate	Std. Error	t value	Pr(> t)
(Intercept)	-0.5831	0.1707	-3.4168	< 0.0001 ***
$\ln(E_{UV}^*)$	-0.5996	0.0730	-8.2122	< 0.0001 ***

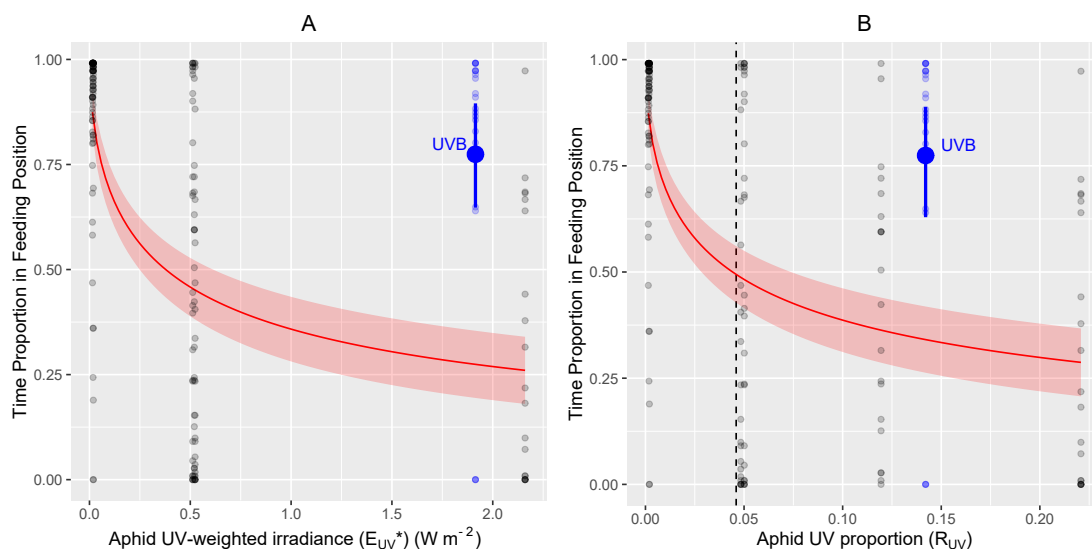


Figure 6.4: Aphid behavioural responses to UV. The proportion of time in a feeding position for all UVA light treatments plotted against (A) aphid-weighted irradiance (E_{UV}^*) and (B) aphid-weighted UV proportion (R_{UV}). Each black point represents a single aphid from a UVA+ or UVA- treatment. The red trendlines show the log-linear GLM predictions and estimated 95% confidence interval for the seven UVA+ and UVA- treatments. Data from the UVB+ experimental treatment are shown independently as small blue points (individual aphids) and a blue point-range representing the mean $\pm 95\%$ confidence intervals. The dashed vertical line in (B) shows the proportion aphid-weighted UV for the standard ASTM G173 Direct Solar Spectrum model as a reference.

The proportional model fit with natural log-transformed R_{UV} had lower residual deviance than the un-transformed equivalent model and was therefore judged a better fitting model. A significant, negative log-linear relationship between UV proportion (R_{UV}) and the proportion of time spent in a feeding position was demonstrated, estimating 50% of aphids in a feeding position when $R_{UV} = 0.044$ (Table 6.6, Figure 6.4.B).

Aphids under UVB+ treatments spent more time in a feeding position than would have been expected under UVA+ treatments of the same aphid-weighted UV irradiance or proportion (77% compared to 34% under a proportional equivalent UVA treatment. Figure 6.4, blue point-ranges).

Table 6.6: Quasibinomial GLM parameters for the proportion of aphids in a feeding position for all UVA experiments (Experiments 1-3) fit against log aphid-weighted UV proportion (R_{UV}). $n = 163$. Significance codes: * = $p < 0.05$, ** = $p < 0.01$, *** = $p < 0.001$.

	Estimate	Std. Error	t value	Pr(> t)
(Intercept)	-1.7621	0.2868	-6.1449	< 0.0001 ***
$\ln(R_{UV})$	-0.5649	0.0690	-8.1905	< 0.0001 ***

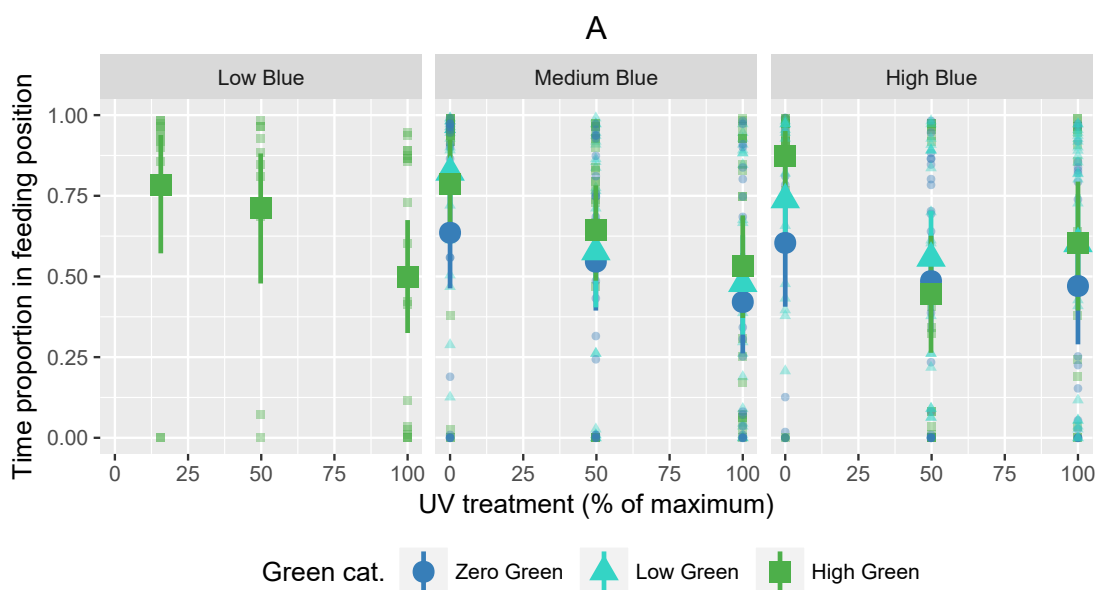


Figure 6.5: Aphid colourspace experiment raw data. Plot shows the proportional aphid response to all light treatments (Time Proportion in Feeding Position). Each small point is an individual aphid. Point-ranges show the mean and estimated 95% confidence intervals for each treatment group. The treatments are expressed in categories determined by the unweighted irradiance from each of the three treatment LEDs (not by aphid visual-weighted response). Blue irradiance category is split by faceting, green irradiance category is shown by point shape and colour and UV irradiance category expressed as a percentage of the maximum on the x axis.

6.3.5 Experiment 5: Expanding the aphid colourspace model

A set of experiments using 21 green/blue/UV light treatments to explore aphid behavioural responses within an environmentally relevant range was conducted using a variable intensity LED array. Time proportion in feeding position was used as the behavioural response variable and this was measured under a range of light treatments (figure 6.5). Both aphid weighted irradiances (E^*) and proportional responses (R) for the three photoreceptors were fit as separate models.

For the irradiance model, natural log transformed values of E_{Green}^* , E_{Blue}^* and E_{UV}^* were fitted as predictors in a binomial GLM with time in feeding position as the response. Model simplification identified the best fitting model as $y \sim \ln E_{\text{UV}}^* + \ln E_{\text{Green}}^*$ which had a lower residual deviance than the untransformed equivalent model $y \sim E_{\text{UV}}^* + E_{\text{Green}}^*$. A quasibinomial error structure was used to account for overdispersion in the data. Aphid-weighted UV irradiance had a significant negative log-linear effect ($\beta = -0.260$) on time spent in feeding position and aphid-weighted green irradiance had a significant positive effect ($\beta = 0.368$) on time spent in feeding position (Table 6.7, Figure 6.6.A and B).

For the irradiance-independent (proportional) model, aphid-weighted UV proportion (R_{UV}) and aphid-weighted GBP ($\text{GBP} = E_{\text{Green}}^*/E_{\text{Blue}}^* + E_{\text{Green}}^*$) were fitted as predictors in a binomial GLM. Natural log transformations were applied to the predictors and were retained where residual deviance was reduced compared to the untransformed models. A quasibinomial error structure was used to account for overdispersion in the data. Model simplification identified the additive model $y \sim \ln R_{\text{UV}} + \text{GBP}$ as the best fitting model. Aphid-weighted UV proportion had a signif-

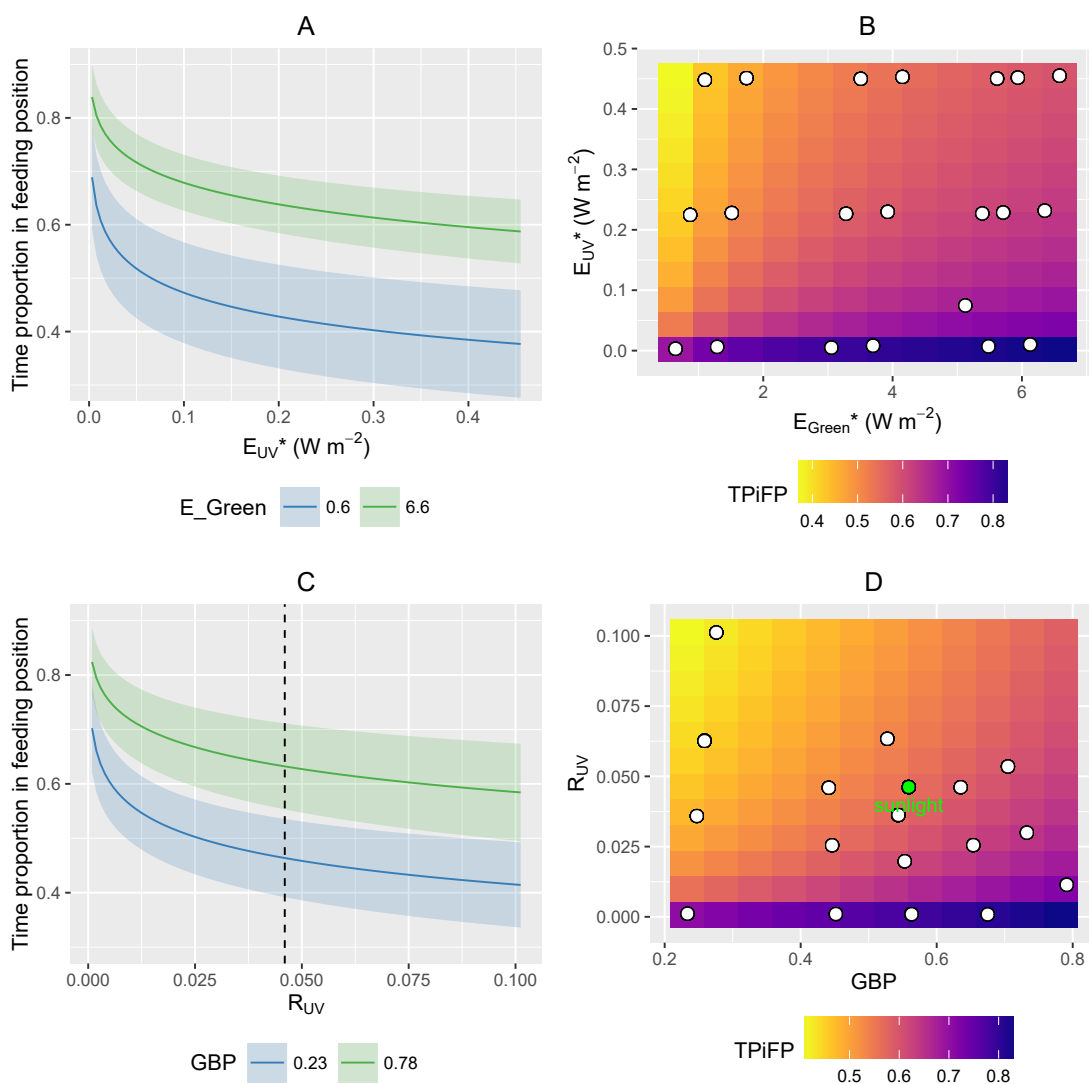


Figure 6.6: Model predictions for effect of irradiance and spectral balance on aphid feeding behaviour. Estimated mean time proportion in feeding position and 95% confidence intervals are shown for the aphid-weighted irradiance model (A). The two line colours represent the extreme experimental aphid-weighted irradiance values ($E_{Green}^* = 0.6$ to 6.6). These predictions are shown as a response surface (B) where colour represents the predicted TPiFP and aphid-weighted green and UV irradiances are the x and y values respectively. The white points represent the experimental treatments. Estimated TPiFP and 95% confidence intervals are shown for the aphid-weighted proportional model (C). The two line colours represent the extreme experimental aphid-weighted Green-Blue Proportion (GBP). For this experiment, the extreme values were 0.23 and 0.78. The dashed line shows the aphid-weighted UV proportion of the reference sunlight spectrum ($R_{UV} = 0.046$). These predictions are shown as a response surface (D) where cell colour represents the predicted mean and GBP and aphid-weighted UV proportion are the x and y values respectively. The white points represent the experimental treatments and the green point shows the spectral balance coordinates of the sunlight reference spectrum.

Table 6.7: Quasibinomial GLM parameters for the model $y \sim \log E_{UV}^* + \log E_{Green}^*$. The response variable was the proportion of time in a feeding position. $n = 420$. Significance codes: * = $p < 0.05$, ** = $p < 0.01$, *** = $p < 0.001$

	Estimate	Std. Error	t value	Pr(> t)	
(Intercept)	-0.5458	0.1983	-2.7522	0.0062	**
$\ln(E_{UV}^*)$	-0.2601	0.0474	-5.4854	< 0.0001	***
$\ln(E_{Green}^*)$	0.3684	0.1153	3.1955	0.0015	**

ificant negative log-linear effect ($\beta = -0.255$) on time in feeding position. The aphid-weighted green:blue proportion had a significant positive effect ($\beta = 1.251$) on time in feeding position (Table 6.8, Figure 6.6.C and D) with aphids in a feeding position for longer in green-biased light environments.

Table 6.8: Quasibinomial GLM parameters for the model $y \sim \ln R_{UV} + GB$. The response variable was the proportion of time in a feeding position. $n = 420$. Significance codes: * = $p < 0.05$, ** = $p < 0.01$, *** = $p < 0.001$

	Estimate	Std. Error	t value	Pr(> t)	
(Intercept)	-1.2224	0.3101	-3.9418	0.0001	**
$\ln(R_{UV})$	-0.2550	0.0486	-5.2490	< 0.0001	***
GBP	1.2510	0.4707	2.6576	0.0082	**

6.3.6 Applying the colourspace model as a predictive tool

The two binomial models identified in the previous section

$$\text{logit}(P) = -0.5458 + (-0.2601 \times \ln(E_{UV}^*)) + (0.3684 \times \ln(E_{Green}^*)) \quad (6.2)$$

and

$$\text{logit}(P) = -1.2224 + (-0.2550 \times \ln(R_{UV})) + (1.2510 \times GBP) \quad (6.3)$$

were used to generate predictions of aphid behaviour under different commercially-relevant light environments (Table 6.9, Figure 6.7).

Table 6.9: Simulated light environments using the ASTM G173 direct spectrum convolved with transmission measurements for the light environments listed below.

Light Environment	Description
C1	Sky under an experimental UVB-blocking plastic
C6	Sky under an experimental UVB-blocking plastic
Canopy	Sky 5 cm below a <i>Brassica</i> canopy
Compost Canopy	Compost substrate 5 cm below a <i>Brassica</i> canopy
Compost	Compost substrate in full sunlight
Leaf	Sky directly below a leaf
Lumitherm	Sky under a standard PE film
Lumisol	Sky under a UV-transparent PE film
Lumivar	Sky under a UV-opaque PE film
Sunlight	Modeled measurement of sky
Tex	Sky under an experimental UVB-blocking PE film

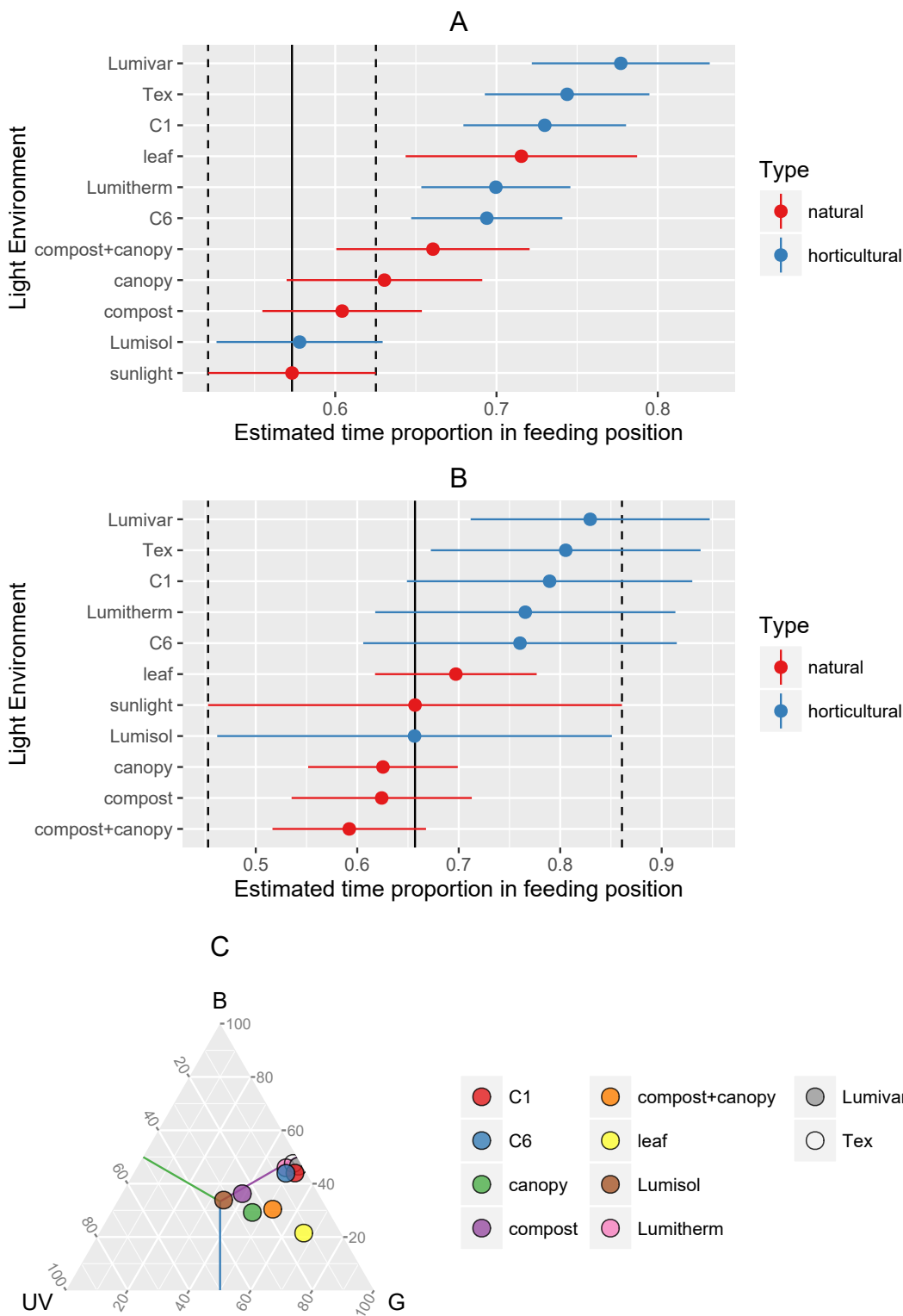


Figure 6.7: Estimated time proportion in feeding position for aphids under different simulated light environments (A,B) and light treatments in aphid colourspace (C). Estimated means and 95% confidence intervals were generated for (A) the proportional model (Table 6.8) and (B) the irradiance model (Table 6.7) computed previously. Red point-ranges are predictions for exposure to spectral balance experienced in natural habitats. Blue point-ranges show the predictions for spectral balance under six horticultural PE film claddings. The solid vertical line shows the prediction for the solar reference spectrum ASTM G173 direct and the dashed line shows the 95% confidence limits for the ASTM prediction. Light environments are shown on a scaled axis (C) with the ASTM G173 direct spectrum at the centre. Light treatments are described in Table 6.9.

Using the proportional model (Figure 6.7.A), the lowest TPiFP was estimated to be under full sunlight (59%). Sunlight filtered with UV-transparent PE films (59%) and full sunlight reflected by compost (60%) were also predicted to have low feeding times. Slightly longer feeding times were predicted under illumination from sunlight transmitted through a partial canopy and reflected by the compost (66%) and illumination from sunlight filtered with a partial canopy (63%). Sunlight filtered through a single leaf predicted a much longer feeding time (72%) which was comparable to sunlight filtered by standard PE films (70%) and by C1 (73%), C6 (69%) and Tex (74%) UVB-blocking PE films. Sunlight filtered by the fully UV-opaque PE film predicted the longest feeding times (78%).

The irradiance model (Figure 6.7.B) predicted the lowest TPiFP under sunlight transmitted through a partial canopy and reflected by the compost (59%), full sunlight reflected by compost (62%) and sunlight filtered by a partial canopy (63%). These were lower feeding times than those predicted under unfiltered sunlight (66%) and sunlight filtered with UV-transparent PE films (66%). Feeding times were predicted to be slightly longer under sunlight transmitted through a single *Brassica* leaf (70%). Longer times were predicted under sunlight filtered with C1 (79%), C6 (76%) and Tex (81%) with the longest feeding time predicted under sunlight filtered with UV-opaque PE film.

Whilst the two models are both able to predict behavioural response for different light environments, the final proportional model had a lower residual deviance ($D = 1072834$) than the final irradiance model ($D = 1074781$) and should therefore be considered a better fitting model. Additionally, the irradiance model predictions had very large confidence intervals. As the model was determined from experimental treatments using relatively low irradiances compared to the field (Maximum experimental irradiance: $E_{\text{Total}}^* = 12 \text{ Wm}^{-2}$, maximum predicted irradiance: $E_{\text{Total}}^* = 280 \text{ Wm}^{-2}$), the confidence intervals are unreliable and so the model predictions are difficult to interpret. Therefore, the proportional model should be considered the more appropriate model, both in interpreting the data presented here and for predicting responses under novel light environments.

6.4 Discussion

The results presented here provide novel evidence that *M. persicae* uses its short-wavelength photoreceptors, not only for flight behaviour by winged morphs (Chyzik et al., 2003; Döring et al., 2007), but also as an important component of the environmental perception mechanism of wingless (apterous) morphs. In this section, I discuss the conceptual models which may be derived from this work, relating *M. persicae* behaviour to its environmental pressures, before discussing the applications of conceptual models to horticultural light design.

6.4.1 A new model for visually-mediated feeding behaviour

Four separate statistical models were used to describe *M. persicae* feeding behaviour in response to changes in spectral balance and irradiance (Table 6.10), and whilst each described the data well enough to be considered a suitable model for the dataset, there are theoretical and practical considerations to be taken into account when selecting the most appropriate model to be used for more general prediction.

Table 6.10: Comparison of the four models used. The GLM formula is the model fit to the data and the mechanistic model is the insect visual mechanism(s) it describes. The opponent column describes whether or not the mechanistic model is a colour opponency mechanism.

Model	Experiment(s)	GLM formula	Mechanistic Model	Opponent?
1	1-3	$y \sim \ln(E_{UV}^*)$	E_{UV}^*	No
2	1-3	$y \sim \ln(R_{UV})$	$E_{UV}^* - E_{Blue}^* - E_{Green}^*$	Yes
3	5	$y \sim \ln(E_{UV}^*) + \ln(E_{Green}^*)$	$E_{UV}^* - E_{Green}^*$	Yes
4	5	$y \sim \ln(R_{UV}) + GBP$	$E_{UV}^* - E_{Blue}^* - E_{Green}^*$ and $E_{Green}^* - E_{Blue}^*$	Yes

For the initial experiments (Experiments 1-3), a 1-dimensional model was fit to the data (Table 6.10, Model 1), where aphid-weighted UV (E_{UV}^*) was used as the sole predictor in the model. This predicts that at a given irradiance threshold, the aphid will respond, irrespective of stimulation of the other photoreceptor types. Previous studies at both an experimental (Chittka et al., 1992) and mechanistic (Borst, 2009) level have shown that most insects use a 2-dimensional colour opponent mechanism: a negative feedback system by which stimulation of one type of photoreceptor has an antagonistic effect on another. This allows relative stimulation of photoreceptors ('colour') to be perceived at widely varying irradiances as would be experienced at different times of the day. A non-opponent mechanism, such as that represented by model one, would not allow this.

However, an opponent mechanism may not be essential in UV perception. In addition to compound eyes, insects have ocelli: simple light perception structures with very limited spatial resolution. In at least one insect species (*Cataglyphis bicolor*, Order: *Hymenoptera*), these organs had high sensitivity to UV and reduced sensitivity to longer wavelengths, in contrast to the compound eye of the same species, which had additional sensitivity at longer wavelengths (Mote and Wehner, 1980). Although ocelli are conventionally associated with Circadian rhythm regulation in aphids (Hardie and Vaz Nunes, 2001), it is possible that these organs may operate as simple wavelength-sensitive switches: at a certain UV intensity, regardless of background ($E_{Green+Blue}^*$) intensity, the photoreceptors respond and elicit a behavioural response. The results presented in this chapter do not support this mechanism in *M. persicae* because UV treatments of the same intensity elicited different behavioural responses dependent on the green and blue intensity (Figure 6.3).

A colour opponent (2-dimensional) model was also fit to the response data from Experiments 1-3. The mechanistic model (Table 6.10, Model 2) described the blue and green photoreceptors as having an antagonistic effect on UV photoreceptors. As the blue and green stimuli increased, the UV response was inhibited. Whilst this model fits the experimental data, the experimental treatments were only varied in the R_{UV} axis and not in the R_{Green} or R_{Blue} axes. Therefore, it is only suitable for predicting changes in R_{UV} and not for changes in the full aphid colourspace (i.e. variation in the Green:Blue ratio).

When behavioural responses to a much greater range of light treatments were tested (Experiment 5 tested 21 different light treatments) to cover a range of illumination colours found in field conditions, only colour opponent mechanisms were appropriate models of the data. The statistical model was fit using irradiance values for green, blue and UV. Blue photoreceptor stimulation was found to be a non-significant predictor in the model and so the final mechanistic model described a simple UV-green opponent system, where the negative effect of UV stimuli were mitigated by the positive effect of green stimulation (Table 6.10, Model 3).

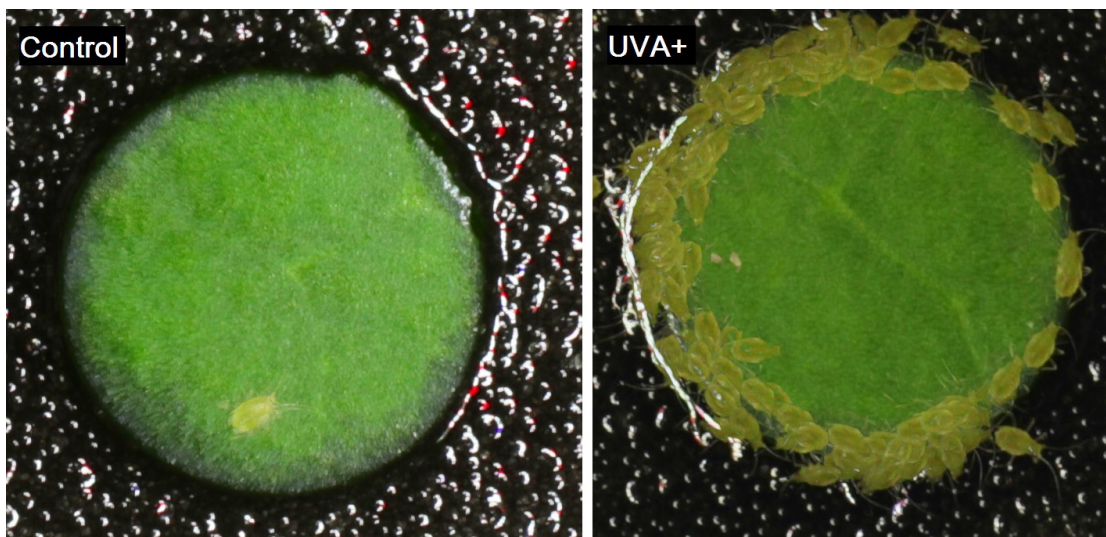


Figure 6.8: Example image stacks from Experiment 1 for Control (E1 UVA-) and UVA+ (E1 UVA+) treatments. Images have been stacked additively to view the positions of a single aphid at each 30 second time point over the one hour experimental duration.

The proportional model fit to the same data (Table 6.10, Model 4) is best explained as a mechanism with two separate components in operation simultaneously: A UV-blue-green opponency (the dominant mechanism) as well as a second green-blue opponency, which operates without input from the UV channel. For reasons discussed in the results, the proportional model is the best choice for predicting responses to untested light environments, such as those presented in Figure 6.7.

6.4.2 UV and green as behavioural cues

In the experimental results presented in this chapter, apterous (wingless) female *M. persicae* spent less time attempting to feed under more UV-rich light environments (Figure 6.4.A). This was most likely due to aphids identifying high UV environments as undesirable and moving in an attempt to find a more desirable feeding location ('desirability' is discussed further below). In Chapter Three, significantly more aphids were located in exposed parts of the plant under low UVA treatments. As it has been well established that *M. persicae*, and many other aphid species, possess photoreceptors capable of perceiving UV wavelengths as short as 300 nm (Döring et al., 2007; Kirchner et al., 2005), it was hypothesised that this positioning was as a direct response to UV perception by the aphid, causing them to move from exposed (typically the upper surfaces of leaves located higher in the canopy) to more sheltered parts of the canopy. In this experimental work, aphids responded rapidly to higher proportional UV by reduced feeding time, spending more time in a non stationary position on the leaf disc or off the leaf disc. It was also observed that in some cases, aphids under high UV circled the edge of the leaf disc (Figure 6.8), likely attempting to move to the underside.

In the *M. persicae* colourspace, solar illumination filtered by a *Brassica* leaf (i.e. fully shaded by a *Brassica* leaf) had higher R_{UV} than semi-UV opaque plastics such as Lumitherm and C6 (Figure 6.7.C). As such, if the visual model were a simple $E_{UV}^* : E_{Green+Blue}^*$ opponency, insects inhabiting a sheltered region of a plant in full sunlight should be more disrupted than an insect inhabiting an exposed feeding site under a semi-UV opaque PE film. However, increases in

R_{Green} act in opponency to increases in R_{UV} , and because the underside of the leaf has much higher R_{Green} values than semi-UV opaque PE films, the underside of the leaf was predicted to be a more attractive feeding environment than a partially UV-attenuated environment, such as that generated by using a Lumitherm PE film to filter sunlight (Figure 6.7.A). Other invertebrates have been shown to prefer UV-attenuated, or shaded environments for feeding. A study using *Aphis glycines* identified this change in distribution for aphids feeding on Soy (*Glycine max*), showing that a greater proportion of aphids inhabited upper leaf surfaces under attenuated-UV treatments (Burdick et al., 2015). Similarly, on tomato plants (*Solanum lycopersicon*) the spider mite *Panonychus citri* showed reduced oviposition preference for upper leaf surfaces under leaves exposed to full sunlight compared to leaves that were shaded (Fukaya et al., 2013).

In this chapter, I also examined the effect of exposure to UVB, however although the colourspace model predicted a behavioural response equal to a moderate UVA treatment (where a relatively large response was observed, Figure 6.3), no behavioural response to UVB exposure from an artificial UVB source was found. The reasons for this are not known, however, one possibility is that a sublethal immobilisation effect of UVB exposure occurred. The irradiance used was very high compared to ambient UK conditions ($I_{\text{CIE}}=0.44 \text{ W m}^{-2}$, UV-index ≈ 18) and so over the period of the experiment (one hour), the dose was approximately equivalent to a UK summer mean daily dose ($\text{Dose}_{\text{CIE}} = 1.6 \text{ kJ m}^{-2}$). This dose would certainly be sufficient to induce a mortality effect, and this may be compounded by the very high irradiance (4.4). As such, reduced motility, and so apparently increased settling, may be observed due to the direct damaging effects of the short wavelength source. An alternative explanation is that the insect photoperceptive organs were damaged by the high irradiance UVB, as was found in a number of taxa at various environmentally-relevant irradiances (Meyer-Rochow et al., 2002). If the ability to perceive UV was inhibited by photoreceptor damage, aphids may be less behaviourally responsive, through interpreting the environment as low in relative UV.

Avoidance of high aphid-visible UV environments is likely to be advantageous to apterous aphids. Feeding sites high in aphid-visible UV are also likely to be exposed to higher levels of shorter wavelength UV. In Chapter Four, I demonstrated that exposure to field-like UVB doses significantly decreased *M. persicae* survival. Field-like UV doses caused increases in mortality in *Hemiptera* (Burdick et al., 2015; Tariq et al., 2015), however these studies did not isolate the direct effect on the insect from potential indirect effects mediated through the plant (see 4.4 for a comprehensive discussion of this problem). Whilst *M. persicae* and possibly other *Hemiptera* (*Aphis glycines*, *Dialeurodes citri*) are negatively affected by exposure to UV doses experienced daily during the UK summer (4.3.4), other species may be more tolerant to living on upper leaf surfaces. This tolerance may be more likely when other, competing selection pressures outweigh the harmful effects of UV exposure, driving physiological adaptation. Movement to the upper surface of the leaf was shown to be advantageous for the aphid *Melanocallis caryaefoliae* when predation risk was high as it reduced contact with predators (Paulsen et al., 2013). This species is black in appearance which could be due to higher concentrations of melanin, an important component of the insect photoprotective mechanism.

Other invertebrates also balance UV exposure with other biotic and abiotic stresses. Spider mite populations were negatively affected by high UV light environments (Sakai et al., 2012; Fukaya et al., 2013; Ohtsuka and Osakabe, 2009; Onzo et al., 2010). Two-spotted spider mite (*Tetranychus urticae*) had much higher adult (Ohtsuka and Osakabe, 2009) and egg (Fukaya et al., 2013) mortality under high UV conditions. In a more UV-tolerant species (*P. citri*), the adults of which spend more time on the upper surface of the leaves than *T. urticae*, egg mortality was also high

when oviposition occurred on exposed leaf surfaces. Therefore, whilst it may be advantageous to inhabit the upper leaf surface when UV exposure is limited or when a life stage of the population is UVB-resistant (as in the case of *P. citri*), the deleterious effects typically render exposed leaf positions uninhabitable. It should be noted that the majority of these experiments used UVB doses comparable to field UVB day doses, however field-like UVA doses were also shown to affect egg survival in at least one species (Onzo et al., 2010). Therefore whilst the effects of UV on survival and fecundity are likely to be driven largely by shorter wavelengths, the impact of longer wavelength UV should not be ignored.

6.4.3 Green-Blue opponency for host finding

A second opponent mechanism was also identified in apterous aphid feeding behaviour (Table 6.10, Model 4). Green-blue opponency occurred in the absence of UV where aphids showed reduced feeding time when the green:blue proportion ($E_{\text{Green}}^*/E_{\text{Green+Blue}}^*$) was reduced (Figure 6.6). This is a relatively unusual light environment for an aphid as the majority of foliage absorbs little green light and so is either transmissive or reflective in the green waveband. Reducing the proportion of aphid-green light in the illumination spectrum reduces the relative proportion of aphid-green light reflected off a leaf surface, therefore making it appear less 'leaf-like' to an insect. Identification of plant material by its high aphid-green saturation and high contrast with the background has been previously identified as a mechanism by which alate aphids first locate a potential host, before using other cues (tactile, exploratory probing, etc.) to establish the suitability for extended feeding (Doring et al., 2004). Apterous aphids may, therefore, also use green:blue proportion to differentiate plant from non-plant, and so if the illumination causes the plant material to be substantially different to leaf material, aphids may reduce their feeding effort and increase movement.

It is also possible that low green:blue proportion light environments cause aphids to incorrectly identify the defensive status of the plant. Anthocyanins, the purple pigments found in foliar and floral tissue, are typically acknowledged to be visual indicators of phenolic status as they have high pleiotropy with other more toxic flavonoids (Johnson and Dowd, 2004). Leaves with low anthocyanin content are highly reflective in the green and less reflective in the blue, whereas leaves with higher anthocyanin content reflect proportionally more blue light (Gitelson et al., 2009, see 1.4.4 for further discussion). Therefore increased anthocyanin content may be detected visually by changes in aphid green:blue proportion. As discussed above, as the aphid green:blue proportion of the illumination spectrum is reduced, the leaf material appears more blue (and so more anthocyanin-rich) to the aphid. Some insects with more sophisticated visual processing systems (*Hymenoptera*) are known to compensate for the colour of the illumination when identifying coloured stimuli (Lotto and Chittka, 2005), however it is not known if aphids are able to make such complex analyses of their environment.

6.4.4 Using the colourspace model to predict behaviour

The approach used in this chapter, where *M. persicae* behavioural responses were mapped to the coordinates within its trichromatic colourspace, is a powerful tool for predicting apterous responses to any light environment. The responses of hemipteran pests to light environments under horticultural PE films are of particular interest to this study, due to the implications for their use in pest control. As such, the simulated light environments within polytunnels clad with

various spectrally-modifying PE films were used to generate predictions of aphid behavioural response (Figure 6.7). Using a simple metric for aphid tolerance (Time Proportion in Feeding Position), this study showed that *M. persicae* may be more tolerant to exposure to full sunlight filtered by C1, Tex and Lumivar PE films than to fully-shaded feeding sites within a plant ('leaf' light environment, Figure 6.7). This means that an aphid on an exposed site under these PE films would be expected to perceive the light environment as though it were a shaded site and, therefore, more readily accept it as a feeding site.

However, spectral balance is not the only predictor of aphid feeding-site acceptance. Previous work shows that *M. persicae* feeding on *Brassica oleracea* had an inherent preference for sheltered leaf surfaces under UV-attenuated light environments (3.3.4, 94% of *M. persicae* found on sheltered leaf surfaces). The results from this chapter indicate that aphids should be highly tolerant to feeding under a UV-absent light environments, with an aphid green:blue proportion identical to midday sunlight (ASTM G173 direct). As there were only relatively few aphids inhabiting exposed sites under field conditions (3.3.4), it is likely that the general preference for sheltered feeding sites is mainly due to non-visually perceived stimuli. This was shown to be due to plant chemical or tactile cues and not due to any gravitational preference for lower leaf surfaces (Simmons, 1999; Sakai et al., 2011b). *Bemisia argentifolii* preference for upper leaf surface was also highly dependent on the host species identity (Simmons, 1999) and so if *M. persicae* was also sensitive to host identity in its feeding site selection, the proportion of aphids inhabiting the exposed surfaces may vary with host.

6.4.5 Implications for horticulture

As has been previously discussed, short wavelength UV (at a dose comparable to UK summer mean day dose) has a deleterious effect on *M. persicae* (Chapter Four). Under normal solar light environments (i.e. exposure to full sunlight), aphids rapidly respond and move to areas of lower R_{UV} . This means that their exposure to harmful UV is minimal. However, C1, C6 and Tex treatments all have relatively low R_{UV} values and, therefore, aphids are more likely to remain in exposed positions to feed. When in these exposed positions, aphids in these light environments receive a higher effective dose of UV than under standard (Lumitherm) or UV-opaque (Lumivar) PE films and so have increased risk of mortality. This translates into lower Population Growth Rate (PGR) and, therefore, smaller populations of insects on plants. The full implications are further discussed in Chapter 7.

6.5 Conclusions

1. The work presented here provides novel evidence that the UV photoreceptor in *M. persicae* is used by apterous (wingless) morphs for identifying areas of high proportional UV (R_{UV}), allowing the insect to avoid these areas and so avoid exposure to harmful short wavelength UV radiation.
2. Experimental mapping of the aphid colourspace showed that feeding effort was determined by the colour opponent mechanism $E_{UV}^* - E_{Blue}^* - E_{Green}^*$, whereby UV inhibits feeding behaviours and aphid-blue and aphid-green light promoted feeding behaviours.

3. A second opponent mechanism between aphid-green and aphid-blue light ($E_{\text{Green}}^* - E_{\text{Blue}}^*$) was also identified. Aphids spent less time attempting to feed on leaf discs when the green:blue proportion was very low and I hypothesise that this is because the plant material appears higher in anthocyanins than when illuminated with higher green:blue proportion light.
4. This has important implications for the design of selectively UV-attenuating horticultural PE films. Where aphid tolerance is desired, and therefore increased feeding in exposed sites, transmission of aphid-UV should be minimised, in order to lower the R_{UV} of the light environment. Alternatively, supplementation (increase) of light in the aphid-blue and aphid-green will have the same effect, reducing the R_{UV} . Finally, if reduced host-acceptance is desired, decreasing the green:blue proportion may reduce the attractiveness of vegetation to wingless (and potentially, winged) aphids.

General Discussion

In this final chapter, I draw together the major findings of the project, first reflecting on how the early literature analysis directed the initial experimental work, then exploring how the unexpected findings of the polytunnel field experiments drove important methodological development, which fundamentally shaped the outcome of this PhD project. I synthesise the findings of the laboratory work in Chapters Four and Six to produce a new model of aphid risk avoidance behaviour and, through this, suggest new hypotheses for future research efforts.

7.1 From initial aims to revised hypotheses

In the introductory chapter, I defined the scope of the project as ‘*Developing knowledge which could bring environmental and economic benefit through improving pest control in protected cropping environments*’. Industry-sponsorship necessitated an approach that made use of the partner company’s expertise in the development of polyethylene (PE) films with novel light transmission properties. Prior to the commencement of this PhD project, Arid Agritec had developed a unique UVB-transmitting, UVA-attenuating PE film, primarily for the control of downy mildew (*Botrytis sp.*) and other plant pathogens (Paul et al., 2012). This unusual modification of the solar spectrum was also expected to affect herbivorous insects, and so the initial stage of the project was a focused synthesis of the literature that brought together three disparate areas of research: applied studies of UV-attenuating PE films for pest control (1.2), the use of colour vision by invertebrate herbivores (1.3), and the roles of ultraviolet (UV) in inducing plant defensive responses (1.4).

Published data from large-scale field experiments consistently showed that attenuation (or partial attenuation) of UV radiation, even when the differences between treatment transmissions were apparently small (e.g. Costa et al., 2002b), caused reductions in the immigration and spread of *Hemiptera* and *Thysanoptera*, which consequently reduced the overall Population Growth Rate (PGR) in crops (1.2). Seemingly at odds with this, the fundamental photoecology community had demonstrated a link between UV-exposure of plants to the induction of plant defensive responses and the subsequent reduction in PGR of herbivorous insects (1.4). However, whereas the

fundamental photoecology studies predominantly manipulated ultraviolet-B (UVB), the applied studies typically manipulated either total UV, or ultraviolet-A (UVA).

A further, key distinction between the two research areas, is that the species studied in the fundamental photoecology sphere were predominantly *Lepidoptera* or other chewing insects, whereas applied experiments focused on the effect on phloem-feeding (*Hemiptera*) and cell-mining (*Thysanoptera*) species. Therefore, whilst there was good understanding of the behavioural mechanisms affecting *Hemiptera* and *Thysanoptera* in crops, the plant-mediated (indirect) effects of UVB exposure on these orders were little-known in 2012. The lack of study in this area may have been due to the experimental challenges of working with *Hemiptera*, for example, the difficulty in sustaining UVB exposure whilst separating direct effect on the insect from plant-mediated effect.

Through synthesising the findings of the fundamental and applied research communities, I identified two mechanisms by which insect pests may interact with UV light:

1. UV is perceived by many insect orders, including *Hemiptera* and *Thysanoptera* (1.3), and is used to enter, or navigate within, a crop (1.2). Therefore, any reduction in UV is likely to reduce the ability of insects to reach or locate host plants. Insect visual perception peaks in the UVA waveband (1.3.1) and, as solar UV irradiance increases with wavelength, it is the longer wavelength solar UV which influences insect visual perception. As such, long wavelength UV-attenuating claddings were predicted to reduce insect immigration and dispersal, consequently reducing the overall PGR within a crop.
2. Some plant defensive responses are sensitive to UV (particularly UVB) exposure, and this has been shown to reduce insect PGR (1.4). Plants grown under fully UV-attenuating claddings were predicted to have aphid populations with higher birth rates due to reduced induction of plant defensive responses. Under solar illumination, plant defence was expected to be positively correlated with the UVB dose.

The first of these mechanisms (inhibition of dispersal through UVA-attenuation) had been well evidenced within the applied literature (1.2-1.3), but few studies had quantified the effect on birth or death rate PGR of phloem-feeding and cell-mining insects under different light environments. Of the limited number of studies in this area, two had evidenced a likely plant-mediated effect of UVB exposure on the aphid *Myzus persicae*. Mewis et al. (2012) had shown a negative effect of plant UVB pre-exposure on the PGR of *M. persicae*, and an earlier study where *M. persicae* and its host were simultaneously exposed, demonstrated changes in phloem chemistry in response to UVB (Kuhlmann et al., 2010). Whilst not conclusive, these studies suggested UVB exposure of plants may induce plant defensive responses relevant to phloem feeders, and so, given scope of the project, this was highlighted as a key research priority.

In accordance with the findings of the literature analysis, the initial experimental work was designed to test a simple hypothesis: that UVB (but not UVA) exposure would promote plant defence and that this would have a negative effect on *M. persicae* (3.1). Through partnership with Arid Agritec, access to a new film, alongside three others which were commercially-available, enabled the testing of a unique, modified solar light environment: where UVA was absent but UVB present (3.2). As both a research tool and a commercial technology, this technology provided unique opportunities to study the effects of UVB and UVA in combination and isolation.

The unexpected findings in Chapter Three, where UVB was found to reduce the PGR in *M. persicae* only in the absence of UVA, suggested that the hypothesis that 'UVB-induced changes in plant

chemistry mediated the interaction between M. persicae and its Brassica host should be rejected for the *Brassica* varieties studied in this instance (3.4). However, through detailed observation of UVA-induced changes in aphid distribution within the plant canopy, I developed a new hypothesis which formed the basis of the remainder of this PhD project. Aphid perception of UV light had been previously identified as a stimulus for take-off and as an orientation cue for flight (1.3.2). I therefore proposed that the decreased proportion of aphids in exposed feeding positions under high-UV treatments was due to aphids perceiving long wavelength UV and responding directly, in order to minimise their exposure to it when attempting to feed.

Aphid PGR under the novel UVB-transmitting, UVA-attenuating PE film was reduced in two of the three experiments and so I argued that UVA-attenuation ‘deceives’ the aphid into increasing the amount of time spent in exposed positions and that this consequently exposes them to harmful doses of UVB, thus increasing the death rate. As the polytunnel field experiments had been subject to inherent variability in environmental conditions, a more refined approach was required to test these hypotheses. Through campaigns of targeted laboratory work, Chapters Four and Six provided crucial evidence to substantiate this mechanism. Within the broad scope of the project (see above), this represents a novel and commercially-advantageous invertebrate pest control method as part of a larger Integrated Pest Management (IPM) approach.

7.2 Key methodological developments

7.2.1 A novel light environment for research

As both a research and a commercial tool, novel PE films with UVA-attenuating/ UVB-transmitting transmission properties represent a significant advancement in the ability to separate short- and long- wavelength responsive mechanisms in plant and animal photobiology. Throughout the project, I utilised these films as both filters of solar radiation (Chapter Three) and for filtering UVB lamps (4.2, 6.2) to produce UVB-biased UV treatments with minimal exposure to longer wavelengths. When used alongside commercial standard, UV-transparent and UV-opaque films, a gradient of both UVA and UVB transmissions is achieved, allowing the separate effects of short- and long-wavelength radiation to be studied in both combination and isolation. As these UVA-attenuating/UVB-transmitting films become commercially available, larger scale applied studies should consider including these films in their experimental work; both as a tool for discriminating short- and long-wavelength mechanisms, and as an approach for improved IPM.

7.2.2 Action spectra for understanding mortality and vision

In this thesis, the use of Biological Spectral Weighting Functions (BSWFs) is discussed in detail, both for the purposes of understanding radiation-induced mortality (Chapter Four) and for the development of a behavioural colourspace model using insect photoreceptor action spectra (Chapter Six). Historically, plant experiments using artificial UVB supplementation typically used doses that were comparable to unweighted field doses, but delivered much higher *effective* doses, consequently exaggerating the negative effects of UVB exposure (Paul and Gwynn-Jones, 2003). As such, photobiological research in plant science has progressed to use both experimental designs and BSWFs to deliver environmentally-relevant wavelengths, quantified in a biologically-relevant framework (e.g. Caldwell et al., 1986; Setlow, 1974). In studies published

to date, where insect response to UVB was tested via the use of artificial UVB supplementation, the same experimental limitations of early plant photobiology experiments were often identified (4.4.3). As such, I used an approach similar to Paul et al. (2005) where non system-specific BSWFs were assessed for their suitability against the data and used to estimate the effective UV dose for inducing mortality in *M. persicae*. As the approach described in this chapter represents a significant conceptual advance from many previous studies of photo-induced mortality in insects, I conclude the chapter with five recommendations for the design of experiments testing the effect of short-wavelength light on insects (4.5). In future work, the erythemally-weighted (CIE) UV dose can be recommended as an appropriate measure of effective UV. Although this BSWF may not be a perfect action spectrum for light-induced mortality in insects (and indeed, other BSWFs fit the aphid mortality data equally well (4.3.2)), the wide availability of erythema dose information mean that laboratory experiments can be easily related to field conditions for extrapolation or interpolation of results (4.4.3).

Chapter Six also makes use of the BSWFs principles to describe spectra as coordinates within a trichromatic insect colourspace (2.4.7), specifically that of *Myzus persicae*. This is a highly useful approach for developing the understanding of insect phototransduction from responses to monochromatic stimuli, to a model based on the fundamental understanding of colour opponent coding (1.3.4). As has been discussed previously (Döring et al., 2007), this model allows visual stimuli to be considered in terms of insect perception, rather than through notional, human-biased descriptions of ‘colour’. The electroretinography (ERG) responses for *M. persicae* had already been measured and so the correct BSWFs for the species could be used, however these data are not always available. For insects for which there is no ERG data available, the BSWF of a taxonomically (and, in ideal circumstances, behaviourally) similar species may be used. Given the extensive number of species with quantified photoreceptor responses (1.3.1), there should be data available at the order level, which should at least approximate the colour perceptive responses.

7.2.3 No-plant mortality assays in *Hemiptera*

A novel method for quantifying aphid mortality was employed, where *M. persicae* was irradiated independently of the plant material in order to assess the effects of single-day exposure to UV (Chapter Four). This approach has not been used with *Hemiptera* previously and so represents the first true assessment of aphid susceptibility to direct UV exposure. Previous work has tested exposure of *Hemiptera* to UV, however this is typically conducted with the aphid located on the plant tissue for the irradiation process (e.g. Burdick et al., 2015; Hu et al., 2013). As such, any UVB-induced effect on plant defence may also be affected and consequently any changes in survival could be attributed to either direct or indirect effects. The approach presented in Chapter Four allows the direct effects to be isolated, however the exposure period cannot be extended because of the likely physiological stress of extended periods without feeding. Future work could compensate for this through using aphids settled on an artificial host medium, typically a nutrient solution encapsulated in Parafilm (Dadd and Mittler, 1965). Feeding aphids could then be irradiated for any period of time and the work could be expanded to examine the multi-generational effects of continuous exposure UV light.

7.2.4 Image analysis tools for behavioural research

Chapter five presents a novel method that utilises low cost technology and open-source software tools to quantify aphid behavioural responses to light (Chapter Five). The benefits of such a system are extensive: very rapid throughput, high spatial and temporal measurement resolution and, through the use of a variable intensity multi-waveband illumination source, the ability to simulate any colour in the aphid colourspace. From an ecological perspective, this offers a convenient method for building colourspace models of insect behavioural responses to light, allowing insight into the mechanisms by which insects use colour as an environmental cue (7.3.1). Understanding insect behaviour under different illumination is also of current relevance to both commercial and research audiences as facilities move from supplementary incandescent to spectrally undefined Light-Emitting Diode (LED) lighting (5.4.2). Certainly, technological advances in all forms of supplementary lighting technology offer attractive opportunities for pest control, through a range of possible behavioural mechanisms (Johansen et al., 2011). Fast-throughput approaches, such as the method presented here, offer the possibility of screening behavioural responses to novel lighting regimes in order to better understand how illumination colour, interval and consistency may be manipulated in order to maximise disruption to invertebrate pests.

7.3 A new model of aphid hazard perception

At the end of the first experimental chapter, I established a detailed hypothesis to explain the reduced PGR of *M. persicae* under the UVB-transmitting, UVA-attenuating PE film (3.5). Building on this early hypothesis, through detailed mortality (Chapter Four) and behavioural (Chapter Six) experiments, I establish the presence of both a log-linear mortality response to UV_{CIE} (4.3) and a behavioural avoidance response driven by a aphid-green:aphid-UV opponent mechanism (6.3). In this section, I synthesise the findings of these chapters into a hazard perception model for the behavioural avoidance of UV hazard in *M. persicae* (Figure 7.1). I show how this may be exploited through current and future technologies and consider the implications for IPM.

7.3.1 Do aphids overestimate the risk of UV exposure?

The green line in Figure 7.1 shows the hazard-avoidance response of *M. persicae* under a gradient of different natural light environments, which an aphid might typically experience under unfiltered sunlight (Figure 7.1.B and C). The simulations predict aphid colourspace and $Dose_{CIE}$ values for full sunlight (Sunlight), sunlight reflected off compost (Compost), sunlight transmitted through a partial canopy (Canopy), sunlight transmitted through a leaf (Leaf) and sunlight transmitted through two leaves (Leafx2) (See 2.4.11 for details of measurement method). This can, therefore, be viewed as the normal model of aphid behavioural response to illumination colour, compared to the subsequent risk to the aphid for that same illumination environment. Representative solar conditions for two geographical regions of commercial relevance been separately modeled: mean UK summer (Figure 7.1.B) and mean Mediterranean summer (Figure 7.1.C). In these models, the behavioural component is calculated using the clear-sky ASTM G173 Direct simulated spectrum (2.4.8) and is treated as an irradiance response and the mortality is calculated from the mean daily dose for the specified geographical region.

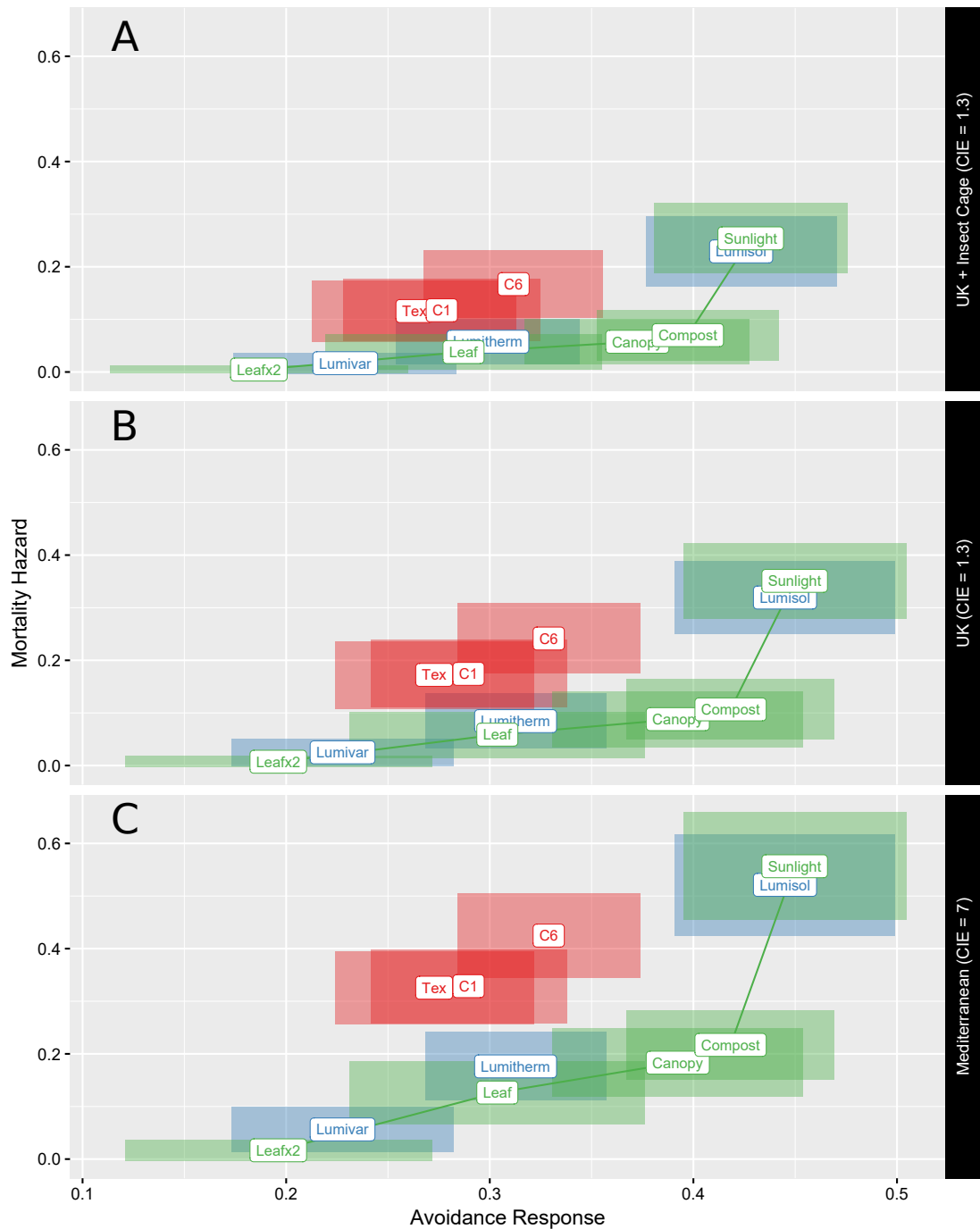


Figure 7.1: Integrated mortality and behaviour models for *Myzus persicae* under different light environments. The mortality hazard is the probability of mortality after a single day dose equivalent (4.3) and the avoidance response is $1 - [\text{Total proportion in feeding position}]$ (6.3). Plots panel: (A) UK summer mean dose ($\text{Dose}_{\text{CIE}} = 1.3 \text{ kJ m}^{-2}$) filtered through the mesh insect cages used in 3.x, (B) UK summer mean dose ($\text{Dose}_{\text{CIE}} = 1.3 \text{ kJ m}^{-2}$), (C) Mediterranean summer mean dose ($\text{Dose}_{\text{CIE}} = 7 \text{ kJ m}^{-2}$). Label position shows the environment coordinates. Translucent boxes show the 95% confidence intervals in both axes. Environment type grouped by colour: green = naturally-experienced environments, blue = commercially-available films, red = experimental UVA-attenuating/UVB-transmitting films. The green line represents the model trajectory through naturally-experienced environments.

The increasing trend shows that as the mortality hazard increases, *M. persicae* responds behaviourally by spending less time in a feeding position. The non-linearity of the natural response trend (green line) implies that aphids either overestimate mortality hazard (respond more than they might be expected to) under top-of-canopy full sunlight, or underestimate the mortality hazard (respond less than might be expected) in more sheltered positions within the canopy. Whilst the latter may be the case, especially where other pressures force sub-optimal feeding positions and behaviours (see 6.4.2), it is presumed that aphids attempt to minimise exposure to harmful agents where possible and so, unnecessary exposure to UV should be selected against. Conversely, over-cautiousness may be an important behavioural trait. Although I did not find any evidence of a sublethal effect of a single dose of UVB (4.3.3, discussed in 4.4.2), the population-level impact of continued exposure, in *M. persicae*, is not known. This measure of mortality may underestimate the overall fitness costs of UV exposure at a long-term population level. I speculate that if this were true, and the costs to the population are indeed higher than may be predicted from the models presented in this thesis, then aphids may be accurately perceiving the level of risk and responding accordingly. However, further work is needed to establish the sublethal effects of continued UV exposure in isolation of plant-mediated effects. This would require methods utilising artificial-feeding media (as described in 7.2.3), which were beyond the means of this project.

Many herbivorous insects show non-random distributions within plants (Severtson et al., 2015), which may be due to a combination of biotic (e.g. tissue nutritional quality, exposure to parasitoids or predators, etc.) and abiotic (e.g. exposure to light, physical dislodgement, etc.) factors, however, the model I present strongly suggests that UV exposure is an important selective pressure and that *M. persicae* has adapted through the evolution of an efficient perception and behavioural avoidance mechanism (Chapter Six). In other systems, tolerance to UV may be a better strategy (Paulsen et al., 2013). Of the four species of aphid which inhabit pecan (*Carya illinoensis*), the black pecan aphid (*Melanocallis caryaefoliae*) inhabits the most exposed parts of the plant and so appears tolerant to solar radiation. As its dark pigmentation is almost certainly a melanin, which is largely opaque to short wavelength solar UVB (Kollias, 1995), it is likely that this is an evolved morphological tolerance to UV exposure. UV tolerance and human visible pigmentation has also been observed in the grain aphid (*Sitobion avenae*), where darker, 'brown' morphs were more resistant to high UVB doses (Hu et al., 2013). This raises interesting questions about the role of pigmentation as a photoprotectant in aphids. Are pigmented species more resistant to short wavelength UV? Do aphids use plant-derived photoprotectants? If so, are plant-derived, colourless (to humans) phenolics (e.g. those reviewed in 1.4.4) also important in aphid photoprotection?

I have also observed that alate 'dispersal' morphs of *M. persicae* are more heavily pigmented than apterous 'reproductive' morphs (Figure 7.2), which raises further questions about the use of pigments for photoprotection. Dispersal morphs are almost certainly exposed to greater UV irradiances than reproductive morphs, and so may have better photoprotective mechanisms. There is some evidence that this is the case in *Hemiptera*. Alate morphs of *Macrosiphum euphorbiae* have been shown to more readily adapt to thermal and UV stress than apterous morphs, illustrating an important fitness trade off between abiotic tolerance and fecundity, which is typically lower in dispersal morphs (Bonte et al., 2012). As such, future work may consider the origins and roles of insect pigmentation in protection against short-wavelength light.

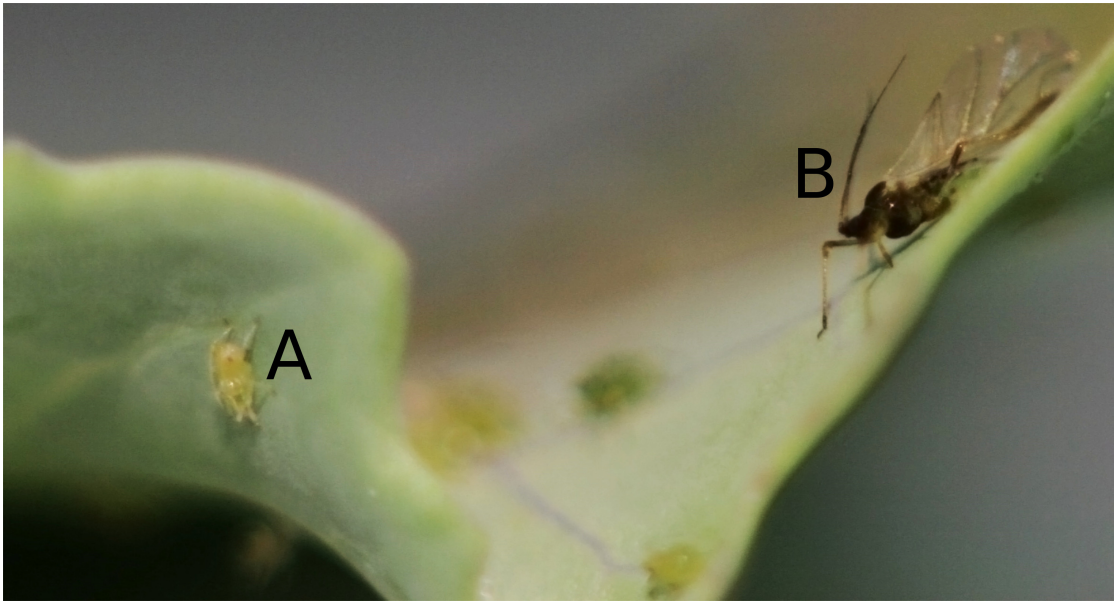


Figure 7.2: Differences in pigmentation between alate and apterous morphs of *Myzus persicae*. Two morphs are shown (A) apterous (asexual) female (B) alate (asexual) female.

7.3.2 UVA as a cue for increased plant defence

A hypothesis not explored in this thesis, is that aphids use UVA as a cue for plant regions which have been exposed to higher UV and so have higher UVB-induced insect defence. Whilst UV exposure of leaves in more sheltered parts of the canopy may indeed be lower, the effect of shading on nutritional quality of leaf tissue is highly variable with studies showing both positive and negative effects of shading on insect feeding preference (Roberts and Paul, 2006). Both in terms of plant defensive chemical composition and the effect on herbivory, natural shading and whole plant UV-attenuation act differently on plants (Roberts and Paul, 2006) and so it is unreliable to transfer hypotheses derived from UV-attenuation experiments to predict the response of insects over a gradient of shading within the plant canopy. It is not fully understood whether the dominant mechanisms in the induction of insect defences are systemic or localised (Ballaré, 2014). If the responses were localised (i.e. only the leaves exposed were affected), one hypothesis might be that insects use visually perceived, high UVA irradiances as cues for regions of the plant that have increased UVB-induced defence. The findings of Chapter Three suggest that UVB-exposure did not induce plant defensive compounds in the two cultivars of *Brassica oleracea* studied, however Mewis et al. (2012) did demonstrate a negative effect of plant UVB pre-exposure on *M. persicae*. The work presented in this thesis strongly suggests that the dominant stress driving the behavioural avoidance mechanism is the hazard presented by high UV exposure, however, this locally-induced plant defence may represent an additional mechanism that could account for the non-linear relationship between avoidance and hazard (Figure 7.1). Aphids which inhabit high UVA environments, as well as being directly damaged by UVB, may be subject to reduced food quality.

7.3.3 Influencing hazard perception for pest suppression

In addition to the hazard perception model for a gradient of naturally-experienced environments, I present the hazards and responses for *M. persicae* under six PE films (Figure 7.1). Figure 7.1

allows comparison of responses between three general light environments: an approximation of the light environment inside the insect cages used for the experimental work in Chapter three (A), the light environment under standard UK field conditions (B), and the light environment predicted in Mediterranean growing environments (C). Whilst the behavioural response changes little between different erythemal daily doses, the magnitude of the mortality hazard increases. As such, *M. persicae* PGR is expected to decrease with erythemal daily dose under all treatments.

Under the three simulated illumination spectra (panels A, B and C), the conventional PE films (Lumitherm, Lumivar and Lumisol, coloured blue) show similar predicted hazard-perception responses to those predicted under natural light environments (coloured green, Figure 7.1). This means that, for a given hazard, aphids are predicted to exhibit avoidance responses under these films similar to those predicted under natural light environments and so largely avoid exposure to short wavelength UV. As such, the use of these films is not predicted to significantly increase or decrease aphid exposure to harmful UV radiation for aphids in a feeding position, compared to the natural model. However, the prototype films (C1, C6, Tex) are positively shifted in the mortality axis, meaning that the direct hazard of UV exposure is higher than the aphid perceives it to be, relative to the naturally-experienced environments. In the early work of this project, I demonstrated a negative effect of UVA-transmitting/UVB-attenuating films on insect PGR compared to the UV-transparent (Lumisol) film (3.3) and subsequently developed a new hypothesis to explain this (3.5, 7.1). The model of hazard perception adds strong evidence that manipulating the spectrum, in the way that these three prototype films do, provides a means to reduce the overall insect PGR through a behavioural mechanism.

The mechanism described above affects PGR through increasing the death rate. Although the early work did not find any evidence that UVB exposure negatively affects *M. persicae* through changes in plant defensive chemistry (3.4), this does not exclude the possibility that other cultivars of *B. oleracea* and, indeed other species, may show much greater UVB-induced changes in plant chemistry, which could subsequently affect PGR, as was observed by Mewis et al. (2012). This mechanism may also be more important for the control of other pest species, however the findings in Chapter Three illustrate that UVB exposure of crops may not be a reliable method of pest management against aphids.

Spectrally-manipulating horticultural claddings also affect the immigration and emigration components of PGR (1.2). Both immigration into the crop (1.2.3) and secondary dispersal within (1.2.4) have been shown to be reduced by UVA-attenuation. For *Hemiptera*, we can make broad predictions of the effect of different light environments on population growth (Table 7.1), however, the relative contribution of each of these mechanisms will determine the overall PGR in a given system. As there is still a great deal of uncertainty, especially in the role of UVB in plant defence against *Hemiptera*, developing further understanding of the relative influence of each of these mechanisms is key to identifying new targets for technological advance.

The prototype UVA-attenuating, UVB-transmitting films offers an improved IPM solution against *Hemiptera*, compared to existing commercial claddings, as they offer characteristics that are likely to have low immigration and within-tunnel dispersal; and high aphid mortality (Table 7.1). Trapping experiments conducted during the same experimental season as the work conducted in Chapter Three suggested that the prototype film, Tex, had a similarly suppressive effect on *Hemiptera* and *Diptera* immigration and dispersal as UV-opaque film (Figure 7.3, C. Wood, *personal communication*). At present, further work is needed to understand the plant-mediated UVB effect on *Hemiptera* before a general conclusion can be made. Certainly, UVB-mediated mecha-

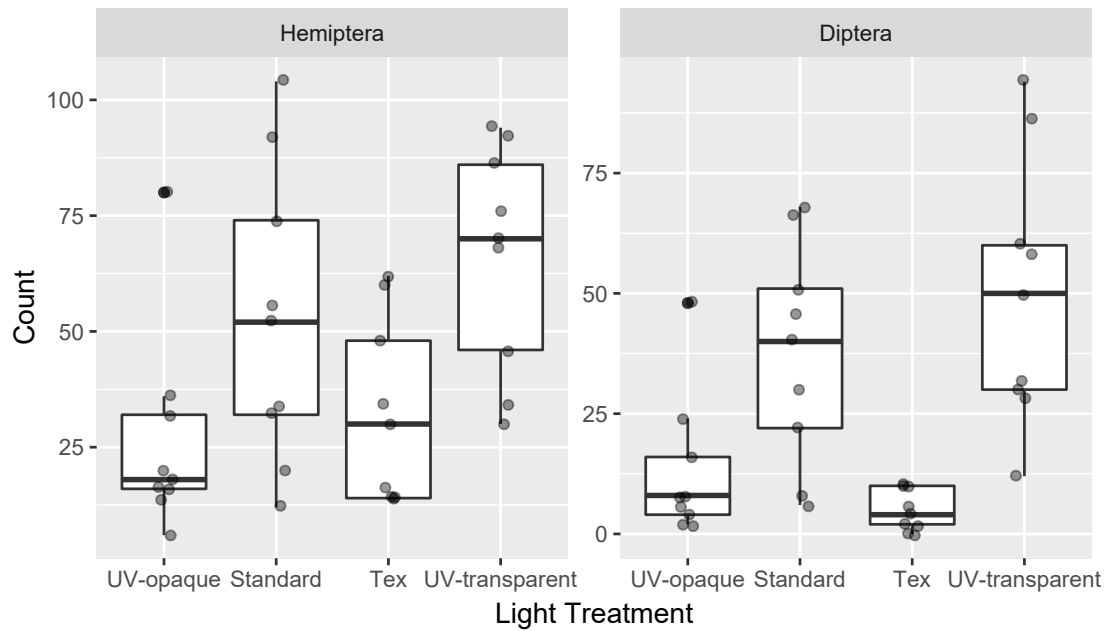


Figure 7.3: Total insects trapped on sticky traps under different PE film claddings. Data are paneled by insect order and each point represents a trap count. Raw data were collected by C. Wood in 2013 for her M.Sc. project and text interpretation are guided by her final report (C. Wood, *personal communication*).

Table 7.1: Mechanisms by which *Hemiptera* may be suppressed under different four different PE film claddings. Immigration and spread estimates are based on 1.2 and the supplementary data presented in Figure 7.3. Plant defence responses are largely unknown in relation to *Hemiptera*, and I include the predictions from the new hypothesis presented in this thesis, termed ‘Direct Damage’.

	Immigration	Dispersal	Plant Defence	Direct Damage
UV-opaque (Lumivar)	Low	Low	?	No effect
Standard (Lumitherm)	Low-Moderate	Low-Moderate	?	No effect
Prototypes (C1, C6, Tex)	Low	Low	?	High
UV-transparent (Lumisol)	High	High	?	No effect

nisms appear far less consistent in their effect on *Hemiptera* than the effects of UVA-attenuation of the new, ‘Direct Damage’ hypothesis described in this thesis. As discussed previously, different aphid species may be differently protected against short-wavelength UV damage, and so it is not known how the ‘Direct Damage’ mechanism of suppression will affect other species. However, given the large number of observations of *Hemiptera* showing preference for less exposed feeding sites (6.4.2), this mechanism may contribute significantly to population suppression across a wide range of species.

Future commercial work should prioritise the establishment of medium- to large- scale field trials in different UV environments to allow the comparison of the three existing commercial with the new UVA-attenuating, UVB-transmitting films. Working with a defined (artificially-introduced) pest species may be appropriate in small-scale experiments where edge effects (small tunnels have a greater edge-to-area ratio) and the inherent stochasticity of pest invasion make studying wild pest population dynamics too challenging. However, a key priority should be sampling experiments with naturally-occurring pest populations in commercial scale tunnels. Trap sampling at entry points and at different distances into the crop should be combined with on-plant counts, in order to construct a comprehensive model of the factors affecting pest population growth. Further resolution may be obtained by caging (with cages which minimally alter spectral balance

and intensity) a proportion of the invading populations, and monitoring age cohort population sizes in order to estimate the birth and death rate of relevant species. At present, very little is known about the potential impact of these films on the immigration and spread of *Lepidoptera*, perhaps because many species of commercial importance are insensitive to coloured sticky traps (minimal reported trap captures in pest invasion experiments, 1.2) or are night flying and so have no or limited colour sensitivity. Larger scale work with *Lepidoptera* in commercial tunnels (i.e. monitoring populations over a whole growing period) could provide much-needed insight into the importance of direct and indirect mechanisms.

Commercial IPM strategies may rely on predators, parasitoids and pathogens of herbivores, and these organisms are also likely to be affected by changes in the crop light environment. A review of the possible implications of spectral modification on their interaction with target pests is beyond the scope of this thesis, however, there is evidence that, in both fungal pathogens (Costa et al., 2012) and hymenopteran parasitoids (Chiel et al., 2006), the effects of manipulating short-wavelength radiation may be highly species specific. Pest control needs must also be balanced with other, equally important demands when selecting films with appropriate UV transmission properties for the crop in question. UVB exposure affects plant characteristics such as morphology and pigmentation (Tsormpatsidis et al., 2008), which are of commercial importance (J. Moore, *personal communication*). There is also increasing evidence that UVB exposure of crops may have human health benefits, through the production of plant secondary metabolites (Schreiner et al., 2012). Regardless of the impact on pest insects, there is a strengthening case for claddings which transmit UVB. The prototype UVA-attenuating, UVB-transmitting PE films may provide many of these benefits, usually obtainable only by using a UV-transparent film, such as the commercially-available Lumisol.

7.4 Conclusions

In concluding this thesis, I wish to emphasise the fundamental shift that occurred, from the early aims and objectives of the General Introduction, to the synthesis of my findings in this chapter. UVB-induced plant defence mechanisms were expected to form a major and substantial component of this project, however, in the early stages of the project, it became apparent that this mechanism was not as important in limiting PGR in *Hemiptera* as was previously thought. The availability and use of new technology, through industrial co-creation, provided a unique opportunity for the project to describe a novel and commercially-relevant mechanism. As UVA-attenuating/UVB-transmitting horticultural claddings become commercially-available and enter field-scale trials, this work forms the basis of our understanding of their potential role in the future of sustainable agriculture.

Bibliography

- Agati, G., Azzarello, E., Pollastri, S., and Tattini, M. (2012). Flavonoids as antioxidants in plants: Location and functional significance. *Plant Science*, 196:67–76.
- Agrell, J., Oleszek, W., Stochmal, A., Olsen, M., and Anderson, P. (2003). Herbivore-induced responses in alfalfa (*Medicago sativa*). *Journal of Chemical Ecology*, 29(2):303–320.
- Alkhedir, H., Karlovsky, P., and Vidal, S. (2010). Effect of light intensity on colour morph formation and performance of the grain aphid *Sitobion avenae* F (Homoptera Aphididae). *Journal of Insect Physiology*, 56(12):1999–2005.
- An, C., Fei, X., Chen, W., and Zhao, Z. (2012). The integrative effects of population density, photoperiod, temperature, and host plant on the induction of alate aphids in *Schizaphis graminum*. *Archives of Insect Biochemistry and Physiology*, 79(4-5):198–206.
- Antignus, Y. (2000). Manipulation of wavelength-dependent behaviour of insects: an IPM tool to impede insects and restrict epidemics of insect-borne viruses. *Virus Research*, 71(1-2):213–20.
- Antignus, Y., Mor, N., Joseph, R. B., Lapidot, M., and Cohen, S. (2006). Ultraviolet-absorbing plastic sheets protect crops from insect pests and from virus diseases vectored by insects. *Environmental Entomology*, 25(5):919–924.
- Antignus, Y., Nestel, D., Cohen, S., Lapidot, M., Greenhouse, U.-d., Affects, E., Attraction, W., Library, T. B., Supply, D., Spa, B., and Kingdom, U. (2001). Ultraviolet-Deficient Greenhouse Environment Affects Whitefly Attraction and Flight-Behaviour. *Environmental Entomology*, 30(2):394–399.
- Aphalo, P. J., Albert, A., McLeod, A. R., Robson, T. M., and Rosenqvist, E. (2012). *Beyond the Visible: A Handbook of Best Practice in Plant UV Photobiology*, volume 2. Helsinki: Yliopisto.
- ASTM International (2012). Standard Tables for Reference Solar Spectral Irradiances: Direct Normal and Hemispherical on 37 Tilted Surface.
- Baguley, T. (2012). *Serious stats: A guide to advanced statistics for the behavioral sciences*. Palgrave Macmillan.
- Ballaré, C. L. (2014). Light Regulation of Plant Defense. *Annual review of plant biology*.
- Ballaré, C. L., Scopel, a. L., Stapleton, a. E., and Yanovsky, M. J. (1996). Solar Ultraviolet-B Radiation Affects Seedling Emergence, DNA Integrity, Plant Morphology, Growth Rate, and Attractiveness to Herbivore Insects in *Datura ferox*. *Plant physiology*, 112(1):161–170.
- Barta, A. and Horváth, G. (2004). Why is it advantageous for animals to detect celestial polarization in the ultraviolet? Skylight polarization under clouds and canopies is strongest in the UV. *Journal of Theoretical Biology*, 226(4):429–437.
- Battisti, A., Marini, L., Pitacco, A., and Larsson, S. (2013). Solar radiation directly affects larval performance of a forest insect. *Ecological Entomology*, 38(6):553–559.

- Becatti, E., Petroni, K., Giuntini, D., Castagna, A., Calvenzani, V., Serra, G., Mensuali-Sodi, A., Tonelli, C., and Ranieri, A. (2009). Solar UV-B Radiation Influences Carotenoid Accumulation of Tomato Fruit through Both Ethylene-Dependent and -Independent Mechanisms. *Journal of Agricultural and Food Chemistry*, 57(22):10979–10989.
- Benelli, G. and Canale, A. (2012). Learning of visual cues in the fruit fly parasitoid *Psytalia concolor* (Szépligeti) (Hymenoptera: Braconidae). *BioControl*, 57(6):767–777.
- Blande, J. D., Turunen, K., and Holopainen, J. K. (2009). Pine weevil feeding on Norway spruce bark has a stronger impact on needle VOC emissions than enhanced ultraviolet-B radiation. *Environmental Pollution*, 157(1):174–180.
- Bohne, F. and Linden, H. (2002). Regulation of carotenoid biosynthesis genes in response to light in *Chlamydomonas reinhardtii*. *Biochimica et biophysica acta*, 1579(1):26–34.
- Bohrerova, Z., Linden, K. G., Grote, I., Orth, H., Wichern, M., Bischoff, A., Cornel, P., and Wagner, M. (2007). Standardizing photoreactivation: comparison of DNA photorepair rate in *Escherichia coli* using four different fluorescent lamps. *Water research*, 41(12):2832–8.
- Bonte, D., Van Dyck, H., Bullock, J. M., Coulon, A., Delgado, M., Gibbs, M., Lehouck, V., Matthyssen, E., Mustin, K., Saastamoinen, M., Schtickzelle, N., Stevens, V. M., Vandewoestijne, S., Baguette, M., Barton, K., Benton, T. G., Chaput-Bardy, A., Clobert, J., Dytham, C., Hovestadt, T., Meier, C. M., Palmer, S. C. F., Turlure, C., and Travis, J. M. J. (2012). Costs of dispersal. *Biological Reviews*, 87(2):290–312.
- Borst, A. (2009). *Drosophila's* view on insect vision. *Current biology : CB*, 19(1):R36–47.
- Brasseur, G. and Solomon, S. (2006). *Aeronomy of the Middle Atmosphere: Chemistry and Physics of the Stratosphere and Mesosphere*. Atmospheric and Oceanographic Sciences Library. Springer.
- Briscoe, A. D. and Chittka, L. (2001). The evolution of color vision in insects. *Annual Review of Entomology*, 46:471–510.
- Britt, A. B. (1996). DNA damage and repair in plants. *Annual Review of Plant Physiology and Plant Molecular Biology*, 47(1):75–100.
- Burdick, S. C., Prischmann-Voldseth, D. A., and Harmon, J. P. (2015). Density and distribution of soybean aphid, *Aphis glycines* Matsumura (Hemiptera: Aphididae) in response to UV radiation. *Population Ecology*, 57(3):457–466.
- Caldwell, M., Camp, L., Warner, C., and Flint, S. (1986). Action Spectra and Their Key Role in Assessing Biological Consequences of Solar UV-B Radiation Change. In *Stratospheric Ozone Reduction, Solar Ultraviolet Radiation and Plant Life*, pages 87–111. Springer-Verlag, Berlin.
- Caputo, C., Rutitzky, M., and Ballaré, C. L. (2006). Solar ultraviolet-B radiation alters the attractiveness of *Arabidopsis* plants to diamondback moths (*Plutella xylostella* L.): impacts on oviposition and involvement of the jasmonic acid pathway. *Oecologia*, 149(1):81–90.
- Carroll, M., Hanlon, A., Hanlon, T., Zangerl, A., and Berenbaum, M. (1997). Behavioral Effects of Carotenoid Sequestration by the Parsnip Webworm *Depressaria pastinacella*. *Journal of Chemical Ecology*, 23(12):2707–2719.
- Carroll, M. J. and Berenbaum, M. R. (2006). Lutein sequestration and furanocoumarin metabolism in parsnip webworms under different ultraviolet light regimes in the montane west. *Journal of Chemical Ecology*, 32(2):277–305.
- Castillo, L., Diaz, M., Gonzalez-Coloma, A., and Rossini, C. (2013). Differential activity against aphid settling of flavones obtained from *Clytostoma callistegioides* (Bignoniaceae). *Industrial Crops and Products*, 44:618–621.
- Chiel, E., Messika, Y., Steinberg, S., and Antignus, Y. (2006). The Effect of UV-absorbing Plastic Sheet on the Attraction and Host Location Ability of Three Parasitoids: *Aphidius colemani*, *Diglyphus isaea* and *Eretmocerus mundus*. *Biocontrol*, 51(1):65–78.

- Chittka, L., Beier, W., Hertep, H., Steinmann, E., and Menzel, R. (1992). Opponent colour coding is a universal strategy to evaluate the photoreceptor inputs in Hymenoptera. *Journal of Comparative Physiology A: Sensory, Neural, and Behavioral Physiology*, 170:545–563.
- Chu, C. C., Chen, T. Y., Natwick, E. T., Fitzgerald, G., Tuck, S., Alexander, P., and Henneberry, T. J. (2005). Light responses by *Frankliniella occidentalis* to white fluorescent light filtered through color films and ultraviolet- and blue- Light Emitting Diodes. *Southwestern Entomologist*, 30(3):149–155.
- Chyzik, R., Dobrinin, S., and Antignus, Y. (2003). Effect of a UV-deficient environment on the biology and flight activity of *Myzus persicae* and its hymenopterous parasite *Aphidius matricariae*. *Phytoparasitica*, 31(5):467–477.
- Close, D. C., Beaoce, C. L., Beadle, C. L., and Beaoce, C. L. (2003). The ecophysiology of foliar anthocyanin. *Botanical Review*, 69(2):149–161.
- Commission Internationale d'Eclairage (1999). ISO 17166:1999(E)/CIE S 007-1998 Erythema Reference Action Spectrum and Standard Erythema Dose.
- Coombe, P. E. (1982). Visual behaviour of the greenhouse whitefly, *Trialeurodes vaporariorum*. *Physiological Entomology*, 7(3):243–251.
- Costa, H. S., Newman, J., and Robb, K. L. (2003). Ultraviolet-blocking greenhouse plastic films for management of insect pests. *Hortscience*, 38(3):465.
- Costa, H. S., Robb, K. L., and Heather S. Costa, K. L. R. (1999). Effects of ultraviolet-absorbing greenhouse plastic films on flight behavior of *Bemisia argentifolii* (Homoptera : Aleyrodidae) and *Frankliniella occidentalis* (Thysanoptera : Thripidae). *Journal of Economic Entomology*, 92(3):557–562.
- Costa, H. S., Robb, K. L., and Wilen, C. A. (2002a). Field trials measuring the effects of ultraviolet-absorbing greenhouse plastic films on insect populations. *Economic Entomology*, 95(1):113–120.
- Costa, H. S., Robb, K. L., and Wilen, C. A. (2002b). Field trials measuring the effects of ultraviolet-absorbing greenhouse plastic films on insect populations. *Journal of Economic Entomology*, 95(1):113–120.
- Costa, L. B., Rangel, D. E. N., Morandi, M. a. B., and Bettiol, W. (2012). Impact of UV-B radiation on *Clonostachys rosea* germination and growth. *World journal of microbiology & biotechnology*, 28(7):2497–504.
- Cowan, T. and Gries, G. (2009). Ultraviolet and violet light: attractive orientation cues for the Indian meal moth, *Plodia interpunctella*. *Entomologia Experimentalis et Applicata*, 131(2):148–158.
- Crawley, M. J. (2007). *The R Book*. Wiley.
- Croft, P. (2006). The Effects of Spectral Modified Filters on Invertebrate Pest Populations. Technical report.
- Dadd, R. H. and Mittler, T. E. (1965). Studies on the artificial feeding of the aphid *Myzus persicae* (Sulzer)-III. Some major nutritional requirements. *Journal of insect physiology*, 11:717–743.
- Dader, B., Gwynn-Jones, D., Moreno, A. A., Winters, A., Fereres, A., D??der, B., Gwynn-Jones, D., Moreno, A. A., Winters, A., and Fereres, A. (2014). Impact of UV-A radiation on the performance of aphids and whiteflies and on the leaf chemistry of their host plants. *Journal of Photochemistry and Photobiology B: Biology*, 138:307–316.
- Davis, J. A., Radcliffe, E. B., and Ragsdale, D. W. (2006). Effects of High and Fluctuating Temperatures on *Myzus persicae* (Hemiptera: Aphididae). *Environ. Entomol.*, 35(6):1461–1468.
- de Costa, F., Yendo, A. C. A., Fleck, J. D., Gosmann, G., and Fett-Neto, A. G. (2013). Accumulation of a bioactive triterpene saponin fraction of *Quillaja brasiliensis* leaves is associated with abiotic and biotic stresses. *Plant Physiology and Biochemistry*, 66:56–62.

- DEFRA (2016). UV Radiation Data - Defra, UK.
- Díaz, B. M., Biurrún, R., Moreno, A., Nebreda, M., Fereres, A., Díaz, B. M., and Biurrún, R. (2006). Impact of ultraviolet-blocking plastic films on insect vectors of virus diseases infesting crisp lettuce. *Hortscience*, 41(3):711–716.
- Díaz, B. M. and Fereres, A. (2007). Ultraviolet-Blocking Materials as a Physical Barrier to Control Insect Pests and Plant Pathogens in Protected Crops. *Pest Technology*, 1(2):85–95.
- Dolzhenko, Y., Berteá, C. M., Occhipinti, A., Bossi, S., and Maffei, M. E. (2010). UV-B modulates the interplay between terpenoids and flavonoids in peppermint (*Mentha x piperita* L.). *Journal of Photochemistry and Photobiology B-Biology*, 100(2):67–75.
- Domingues, A. P., Shimizu, M. M., Moura, J., Catharino, R. R., Ramos, R. A., Ribeiro, R. V., and Mazzafera, P. (2012). Looking for the Physiological Role of Anthocyanins in the Leaves of *Coffea arabica*. *Photochemistry and Photobiology*, 88(4):928–937.
- Dong, Z., YiMin, D., Jie, Y., Li, Z., HuiYan, Z., ZuQing, H., and XiangShun, H. (2014). Effects of UV-B radiation in successive generations on the activities of protective enzymes in the grain aphid, *Sitobion avenae* (Hemiptera: Aphididae). *Acta Entomologica Sinica*, 57(7):762–768.
- Döring, T. F., Chittka, L., and Döring, T. F. (2007). Visual ecology of aphids—a critical review on the role of colours in host finding. *Arthropod-Plant Interactions*, 1(1):3–16.
- Döring, T. F. and Kirchner, S. M. (2007). Preliminary characterisation of the spectral sensitivity in the cabbage aphid with electroretinogram recordings (Hemiptera : Aphididae). *Entomologia Generalis*, 30(3):233–234.
- Döring, T. F., Kirchner, S. M., Kuhne, S., Saucke, H., Döring, T. F., and Kühne, S. (2004). Response of alate aphids to green targets on coloured backgrounds. *Entomologia Experimentalis Et Applicata*, 113(1):53–61.
- Doukas, D. and Payne, C. C. (2007). The use of ultraviolet-blocking films in insect pest management in the UK; effects on naturally occurring arthropod pest and natural enemy populations in a protected cucumber crop. *Annals of Applied Biology*, 151(2):221–231.
- Dudareva, N., Klempien, A., Muhlemann, J. K., Kaplan, I., Muhlemann, K., and Kaplan, I. (2013). Biosynthesis, function and metabolic engineering of plant volatile organic compounds. *New Phytologist*, 198(1):16–32.
- Dyer, a. G. (2004). Bumblebee search time without ultraviolet light. *Journal of Experimental Biology*, 207(10):1683–1688.
- Dyer, A. G., Boyd-Gerny, S., McLoughlin, S., Rosa, M. G. P., Simonov, V., and Wong, B. B. M. (2012). Parallel evolution of angiosperm colour signals: common evolutionary pressures linked to hymenopteran vision. *Proceedings of the Royal Society B-Biological Sciences*, 279(1742):3606–3615.
- Egelhaaf, M. and Kern, R. (2002). Vision in flying insects. *Current Opinion in Neurobiology*, 12(6):699–706.
- Fereres, A. and Moreno, A. (2009). Behavioural aspects influencing plant virus transmission by homopteran insects. *Virus research*, 141(2):158–68.
- Fioletov, V., Kerr, J. B., and Fergusson, A. (2010). The UV Index: Definition, Distribution and Factors Affecting It. *Source Canadian Journal of Public Health / Revue Canadienne de Santé Publique*, 10188(4).
- Foggo, A., Higgins, S., Wargent, J. J., and Coleman, R. a. (2007). Tri-trophic consequences of UV-B exposure: plants, herbivores and parasitoids. *Oecologia*, 154(3):505–12.
- Fondom, N. Y., Castro-Nava, S., and Huerta, A. J. (2009). Photoprotective mechanisms during leaf ontogeny: cuticular development and anthocyanin deposition in two morphs of *Agave striata* that differ in leaf coloration. *Botany-Botanique*, 87(12):1186–1197.

- Frentiu, F. D., Bernard, G. D., Cuevas, C. I., Sison-Mangus, M. P., Prudic, K. L., and Briscoe, A. D. (2007). Adaptive evolution of color vision as seen through the eyes of butterflies. *Proceedings of the National Academy of Sciences of the United States of America*, 104:8634–40.
- Fukaya, M., Uesugi, R., Ohashi, H., Sakai, Y., Sudo, M., Kasai, A., Kishimoto, H., and Osakabe, M. (2013). Tolerance to Solar Ultraviolet-B Radiation in the Citrus Red Mite, An Upper Surface User of Host Plant Leaves. *Photochemistry and Photobiology*, 89(2):424–431.
- Gao, S., Takemura, S.-Y., Ting, C.-Y., Huang, S., Lu, Z., Luan, H., Rister, J., Thum, A. S., Yang, M., Hong, S.-T., Wang, J. W., Odenwald, W. F., White, B. H., Meinertzhagen, I. A., and Lee, C.-H. (2008). The neural substrate of spectral preference in *Drosophila*. *Neuron*, 60(2):328–42.
- Gencer, N. S., Coskuncu, K. S., and Kumral, N. A. (2006). The colonization preference and population trends of larval fig psylla, *Homotoma ficus* L. (Hemiptera: Homotomidae). *Journal of Pest Science*, 80(1):1–8.
- Ghanem, I. and Shamma, M. (2007). Effect of non-ionizing radiation (UVC) on the development of *Trogoderma granarium* Everts. *Journal of Stored Products Research*, 43(4):362–366.
- Ghosh, B. (2000). Polyamines and plant alkaloids. *Indian journal of experimental biology*, 38(11):1086–91.
- Gil, M., Pontin, M., Berli, F., Bottini, R., and Piccoli, P. (2012). Metabolism of terpenes in the response of grape (*Vitis vinifera* L.) leaf tissues to UV-B radiation. *Phytochemistry*, 77:89–98.
- Gitelson, A. A., Chivkunova, O. B., and Merzlyak, M. N. (2009). Nondestructive estimation of anthocyanins and chlorophylls in anthocyanic leaves. *American Journal of Botany*, 96(10):1861–1868.
- Giurfa, M. and Menzel, R. (1997). Insect visual perception: complex abilities of simple nervous systems. *Current Opinion in Neurobiology*, 7(4):505–513.
- Goławska, S., Lukasik, I., and Goławska, S. (2012a). Antifeedant activity of luteolin and genistein against the pea aphid, *Acyrtosiphon pisum*. *Journal of Pest Science*, 85(4):443–450.
- Goławska, S., Lukasik, I., Wojcicka, A., and Sytykiewicz, H. (2012b). Relationship between saponin content in alfalfa and aphid development. *Acta Biologica Cracoviensia Series Botanica*, 54(2):39–46.
- Gonzalez, A., Rodriguez, R., Banon, S., Franco, J. A., and Fernandez, J. A. (2001). The influence of photoselective plastic films as greenhouse cover on sweet pepper yield and on insect pest levels. In Fernandez, J. A., Martinez, P. F., and Castilla, N., editors, *Proceedings of the Fifth International Symposium on Protected Cultivation in Mild Winter Climates: Current Trends for Sustainable Technologies, Vols I and II*, number 559, pages 233–238. International Society Horticultural Science, Leuven 1.
- Grant-Petersson, J. and Renwick, J. A. A. (1996). Effects of ultraviolet-B exposure of *Arabidopsis thaliana* on herbivory by two crucifer-feeding insects (Lepidoptera). *Environmental Entomology*, 25(1):135–142.
- Gregianini, T. S., da Silveira, V. C., Porto, D. D., Kerber, V. A., Henriques, A. T., and Fett-Neto, A. G. (2003). The Alkaloid Brachycerine is Induced by Ultraviolet Radiation and is a Singlet Oxygen Quencher[¶]. *Photochemistry and Photobiology*, 78(5):470–474.
- Gunn, A. (1998). The determination of larval phase coloration in the African armyworm, *Spodoptera exempta* and its consequences for thermoregulation and protection from UV light. *Entomologia Experimentalis et Applicata*, 86(2):125–133.
- Güven, E., Pandr, D., and Ba, H. (2015). UV radiation-induced oxidative stress and DNA damage on Mediterranean flour moth, *Ephestia kuehniella* Zeller (Lepidoptera: Pyralidae) larvae. *Turkish Journal of Entomology*, 39(1).
- Hadfield, J. D. (2010). MCMC Methods for Multi-Response Generalized Linear Mixed Models: The MCMCglmm R Package. *Journal of Statistical Software*, 33(2):1–22.

- Hamilton, W. D. and Brown, S. P. (2001). Autumn tree colours as a handicap signal. *Proceedings of the Royal Society B-Biological Sciences*, 268:1489–1493.
- Han, B., Zhang, Q.-H., and Byers, J. a. (2012). Attraction of the tea aphid, *Toxoptera aurantii*, to combinations of volatiles and colors related to tea plants. *Entomologia Experimentalis et Applicata*, 144(3):258–269.
- Harborne, J. B. and Williams, C. A. (2000). Advances in flavonoid research since 1992. *Phytochemistry*, 55(6):481–504.
- Hardie, J. (1989). Spectral specificity for targeted flight in the black bean aphid, *Aphis fabae*. *J. hecr Physiol*, 35(8):619–626.
- Hardie, J. and Vaz Nunes, M. (2001). Aphid photoperiodic clocks. *Journal of Insect Physiology*, 47(8):821–832.
- Hatcher, P. E. and Paul, N. D. (1994). The effect of elevated UV-B radiation on herbivory of pea by *Autographa gamma*. *Entomologia Experimentalis Et Applicata*, 71(3):227–233.
- Hatcher, P. E., Paul, N. D., Ayres, P. G., and Whittaker, J. B. (1997). Nitrogen Fertilization Affects Interactions Between the Components of an Insect-Fungus- Plant Tripartite System. *Source: Functional Ecology Functional Ecology*, 11(11):537–544.
- Heath, J. J., Cipollini, D. F., Stireman, J. O., Stireman III, J. O., Stireman, J. O., and Stireman III, J. O. (2012). The role of carotenoids and their derivatives in mediating interactions between insects and their environment. *Arthropod-Plant Interactions*, 7(1):1–20.
- Hectors, K. (2010). *UV-B acclimation in Arabidopsis thaliana: A multidisciplinary approach*. PhD thesis.
- Herbert, P. D. N. and Emery, C. J. (1990). The adaptive significance of cuticular pigmentation in *Daphnia*. *Functional Ecology*, 4(5):703–710.
- Hopkins, R. J., van Dam, N. M., and van Loon, J. J. a. (2009). Role of Glucosinolates in Insect-Plant Relationships and Multitrophic Interactions. In *Annual Review of Entomology*, volume 54, pages 57–83. Annual Reviews, Palo Alto.
- Hori, M., Shibuya, K., Sato, M., and Saito, Y. (2014). Lethal effects of short-wavelength visible light on insects. *Scientific Reports*, 4:7383.
- Hu, Z.-Q., Zhao, H.-Y., and Thieme, T. (2013). The Effects of Enhanced Ultraviolet-B Radiation on the Biology of Green and Brown Morphs of *Sitobion avenae* (Hemiptera: Aphididae). *Environ. Entomol*, 42(3):578–585.
- Hughes, N. M., Smith, W. K., and Gould, K. S. (2010). Red (anthocyanic) leaf margins do not correspond to increased phenolic content in New Zealand *Veronica* spp. *Annals of Botany*, 105(4):647–654.
- Hussain, S. S., Ali, M., Ahmad, M., and Siddique, K. H. M. (2011). Polyamines: natural and engineered abiotic and biotic stress tolerance in plants. *Biotechnology advances*, 29(3):300–11.
- Imafuku, M. (2008). Variation in UV light reflected from the wings of *Favonius* and *Quercusia* butterflies. *Entomological Science*, 11(1):75–80.
- International Commission on Non-Ionising Radiation (2004). ICNIRP guidelines on limits of exposure to ultraviolet radiation of wavelengths between 180nm and 400nm (incoherent optical radiation). *Health Physics*, 87(2):171–186.
- Irwin, M. E., Kampmeier, G. E., and Weisser, W. W. (2007). Aphid Movement: Process and Consequences. In van Emden, H. F. and Harrington, R., editors, *Aphids as Crop Pests*, pages 153–186. CABI, Wallingford.
- Izaguirre, M. M., Mazza, C. A., Svatos, A., Baldwin, I. T., Ballare, C. L., and Ballaré, C. L. (2007). Solar ultraviolet-B radiation and insect herbivory trigger partially overlapping phenolic responses in *Nicotiana attenuata* and *Nicotiana longiflora*. *Annals of Botany*, 99(1):103–109.

- Johansen, N. S., Vanninen, I., Pinto, D. M., Nissinen, a. I., Shipp, L., and Vänninen, I. (2011). In the light of new greenhouse technologies: 2. Direct effects of artificial lighting on arthropods and integrated pest management in greenhouse crops. *Annals of Applied Biology*, 159(1):1–27.
- Johnson, E. T. and Dowd, P. F. (2004). Differentially enhanced insect resistance, at a cost, in *Arabidopsis thaliana* constitutively expressing a transcription factor of defensive metabolites. *Journal of agricultural and food chemistry*, 52(16):5135–8.
- Josuttis, M., Dietrich, H., Treutter, D., Will, F., Linnemannstons, L., and Kruger, E. (2010). Solar UVB Response of Bioactives in Strawberry (*Fragaria x ananassa* Duch. L.): A Comparison of Protected and Open-Field Cultivation. *Journal of Agricultural and Food Chemistry*, 58(24):12692–12702.
- Keller, M. D., Leahy, D. J., Norton, B. J., Johanson, T., Mullen, E. R., Marvit, M., and Makagon, A. (2016). Laser induced mortality of *Anopheles stephensi* mosquitoes. *Scientific Reports*, 6:20936.
- Kigathi, R. and Poehling, H.-M. M. (2012). UV-absorbing films and nets affect the dispersal of western flower thrips, *Frankliniella occidentalis* (Thysanoptera: Thripidae). *Journal of Applied Entomology*, 136(10):761–771.
- Kim, J. H., Lee, B. W., Schroeder, F. C., and Jander, G. (2008a). Identification of indole glucosinolate breakdown products with antifeedant effects on *Myzus persicae* (green peach aphid). *Plant Journal*, 54(6):1015–1026.
- Kim, J. H., Lee, B. W., Schroeder, F. C., and Jander, G. (2008b). Identification of indole glucosinolate breakdown products with antifeedant effects on *Myzus persicae* (green peach aphid). *The Plant journal : for cell and molecular biology*, 54(6):1015–26.
- Kirchner, S. M., Döring, T. F., Saucke, H., and Doring, T. F. (2005). Evidence for trichromacy in the green peach aphid, *Myzus persicae* (Sulz.) (Hemiptera: Aphididae). *Journal of insect physiology*, 51(11):1255–60.
- Kishi, M., Wakakuwa, M., Kansako, M., Inuma, T., and Arikawa, K. (2013). Action Spectrum of Phototactic Behavior and Compound Eye Spectral Sensitivity in the Yellow Tea Thrips. *Japanese journal of applied entomology and zoology*, 58:13–16.
- Kloth, K. J., Ten Broeke, C. J., Thoen, M. P., Hanhart-van den Brink, M., Wieggers, G. L., Krips, O. E., Noldus, L. P., Dicke, M., and Jongasma, M. A. (2015). High-throughput phenotyping of plant resistance to aphids by automated video tracking. *Plant methods*, 11(1):4.
- Kollias, N. (1995). *The spectroscopy of human melanin pigmentation*. Number JANUARY 1995.
- Kos, M., Broekgaarden, C., Kabouw, P., Lenferink, K. O., Poelman, E. H., Vet, L. E. M., Dicke, M., and van Loon, J. J. A. (2011). Relative importance of plant-mediated bottom-up and top-down forces on herbivore abundance on *Brassica oleracea*. *Functional Ecology*, 25(5):1113–1124.
- Kos, M., Houshyani, B., Achhami, B. B., Wietsma, R., Gols, R., Weldegergis, B. T., Kabouw, P., Bouwmeester, H. J., Vet, L. E. M., Dicke, M., and van Loon, J. J. a. (2012). Herbivore-mediated effects of glucosinolates on different natural enemies of a specialist aphid. *Journal of chemical ecology*, 38(1):100–15.
- Kuhlmann, F. and Müller, C. (2009). Development-dependent effects of UV radiation exposure on broccoli plants and interactions with herbivorous insects. *Environmental and Experimental Botany*, 66(1):61–68.
- Kuhlmann, F., Muller, C., and Müller, C. (2009). Independent responses to ultraviolet radiation and herbivore attack in broccoli. *Journal of Experimental Botany*, 60(12):3467–3475.
- Kuhlmann, F., Muller, C., and Müller, C. (2010). UV-B impact on aphid performance mediated by plant quality and plant changes induced by aphids. *Plant Biology*, 12(4):676–684.
- Kumar, P. and Poehling, H. M. (2006). UV-blocking plastic films and nets influence vectors and virus transmission on greenhouse tomatoes in the humid tropics. *Environmental Entomology*, 35(4):1069–1082.

- Kuzina, V., Ekstrom, C. T., Andersen, S. B., Nielsen, J. K., Olsen, C. E., and Bak, S. (2009). Identification of Defense Compounds in *Barbarea vulgaris* against the Herbivore *Phyllotreta nemorum* by an Ecometabolomic Approach. *Plant Physiology*, 151(4):1977–1990.
- Labsphere (2015). Technical Guide: Integrating Sphere Radiometry and Photometry.
- Langley, S. a., Tilmon, K. J., Cardinale, B. J., and Ives, A. R. (2006). Learning by the parasitoid wasp, *Aphidius ervi* (Hymenoptera: Braconidae), alters individual fixed preferences for pea aphid color morphs. *Oecologia*, 150(1):172–9.
- Laposi, R., Veres, S., Lakatos, G., Olah, V., Fieldsend, A., and Meszaros, I. (2009). Responses of leaf traits of European beech (*Fagus sylvatica* L.) saplings to supplemental UV-B radiation and UV-B exclusion. *Agricultural and Forest Meteorology*, 149(5):745–755.
- Lattanzio, V., Arpaia, S., Cardinali, A., Di Venere, D., and Linsalata, V. (2000). Role of endogenous flavonoids in resistance mechanism of *Vigna* to aphids. *Journal of Agricultural and Food Chemistry*, 48(11):5316–5320.
- Legarrea, S., Betancourt, M., Plaza, M., Fraile, a., Garcia-Arenal, F., Fereres, A., García-Arenal, F., and Fereres, A. (2012a). Dynamics of nonpersistent aphid-borne viruses in lettuce crops covered with UV-absorbing nets. *Virus Research*, 165(1):1–8.
- Legarrea, S., Diaz, B. M., Plaza, M., Barrios, L., Morales, I., Viñuela, E., Vinuela, E., and Fereres, A. (2012b). Diminished UV radiation reduces the spread and population density of *Macrosiphum euphorbiae* (Thomas) Hemiptera: Aphididae in lettuce crops. *Horticultural Science*, 39(2):74–80.
- Legarrea, S., Karnieli, A., Fereres, A., and Weintraub, P. G. (2010). Comparison of UV-absorbing nets in pepper crops: spectral properties, effects on plants and pest control. *Photochemistry and photobiology*, 86(2):324–30.
- Legarrea, S., Weintraub, P. G., Plaza, M., Viñuela, E., Fereres, A., Vinuela, E., Fereres, A., Viñuela, E., Fereres, A., and Vinuela, E. (2012c). Dispersal of aphids, whiteflies and their natural enemies under photoselective nets. *BioControl*, 57(4):523–532.
- Llusia, J., Llorens, L., Bernal, M., Verdaguer, D., and Penuelas, J. (2012). Effects of UV radiation and water limitation on the volatile terpene emission rates, photosynthesis rates, and stomatal conductance in four Mediterranean species. *Acta Physiologiae Plantarum*, 34(2):757–769.
- Lotto, R. B. and Chittka, L. (2005). Seeing the light: illumination as a contextual cue to color choice behavior in bumblebees. *Proceedings of the National Academy of Sciences of the United States of America*, 102(10):3852–6.
- Luft, P. A., Paine, T. D., and Walker, G. P. (2001). Interactions of colonisation density and leaf environments on survival of *Trioza eugeniae* nymphs. *Ecological Entomology*, 26:263–270.
- Lydon, J., Casale, J. F., Hyesuk, K., Sullivan, J. H., Daughtry, C. S. T., and Bailey, B. (2009). The Effects of Ambient Solar UV Radiation on Alkaloid Production by *Erythroxylum novogranatense* var. *novogranatense*. *Photochemistry & Photobiology*, 85(5):1156–1161.
- Malone, L. a., Barraclough, E. I., Lin-Wang, K., Stevenson, D. E., and Allan, A. C. (2009). Effects of red-leaved transgenic tobacco expressing a MYB transcription factor on two herbivorous insects, *Spodoptera litura* and *Helicoverpa armigera*. *Entomologia Experimentalis Et Applicata*, 133(2):117–127.
- Margaritopoulos, J. T., Tsitsipis, J. a., and Prophetou-Athanasiadou, D. a. (2002). An interval timer controls the production of sexual morphs in *Myzus persicae* (Homoptera: Aphididae). *Physiological Entomology*, 27(3):251–255.
- Markham, K. R., Ryan, K. G., Bloor, S. J., and Mitchell, K. A. (1998). An increase in the luteolin : apigenin ratio in *Marchantia polymorpha* on UV-B enhancement. *Phytochemistry*, 48(5):791–794.

- Markwick, N. P., Poulton, J., Espley, R. V., Rowan, D. D., McGhie, T. K., Wadasinghe, G., Wohlers, M., Jia, Y. L., and Allan, A. C. (2013). Red-foliaged apples affect the establishment, growth, and development of the light brown apple moth, *Epiphyas postvittana*. *Entomologia Experimentalis Et Applicata*, 146(2):261–275.
- Matsumoto, Y., Wakakuwa, M., Yukuhiro, F., Arikawa, K., and Noda, H. (2014). Attraction to Different Wavelength Light Emitting Diodes LEDs, the Compound Eye Structure, and opsin Genes in *Nilaparvata lugens*. *J. Appl. Entomol. Zool*, 58:111–118.
- Matsuura, H. N. and Fett-Neto, A. G. (2013). The major indole alkaloid N,-D-glucopyranosyl vincosamide from leaves of *Psychotria leiocarpa* Cham. & Schltdl. is not an antifeedant but shows broad antioxidant activity. *Natural Product Research*, 27(4-5):402–411.
- Mazza, C. a., Izaguirre, M. M., Curiale, J., and Ballaré, C. L. (2010). A look into the invisible: ultraviolet-B sensitivity in an insect (*Caliothrips phaseoli*) revealed through a behavioural action spectrum. *Proceedings. Biological sciences / The Royal Society*, 277(1680):367–373.
- Mazza, C. A., Zavala, J., Scopel, a. L., Ballaré, C. L., and Ballare, C. L. (1999). Perception of solar UVB radiation by phytophagous insects: Behavioral responses and ecosystem implications. *Proceedings of the National Academy of Sciences of the United States of America*, 96(3):980–985.
- McCall, A. C., Murphy, S. J., Venner, C., and Brown, M. (2013). Florivores prefer white versus pink petal color morphs in wild radish, *Raphanus sativus*. *Oecologia*, 172(1):189–95.
- McCloud, E. S. and Berenbaum, M. (1999). Effects of enhanced UV-B radiation on a weedy forb (*Plantago lanceolata*) and its interactions with a generalist and specialist herbivore. *Entomologia Experimentalis Et Applicata*, 93(3):233–247.
- Meijkamp, B., Aerts, A., Van de Staaij, J., Tosserams, M., Wilfried, E., and Rozema, J. (1999). Effects of UV-B on secondary metabolites in plants. In Rozema, J., editor, *Stratospheric Ozone Depletion: The Effects of Enhanced Uv-B Radiation on Terrestrial Ecosystems*, chapter 5. Backhuys Publishers, Leiden.
- Meng, J.-Y., Zhang, C.-Y., Zhu, F., Wang, X.-P., and Lei, C.-L. (2009). Ultraviolet light-induced oxidative stress: Effects on antioxidant response of *Helicoverpa armigera* adults. *Journal of Insect Physiology*, 55(6):588–592.
- Mewis, I., Schreiner, M., Nguyen, C. N., Krumbein, A., Ulrichs, C., Lohse, M., Zrenner, R., and Chau Nhi, N. (2012). UV-B irradiation changes specifically the secondary metabolite profile in broccoli sprouts: induced signaling overlaps with defense response to biotic stressors. *Plant & cell physiology*, 53(9):1546–1560.
- Meyer-Rochow, V., Kashiwagi, T., and Eguchi, E. (2002). Selective photoreceptor damage in four species of insects induced by experimental exposures to UV-irradiation. *Micron*, 33(1):23–31.
- Möller, R. (2002). Insects could exploit UV-green contrast for Landmark navigation. *Journal of theoretical biology*, 214(4):619–31.
- Mote, M. I. and Wehner, R. (1980). Journal of Comparative Physiology. A Functional Characteristics of Photoreceptors in the Compound Eye and Ocellus of the Desert Ant, *Cataglyphis bicolor*. *Physiol*, 137:63–71.
- Müller, C. B., Williams, I. S., and Hardie, J. (2001). The role of nutrition, crowding and interspecific interactions in the development of winged aphids. *Ecological Entomology*, 26(3):330–340.
- Müller, M., Buchbauer, G., and Muller, M. (2011). Essential oil components as pheromones. A review. *Flavour and Fragrance Journal*, 26(6):357–377.
- Murata, Y. and Osakabe, M. (2013). The BunsenRoscoe reciprocity law in ultraviolet-B-induced mortality of the two-spotted spider mite *Tetranychus urticae*. *Journal of Insect Physiology*, 59(3):241–247.
- Murata, Y. and Osakabe, M. (2014). Factors affecting photoreactivation in UVB-irradiated herbivorous spider mite (*Tetranychus urticae*). *Experimental & applied acarology*, 63(2):253–65.

- Musil, C. F. (1995). Differential effects of elevated ultraviolet-B radiation on the photochemical and reproductive performances of dicotyledonous and monocotyledonous arid-environment ephemerals. *Plant, Cell and Environment*, 18(8):844–854.
- Mutwiwa, U. N., Borgemeister, C., Von Elsner, B., and Tantau, H. J. (2005). Effects of UV-absorbing plastic films on greenhouse whitefly (Homoptera : Aleyrodidae). *Journal of Economic Entomology*, 98(4):1221–1228.
- Naranjo, S. E. (2007). Survival and Movement of Bemisia tabaci (Homoptera: Aleyrodidae) Crawlers on Cotton. *Southwestern Entomologist*, 32(1):17–23.
- NASA (2016). Giovanni visualisation tool.
- Nathans, J. (1999). The Evolution and Physiology of Human Color Vision. *Neuron*, 24(2):299–312.
- Noldus, L. P., Spink, A. J., and Tegelenbosch, R. A. (2002). Computerised video tracking, movement analysis and behaviour recognition in insects. *Computers and Electronics in Agriculture*, 35(2-3):201–227.
- Ohtsuka, K. and Osakabe, M. M. (2009). Deleterious Effects of UV-B Radiation on Herbivorous Spider Mites: They Can Avoid It by Remaining on Lower Leaf Surfaces. *Environmental Entomology*, 38(3):920–929.
- Onzo, A., Sabelis, M. W., and Hanna, R. (2010). Effects of ultraviolet radiation on predatory mites and the role of refuges in plant structures. *Environmental entomology*, 39(2):695–701.
- Osorio, D. and Vorobyev, M. (2008). A review of the evolution of animal colour vision and visual communication signals. *Vision research*, 48(20):2042–51.
- Paul, N. D. and Gwynn-Jones, D. (2003). Ecological roles of solar UV radiation: towards an integrated approach. *Trends in Ecology & Evolution*, 18(1):48–55.
- Paul, N. D., Jacobson, R. J., Taylor, A., Wargent, J. J., and Moore, J. P. (2005). The use of wavelength-selective plastic cladding materials in horticulture: understanding of crop and fungal responses through the assessment of biological spectral weighting functions. *Photochemistry and photobiology*, 81(5):1052–60.
- Paul, N. D., Moore, J. P., McPherson, M., Lambourne, C., Croft, P., Heaton, J. C., and Wargent, J. J. (2012). Ecological responses to UV radiation: interactions between the biological effects of UV on plants and on associated organisms. *Physiologia Plantarum*, 145(4):565–581.
- Paulsen, C., Cottrell, T., and Ruberson, J. (2013). Distribution of the black pecan aphid, *Melanocallis caryaefoliae*, on the upper and lower surface of pecan foliage. *Entomologia Experimentalis et Applicata*, 146(2):252–260.
- Pérez, J., Rojas, J. C., Montoya, P., Liedo, P., González, F. J., and Castillo, A. (2011). Size, shape and hue modulate attraction and landing responses of the braconid parasitoid *Fopius arisanus* to fruit odour-baited visual targets. *BioControl*, 57(3):405–414.
- Pettersson, J., Tjallingii, W. F., and Hardie, J. (2007). Host-plant Selection and Feeding. In *Aphids as crop pests*, pages 87–114. CAB International.
- Pfeiffer, K. and Homberg, U. (2007). Coding of Azimuthal Directions via Time-Compensated Combination of Celestial Compass Cues. *Current Biology*, 17(11):960–965.
- Pollastri, S. and Tattini, M. (2011). Flavonols: old compounds for old roles. *Annals of Botany*, 108(7):1225–1233.
- Prokopy, R. J. and Owens, E. D. (1983). Visual detection of plants by herbivorous insects. *Ann. Rev. Entomol.*, 28:337–64.
- Quaite, F. E., Sutherland, B. M., and Sutherland, J. C. (1992). Action spectrum for DNA damage in alfalfa lowers predicted impact of ozone depletion. *Nature*, 358(August 1992):576–578.

- R Core Team (2013). R: A Language and Environment for Statistical Computing.
- Raviv, M., Antignus, Y., and Yishay, R. (2004). Invited Review UV Radiation Effects on Pathogens and Insect Pests of Greenhouse-Grown Crops. *Photochemistry and Photobiology*, 79(3):219–226.
- Rechner, O. and Poehling, H.-m. (2014). UV exposure induces resistance against herbivorous insects in broccoli. *Journal of plant diseases and protection*, 121(3):125–132.
- Renshaw, E. (1993). *Modelling Populations in Space and Time*. Cambridge University Press, 2nd edition.
- Rigollier, C., Bauer, O., and Wald, L. (2000). On the clear sky model of the ESRA -European Solar Radiation Atlas with respect to the Heliosat method. *Solar Energy*, 68(1):33–48.
- Roberts, M. R. and Paul, N. D. (2006). Seduced by the dark side: integrating molecular and ecological perspectives on the influence of light on plant defence against pests and pathogens. *New Phytologist*, pages 849–858.
- Rozema, J., VandeStaaïj, J., Bjorn, L. O., and Caldwell, M. (1997). UV-B as an environmental factor in plant life: Stress and regulation. *Trends in Ecology & Evolution*, 12(1):22–28.
- Ryan, K. G., Swinny, E. E., Winefield, C., and Markham, K. R. (2001). Flavonoids and UV photoprotection in Arabidopsis mutants. *Zeitschrift Fur Naturforschung C-a Journal of Biosciences*, 56(9-10):745–754.
- Sakai, H., Katayama, H., Oguma, K., and Ohgaki, S. (2011a). Effect of photoreactivation on ultraviolet inactivation of *Microcystis aeruginosa*. *Water science and technology : a journal of the International Association on Water Pollution Research*, 63(6):1224–9.
- Sakai, Y., Sudo, M., and Osakabe, M. (2011b). A comparison of the effects of gravity and the nutritional advantage of leaf surfaces on fecundity in the two-spotted spider mite (Acari: Tetranychidae). *Journal of the Acarological Society of Japan*, 21(1):1–6.
- Sakai, Y., Sudo, M., and Osakabe, M. (2012). Seasonal changes in the deleterious effects of solar ultraviolet-B radiation on eggs of the twospotted spider mite, *Tetranychus urticae* (Acari: Tetranychidae). *Applied Entomology and Zoology*, 47(1):67–73.
- Sal, J., Velázquez, E., Legarrea, S., Aguado, P., Fereres, A., Morales, I., and Del, P. (2008). Influence of UV-absorbing nets in the population of *Macrosiphum euphorbiae* (Homoptera: Aphididae) and the parasitoid *Aphidius ervi* (Hymenoptera: Aphidiidae) in lettuce crops. (Viñuela 2005).
- Sambaraju, K. R. and Phillips, T. W. (2008). Responses of Adult *Plodia interpunctella* (Hübner) (Lepidoptera: Pyralidae) to Light and Combinations of Attractants and Light. *Journal of Insect Behavior*, 21(5):422–439.
- Sato, Y., Abe, M., Sasaki, F., Nakamura, M., Akayanagi, S. T., and Negishi, S. (2010). UVB-induced Damage and Photoreactivation in the Integument of the Terrestrial Isopod *Armadillidium vulgare*. *Hiyoshi Review of Natural Science*, 47(1):1–13.
- Schaefer, H. M. and Rolshausen, G. (2006). Plants on red alert: do insects pay attention? *Bioessays*, 28(1):65–71.
- Schreiner, M., Mewis, I., Huyskens-Keil, S., Jansen, M. A. K., Zrenner, R., Winkler, J. B., O'Brien, N., Krumbein, A., O'Brien, N., and Krumbein, A. (2012). UV-B-Induced Secondary Plant Metabolites - Potential Benefits for Plant and Human Health. *Critical Reviews in Plant Sciences*, 31(3):229–240.
- Searle, J. and Mittler, T. (1982). OF THE APHID MYZUS PERSICAE , IN RELATION TO PHOTOPERIOD. *J. Insect Physiol.*, 28(3):213–220.
- Sempruch, C., Horbowicz, M., Kosson, R., and Leszczynski, B. (2012). Biochemical interactions between triticales (Triticosecale; Poaceae) amines and bird cherry-oat aphid (*Rhopalosiphum padi*; Aphididae). *Biochemical Systematics and Ecology*, 40:162–168.

- Sempruch, C., Leszczyński, B., and Kozik, A. (2010). The influence of selected plant polyamines on feeding and survival of grain aphid (*Sitobion avenae* F.). *Pesticides*, 1-4:15–20.
- Setlow, R. B. (1974). The wavelengths in sunlight effective in producing skin cancer: a theoretical analysis. *Proceedings of the National Academy of Sciences of the United States of America*, 71(9):3363–6.
- Severtson, D., Flower, K., and Nansen, C. (2015). Nonrandom Distribution of Cabbage Aphids (Hemiptera: Aphididae) in Dryland Canola (Brassicales: Brassicaceae). *Environmental Entomology*, 44(3).
- Shimoda, M. and Honda, K.-i. (2013). Insect reactions to light and its applications to pest management. *Applied Entomology and Zoology*, 48(4):413–421.
- Simmonds, M. S. J. (2003). Flavonoid-insect interactions: recent advances in our knowledge. *Phytochemistry*, 64(1):21–30.
- Simmons, A. M. (1999). Nymphal survival and movement of crawlers of *Bemisia argentifolii* (Homoptera: Aleyrodidae) on leaf surfaces of selected vegetables. *Environmental entomology*, 28(2):212–6.
- Sisa, M., Bonnet, S. L., Ferreira, D., and Van der Westhuizen, J. H. (2010). Photochemistry of Flavonoids. *Molecules*, 15(8):5196–5245.
- SoDa (2016). SoDa solar radiation data.
- Solovchenko, a. E. and Merzlyak, M. N. (2008). Screening of Visible and UV Radiation as a Photoprotective Mechanism in Plants. *Russian Journal of Plant Physiology*, 55(6):719–737.
- Tariq, K., Noor, M., Saeed, S., and Zhang, H. (2015). The Effect of Ultraviolet-A Radiation Exposure on the Reproductive Ability, Longevity, and Development of the *Dialeurodes citri* (Homoptera: Aleyrodidae) F1 Generation. *Environmental Entomology*, 44(6):1614–1618.
- Thoen, M. P. M., Kloth, K. J., Wieggers, G. L., Krips, O. E., Noldus, L. P. J. J., Dicke, M., and Jongsma, M. A. (2016). Automated video tracking of thrips behavior to assess host-plant resistance in multiple parallel two-choice setups. *Plant methods*, 12:1.
- Tsormpatsidis, E., Henbest, R., Davis, F., Battey, N., Hadley, P., and Wagstaffe, a. (2008). UV irradiance as a major influence on growth, development and secondary products of commercial importance in Lollo Rosso lettuce Revolution' grown under polyethylene films. *Environmental and Experimental Botany*, 63(1-3):232–239.
- Vänninen, I., Pinto, D., a.I. Nissinen, Johansen, N., and Shipp, L. (2010). In the light of new greenhouse technologies: 1. Plant-mediated effects of artificial lighting on arthropods and tritrophic interactions. *Annals of Applied Biology*, 157(3):393–414.
- Vorobyev, M. and Brandt, R. (1997). How do insect pollinators discriminate colors? *Israel Journal of Plant Sciences*, 45(2-3):103–113.
- Wei, X. C., Zhang, X. H., Shen, D., Wang, H. P., Wu, Q. J., Lu, P., Qiu, Y., Song, J. P., Zhang, Y. J., and Li, X. X. (2013). Transcriptome Analysis of *Barbarea vulgaris* Infested with Diamondback Moth (*Plutella xylostella*) Larvae. *Plos One*, 8(5).
- Wink, M. (1992). The Role of Quinolizidine Alkaloids in Plant-Insect Interactions. In Bernays, E., editor, *Insect-Plant Interactions*, volume 4, chapter 5, pages 131–166. CRC Press.
- Woodall, G. S. and Stewart, G. R. (1998). Do anthocyanins play a role in UV protection of the red juvenile leaves of *Syzygium*? *Journal of Experimental Botany*, 49(325):1447–1450.
- YiMin, D., Ping, W., Jie, Y., Dong, Z., GuangYu, L., HuiYan, Z., ZuQing, H., and XiangShun, H. (2014). Effects of UV-B radiation intensity and duration on the growth, development and fecundity of *Sitobion avenae* (Hemiptera: Aphididae). *Acta Entomologica Sinica*, 57(12):1395–1401.

- Zavala, J. A., Scopel, A. L., and Ballaré, C. L. (2001). Effects of ambient UV-B radiation on soybean crops: Impact on leaf herbivory by *Anticarsia gemmatalis*. *Ecology*, 156(2):121–130.
- Zhang, C.-Y., Meng, J.-Y., Wang, X.-P., Zhu, F., and Lei, C.-L. (2011a). Effects of UV-A exposures on longevity and reproduction in *Helicoverpa armigera*, and on the development of its F1 generation. *Insect Science*, 18(6):697–702.
- Zhang, C.-Y., Meng, J.-Y., Wang, X.-P., Zhu, F., and Lei, C.-L. (2011b). Effects of UV-A exposures on longevity and reproduction in *Helicoverpa armigera*, and on the development of its F1 generation. *Insect Science*, 18(6):697–702.
- Zhang, Y., Wang, X.-X., Zhang, Z.-F., Chen, N., Zhu, J.-Y., Tian, H.-G., Fan, Y.-L., and Liu, T.-X. (2016). Pea aphid *Acyrtosiphon pisum* sequesters plant-derived secondary metabolite L-DOPA for wound healing and UVA resistance. *Nature Publishing Group*, 6:23618.
- Zu-Qing, H., Hui-Yan, Z., and Thomas, T. (2013). Probing behaviors of *Sitobion avenae* (Hemiptera: Aphididae) on enhanced UV-B irradiated plants. *Archives of Biological Sciences*, 65(1):247–254.